TARGETING CDK4 AND CDK6 IN COMBINATION CANCER THERAPY

RELATED APPLICATION

[0001] This application claims the benefit of U.S. Provisional Application No. 61/012,403, filed December 7, 2007, which is incorporated herein by reference in its entirety.

BACKGROUND OF THE INVENTION

Field of the Invention

[0002] The present invention relates to certain compounds and to methods for the preparation and the use of certain compounds in the fields of chemistry and medicine.

Description of the Related Art

[0003] Cancer is a leading cause of death in the United States. Despite significant efforts to find new approaches for treating cancer, the primary treatment options remain surgery, chemotherapy and radiation therapy, either alone or in combination. Surgery and radiation therapy, however, are generally useful only for fairly defined types of cancer, and are of limited use for treating patients with disseminated disease. Chemotherapy is the method that is generally useful in treating patients with metastatic cancer or diffuse cancers such as leukemias. Although chemotherapy can provide a therapeutic benefit, it often fails to result in cure of the disease due to the patient's cancer cells becoming resistant to the chemotherapeutic agent. Due, in part, to the likelihood of cancer cells becoming resistant to a chemotherapeutic agent, such agents are commonly used in combination to treat patients.

[0004] Therefore, a need exists for additional chemotherapeutics agents to treat cancer. A continuing effort is being made by individual investigators, academia and companies to identify new, potentially useful chemotherapeutic agents.

[0005] Marine-derived natural products are a rich source of potential new anti-cancer agents and anti-microbial agents. The oceans are massively complex and house a diverse assemblage of microbes that occur in environments of extreme variations in pressure, salinity, and temperature. Marine microorganisms have therefore developed unique metabolic and physiological capabilities that not only ensure survival in extreme and varied habitats, but also offer the potential to produce metabolites that would not be observed from terrestrial

microorganisms (Okami, Y. 1993 *J Mar Biotechnol* **1**:59). Representative structural classes of such metabolites include terpenes, peptides, polyketides, and compounds with mixed biosynthetic origins. Many of these molecules have demonstrable anti-tumor, anti-bacterial, anti-fungal, anti-inflammatory or immunosuppressive activities (Bull, A.T. *et al.* 2000 *Microbiol Mol Biol Rev* **64**:573; Cragg, G.M. & D.J. Newman 2002 *Trends Pharmacol Sci* **23**:404; Kerr, R.G. & S.S. Kerr 1999 *Exp Opin Ther Patents* **9**:1207; Moore, B.S 1999 *Nat Prod Rep* **16**:653; Faulkner, D.J. 2001 *Nat Prod Rep* **18**:1; Mayer, A. M. & V.K. Lehmann 2001 *Anticancer Res* **21**:2489), validating the utility of this source for isolating invaluable therapeutic agents. Further, the isolation of novel anti-cancer and anti-microbial agents that represent alternative mechanistic classes to those currently on the market will help to address resistance concerns, including any mechanism-based resistance that may have been engineered into pathogens for bioterrorism purposes.

SUMMARY OF THE INVENTION

[0006] The embodiments disclosed herein generally relate to chemical compounds, including heterocyclic compounds and analogs thereof. Some embodiments are directed to the use of compounds as proteasome inhibitors.

[0007] In other embodiments, the compounds are used to treat neoplastic diseases, for example, to inhibit the growth of tumors, cancers and other neoplastic tissues. The methods of treatment disclosed herein can be employed with any patient suspected of carrying tumorous growths, cancers, or other neoplastic growths, either benign or malignant ("tumor" or "tumors" as used herein encompasses tumors, cancers, disseminated neoplastic cells and localized neoplastic growths). Examples of such growths include but are not limited to hematological malignancies including Waldenström's Macroglobulinemia, myelomas (e.g., multiple myeloma), lymphomas, and leukemias; breast cancers; osteosarcomas, angiosarcomas, fibrosarcomas and other sarcomas; sinus tumors; ovarian, uretal, bladder, prostate and other genitourinary cancers; colon, esophageal and stomach cancers and other gastrointestinal cancers; rectal cancers; lung cancers; pancreatic cancers; liver cancers; kidney cancers; endocrine cancers; skin cancers; melanomas; angiomas; and brain or central nervous system (CNS; glioma) cancers. In general, the tumor or growth to be treated can be any tumor or cancer, primary or secondary. Certain embodiments relate to methods of treating neoplastic diseases in animals. The method can

include, for example, administering an effective amount of a compound to a patient in need thereof. Other embodiments relate to the use of compounds in the manufacture of a pharmaceutical or medicament for the treatment of a neoplastic disease.

[0008] The compounds can be administered or used in combination with treatments such as chemotherapy, radiation, and biologic therapies. In some embodiments the compounds can be administered or used with one or more other chemotherapeutic agents. In one embodiment, the compounds are administered in combination with PD 0332991. Examples of other chemotherapeutics include alkaloids, alkylating agents, antibiotics, antimetabolites, enzymes, hormones, platinum compounds, immunotherapeutics (antibodies, T-cells, epitopes), BRMs, and the like. Examples include, Vincristine, Vinblastine, Vindesine, Paclitaxel (Taxol), Docetaxel, topoisomerase inhibibitors epipodophyllotoxins (Etoposide (VP-16), Teniposide (VM-26)), Camptothecin, nitrogen mustards (cyclophosphamide), Nitrosoureas, Carmustine, lomustine, dacarbazine, hydroxymethylmelamine, thiotepa and mitocycin C, Dactinomycin (Actinomycin D), anthracycline antibiotics (Daunorubicin, Daunomycin, Cerubidine), Doxorubicin (Adriamycin), Idarubicin (Idamycin), Anthracenediones (Mitoxantrone), Bleomycin (Blenoxane), Plicamycin (Mithramycin, Antifolates (Methotrexate (Folex, Mexate)), purine antimetabolites (6-mercaptopurine (6-MP, Purinethol) and 6- thioguanine (6-TG). The two major anticancer drugs in this category are 6-mercaptopurine and 6-thioguanine, Chlorodeoxyadenosine and Pentostatin, Pentostatin (2'-deoxycoformycin), pyrimidine antagonists, Avastin, Leucovorin, Oxaliplatin, fluoropyrimidines (5-fluorouracil(Adrucil), 5-fluorodeoxyuridine (FdUrd) (Floxuridine)), Cytosine Arabinoside (Cytosar, ara-C), Fludarabine, L-ASPARAGINASE, Hydroxyurea, glucocorticoids, antiestrogens, tamoxifen, nonsteroidal antiandrogens, flutamide, aromatase inhibitors Anastrozole(Arimidex), Cisplatin, 6-Mercaptopurine and Thioguanine, Methotrexate, Cytoxan, Cytarabine, L-Asparaginase, Steroids: Prednisone and Dexamethasone. Also, proteasome inhibitors such as bortezomib and carfilzomib can be used in combination with the instant compounds, for example. Examples of biologics can include agents such as TRAIL antibodies to TRAIL, integrins such as alpha-V-beta-3 ($\alpha V\beta 3$) and / or other cytokine/growth factors that are involved in angiogenesis, VEGF, EGF, FGF and PDGF. In some aspects, the compounds can be conjugated to or delivered with an antibody.

[0009] In other embodiments, the other chemotherapeutic agents include histone deacetylase inhibitors (HDACi). In various embodiments, the HDACi is selected from the group consisting of:

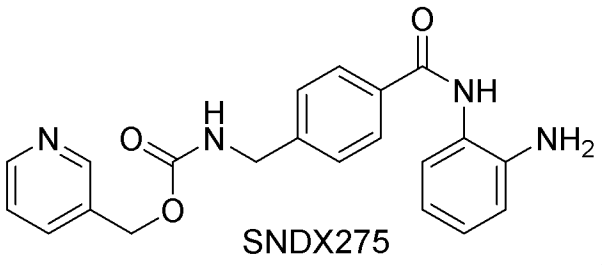

SNDX275,

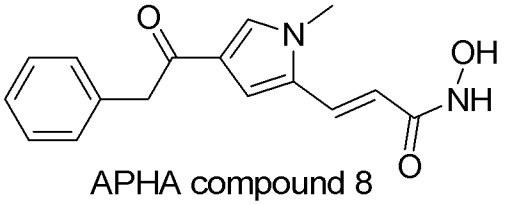

APHA compound 8,

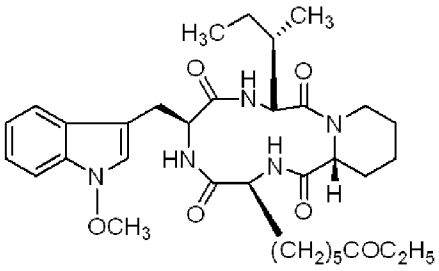

Apicidin,

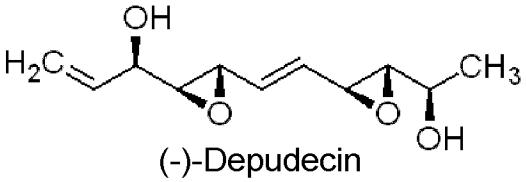

(-)-Depudecin,

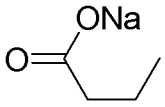

Sodium Butyrate,

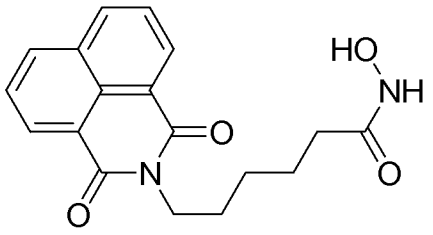

Scriptaid ,

Sirtinol ,

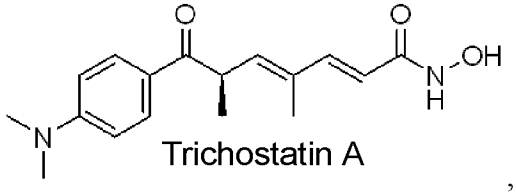

Trichostatin A ,

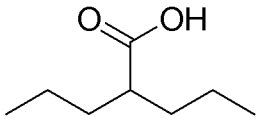

Valproic acid , and

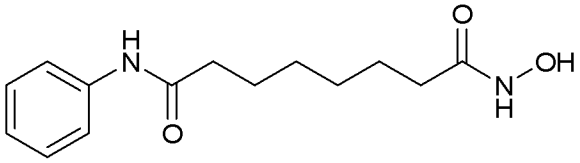

Vorinostat (suberoylanilide hydroxamic acid (SAHA)) .

[0010] In other embodiments, the other chemotherapeutics include vascular disrupting agents (VDA). Examples of such VDAs include combratostatin CA4P and NPI-2358. NPI-2358 is represented by the following formula:

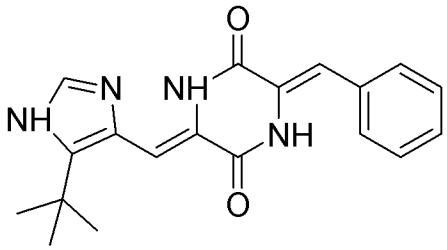

NPI-2358

[0011] Some embodiments relate to uses of a structure of Formula I, or a pharmaceutically acceptable salt or pro-drug ester thereof:

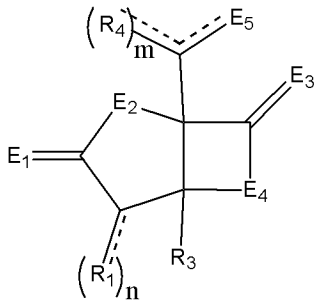

Formula I

wherein R_1, R_3, and R_4 separately may include a hydrogen, a halogen, a mono-substituted, a poly-substituted or an unsubstituted variant of the following residues: saturated C_1-C_{24} alkyl, unsaturated C_2-C_{24} alkenyl or C_2-C_{24} alkynyl, acyl, acyloxy, alkyloxycarbonyloxy, aryloxycarbonyloxy, cycloalkyl, cycloalkenyl, alkoxy, cycloalkoxy, aryl, heteroaryl, arylalkoxy carbonyl, alkoxy carbonylacyl, amino, aminocarbonyl, aminocarboyloxy, nitro, azido, phenyl, cycloalkylacyl, hydroxy, alkylthio, arylthio, oxysulfonyl, carboxy, cyano, thio, sulfoxide, sulfone, sulfonate esters, thiocyano, boronic acids and esters, and halogenated alkyl including polyhalogenated alkyl;

wherein m is equal to 1 or 2;

wherein n is equal to 1 or 2;

wherein each of E_1, E_2, E_3 and E_4 is a substituted or unsubstituted heteroatom; and

wherein E_5 may include OH, O, OR_{10}, S, SR_{11}, SO_2R_{11}, NH, NH_2, NOH, NHOH, NR_{12}, and $NHOR_{13}$;

[0012] Other embodiments relate to methods of treating a neoplastic disease in an animal. The methods can include, for example, administering to the animal, a therapeutically effective amount of a compound of a formula selected from Formula I, and pharmaceutically acceptable salts and pro-drug esters thereof.

[0013] Further embodiments relate to pharmaceutical compositions which include a compound of a formula selected from Formula I.

[0014] Still further embodiments relate to methods of inhibiting the growth of a cancer cell. The methods can include, for example, contacting a cancer cell with a compound of a formula selected from Formula I and pharmaceutically acceptable salts and pro-drug esters thereof.

BRIEF DESCRIPTION OF THE DRAWINGS

[0015] The accompanying drawings, which are incorporated in and form part of the specification, merely illustrate certain preferred embodiments of the present invention. Together with the remainder of the specification, they are meant to serve to explain preferred modes of making certain compounds of the invention to those of skilled in the art. In the drawings:

[0016] FIG. 1A is a graph showing MM1.S cells cultured in the presence and absence of 0.25 μM PD 0332991 for 24 hours before treatment with 4 nM salinosporamide A for 24 hours.

[0017] FIG. 1B is a plot of total viable cells, BrdU uptake.

[0018] FIG. 1C is a graph of the loss of mitochondria depolarization as assayed using JC-1 dye.

[0019] FIG. 2A is a graph showing MM cells culture with PD 0332991 (2 μM) for 4 or 17 hours before additional culturing in the presence or absence of PD 0332991, bortezomib or salinosporamide A for 24 hours. PARP cleavage was analyzed by immunoblotting. PARP and its cleaved product are as indicated. Actin is shown as loading control. F. MM cells were treated with PD 0332991 (2 μM) and bortezomib (6 nM) for 3 days (d 3), and after rinsing in media cultured with salinosporamide A (4 nM) or PD 0332991 (2 μM), or both until day 7.

[0020] FIG. 2B is a graph of percent viable MM cells treated with PD 0332991 (2 μM) and bortezomib (6 nM) for 3 days (d 3), and after rinsing in media cultured with salinosporamide A (4 nM) or PD 0332991 (2 μM), or both until day 7.

[0021] FIG. 2C is a graph showing MM cells cultured with PD 0332991 (2 μM) and bortezomib or salinosporamide A for 72 hours. Total viable cells were determined by trypan blue exclusion and presented as percentage of input. Error bars represent cell counts in triplicates.

DETAILED DESCRIPTION OF THE PREFERRED EMBODIMENT

[0022] Numerous references are cited herein. The references cited herein, including the U.S. patents cited herein, are each to be considered incorporated by reference in their entirety into this specification.

[0023] Embodiments of the invention include, but are not limited to, providing a method for the preparation of compounds, including compounds, for example, those described herein and analogs thereof, and to providing a method for producing pharmaceutically acceptable anti-cancer compositions. The methods can include the compositions in relatively high yield, wherein the compounds and/or their derivatives are among the active ingredients in these compositions. Other embodiments relate to providing novel compounds not obtainable by currently available methods. Furthermore, embodiments relate to methods of treating cancers, particularly those affecting humans. In some embodiments, one or more formulae, one or more compounds, or groups of compounds can be specifically excluded from use in any one or more of the methods of treating the conditions described herein. As one illustrative example, compounds of Formula I-16 can be excluded in some embodiments from the methods of treating cancer generally, for example, or a specific type of cancer. The methods may include, for example, the step of administering an effective amount of a member of a class of new compounds. Preferred embodiments relate to the compounds and methods of making and using such compounds disclosed herein, but not necessarily in all embodiments of the present invention, these objectives are met.

[0024] For the compounds described herein, each stereogenic carbon can be of R or S configuration. Although the specific compounds exemplified in this application can be depicted in a particular configuration, compounds having either the opposite stereochemistry at any given chiral center or mixtures thereof are also envisioned. When chiral centers are found in the derivatives of this invention, it is to be understood that the compounds encompass all possible stereoisomers.

[0025] The cyclin-dependent kinase Cdk4 and Cdk6 are frequently deregulated in cancer, and required to maintain breast tumorigenesis (Yu et al., 2006). Coupled with cyclin D overexpression, aberrant elevation of Cdk4 or Cdk6 promotes cell cycle reentry and progression through G1 by overriding inhibition by the INK4 family of Cdk inhibitors (CKI)s and titrating the Cip/Kip CKls that attenuate cyclin E-Cdk2. Targeting Cdk4 and Cdk6 may therefore improve the efficacy of cancer therapy in particular during aggressive tumor growth and relapse, but no specific cell cycle-based cancer therapy has been available.

[0026] Multiple myeloma (MM), the second most common hematopoietic cancer, is treatable but invariably fatal. In MM, malignant plasma cells retain the self-renewing potential as opposed to normal plasma cells, which are permanently withdrawn from the cell cycle.In the stable phase of the disease, myeloma cells accumulate in the bone marrow (BM) mainly due to impaired apoptosis. However, they re-enter the cell cycle and proliferate without restraint during relapse and drug resistance. Ultimately, all MM becomes refractory to treatment as current chemotherapies center on empirical cytotoxic killing.

[0027] Multiple lines of evidence suggest that deregulation of Cdk4 and Cdk6 is pivotal to the loss of cell cycle control in MM. Gene targeting and *in vitro* studies first demonstrated that inhibition of Cdk4 and Cdk6 by the physiologic CKI, $p18^{INK4C}$, is required for cell cycle termination during plasma cell differentiation in the immune response. Deletion and inactivation of the INK4a CKI genes in MM cell lines have been reported. Overexpression of cyclin D1 or D3 is frequent in MM, but insufficient to promote cell cycle progression through G1 in primary human BM myeloma cells. Rather, proliferation of primary human BM myeloma cells in vivo is preceded by mutually exclusive co-activation of Cdk4-cyclin 01 or Cdk6-cyclin 02 specific for each case of MM. These results suggest that Cdk4 and Cdk6 are promising targets for cell cycle control in MM.

[0028] PD 0332991 is an orally bioactive, cell-permeable pyridopyrimidine that potently and selectively inhibits Cdk4 and Cdk6 (IC50, 0.01 μM) (Fry et al., Specific Inhibition of Cyclin-dependent Kinase 4/6 by PD 0332991 and Associated Antitumor Activity in Human Tumore Xenografts, Mol. Cancer Ther. 3, 1427-1438, 2004). PD 0332991 has the chemical structure:

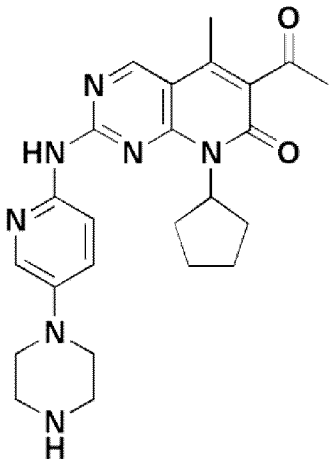

At concentrations specific for inhibition of Cdk4/6 (below 5 μM) PD 0332991 has little or no activity against 42 additional kinases including Cdk2 (Fry et al., 2004), in contrast to other Cdk inhibitors that have been used in clinical trials such as flavopiridol and R-roscovitin. Consistent with observations in solid tumor cell lines in vitro and in xenografts (Fry et al., 2004), inhibition of Cdk4/6 by PD 0332991 (IC50, 0.06 μM) leads to rapid and exclusive G1 arrest unaccompanied by apoptosis in primary BM myeloma cells ex vivo, and profoundly suppresses human myeloma tumor growth in xenografts. Emerging evidence further suggests that PD 0332991 is effective in inhibiting Cdk4/6 in mantle cell lymphoma cells ex vivo and acute myeloid leukemia cells ex vivo and in xenografts. However, as a competitive inhibitor of ATP binding to Cdk4 and Cdk6, PD 0332991 is reversible (Fry et al., 2004). Tumor growth in the myeloma xenografts resumes upon discontinuation of PD 0332991 treatment, suggesting that to optimize targeting Cdk4 and Cdk6 in cancer, a combination therapy is necessary.

[0029] To develop a cell cycle-based combination therapy, it was shown that by inducing synchronously 8 phase entry upon release of PD 03232991-induced G1 block or by prolonging G1 arrest, selective inhibition of Cdk4 and Cdk6 by PD 0332991 not only prevents proliferation but also primes myeloma cells to killing by cytotoxic drugs. These include bortezomib, a reversible 208 proteasome inhibitor effective in treating some but not all cases of myeloma, salinosporamide A (herein the compound of Formula I-16), an irreversible proteasome

inhibitor derived from fermentation of Salinospora which also induces apoptosis in myeloma cells, and dexamethasone, a steroid widely used in cancer therapy. Synergistic killing of tumor cells is rooted in cell cycle-dependent induction of mitochondrial depolarization and caspase activation, which overcomes chemoresistance in primary myeloma cells and induces synergistic tumor repression in xenografts. These findings provide the first evidence that selective targeting of Cdk4 and Cdk6 by PD 0332991 in combination therapy is a promising new mechanism-based therapeutic strategy for multiple myeloma.

[0030] The targeting of Cdk4 and Cdk6 induces synergistic killing by two strategies. First, synchronization of S phase entry enhances preferential killing of cycling MM cells by chemotherapy. BrdU labeling is used to circumvent complication due to cell death. In addition, prolonging G1 arrest primes cells to killing by disrupting the coupling between cellular function and cell cycle. There is no induction of apoptosis by PD 0332991 alone in myeloma cells.

[0031] Whether a cancer cell chooses to die in response to cytotoxic signals depends largely on the interactions between the anti-apoptotic and proapoptotic members of the Bcl-2 protein family (Adams, 2003). There is dynamic regulation of the partnership between anti-apoptotic Bcl-2 family proteins and proapoptotic BH3-only proteins. Noxa opposes the activation of bortezomib. Bim plays an essential role in lymphocyte homeostasis in development and physiologic immune response, in part due to its ability to engage all pro-survival Bcl-2 family proteins. In myeloma cells, Bim and Noxa play central roles in neutralizing the pro-survival function of Mcl-1 and Bcl-2, which are highly expressed and were found to associate with Bim. This synergistically is regulated by the combination therapy at multiple levels – mRNA, Erk, and association with Mcl-1 and Bcl-2 but not Bcl-xl.

[0032] The proapoptotic multidomain-proteins Bax and Bak are critical mediators of apoptosis as cells deficient for both Bax and Bak are resistant to most dead stimuli. Upon activation, Bax and Bak oligomerize and permeabilize the mitochondrial outer membrane allowing the release of cytochrome c and other proapoptotic factors such as Smac into the cytosol (Cory and Adams, 2002). The released cytochrome c binds to procaspase-9 and apoptosis protease-activating factor-1 (Apaf-1) to form an apoptosome complex that induces the autoactivation of caspase-9, initiating activation cascade of apoptosis (Wang, 2001). Bak but not Bax is differentially activated and associated with the membrane. There is a model in which

BH3-only proteins indirectly activate Bax and Bak by antagonizing the guarding of Bax or Bak activation by the pro-survival member of BcI-2 family protein (Willis et aI., 2005 and 2007).

[0033] PD 03232991-based combination therapy can overcome drug resistance and suppress tumor growth. PD 03232991 is orally bioactive and the first potent and specific Cdk4/6 inhibitor. Induction of G1 arrest is more attainable physiologically then cell cycle synchronization. Within the limit of an ex vivo culture system PD 03232991-based combination therapy showed more effectiveness in MM cells isolated from relapsed disease. There was also a conversion of resistance to sensitive by selection of cytotoxic partners which results in a lowering of the threshold of killing in combination therapy.

[0034] In addition to the ex vivo model, there is also an in vivo model lowering the dose. In animal models, PD 03232991 induced G1 arrest due to the decay kinetics of plasma PD 03232991 in mice.

[0035] Cdk4/6 can be targeted in cancer therapy in many cancers.

[0036] Accordingly, in some embodiments, PD 3232991 is administered in combination with a proteasome inhibitor to synergistically treat cancer. In some embodiments, the proteasome inhibitor is a compound of Formula I (e.g., a compound of Formula I-16). In some embodiments, the cancer is a hematological malignancy (e.g., multiple myeloma).

Compounds of Formula I

[0037] In some embodiments, compounds for use as described herein are represented by Formula I:

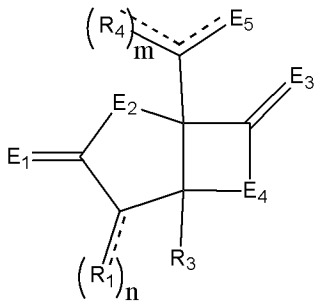

Formula I

[0038] In certain embodiments the substituent(s) R_1, R_3, and R_4 separately may include a hydrogen, a halogen, a mono-substituted, a poly-substituted or an unsubstituted variant of the following residues: saturated C_1-C_{24} alkyl, unsaturated C_2-C_{24} alkenyl or C_2-C_{24} alkynyl, acyl, acyloxy, alkyloxycarbonyloxy, aryloxycarbonyloxy, cycloalkyl, cycloalkenyl, alkoxy,

cycloalkoxy, aryl, heteroaryl, arylalkoxy carbonyl, alkoxy carbonylacyl, amino, aminocarbonyl, aminocarboyloxy, nitro, azido, phenyl, cycloalkylacyl, hydroxy, alkylthio, arylthio, oxysulfonyl, carboxy, cyano, thio, sulfoxide, sulfone, sulfonate esters, thiocyano, boronic acids and esters, and halogenated alkyl including polyhalogenated alkyl. Further, in certain embodiments, each of E_1, E_2, E_3 and E_4 can be a substituted or unsubstituted heteroatom, for example, a heteroatom or substituted heteroatom selected from the group consisting of nitrogen, sulfur and oxygen.

[0039] In some embodiments n can be equal to 1, while in others it can be equal to 2. When n is equal to 2, the substituents can be the same or can be different. Furthermore, in some embodiments R_3 is not a hydrogen. m can be equal to 1 or 2, and when m is equal to 2, R_4 can be the same or different.

[0040] E_5 can be, for example, OH, O, OR_{10}, S, SR_{11}, SO_2R_{11}, NH, NH_2, NOH, NHOH, NR_{12}, and $NHOR_{13}$, wherein $R_{10\text{-}13}$ may separately include, for example, hydrogen, a substituted or unsubstituted of any of the following: alkyl, an aryl, a heteroaryl, and the like. Also, R_1 can be CH_2CH_2X, wherein X can be, for example, H, F, Cl, Br, and I. R_3 can be methyl. Furthermore, R_4 may include a cyclohexyl. Also, each of E_1, E_3 and E_4 can be O and E_2 can be NH. Preferably, R_1 can be CH_2CH_2X, wherein X is selected from the group consisting of H, F, Cl Br, and I; wherein R_4 may include a cyclohexyl; wherein R_3 can be methyl; and wherein each of E_1, E_3 and E_4 separately can be O and E_2 can be NH.

[0041] In some embodiments, R_2 is not cyclohex-2-enyl carbinol when one of the R_1 substituents is ethyl or chloroethyl and R_3 is methyl.

[0042] In some embodiments, preferably R_1 is a substituted or unsubstituted C_1 to C_5 alkyl. For example, methyl, ethyl, propyl, isopropyl, butyl, isobutyl, tert-butyl, and pentyl are preferred. In some embodiments, R_1 is not a substituted or unsubstituted, unbranched C_6 alkyl.

[0043] For example, an exemplary compound of Formula I has the following structure I-1:

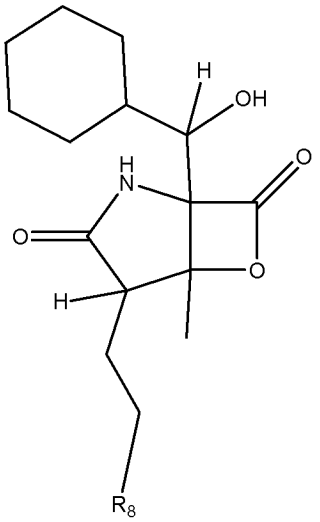

Formula I-1

[0044] R_8 may include, for example, hydrogen, fluorine, chlorine, bromine and iodine.

[0045] Exemplary stereochemistry can be as follows:

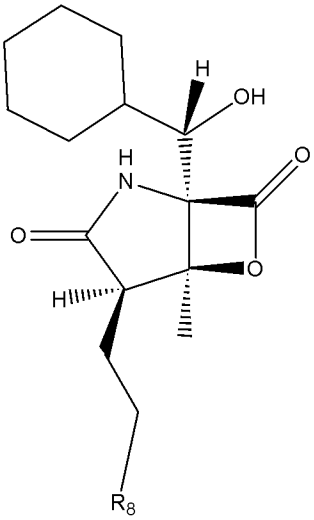

[0046] In preferred embodiments, the compound of Formula I has any of the following structures:

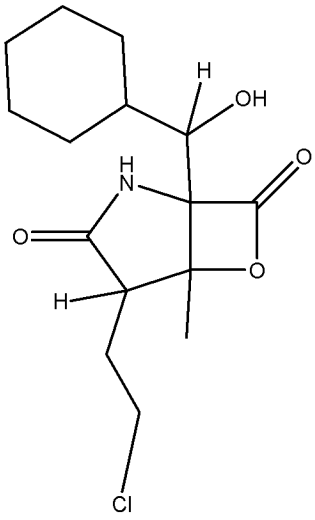

Formula I-2

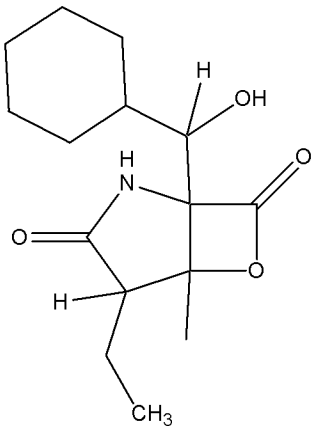

Formula I-3

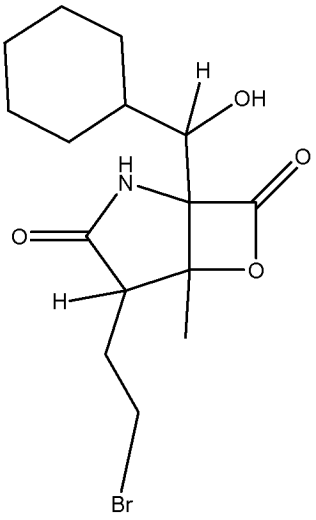

Formula I-4

[0047] The following is exemplary stereochemistry for compounds having the structures I-2, I-3, and I-4, respectively:

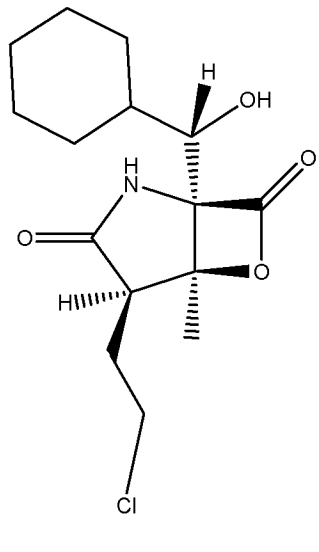

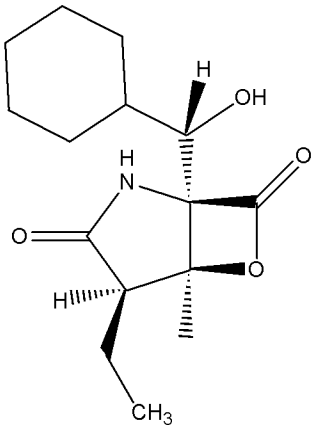

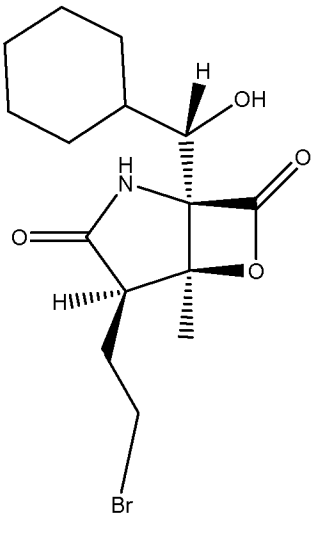

[0048] In other embodiments wherein R_4 may include a 7-oxa-bicyclo[4.1.0]hept-2-yl). An exemplary compound of Formula I is the following structure I-5:

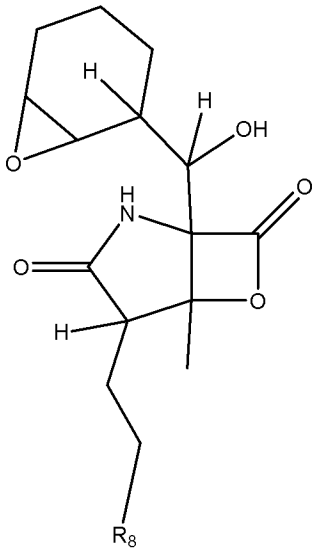

Formula I-5

[0049] R_8 may include, for example, hydrogen, fluorine, chlorine, bromine and iodine.

[0050] The following are examples of compounds having the structure of Formula I-5:

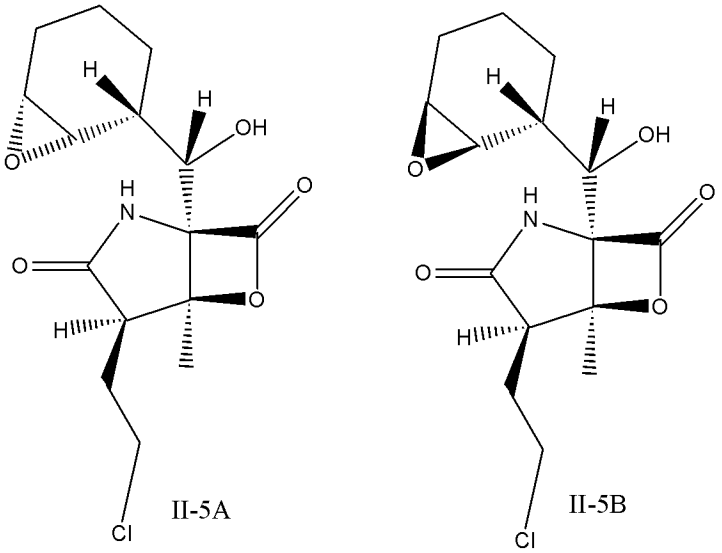

FORMULAE I-5A AND I-5B

[0051] In still further embodiments, at least one R_4 may include a substituted or an unsubstituted branched alkyl. For example, a compound of Formula I can be the following structure I-6:

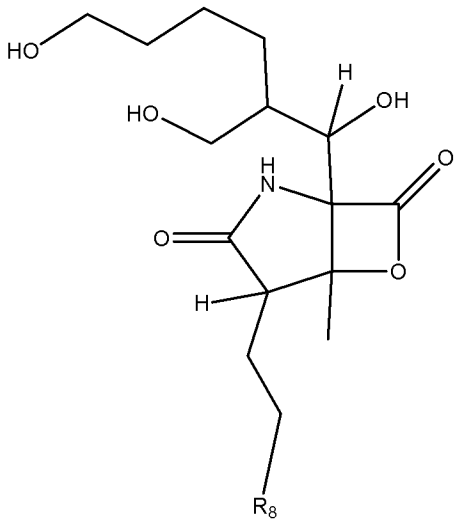

Formula I-6

[0052] R_8 may include, for example, hydrogen, fluorine, chlorine, bromine and iodine.

[0053] The following is exemplary stereochemistry for a compound having the structure of Formula I-6:

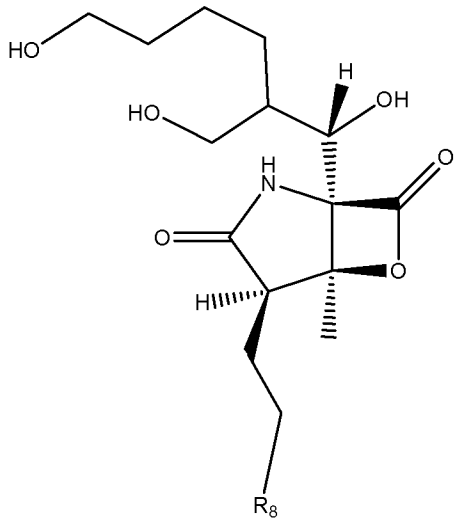

[0054] As another example, the compound of Formula I can be the following structure I-7:

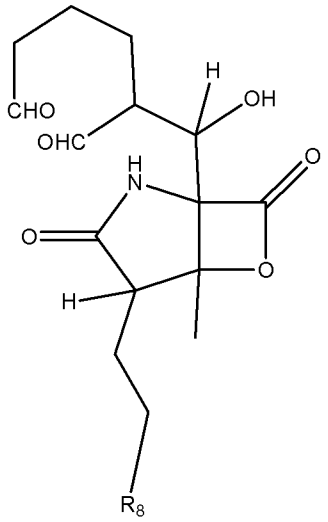

Formula I-7

[0055] R_8 may include, for example, hydrogen, fluorine, chlorine, bromine and iodine.

[0056] The following is exemplary stereochemistry for a compound having the structure of Formula I-7:

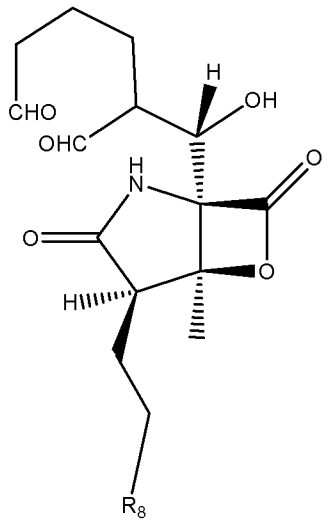

[0057] In other embodiments, at least one R_4 can be a cycloalkyl and E_5 can be an oxygen. An exemplary compound of Formula I can be the following structure I-8:

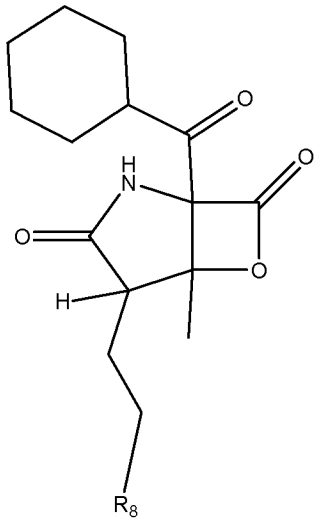

Formula I-8

[0058] R_8 may include, for example, hydrogen (I-8A), fluorine (I-8B), chlorine (I-8C), bromine (I-8D) and iodine (I-8E).

[0059] The following is exemplary stereochemistry for a compound having the structure of Formula I-8:

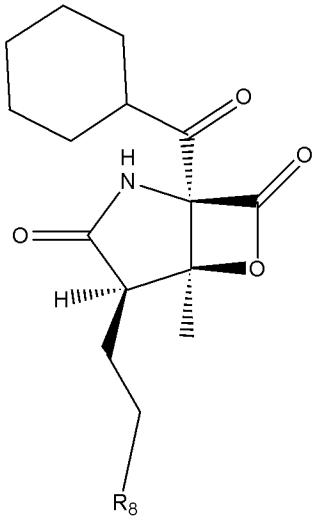

[0060] In some embodiments E5 can be an amine oxide, giving rise to an oxime. An exemplary compound of Formula I has the following structure I-9:

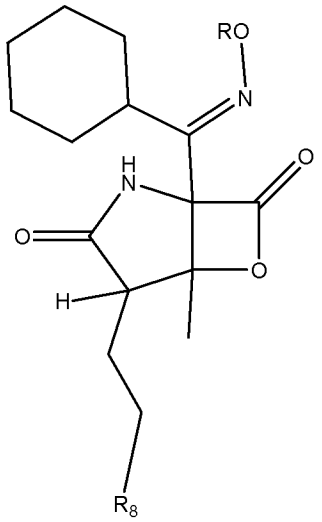

Formula I-9

[0061] R_8 may include, for example, hydrogen, fluorine, chlorine, bromine and iodine; R can be hydrogen, and a substituted or unsubstituted alkyl, aryl, or heteroaryl, and the like.

[0062] The following is exemplary stereochemistry for a compound having the structure of Formula I-9:

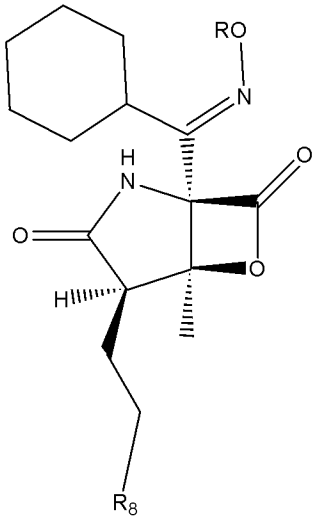

[0063] A further exemplary compound of Formula I has the following structure I-10:

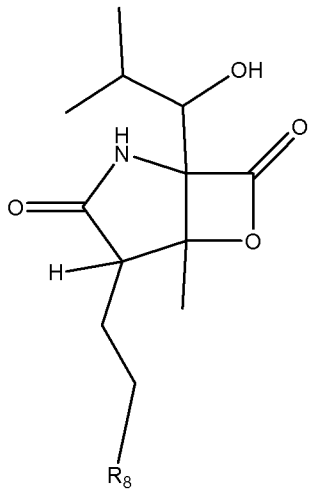

Formula I-10

[0064] R_8 may include, for example, hydrogen, fluorine, chlorine, bromine and iodine.

[0065] The following is exemplary stereochemistry for a compound having the structure of Formula I-10:

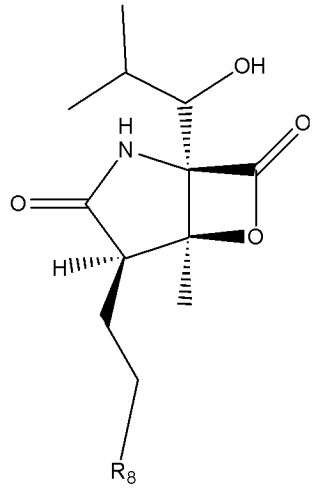

[0066] In some embodiments, E_5 can be NH_2. An exemplary compound of Formula I has the following structure I-11:

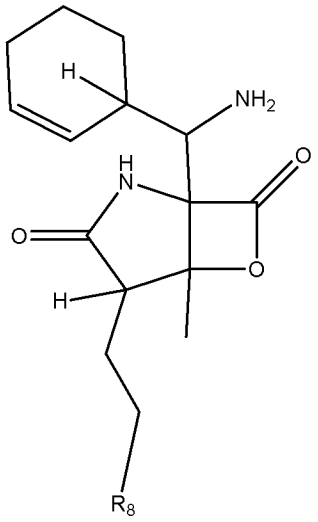

Formula I-11

[0067] R_8 may include, for example, hydrogen, fluorine, chlorine, bromine and iodine.

[0068] The following is exemplary stereochemistry for a compound having the structure of Formula I-11:

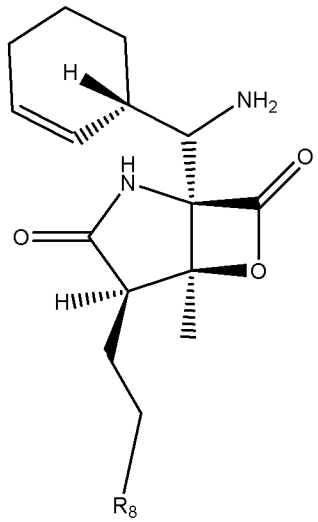

[0069] In some embodiments, at least one R_4 may include a cycloalkyl and E_5 can be NH_2. An exemplary compound of Formula I has the following structure I-12:

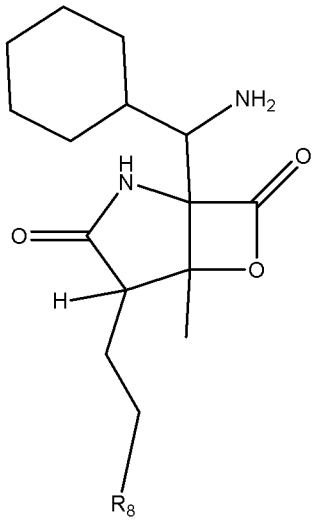

Formula I-12

[0070] R_8 may include, for example, hydrogen, fluorine, chlorine, bromine and iodine.

[0071] The following is exemplary stereochemistry for a compound having the structure of Formula I-12:

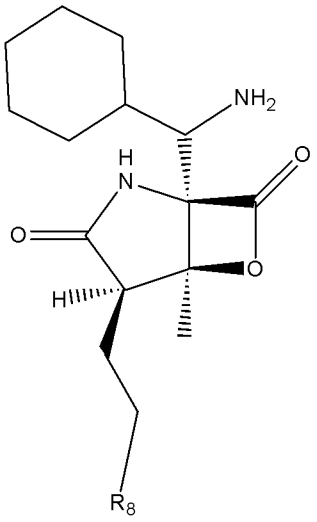

[0072] A further exemplary compound of Formula I has the following structure I-13:

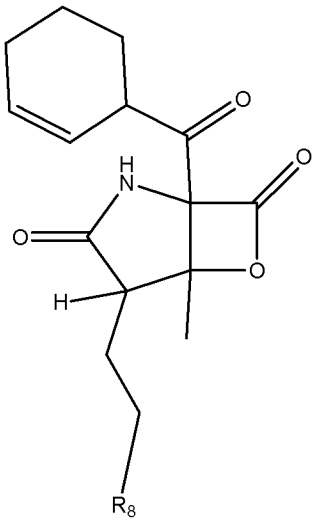

FORMULA I-13

[0073] R_8 may include, for example, hydrogen (I-13A), fluorine (I-13B), chlorine (I-13C), bromine (I-13D) and iodine (I-13E).

[0074] The following is exemplary stereochemistry for a compound having the structure of Formula I-13:

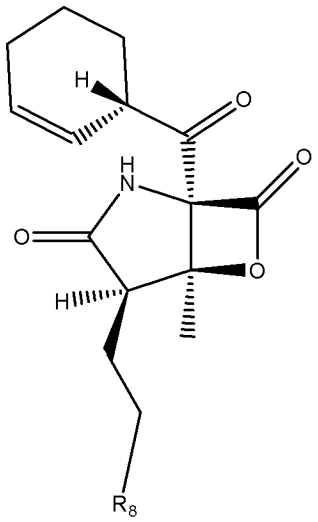

[0075] A still further exemplary compound of Formula I has the following structure I-14:

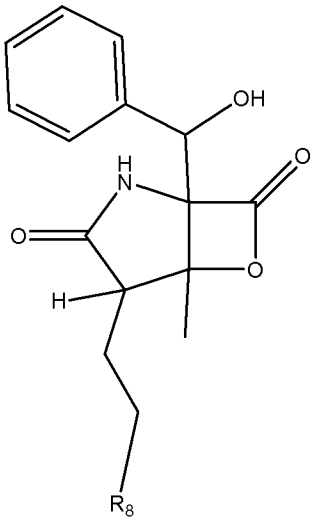

FORMULA I-14

[0076] R_8 may include, for example, hydrogen, fluorine, chlorine, bromine and iodine.

[0077] The following is exemplary stereochemistry for a compound having the structure of Formula I-14:

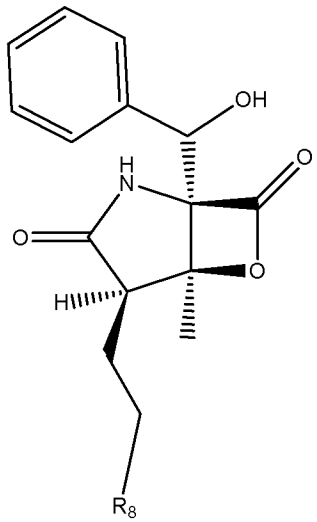

[0078] In some embodiments, the compounds of Formula I, may include as R_4 at least one cycloalkene, for example. Furthermore, in some embodiments, the compounds may

include a hydroxy at E_5, for example. A further exemplary compound of Formula I has the following structure I-15:

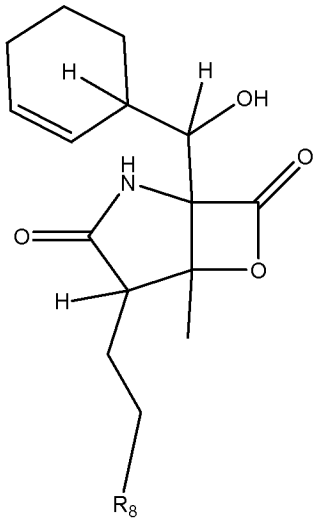

Formula I-15

[0079] R_8 may include, for example, hydrogen, fluorine, chlorine, bromine and iodine.

[0080] Exemplary stereochemistry can be as follows:

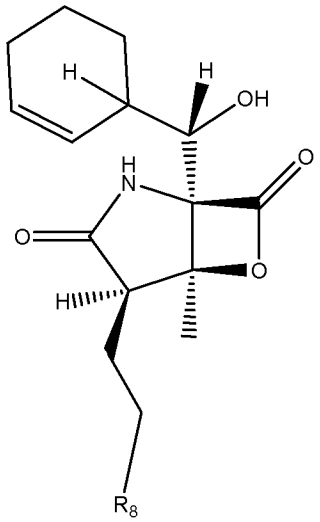

[0081] The following is exemplary stereochemistry for compounds having the structures I-16, I-17, I-18, and I-19, respectively:

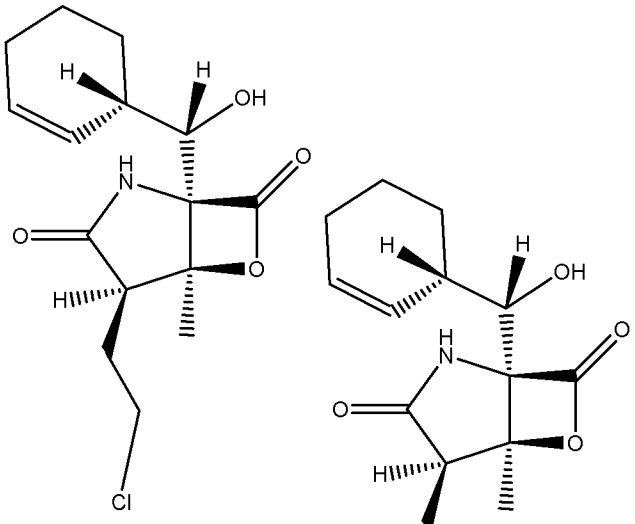

I-16

I-17

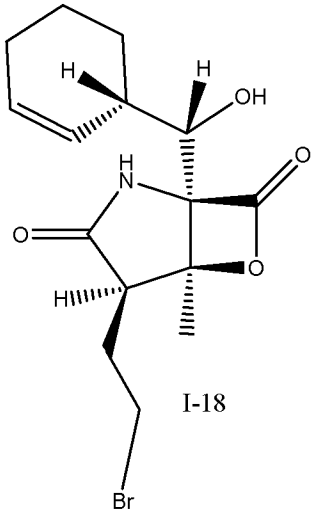

I-18

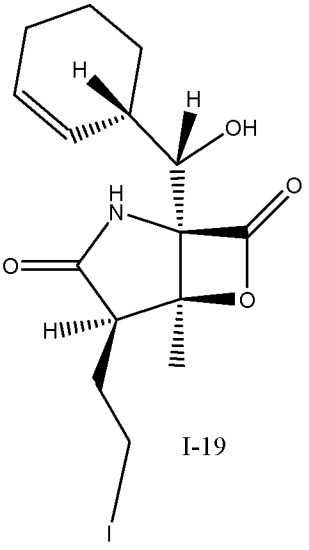

I-19

[0082] The compound of Formula I-16 is also known as salinosporamide A. The compounds of Formulae I-16, I-17, I-18 and I-19 can be obtained by fermentation, synthesis, or semi-synthesis and isolated/purified as set forth below. Furthermore, the compounds of Formulae I-16, I-17, I-18 and I-19 can be used, and are referred to, as "starting materials" to make other compounds described herein.

[0083] In some embodiments, the compounds of Formula I, may include a methyl group as R_1, for example. A further exemplary compound, Formula I-20, has the following structure and stereochemistry:

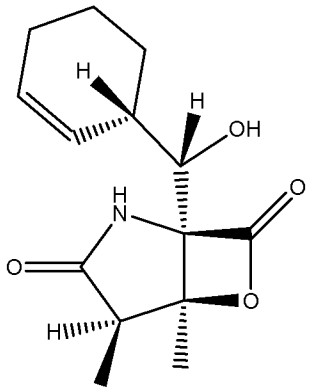

I-20

[0084] In some embodiments, the compounds of Formula I, may include hydroxyethyl as R_1, for example. A further exemplary compound, Formula I-21, has the following structure and stereochemistry:

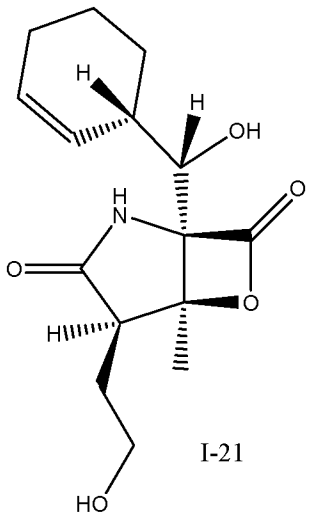

I-21

[0085] In some embodiments, the hydroxyl group of Formula I-21 can be esterified such that R_1 may include ethylpropionate, for example. An exemplary compound, Formula I-22, has the following structure and stereochemistry:

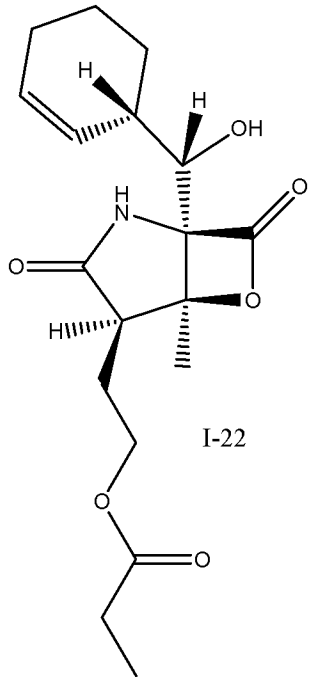

I-22

[0086] In some embodiments, the compounds of Formula I may include an ethyl group as R_3, for example. A further exemplary compound of Formula I has the following structure I-23:

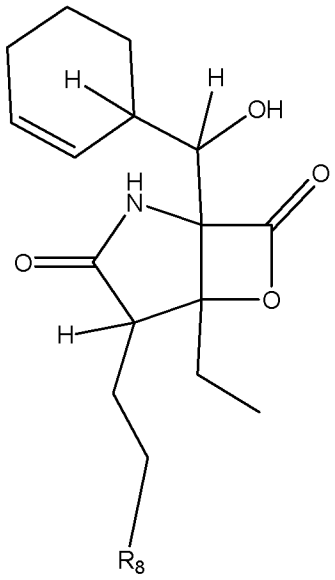

I-23

[0087] R_8 may include, for example, hydrogen, fluorine, chlorine, bromine and iodine. Exemplary stereochemistry can be as follows:

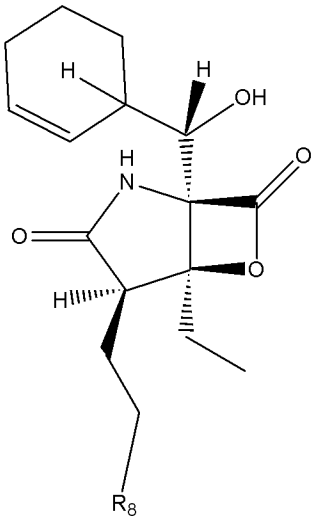

[0088] In some embodiments, the compounds of Formula I-23 may have the following structure and stereochemistry, exemplified by Formula I-24C, where R_8 is chlorine:

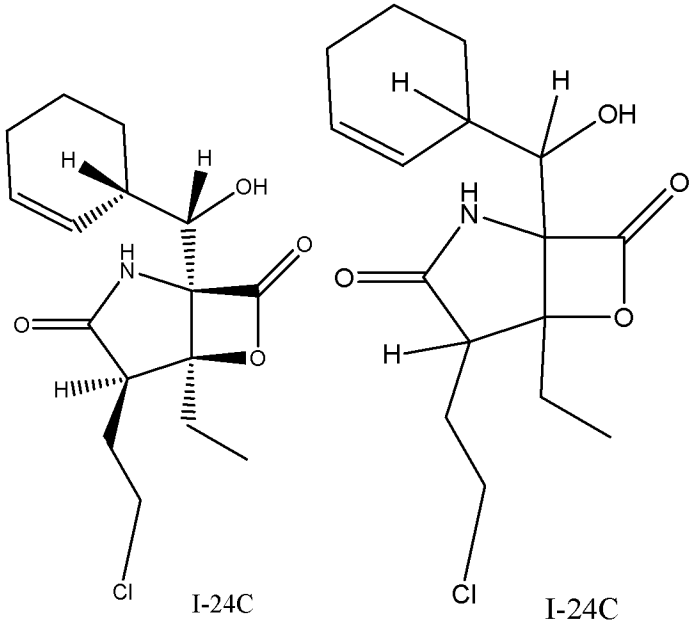

I-24C I-24C

[0089] In some embodiments, the compounds of Formula I-15 may have the following stereochemistry, exemplified by the compound of Formula I-25, where R_8 is chlorine:

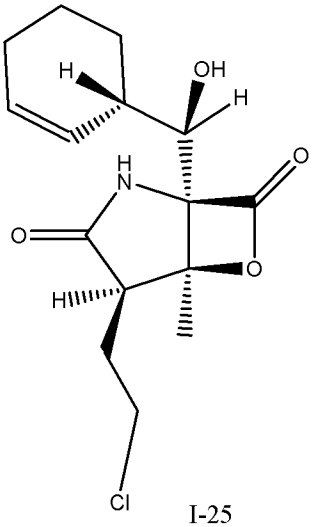

I-25

[0090] In some embodiments, the compound of Formula I-15 may have the following stereochemistry, exemplified by the compound of Formula I-26, where R_8 is chlorine:

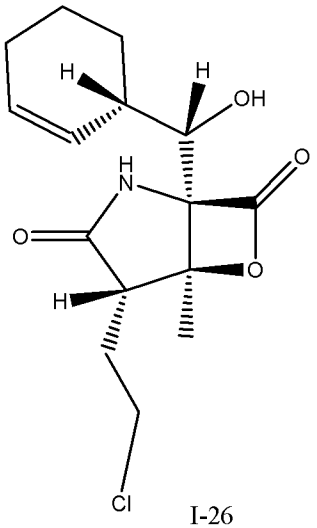

I-26

[0091] In some embodiments, the compound of Formula I may have the following structure and stereochemistry, exemplified by Formula I-27, where R_1 is ethyl:

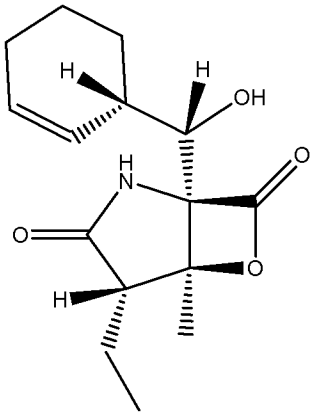

I-27

[0092] In some embodiments, the compound of Formula I may have the following structure and stereochemistry, exemplified by Formula I-28, where R_1 is methyl:

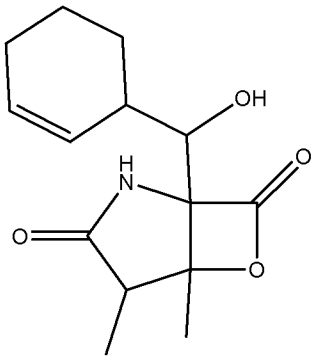

I-28

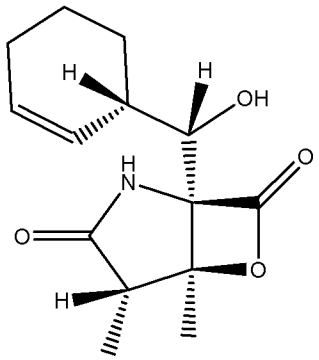

I-28

[0093] In some embodiments, the compounds of Formula I may include azidoethyl as R_1, for example. A further exemplary compound, Formula I-29, has the following structure and stereochemistry:

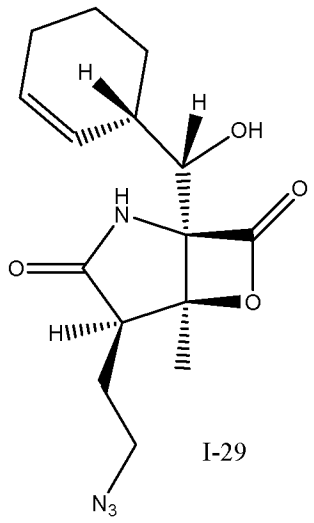

I-29

[0094] In some embodiments, the compounds of Formula I may include propyl as R_1, for example. A further exemplary compound, Formula I-30, has the following structure and stereochemistry:

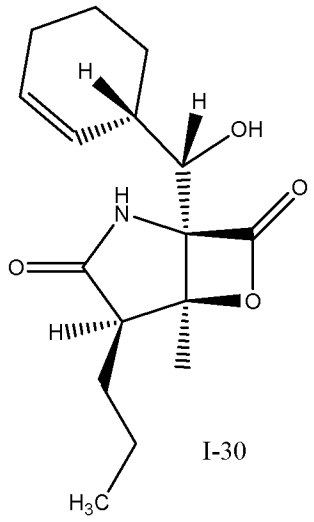

I-30

[0095] Still further exemplary compounds, Formulae I-31 and I-32, have the following structure and stereochemistry:

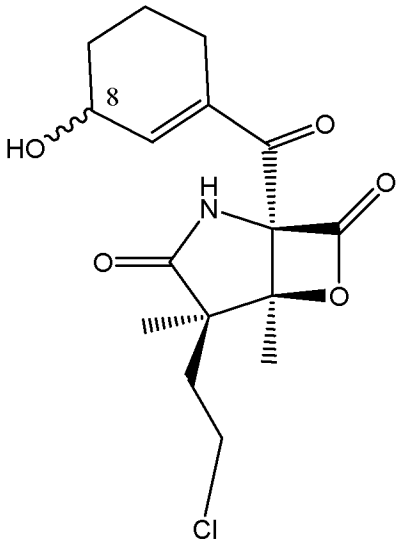

Formula I-31 and I-32

[0096] Other exemplary compounds, Formulae I-33, I-34, I-35 and I-36, have the following structure and stereochemistry:

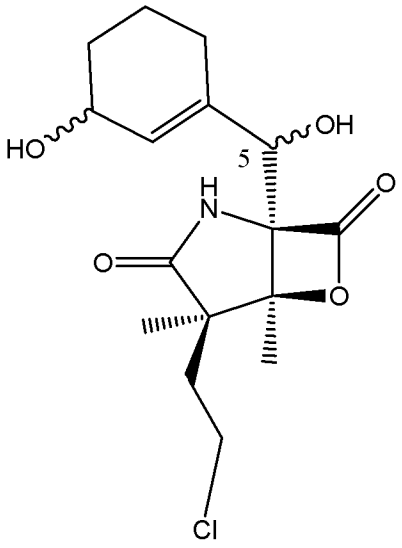

Formula I-33 – I-36

[0097] In some embodiments, the compound of Formula I may include cyanoethyl as R_1; for example, the compound of Formula I-37 has the following structure and stereochemistry:

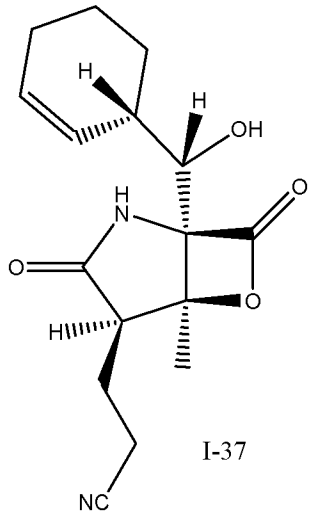

I-37

[0098] In another embodiment, the compound of Formula I may include ethylthiocyanate as R_1; for example, the compound of Formula I-38 has the following structure and stereochemistry:

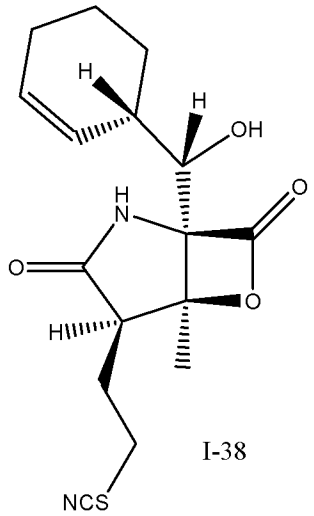

I-38

[0099] In some embodiments, the compounds of Formula I may include a thiol as R_1, for example. A further exemplary compound, Formula I-39, has the following structure and stereochemistry, where R= H, alkyl, aryl, or substituted alkyl or aryl:

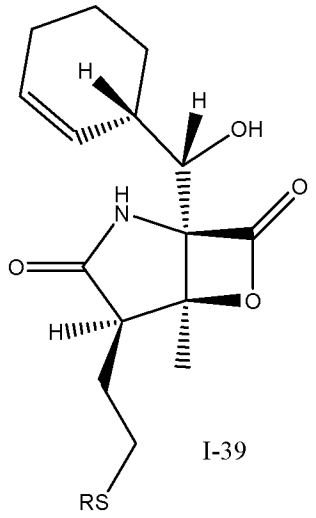

I-39

[0100] In a further exemplary compound, the sulfur of the compound of Formula I-39 can be oxidized to a sulfoxide (n=1) or sulfone (n=2), for example, as in the compound of Formula I-40:

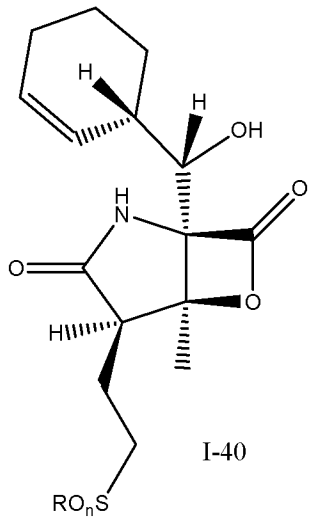

I-40

[0101] In some embodiments, the substituent R_1 of the compound of Formula I may include a leaving group, for example, a halogen, as in compounds I-18 or I-19, or another leaving group, such as a sulfonate ester. One example is the methane sulfonate (mesylate) of Formulae I-41A:

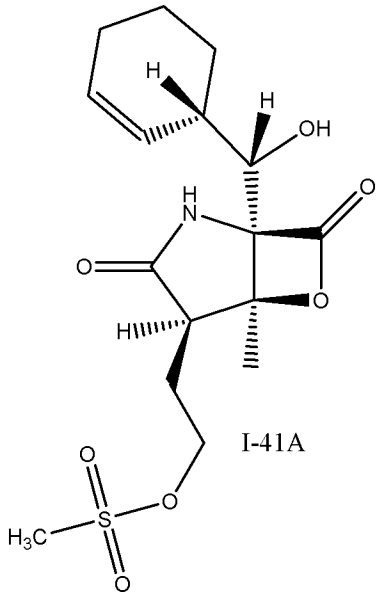

I-41A

[0102] Another embodiment is the tosylate of Formula I-41B

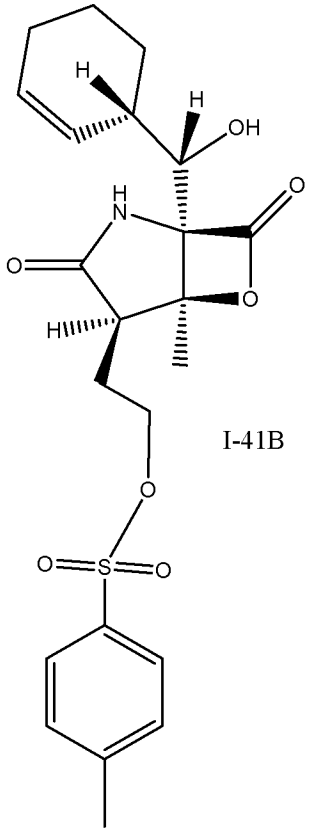

I-41B

[0103] In some embodiments, the substituent R_1 of the compound of Formula I may include electron acceptors. The electron acceptor can be, for example, a Lewis acid, such as a boronic acid or ester. An exemplary compound, Formula I-42, has the following structure and

stereochemistry, where n = 0, 1, 2, 3, 4, 5, or 6, for example, and where R=H or alkyl, for example:

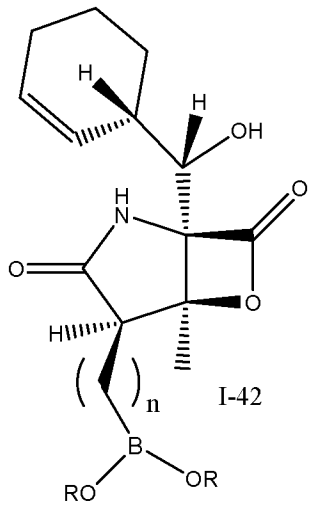

I-42

[0104] Further exemplary compounds of Formula I-42 are the compounds of Formula I-42A, where n=2 and R=H, and the compound of Formula I-42B, where n=1 and R=H:

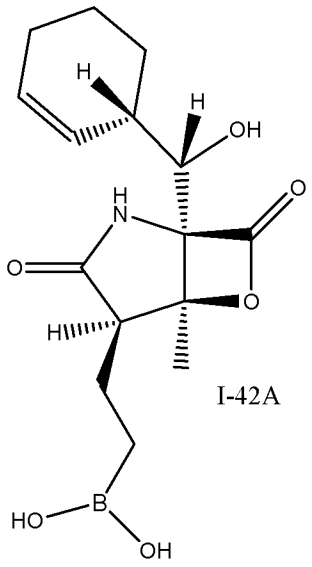

I-42A

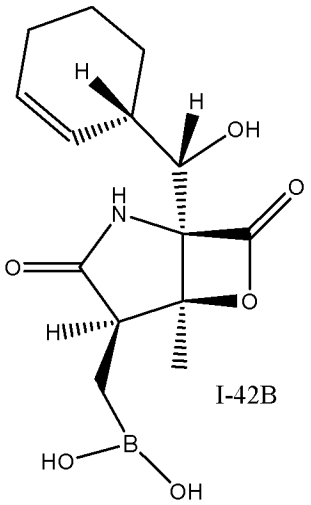

I-42B

[0105] In some embodiments where the substituent R_1 of the compound of Formula I includes an electron acceptor, the electron acceptor can be, for example, a Michael acceptor. An exemplary compound, Formula I-43 has the following structure, where n = 0, 1, 2, 3, 4, 5, 6, and

where Z is an electron withdrawing group, for example, CHO, COR, COOR, $CONH_2$, CN, NO_2, SOR, SO_2R, etc:

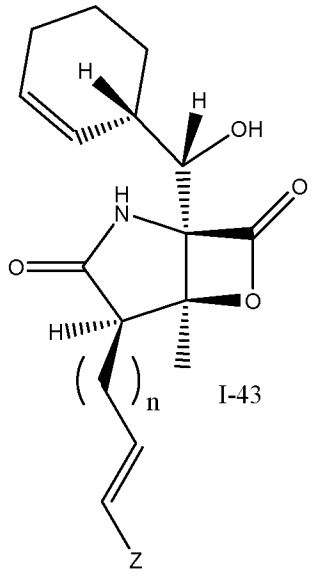

I-43

[0106] A further exemplary compound of Formula I-43 is the compound of Formula I-43A, where n=1 and $Z=CO_2CH_3$:

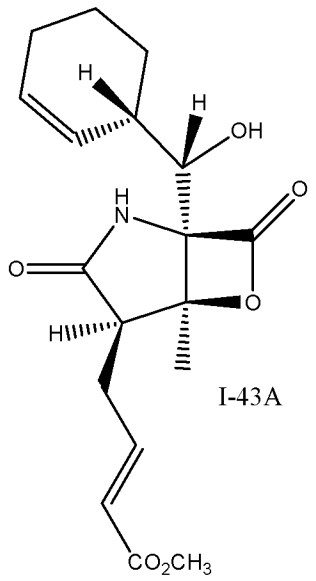

I-43A

[0107] In some embodiments, the compounds can be prodrug esters or thioesters of the compounds of Formula I. For example, the compound of Formula I-44 (a prodrug thioester of the compound of Formula I-16) has the following structure and stereochemistry:

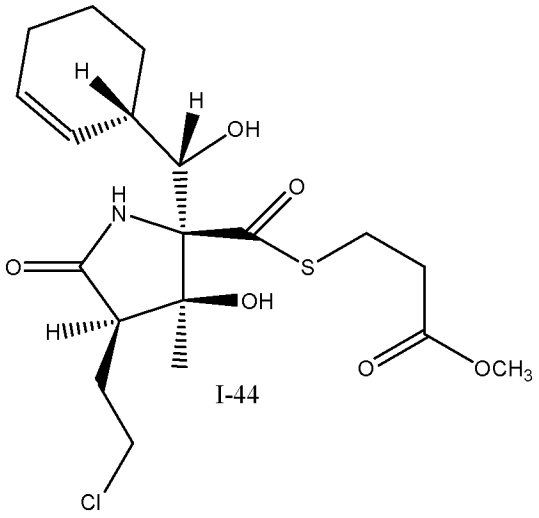

I-44

[0108] In some embodiments, the compounds of Formula I may include an alkenyl group as R_1, for example, ethylenyl. A further exemplary compound, Formula I-46, has the following structure and stereochemistry:

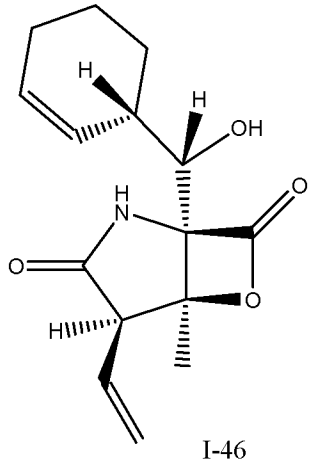

I-46

[0109] In some embodiments, the compounds can be prodrug esters or thioesters of the compounds of Formula I. For example, the compound of Formula I-47 (a prodrug thioester of the compound of Formula I-17) has the following structure and stereochemistry:

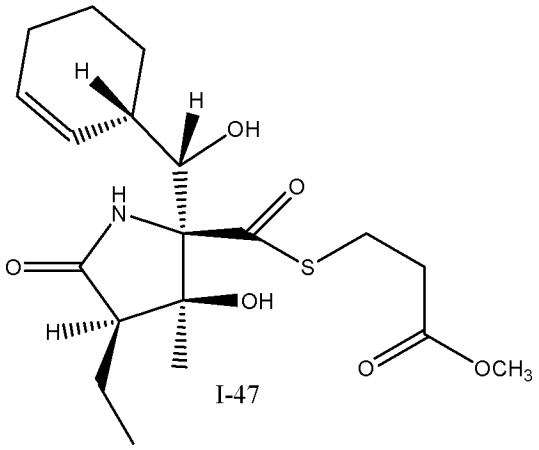

I-47

[0110] In some embodiments, the compounds can be prodrug esters or thioesters of the compounds of Formula I. For example, the compound of Formula I-48 has the following structure and stereochemistry:

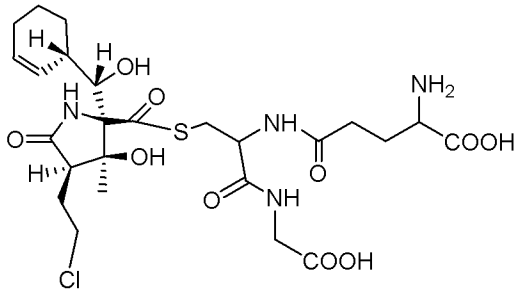

I-48

[0111] Other exemplary compound, Formula I-49 has the following structure and stereochemistry:

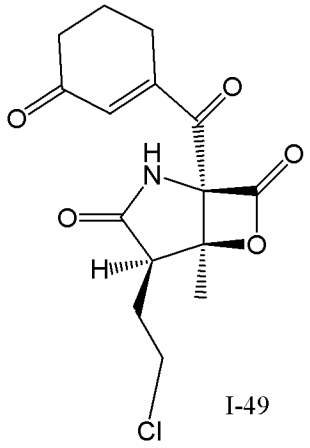

I-49

[0112] In some embodiments, the compound can be prodrug ester or thioester of the compounds of Formula I. For example, the compound of Formula I-50 (prodrug ester of the compound of Formula I-16) has the following structure and stereochemistry:

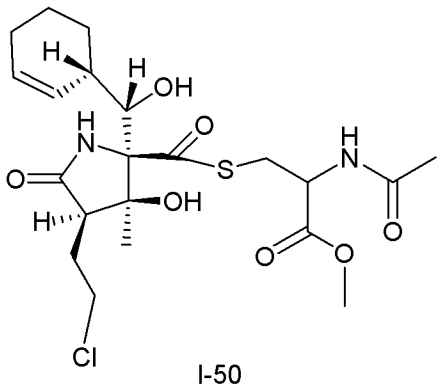

I-50

[0113] Certain embodiments also provide pharmaceutically acceptable salts and pro-drug esters or throesters of the compound of Formulae I, and provide methods of obtaining and purifying such compounds by the methods disclosed herein.

[0114] The term "pro-drug ester," especially when referring to a pro-drug ester of the compound of Formula I synthesized by the methods disclosed herein, refers to a chemical derivative of the compound that is rapidly transformed *in vivo* to yield the compound, for example, by hydrolysis in blood or inside tissues. The term "pro-drug ester" refers to derivatives of the compounds disclosed herein formed by the addition of any of several ester- or thioester-forming groups that are hydrolyzed under physiological conditions. Examples of pro-drug ester groups include pivoyloxymethyl, acetoxymethyl, phthalidyl, indanyl and methoxymethyl, as well as other such groups known in the art, including a (5-R-2-oxo-1,3-dioxolen-4-yl)methyl group. Other prodrugs can be prepared by preparing a corresponding thioester of the compound, for example, by reacting with an appropriate thiol, such as thiophenol, Cysteine or derivatives thereof, or propanethiol, for example. Other examples of pro-drug ester groups can be found in, for example, T. Higuchi and V. Stella, in "Pro-drugs as Novel Delivery Systems", Vol. 14, A.C.S. Symposium Series, American Chemical Society (1975); and "Bioreversible Carriers in Drug Design: Theory and Application", edited by E. B. Roche, Pergamon Press: New York, 14-21 (1987) (providing examples of esters useful as prodrugs for compounds containing carboxyl groups). Each of the above-mentioned references is hereby incorporated by reference in its entirety.

[0115] The term "pharmaceutically acceptable salt," as used herein, and particularly when referring to a pharmaceutically acceptable salt of a compound, including Formulae I, and Formula I as produced and synthesized by the methods disclosed herein, refers to any pharmaceutically acceptable salts of a compound, and preferably refers to an acid addition salt of a compound. Preferred examples of pharmaceutically acceptable salt are the alkali metal salts (sodium or potassium), the alkaline earth metal salts (calcium or magnesium), or ammonium salts derived from ammonia or from pharmaceutically acceptable organic amines, for example C_1-C_7 alkylamine, cyclohexylamine, triethanolamine, ethylenediamine or tris-(hydroxymethyl)-aminomethane. With respect to compounds synthesized by the method of this embodiment that are basic amines, the preferred examples of pharmaceutically acceptable salts are acid addition salts of pharmaceutically acceptable inorganic or organic acids, for example, hydrohalic, sulfuric, phosphoric acid or aliphatic or aromatic carboxylic or sulfonic acid, for example acetic, succinic, lactic, malic, tartaric, citric, ascorbic, nicotinic, methanesulfonic, p-toluensulfonic or naphthalenesulfonic acid.

[0116] Preferred pharmaceutical compositions disclosed herein include pharmaceutically acceptable salts and pro-drug esters of the compound of Formulae I obtained and purified by the methods disclosed herein. Accordingly, if the manufacture of pharmaceutical formulations involves intimate mixing of the pharmaceutical excipients and the active ingredient in its salt form, then it is preferred to use pharmaceutical excipients which are non-basic, that is, either acidic or neutral excipients.

[0117] It will be also appreciated that the phrase "compounds and compositions comprising the compound," or any like phrase, is meant to encompass compounds in any suitable form for pharmaceutical delivery, as discussed in further detail herein. For example, in certain embodiments, the compounds or compositions comprising the same may include a pharmaceutically acceptable salt of the compound.

[0118] The term "halogen atom," as used herein, means any one of the radio-stable atoms of column 7 of the Periodic Table of the Elements, *i.e.*, fluorine, chlorine, bromine, or iodine, with bromine and chlorine being preferred.

[0119] The term "alkyl," as used herein, means any unbranched or branched, substituted or unsubstituted, saturated hydrocarbon, with C_1-C_{24} preferred, and C_1-C_6 hydrocarbons being preferred, with methyl, ethyl, propyl, isopropyl, butyl, isobutyl, and tert-

butyl, and pentyl being most preferred. Among the substituted, saturated hydrocarbons, C_1-C_{24} are preferred, with C_1-C_6 mono- and di- and per-halogen substituted saturated hydrocarbons and amino-substituted hydrocarbons more preferred.

[0120] The term "substituted" has its ordinary meaning, as found in numerous contemporary patents from the related art. See, for example, U.S. Patent Nos. 6,509,331; 6,506,787; 6,500,825; 5,922,683; 5,886,210; 5,874,443; and 6,350,759; all of which are incorporated herein in their entireties by reference. Specifically, the definition of substituted is as broad as that provided in U.S. Patent No. 6,509,331, which defines the term "substituted alkyl" such that it refers to an alkyl group, preferably of from 1 to 10 carbon atoms, having from 1 to 5 substituents, and preferably 1 to 3 substituents, selected from the group consisting of alkoxy, substituted alkoxy, cycloalkyl, substituted cycloalkyl, cycloalkenyl, substituted cycloalkenyl, acyl, acylamino, acyloxy, amino, substituted amino, aminoacyl, aminoacyloxy, oxyacylamino, cyano, halogen, hydroxyl, carboxyl, carboxylalkyl, keto, thioketo, thiol, thioalkoxy, substituted thioalkoxy, thiocyanate, aryl, aryloxy, heteroaryl, heteroaryloxy, heterocyclic, heterocyclooxy, hydroxyamino, alkoxyamino, nitro, azido, boronric acid, boronic ester --SO-alkyl, --SO-substituted alkyl, --SO-aryl, --SO-heteroaryl, --SO_2-alkyl, --SO_2-substituted alkyl, --SO_2-aryl, --SO_2-heteroaryl, --OSO-alkyl, --OSO-substituted alkyl, --OSO-aryl, --OSO-heteroaryl, --OSO_2-alkyl, --OSO_2-substituted alkyl, --OSO_2-aryl, and --OSO_2-heteroaryl. The other above-listed patents also provide standard definitions for the term "substituted" that are well-understood by those of skill in the art.

[0121] The term "cycloalkyl" refers to any non-aromatic hydrocarbon ring, preferably having five to twelve atoms comprising the ring. The term "acyl" refers to alkyl or aryl groups derived from an oxoacid, with an acetyl group being preferred.

[0122] The term "alkenyl," as used herein, means any unbranched or branched, substituted or unsubstituted, unsaturated hydrocarbon including polyunsaturated hydrocarbons, with C_1-C_6 unbranched, mono-unsaturated and di-unsaturated, unsubstituted hydrocarbons being preferred, and mono-unsaturated, di-halogen substituted hydrocarbons being most preferred. The term "cycloalkenyl" refers to any non-aromatic hydrocarbon ring, preferably having five to twelve atoms comprising the ring.

[0123] The terms "aryl," "substituted aryl," "heteroaryl," and "substituted heteroaryl," as used herein, refer to aromatic hydrocarbon rings, preferably having five, six, or

seven atoms, and most preferably having six atoms comprising the ring. "Heteroaryl" and "substituted heteroaryl," refer to aromatic hydrocarbon rings in which at least one heteroatom, *e.g.*, oxygen, sulfur, or nitrogen atom, is in the ring along with at least one carbon atom. The term "heterocycle" or "heterocyclic" refer to any cyclic compound containing one or more heteroatoms. The substituted aryls, heterocycles and heteroaryls can be substituted with any substituent, including those described above and those known in the art.

[0124] The term "alkoxy" refers to any unbranched, or branched, substituted or unsubstituted, saturated or unsaturated ether, with C_1-C_6 unbranched, saturated, unsubstituted ethers being preferred, with methoxy being preferred, and also with dimethyl, diethyl, methyl-isobutyl, and methyl-tert-butyl ethers also being preferred. The term "cycloalkoxy" refers to any non-aromatic hydrocarbon ring, preferably having five to twelve atoms comprising the ring. The term "alkoxy carbonyl" refers to any linear, branched, cyclic, saturated, unsaturated, aliphatic or aromatic alkoxy attached to a carbonyl group. The examples include methoxycarbonyl group, ethoxycarbonyl group, propyloxycarbonyl group, isopropyloxycarbonyl group, butoxycarbonyl group, sec-butoxycarbonyl group, tert-butoxycarbonyl group, cyclopentyloxycarbonyl group, cyclohexyloxycarbonyl group, benzyloxycarbonyl group, allyloxycarbonyl group, phenyloxycarbonyl group, pyridyloxycarbonyl group, and the like.

[0125] The terms "pure," "purified," "substantially purified," and "isolated" as used herein refer to the compound of the embodiment being free of other, dissimilar compounds with which the compound, if found in its natural state, would be associated in its natural state. In certain embodiments described as "pure," "purified," "substantially purified," or "isolated" herein, the compound may comprise at least 0.5%, 1%, 5%, 10%, or 20%, and most preferably at least 50% or 75% of the mass, by weight, of a given sample.

[0126] The terms "derivative," "variant," or other similar term refers to a compound that is an analog of the other compound.

[0127] Certain of the compounds of Formula I can be obtained and purified or can be obtained via semi-synthesis from purified compounds as set forth herein. Generally, without being limited thereto, the compounds of Formula I-15, preferably, Formulae I-16, I-17, I-18 and I-19, can be obtained synthetically or by fermentation. Exemplary fermentation procedures are provided below. Further, the compounds of Formula I-15, preferably, Formulae I-16, I-17, I-18

and I-19 can be used as starting compounds in order to obtain/synthesize various of the other compounds described herein. Exemplary non-limiting syntheses are provided herein.

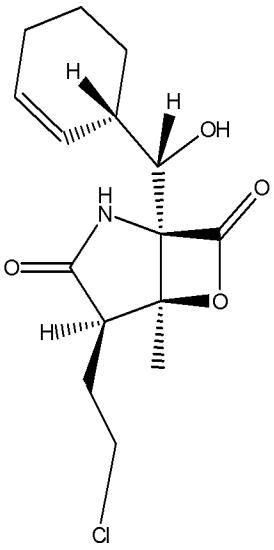

Formula I-16

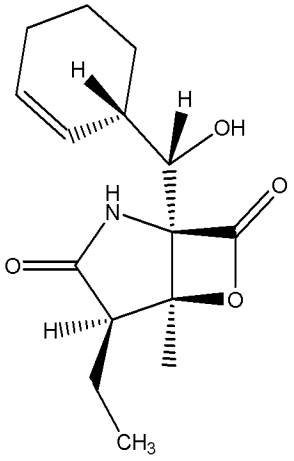

Formula I-17

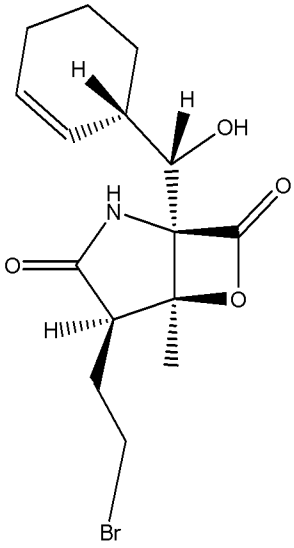

Formula I-18

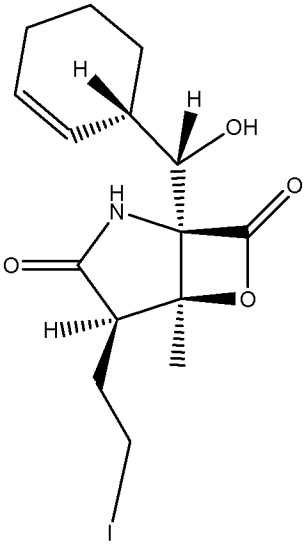

Formula I-19

[0128] Formula I-16 may be produced through a high-yield saline fermentation (~350 - 400 mg/L) and modifications of the conditions have yielded new analogs in the fermentation extracts. Additional analogs can be generated through directed biosynthesis. Directed biosynthesis is the modification of a natural product by adding biosynthetic precursor analogs to the fermentation of producing microorganisms (Lam, *et al.*, *J Antibiot (Tokyo)* 44:934 (1991),

Lam, *et al.*, *J Antibiot (Tokyo)* 54:1 (2001); which is hereby incorporated by reference in its entirety).

[0129] Exposing the producing culture to analogs of acetic acid, phenylalanine, valine, butyric acid, shikimic acid, and halogens, preferably, other than chlorine, can lead to the formation of new analogs. The new analogs produced can be easily detected in crude extracts by HPLC and LC-MS. For example, after manipulating the medium with different concentrations of sodium bromide, a bromo-analog, Formula I-18, was successfully produced in shake-flask culture at a titer of 14 mg/L.

[0130] A second approach to generate analogs is through biotransformation. Biotransformation reactions are chemical reactions catalyzed by enzymes or whole cells containing these enzymes. Zaks, A., *Curr Opin Chem Biol* 5:130 (2001). Microbial natural products are ideal substrates for biotransformation reactions as they are synthesized by a series of enzymatic reactions inside microbial cells. Riva, S., *Curr Opin Chem Biol* 5:106 (2001).

[0131] Given the structure of the described compounds, including those of Formula I-15, for example, the possible biosynthetic origins are acetyl-CoA, ethylmalonyl-CoA, phenylalanine and chlorine. Ethylmalonyl-CoA is derived from butyryl-CoA, which can be derived either from valine or crotonyl-CoA. Liu, *et al.*, *Metab Eng* 3:40 (2001). Phenylalanine is derived from shikimic acid.

[0132] Alternatively, compositions such as Formula I-16 and its analogs may be produced synthetically, e.g., such as described in United States Application Serial No. 11/697,689, which is incorporated by reference in its entirety.

Production of Compounds of Formulae I-16, I-17, I-18, I-20, I-24C, I-26, I-27 and I-28

[0133] The production of compounds of Formulae I-16, I-17, I-18, I-20,I-24C, I-26, I-27 and I-28 can be carried out by cultivating strain CNB476 and strain NPS21184, a natural variant of strain CNB476, in a suitable nutrient medium under conditions described herein, preferably under submerged aerobic conditions, until a substantial amount of compounds are detected in the fermentation; harvesting by extracting the active components from the fermentation broth with a suitable solvent; concentrating the solvent containing the desired components; then subjecting the concentrated material to chromatographic separation to isolate the compounds from other metabolites also present in the cultivation medium.

[0134] The culture (CNB476) was deposited on June 20, 2003 with the American Type Culture Collection (ATCC) in Rockville, MD and assigned the ATCC patent deposition number PTA-5275. Strain NPS21184, a natural variant of strain CNB476, was derived from strain CNB476 as a single colony isolate. Strain NPS21184 has been deposited to ATCC on April 27, 2005. The ATCC deposit meets all of the requirements of the Budapest treaty. The culture is also maintained at and available from Nereus Pharmaceutical Culture Collection at 10480 Wateridge Circle, San Diego, CA 92121. In addition to the specific microorganism described herein, it should be understood that mutants, such as those produced by the use of chemical or physical mutagens including X-rays, etc. and organisms whose genetic makeup has been modified by molecular biology techniques, may also be cultivated to produce the starting compounds of Formulae I-16, I-17, and I-18.

Fermentation of strain CNB476 and strain NPS21184

[0135] Production of compounds can be achieved at temperature conducive to satisfactory growth of the producing organism, e.g. from 16 degree C to 40 degree C, but it is preferable to conduct the fermentation at 22 degree C to 32 degree C. The aqueous medium can be incubated for a period of time necessary to complete the production of compounds as monitored by high pressure liquid chromatography (HPLC), preferably for a period of about 2 to 10 days, on a rotary shaker operating at about 50 rpm to 400 rpm, preferably at 150 rpm to 250 rpm, for example. The production of the compounds can also be achieved by cultivating the production strain in a bioreactor, such as a fermentor system that is suitable for the growth of the production strain.

[0136] Growth of the microorganisms can be achieved by one of ordinary skill of the art by the use of appropriate medium. Broadly, the sources of carbon include glucose, fructose, mannose, maltose, galactose, mannitol and glycerol, other sugars and sugar alcohols, starches and other carbohydrates, or carbohydrate derivatives such as dextran, cerelose, as well as complex nutrients such as oat flour, corn meal, millet, corn, and the like. The exact quantity of the carbon source that is utilized in the medium will depend in part, upon the other ingredients in the medium, but an amount of carbohydrate between 0.5 to 25 percent by weight of the medium can be satisfactorily used, for example. These carbon sources can be used individually or several

such carbon sources can be combined in the same medium, for example. Certain carbon sources are preferred as hereinafter set forth.

[0137] The sources of nitrogen include amino acids such as glycine, arginine, threonine, methionine and the like, ammonium salt, as well as complex sources such as yeast extracts, corn steep liquors, distiller solubles, soybean meal, cotttonseed meal, fish meal, peptone, and the like. The various sources of nitrogen can be used alone or in combination in amounts ranging from 0.5 to 25 percent by weight of the medium, for example.

[0149] Among the nutrient inorganic salts, which can be incorporated in the culture media, are the customary salts capable of yielding sodium, potassium, magnesium, calcium, phosphate, sulfate, chloride, carbonate, and like ions. Also included are trace metals such as cobalt, manganese, iron, molybdenum, zinc, cadmium, and the like.

Pharmaceutical Compositions

[0138] In one embodiment, the compounds disclosed herein are used in pharmaceutical compositions. The compounds preferably can be produced by the methods disclosed herein. The compounds can be used, for example, in pharmaceutical compositions comprising a pharmaceutically acceptable carrier prepared for storage and subsequent administration. Also, embodiments relate to a pharmaceutically effective amount of the products and compounds disclosed above in a pharmaceutically acceptable carrier or diluent. Acceptable carriers or diluents for therapeutic use are well known in the pharmaceutical art, and are described, for example, in Remington's Pharmaceutical Sciences, Mack Publishing Co. (A.R. Gennaro edit. 1985), which is incorporated herein by reference in its entirety. Preservatives, stabilizers, dyes and even flavoring agents can be provided in the pharmaceutical composition. For example, sodium benzoate, ascorbic acid and esters of p-hydroxybenzoic acid can be added as preservatives. In addition, antioxidants and suspending agents can be used.

[0139] The compositions can be formulated and used as tablets, capsules, or elixirs for oral administration; suppositories for rectal administration; sterile solutions, suspensions for injectable administration; patches for transdermal administration, and sub-dermal deposits and the like. Injectables can be prepared in conventional forms, either as liquid solutions or suspensions, solid forms suitable for solution or suspension in liquid prior to injection, or as emulsions. Suitable excipients are, for example, water, saline, dextrose, mannitol, lactose, lecithin, albumin, sodium glutamate, cysteine hydrochloride, and the like. In addition, if desired,

the injectable pharmaceutical compositions may contain minor amounts of nontoxic auxiliary substances, such as wetting agents, pH buffering agents, and the like. If desired, absorption enhancing preparations (for example, liposomes), can be utilized.

[0140] Pharmaceutical formulations for parenteral administration include aqueous solutions of the active compounds in water-soluble form. Additionally, suspensions of the active compounds can be prepared as appropriate oily injection suspensions. Suitable lipophilic solvents or vehicles include fatty oils such as sesame oil, or other organic oils such as soybean, grapefruit or almond oils, or synthetic fatty acid esters, such as ethyl oleate or triglycerides, or liposomes. Aqueous injection suspensions may contain substances that increase the viscosity of the suspension, such as sodium carboxymethyl cellulose, sorbitol, or dextran. Optionally, the suspension may also contain suitable stabilizers or agents that increase the solubility of the compounds to allow for the preparation of highly concentrated solutions.

[0141] Pharmaceutical preparations for oral use can be obtained by combining the active compounds with solid excipient, optionally grinding a resulting mixture, and processing the mixture of granules, after adding suitable auxiliaries, if desired, to obtain tablets or dragee cores. Suitable excipients are, in particular, fillers such as sugars, including lactose, sucrose, mannitol, or sorbitol; cellulose preparations such as, for example, maize starch, wheat starch, rice starch, potato starch, gelatin, gum tragacanth, methyl cellulose, hydroxypropylmethyl-cellulose, sodium carboxymethylcellulose, and/or polyvinylpyrrolidone (PVP). If desired, disintegrating agents can be added, such as the cross-linked polyvinyl pyrrolidone, agar, or alginic acid or a salt thereof such as sodium alginate. Dragee cores are provided with suitable coatings. For this purpose, concentrated sugar solutions can be used, which may optionally contain gum arabic, talc, polyvinyl pyrrolidone, carbopol gel, polyethylene glycol, and/or titanium dioxide, lacquer solutions, and suitable organic solvents or solvent mixtures. Dyestuffs or pigments can be added to the tablets or dragee coatings for identification or to characterize different combinations of active compound doses. For this purpose, concentrated sugar solutions can be used, which may optionally contain gum arabic, talc, polyvinyl pyrrolidone, carbopol gel, polyethylene glycol, and/or titanium dioxide, lacquer solutions, and suitable organic solvents or solvent mixtures. Dyestuffs or pigments can be added to the tablets or dragee coatings for identification or to characterize different combinations of active compound doses. Such formulations can be made using methods known in the art (see, for example, U.S. Patent Nos. 5,733,888 (injectable

compositions); 5,726,181 (poorly water soluble compounds); 5,707,641 (therapeutically active proteins or peptides); 5,667,809 (lipophilic agents); 5,576,012 (solubilizing polymeric agents); 5,707,615 (anti-viral formulations); 5,683,676 (particulate medicaments); 5,654,286 (topical formulations); 5,688,529 (oral suspensions); 5,445,829 (extended release formulations); 5,653,987 (liquid formulations); 5,641,515 (controlled release formulations) and 5,601,845 (spheroid formulations); all of which are incorporated herein by reference in their entireties.

[0142] Further disclosed herein are various pharmaceutical compositions well known in the pharmaceutical art for uses that include topical, intraocular, intranasal, and intraauricular delivery. Pharmaceutical formulations include aqueous ophthalmic solutions of the active compounds in water-soluble form, such as eyedrops, or in gellan gum (Shedden et al., *Clin. Ther.*, 23(3):440-50 (2001)) or hydrogels (Mayer et al., *Ophthalmologica*, 210(2):101-3 (1996)); ophthalmic ointments; ophthalmic suspensions, such as microparticulates, drug-containing small polymeric particles that are suspended in a liquid carrier medium (Joshi, A. 1994 *J Ocul Pharmacol* **10**:29-45), lipid-soluble formulations (Alm et al., *Prog. Clin. Biol. Res.*, 312:447-58 (1989)), and microspheres (Mordenti, *Toxicol. Sci.*, 52(1):101-6 (1999)); and ocular inserts. All of the above-mentioned references, are incorporated herein by reference in their entireties. Such suitable pharmaceutical formulations are most often and preferably formulated to be sterile, isotonic and buffered for stability and comfort. Pharmaceutical compositions may also include drops and sprays often prepared to simulate in many respects nasal secretions to ensure maintenance of normal ciliary action. As disclosed in Remington's Pharmaceutical Sciences (Mack Publishing, 18th Edition), which is incorporated herein by reference in its entirety, and well-known to those skilled in the art, suitable formulations are most often and preferably isotonic, slightly buffered to maintain a pH of 5.5 to 6.5, and most often and preferably include anti-microbial preservatives and appropriate drug stabilizers. Pharmaceutical formulations for intraauricular delivery include suspensions and ointments for topical application in the ear. Common solvents for such aural formulations include glycerin and water.

[0143] When used as an anti-cancer compound, for example, the compounds of Formulae I or compositions including Formulae I can be administered by either oral or non-oral pathways. When administered orally, it can be administered in capsule, tablet, granule, spray, syrup, or other such form. When administered non-orally, it can be administered as an aqueous suspension, an oily preparation or the like or as a drip, suppository, salve, ointment or the like,

when administered via injection, subcutaneously, intraperitoneally, intravenously, intramuscularly, or the like.

[0144] In one embodiment, the anti-cancer agent can be mixed with additional substances to enhance their effectiveness.

Methods of Administration

[0145] In an alternative embodiment, the disclosed chemical compounds and the disclosed pharmaceutical compositions are administered by a particular method as an anti-microbial. Such methods include, among others, (a) administration though oral pathways, which administration includes administration in capsule, tablet, granule, spray, syrup, or other such forms; (b) administration through non-oral pathways, which administration includes administration as an aqueous suspension, an oily preparation or the like or as a drip, suppository, salve, ointment or the like; administration via injection, subcutaneously, intraperitoneally, intravenously, intramuscularly, intradermally, or the like; as well as (c) administration topically, (d) administration rectally, or (e) administration vaginally, as deemed appropriate by those of skill in the art for bringing the compound of the present embodiment into contact with living tissue; and (f) administration via controlled released formulations, depot formulations, and infusion pump delivery. As further examples of such modes of administration and as further disclosure of modes of administration, disclosed herein are various methods for administration of the disclosed chemical compounds and pharmaceutical compositions including modes of administration through intraocular, intranasal, and intraauricular pathways.

[0146] The pharmaceutically effective amount of the compositions that include the described compounds required as a dose will depend on the route of administration, the type of animal, including human, being treated, and the physical characteristics of the specific animal under consideration. The dose can be tailored to achieve a desired effect, but will depend on such factors as weight, diet, concurrent medication and other factors which those skilled in the medical arts will recognize.

[0147] In practicing the methods of the embodiment, the products or compositions can be used alone or in combination with one another, or in combination with other therapeutic or diagnostic agents. These products can be utilized *in vivo*, ordinarily in a mammal, preferably in a human, or *in vitro*. In employing them *in vivo*, the products or compositions can be

administered to the mammal in a variety of ways, including parenterally, intravenously, subcutaneously, intramuscularly, colonically, rectally, vaginally, nasally or intraperitoneally, employing a variety of dosage forms. Such methods may also be applied to testing chemical activity *in vivo*.

[0148] As will be readily apparent to one skilled in the art, the useful *in vivo* dosage to be administered and the particular mode of administration will vary depending upon the age, weight and mammalian species treated, the particular compounds employed, and the specific use for which these compounds are employed. The determination of effective dosage levels, that is the dosage levels necessary to achieve the desired result, can be accomplished by one skilled in the art using routine pharmacological methods. Typically, human clinical applications of products are commenced at lower dosage levels, with dosage level being increased until the desired effect is achieved. Alternatively, acceptable *in vitro* studies can be used to establish useful doses and routes of administration of the compositions identified by the present methods using established pharmacological methods.

[0149] In non-human animal studies, applications of potential products are commenced at higher dosage levels, with dosage being decreased until the desired effect is no longer achieved or adverse side effects disappear. The dosage may range broadly, depending upon the desired affects and the therapeutic indication. Typically, dosages can be between about 10 microgram/kg and 100 mg/kg body weight, preferably between about 100 microgram/kg and 10 mg/kg body weight. Alternatively dosages can be based and calculated upon the surface area of the patient, as understood by those of skill in the art. Administration is preferably oral on a daily or twice daily basis.

[0150] The exact formulation, route of administration and dosage can be chosen by the individual physician in view of the patient's condition. *See* for example, Fingl *et al.*, in The Pharmacological Basis of Therapeutics, 1975, which is incorporated herein by reference in its entirety. It should be noted that the attending physician would know how to and when to terminate, interrupt, or adjust administration due to toxicity, or to organ dysfunctions. Conversely, the attending physician would also know to adjust treatment to higher levels if the clinical response were not adequate (precluding toxicity). The magnitude of an administrated dose in the management of the disorder of interest will vary with the severity of the condition to be treated and to the route of administration. The severity of the condition may, for example, be

evaluated, in part, by standard prognostic evaluation methods. Further, the dose and perhaps dose frequency, will also vary according to the age, body weight, and response of the individual patient. A program comparable to that discussed above can be used in veterinary medicine.

[0151] Depending on the specific conditions being treated, such agents can be formulated and administered systemically or locally. A variety of techniques for formulation and administration can be found in Remington's Pharmaceutical Sciences, 18th Ed., Mack Publishing Co., Easton, PA (1990), which is incorporated herein by reference in its entirety. Suitable administration routes may include oral, rectal, transdermal, vaginal, transmucosal, or intestinal administration; parenteral delivery, including intramuscular, subcutaneous, intramedullary injections, as well as intrathecal, direct intraventricular, intravenous, intraperitoneal, intranasal, or intraocular injections.

[0152] For injection, the agents of the embodiment can be formulated in aqueous solutions, preferably in physiologically compatible buffers such as Hanks' solution, Ringer's solution, or physiological saline buffer. For such transmucosal administration, penetrants appropriate to the barrier to be permeated are used in the formulation. Such penetrants are generally known in the art. Use of pharmaceutically acceptable carriers to formulate the compounds herein disclosed for the practice of the embodiment into dosages suitable for systemic administration is within the scope of the embodiment. With proper choice of carrier and suitable manufacturing practice, the compositions disclosed herein, in particular, those formulated as solutions, can be administered parenterally, such as by intravenous injection. The compounds can be formulated readily using pharmaceutically acceptable carriers well known in the art into dosages suitable for oral administration. Such carriers enable the compounds of the embodiment to be formulated as tablets, pills, capsules, liquids, gels, syrups, slurries, suspensions and the like, for oral ingestion by a patient to be treated.

[0153] Agents intended to be administered intracellularly can be administered using techniques well known to those of ordinary skill in the art. For example, such agents can be encapsulated into liposomes, then administered as described above. All molecules present in an aqueous solution at the time of liposome formation are incorporated into the aqueous interior. The liposomal contents are both protected from the external micro-environment and, because liposomes fuse with cell membranes, are efficiently delivered into the cell cytoplasm.

Additionally, due to their hydrophobicity, small organic molecules can be directly administered intracellularly.

[0154] Determination of the effective amounts is well within the capability of those skilled in the art, especially in light of the detailed disclosure provided herein. In addition to the active ingredients, these pharmaceutical compositions may contain suitable pharmaceutically acceptable carriers comprising excipients and auxiliaries which facilitate processing of the active compounds into preparations which can be used pharmaceutically. The preparations formulated for oral administration can be in the form of tablets, dragees, capsules, or solutions. The pharmaceutical compositions can be manufactured in a manner that is itself known, for example, by means of conventional mixing, dissolving, granulating, dragee-making, levitating, emulsifying, encapsulating, entrapping, or lyophilizing processes.

[0155] Compounds disclosed herein can be evaluated for efficacy and toxicity using known methods. For example, the toxicology of a particular compound, or of a subset of the compounds, sharing certain chemical moieties, can be established by determining *in vitro* toxicity towards a cell line, such as a mammalian, and preferably human, cell line. The results of such studies are often predictive of toxicity in animals, such as mammals, or more specifically, humans. Alternatively, the toxicity of particular compounds in an animal model, such as mice, rats, rabbits, dogs or monkeys, can be determined using known methods. The efficacy of a particular compound can be established using several art recognized methods, such as *in vitro* methods, animal models, or human clinical trials. Art-recognized *in vitro* models exist for nearly every class of condition, including the conditions abated by the compounds disclosed herein, including cancer, cardiovascular disease, and various immune dysfunction, and infectious diseases. Similarly, acceptable animal models can be used to establish efficacy of chemicals to treat such conditions. When selecting a model to determine efficacy, the skilled artisan can be guided by the state of the art to choose an appropriate model, dose, and route of administration, and regime. Of course, human clinical trials can also be used to determine the efficacy of a compound in humans.

[0156] When used as an anti-cancer agent, the compounds disclosed herein can be administered by either oral or a non-oral pathways. When administered orally, it can be administered in capsule, tablet, granule, spray, syrup, or other such form. When administered non-orally, it can be administered as an aqueous suspension, an oily preparation or the like or as

a drip, suppository, salve, ointment or the like, when administered via injection, subcutaneously, intraperitoneally, intravenously, intramuscularly, intradermally, or the like. Controlled release formulations, depot formulations, and infusion pump delivery are similarly contemplated.

[0157] The compositions disclosed herein in pharmaceutical compositions may also comprise a pharmaceutically acceptable carrier. Such compositions can be prepared for storage and for subsequent administration. Acceptable carriers or diluents for therapeutic use are well known in the pharmaceutical art, and are described, for example, in Remington's Pharmaceutical Sciences, Mack Publishing Co. (A.R. Gennaro edit. 1985). For example, such compositions can be formulated and used as tablets, capsules or solutions for oral administration; suppositories for rectal or vaginal administration; sterile solutions or suspensions for injectable administration. Injectables can be prepared in conventional forms, either as liquid solutions or suspensions, solid forms suitable for solution or suspension in liquid prior to injection, or as emulsions. Suitable excipients include, but are not limited to, saline, dextrose, mannitol, lactose, lecithin, albumin, sodium glutamate, cysteine hydrochloride, and the like. In addition, if desired, the injectable pharmaceutical compositions may contain minor amounts of nontoxic auxiliary substances, such as wetting agents, pH buffering agents, and the like. If desired, absorption enhancing preparations (for example, liposomes), can be utilized.

[0158] The pharmaceutically effective amount of the composition required as a dose will depend on the route of administration, the type of animal being treated, and the physical characteristics of the specific animal under consideration. The dose can be tailored to achieve a desired effect, but will depend on such factors as weight, diet, concurrent medication and other factors which those skilled in the medical arts will recognize.

[0159] The products or compositions of the embodiment, as described above, can be used alone or in combination with one another, or in combination with other therapeutic or diagnostic agents. These products can be utilized *in vivo* or *in vitro*. The useful dosages and the most useful modes of administration will vary depending upon the age, weight and animal treated, the particular compounds employed, and the specific use for which these composition or compositions are employed. The magnitude of a dose in the management or treatment for a particular disorder will vary with the severity of the condition to be treated and to the route of administration, and depending on the disease conditions and their severity, the compositions can be formulated and administered either systemically or locally. A variety of techniques for

formulation and administration can be found in Remington's Pharmaceutical Sciences, 18th ed., Mack Publishing Co., Easton, PA (1990).

[0160] To formulate the compounds of Formulae I as an anti-cancer agent, known surface active agents, excipients, smoothing agents, suspension agents and pharmaceutically acceptable film-forming substances and coating assistants, and the like can be used. Preferably alcohols, esters, sulfated aliphatic alcohols, and the like can be used as surface active agents; sucrose, glucose, lactose, starch, crystallized cellulose, mannitol, light anhydrous silicate, magnesium aluminate, magnesium methasilicate aluminate, synthetic aluminum silicate, calcium carbonate, sodium acid carbonate, calcium hydrogen phosphate, calcium carboxymethyl cellulose, and the like can be used as excipients; magnesium stearate, talc, hardened oil and the like can be used as smoothing agents; coconut oil, olive oil, sesame oil, peanut oil, soya can be used as suspension agents or lubricants; cellulose acetate phthalate as a derivative of a carbohydrate such as cellulose or sugar, or methylacetate-methacrylate copolymer as a derivative of polyvinyl can be used as suspension agents; and plasticizers such as ester phthalates and the like can be used as suspension agents. In addition to the foregoing preferred ingredients, sweeteners, fragrances, colorants, preservatives and the like can be added to the administered formulation of the compound produced by the method of the embodiment, particularly when the compound is to be administered orally.

[0161] The compounds and compositions can be orally or non-orally administered to a human patient in the amount of about 0.001 mg/kg/day to about 10,000 mg/kg/day of the active ingredient, and more preferably about 0.1 mg/kg/day to about 100 mg/kg/day of the active ingredient at, preferably, one time per day or, less preferably, over two to about ten times per day. Alternatively and also preferably, the compound produced by the method of the embodiment may preferably be administered in the stated amounts continuously by, for example, an intravenous drip. Thus, for the example of a patient weighing 70 kilograms, the preferred daily dose of the active ingredient would be about 0.07 mg/day to about 700 gm/day, and more preferable, 7 mg/day to about 7 grams/day. Nonetheless, as will be understood by those of skill in the art, in certain situations it can be necessary to administer the anti-cancer compound of the embodiment in amounts that excess, or even far exceed, the above-stated, preferred dosage range to effectively and aggressively treat particularly advanced cancerss or infections.

[0162] In the case of using the cancer produced by methods of the embodiment as a biochemical test reagent, the compound produced by methods of the embodiment inhibits the progression of the disease when it is dissolved in an organic solvent or hydrous organic solvent and it is directly applied to any of various cultured cell systems. Usable organic solvents include, for example, methanol, methylsulfoxide, and the like. The formulation can, for example, be a powder, granular or other solid inhibitor, or a liquid inhibitor prepared using an organic solvent or a hydrous organic solvent. While a preferred concentration of the compound produced by the method of the embodiment for use as an anticancer compound is generally in the range of about 1 to about 100 μg/ml, the most appropriate use amount varies depending on the type of cultured cell system and the purpose of use, as will be appreciated by persons of ordinary skill in the art. Also, in certain applications it can be necessary or preferred to persons of ordinary skill in the art to use an amount outside the foregoing range.

[0163] In one embodiment, the method of using a compound as an anti-cancer involves administering an effective amount of any of the compounds of Formulae I or compositions of those compounds. In a preferred embodiment, the method involves administering the compound represented by Formula I, to a patient in need of an anti-cancer agent, until the need is effectively reduced or more preferably removed.

[0164] As will be understood by one of skill in the art, "need" is not an absolute term and merely implies that the patient can benefit from the treatment of the anti-cancer agent in use. By "patient" what is meant is an organism that can benefit by the use of an anti-cancer agent. For example, any organism with cancer, such as, WM. In one embodiment, the patient's health may not require that an anti-cancer agent be administered, however, the patient may still obtain some benefit by the reduction of the level of cancer cells present in the patient, and thus be in need. In one embodiment, the anti- anti-cancer agent is effective against one type of cancer, but not against other types; thus, allowing a high degree of selectivity in the treatment of the patient. In choosing such an anti-cancer agent, the methods and results disclosed in the Examples can be useful. In still further embodiments, the anti-cancer agent is effective against a broad spectrum of cancers or all cancers. Examples of cancers, against which the compounds can be effective include WM, a colorectal carcinoma, a prostate carcinoma, a breast adenocarcinoma, a non-small cell lung carcinoma, an ovarian carcinoma, multiple myelomas, a melanoma, and the like.

[0165] "Therapeutically effective amount," "pharmaceutically effective amount," or similar term, means that amount of drug or pharmaceutical agent that will result in a biological or medical response of a cell, tissue, system, animal, or human that is being sought. In a preferred embodiment, the medical response is one sought by a researcher, veterinarian, medical doctor, or other clinician.

[0166] "Anti-cancer agent" refers to a compound or composition including the compound that reduces the likelihood of survival of a cancer cell. In one embodiment, the likelihood of survival is determined as a function of an individual cancer cell; thus, the anti-cancer agent will increase the chance that an individual cancer cell will die. In one embodiment, the likelihood of survival is determined as a function of a population of cancer cells; thus, the anti-cancer agent will increase the chances that there will be a decrease in the population of cancer cells. In one embodiment, anti-cancer agent means chemotherapeutic agent or other similar term.

[0167] A "chemotherapeutic agent" is a chemical compound useful in the treatment of a neoplastic disease, such as cancer. Examples of chemotherapeutic agents include alkylating agents, such as a nitrogen mustard, an ethyleneimine and a methylmelamine, an alkyl sulfonate, a nitrosourea, and a triazene, folic acid antagonists, anti-metabolites of nucleic acid metabolism, antibiotics, pyrimidine analogs, 5-fluorouracil, cisplatin, purine nucleosides, amines, amino acids, triazol nucleosides, corticosteroids, a natural product such as a vinca alkaloid, an epipodophyllotoxin, an antibiotic, an enzyme, a taxane, and a biological response modifier or antibodies to biological response modifiers or other agents; miscellaneous agents such as a platinum coordination complex, an anthracenedione, an anthracycline, a substituted urea, a methyl hydrazine derivative, or an adrenocortical suppressant; or a hormone or an antagonist such as an adrenocorticosteroid, a progestin, an estrogen, an antiestrogen, an androgen, an antiandrogen, or a gouadotropin-releasing hormone analog. Specific examples include Adriamycin, Doxorubicin, 5-Fluorouracil, Cytosine arabinoside ("Ara-C"), Cyclophosphamide, Thiotepa, Busulfan, Cytoxin, Taxol, Toxotere, Methotrexate, Cisplatin, Melphalan, Vinblastine, Bleomycin, Etoposide, Ifosfamide, Mitomycin C, Mitoxantrone, Vincreistine, Vinorelbine, Carboplatin, Teniposide, Daunomycin, Carminomycin, Aminopterin, Dactinomycin, Mitomycins, Esperamicins, Melphalan, and other related nitrogen mustards. Also included in

this definition are hormonal agents that act to regulate or inhibit hormone action on tumors, such as tamoxifen and onapristone.

[0168] The anti-cancer agent may act directly upon a cancer cell to kill the cell, induce death of the cell, to prevent division of the cell, and the like. Alternatively, the anti-cancer agent may indirectly act upon the cancer cell by limiting nutrient or blood supply to the cell, for example. Such anti-cancer agents are capable of destroying or suppressing the growth or reproduction of cancer cells, such as a colorectal carcinoma, a prostate carcinoma, a breast adenocarcinoma, a non-small cell lung carcinoma, an ovarian carcinoma, multiple myelomas, a melanoma, and the like.

[0169] In one embodiment, a described compound, preferably a compound having the Formulae I, including those as described herein, is considered an effective anti-cancer agent if the compound can influence 10% of the cancer cells, for example. In a more preferred embodiment, the compound is effective if it can influence 10 to 50% of the cancer cells. In an even more preferred embodiment, the compound is effective if it can influence 50-80% of the cancer cells. In an even more preferred embodiment, the compound is effective if it can influence 80-95% of the cancer cells. In an even more preferred embodiment, the compound is effective if it can influence 95-99% of the cancer cells. "Influence" is defined by the mechanism of action for each compound. For example, if a compound prevents the division of cancer cells, then influence is a measure of prevention of cancer cell division. Not all mechanisms of action need be at the same percentage of effectiveness. In an alternative embodiment, a low percentage effectiveness can be desirable if the lower degree of effectiveness is offset by other factors, such as the specificity of the compound, for example. Thus a compound that is only 10% effective, for example, but displays little in the way of harmful side-effects to the host, or non-harmful microbes or cells, can still be considered effective.

[0170] In one embodiment, the compounds described herein are administered simply to remove cancer cells and need not be administered to a patient. For example, the compounds can be administered *ex vivo* to a cell sample, such as a bone marrow or stem cell transplant to ensure that only non-cancerous cells are introduced into the recipient. After the compounds are administered they may optionally be removed. Whether or not this is an option will depend upon the relative needs of the situation and the risks associated with the compound, which in part can be determined as described in the Examples below.

[0171] The following non-limiting examples are meant to describe the preferred embodiments of the methods. Variations in the details of the particular methods employed and in the precise chemical compositions obtained will undoubtedly be appreciated by those of skill in the art.

EXAMPLES

EXAMPLE 1

FERMENTATION OF COMPOUND OF FORMULAE I-16, I-17, I-20, I-24C, I-26 AND I-28 USING STRAIN CNB476

[0172] Strain CNB476 was grown in a 500-ml flask containing 100 ml of vegetative medium consisting of the following per liter of deionized water: glucose, 4 g; Bacto tryptone, 3 g; Bacto casitone, 5 g; and synthetic sea salt (Instant Ocean, Aquarium Systems), 30 g. The first seed culture was incubated at 28 degree C for 3 days on a rotary shaker operating at 250 rpm. Five ml each of the first seed culture was inoculated into three 500-ml flasks containing of 100 ml of the vegetative medium. The second seed cultures were incubated at 28 degree C and 250 rpm on a rotary shaker for 2 days. Five ml each of the second seed culture was inoculated into thirty-five 500-ml flasks containing of 100 ml of the vegetative medium. The third seed cultures were incubated at 28 degree and 250 rpm on a rotary shaker for 2 days. Five ml each of the third seed culture was inoculated into four hundred 500-ml flasks containing 100 ml of the Production Medium A consisting of the following per liter of deionized water: starch, 10 g; yeast extract, 4 g; Hy-Soy, 4 g; ferric sulfate, 40 mg; potassium bromide, 100 mg; calcium carbonate, 1 g; and synthetic sea salt (Instant Ocean, Aquarium Systems), 30 g. The production cultures were incubated at 28 degree C and 250 rpm on roatry shakers for 1 day. Approximately 2 to 3 grams of sterile Amberlite XAD-7 resin were added to the production cultures. The production cultures were further incubated at 28 degree C and 250 rpm on rotary shakers for 5 days and achieved a titer of Compound I-16 of about 200 mg/L. The culture broth was filtered through cheese cloth to recover the Amberlite XAD-7 resin. The resin was extracted with 2 times 6 liters ethyl acetate followed by 1 time 1.5 liters ethyl acetate. The combined extracts were dried in vacuo. The dried extract, containing 3.8 grams the compound of Formula I-16 and lesser quantities of compounds of formulae I-20 and I-24C, was then processed for the recovery of the compounds of Formula I-16, I-20, I-24C, I-26 and I-28.

EXAMPLE 2

FERMENTATION OF COMPOUNDS I-16, I-17, I-20, I-24C, I-26 AND I-28 USING STRAIN NPS21184

[0173] Strain NPS21184 was grown in a 500-ml flask containing 100 ml of vegetative medium consisting of the following per liter of deionized water: glucose, 8 g; yeast extract, 6 g; Hy-Soy, 6 g; and synthetic sea salt (Instant Ocean, Aquarium Systems), 30 g. The first seed culture was incubated at 28 degree C for 3 days on a rotary shaker operating at 250 rpm. Five ml of the first seed culture was inoculated into 500-ml flask containing of 100 ml of the vegetative medium. The second seed cultures were incubated at 28 degree C and 250 rpm on a rotary shaker for 2 days. Five ml each of the second seed culture was inoculated into 500-ml flask containing of 100 ml of the vegetative medium. The third seed cultures were incubated at 28 degree and 250 rpm on a rotary shaker for 2 days. Five ml each of the third seed culture was inoculated into 500-ml flask containing 100 ml of the Production Medium B consisting of the following per liter of deionized water: starch, 20 g; yeast extract, 4 g; Hy-Soy, 8 g; ferric sulfate, 40 mg; potassium bromide, 100 mg; calcium carbonate, 1 g; and synthetic sea salt (Instant Ocean, Aquarium Systems), 30 g. The production cultures were incubated at 28 degree C and 250 rpm on rotary shakers for 1 day. Approximately 2 to 3 grams of sterile Amberlite XAD-7 resin were added to the production culture. The production culture was further incubated at 28 degree C and 250 rpm on rotary shaker for 4 days and achieved a titer of 350 – 400 mg/L for Compound I-16.

[0174] Alternatively, the production of the compounds can be achieved in a 42L fermentor system using strain NPS21184. Strain NPS21184 was grown in a 500-ml flask containing 100 ml of vegetative medium consisting of the following per liter of deionized water: glucose, 8 g; yeast extract, 6 g; Hy-Soy, 6 g; and synthetic sea salt (Instant Ocean, Aquarium Systems), 30 g. The first seed culture was incubated at 28 degree C for 3 days on a rotary shaker operating at 250 rpm. Five ml of the first seed culture was inoculated into 500-ml flask containing of 100 ml of the vegetative medium. The second seed cultures were incubated at 28 degree C and 250 rpm on a rotary shaker for 2 days. Twenty ml each of the second seed culture was inoculated into 2.8L Fernbach flask containing of 400 ml of the vegetative medium. The third seed cultures were incubated at 28 degree and 250 rpm on a rotary shaker for 2 days. 1.2L

of the third seed culture was inoculated into a 42L fermentor containing 26L of Production Medium A. Production Medium B and Production Medium C, with the following composition, can also be used. Production Medium C consisting of the following per liter of deionized water: starch, 15 g; yeast extract 6 g; Hy-Soy, 6 g; ferric sulfate, 40 mg; potassium bromide, 100 mg; calcium carbonate, 1 g; and synthetic sea salt (Instant Ocean, Aquarium Systems), 30 g. The fermentor cultures were operated at the following parameters: temperature, 28 degree C; agitation, 200 rpm; aeration, 13L/min and back pressure, 4.5 psi. At 36 to 44 hours of the production cycle, approximately 600 grams of sterile Amberlite XAD-7 resin were added to the fermentor culture. The production culture was further incubated at the above operating parameters until day 4 of the production cycle. The aeration rate was lowered to 8L/min. At day 5 of the production cycle, the fermentor culture achieved a titer of about 300 mg/L for Compound I-16. The culture broth was filtered through cheese cloth to recover the Amberlite XAD-7 resin. The resin was extracted with 2 times 4.5L liters ethyl acetate followed by 1 time 1.5 liters ethyl acetate. The combined extracts were dried in vacuo. The dried extract was then processed for the recovery of the Compounds of Formulae I-16, I-17, I-20, I-24C, I-26 and I-28.

EXAMPLE 3

PURIFICATION OF COMPOUND OF FORMULAE I-16, I-20, I-24C, I-26 AND I-28

3A: Purification of Compound of Formulae I-16, I-20, I-24C, I-26 and I-28

[0175] The pure compounds of Formulae I-16, I-20 I-24C, I-26 and I-28 were obtained by flash chromatography followed by HPLC. Eight grams crude extract containing 3.8 grams of the compound of Formula I-16 and lesser quantities of I-20, I-24C, I-26 and I-28 was processed by flash chromatography using Biotage Flash40i system and Flash 40M cartridge (KP-Sil Silica, 32-63 μm, 90 grams). The flash chromatography was developed by the following step gradient:

1. Hexane (1L)
2. 10% Ethyl acetate in hexane (1L)
3. 20% Ethyl acetate in hexane, first elution (1L)
4. 20% Ethyl acetate in hexane, second elution (1L)
5. 20% Ethyl acetate in hexane, third elution (1L)
6. 25% Ethyl acetate in hexane (1L)

7. 50% Ethyl acetate in hexane (1L)
8. Ethyl acetate (1L)

[0176] Fractions containing the compound of Formula I-16 in greater or equal to 70% UV purity by HPLC were pooled and subject to HPLC purification, as described below, to obtain I-16, along with I-20 and I-24C, each as pure compounds

Column	Phenomenex Luna 10u Silica
Dimensions	25 cm X 21.2 mm ID
Flow rate	25 ml/min
Detection	ELSD
Solvent	Gradient of 24% EtOAc/hexane for 19 min, 24% EtOAc/hexane to 100%EtOAc in 1 min, then 100% EtOAc for 4 min

[0177] The fraction enriched in compound of Formula I-16 (described above; ~ 70% pure with respect to I-16) was dissolved in acetone (60mg/ml). Aliquots (950 ul) of this solution were injected onto a normal-phase HPLC column using the conditions described above. Compound I-16 typically eluted after 14 minutes and compounds I-24C and I-26 co-eluted as a single peak at 11 min. When parent samples containing compounds I-17, I-20 and I-28 were processed, compound I-17 eluted at 22 minutes, while I-20 and I-28 co-eluted at 23 minutes during the 100% ethyl acetate wash. Fractions containing compound I-16 and minor analogs were pooled based on composition of compounds present, and evaporated under reduced pressure on a rotary evaporator. This process yielded pure Compound A, as well as separate fractions containing minor compounds I-20, I-24C, I-26 and I-28, which were further purified as described below.

[0178] Sample containing I-24C and I-26 generated from the process described above were further separated using reversed-phase preparative HPLC as follows. The sample containing I-24C (70 mg) was dissolved in acetonitrile at a concentration of 10 mg/ml, and 500 µl was loaded on an HPLC column of dimensions 21 mm i.d. by 15 cm length containing Eclipse

XDB-C18 support. The solvent gradient increased linearly from 15% acetonitrile /85% water to 100% acetonitrile over 23 minutes at a flow rate of 14.5 ml/min. The solvent composition was held at 100% acetonitrile for 3 minutes before returning to the starting solvent mixture. Compound I-26 eluted at 17.5 minutes while compound I-24C eluted at 19 minutes under these conditions.

[0179] Crystalline I-26 was obtained using a vapor diffusion method. Compound I-26 (15 mg) was dissolved in 100 µl of acetone in a 1.5 ml v-bottom HPLC vial. This vial was then placed inside a larger sealed vessel containing 1 ml of pentane. Crystals suitable for X-ray crystallography experiments were observed along the sides and bottom of the inner vial after 48 hours of incubation at 4 °C. Crystallography data was collected on a Bruker SMART APEX CCD X-ray diffractometer (F(000)= 2656, $Mo_{K\alpha}$ radiation, λ=0.71073 Å, μ=0.264 mm^{-1}, T=100K) at the UCSD Crystallography Lab and the refinement method used was full-matrix least-squares on F^2. Crystal data NPI-2065: $C_{15}H_{20}ClNO_4$, MW=313.77, tetragonal, space group P4(1)2(1)2, a= b=11.4901(3) Å , c= 46.444(2) Å, $\alpha=\beta=\gamma=90°$, vol=6131.6(3) $Å^3$, Z=16, ρ_{calcd}=1.360 g cm^{-3}, crystal size, 0.30 x 0.15 x 0.07 mm^3, θ range, 1.75-26.00°, 35367 reflections collected, 6025 independent reflections (R_{int}=0.0480), final R indices *($I>2\sigma(I)$)*: R_1=0.0369, wR_2=0.0794, GOF=1.060.

[0180] In order to separate I-28 from I-20, a reverse-phase isocratic method was employed. Sample (69.2 mg) containing both compounds was dissolved in acetonitrile to a concentration of 10 mg/ml, and 500 µl was loaded on a reverse-phase HPLC column (ACE 5 C18-HL, 15 cm X 21 mm ID) per injection. An isocratic solvent system of 27% acetonitrile/ 63% water at flow rate of 14.5 ml/min was used to separate compounds I-28 and I-20, which eluted after 14 and 16 minutes, respectively. Fractions containing compounds of interest were immediately evaporated under reduced pressure at room temperature on a rotary evaporator. Samples were then loaded onto a small column of silica and eluted with 10 ml of 70% hexane/30% acetone to remove additional impurities.

[0181] Samples generated from the preparative normal-phase HPLC method described above that contained I-20, but which were free of I-28 could also be triturated with 100% EtOAc to remove minor lipophilic impurities.

[0182] Compound of Formula I-16: UV (Acetonitrile/ H_2O) λ_{max} 225(sh) nm. Low Res. Mass: m/z 314 (M+H), 336 (M+Na).

[0183] Compound of Formula I-20: UV (Acetonitrile/ H_2O) λ_{max} 225(sh) nm. Low Res. Mass: m/z 266 (M+H); HRMS (ESI), *m/z* 266.1396 (M+H), Δ_{calc}= 1.2 ppm.

[0184] Compound of Formula I-24C: UV (Acetonitrile/ H_2O) λ_{max} 225(sh) nm. Low Res. Mass: m/z 328 (M+H), 350 (M+Na); HRMS (ESI), *m/z* 328.1309 (M+H), Δ_{calc}= -2.0 ppm, $C_{16}H_{23}NO_4Cl$.

[0185] Compound of Formula I-26: UV (Acetonitrile/ H_2O) λ_{max} 225(sh) nm; HRMS (ESI), *m/z* 314.1158 (M+H), Δ_{calc}= -0.4 ppm, $C_{15}H_{21}NO_4Cl$.

[0186] Compound of Formula I-28: UV (Acetonitrile/ H_2O) λ_{max} 225(sh) nm; HRMS (ESI), *m/z* 266.1388 (M+H), Δ_{calc}= -1.8 ppm, $C_{14}H_{20}NO_4$.

EXAMPLE 4

FERMENTATION OF COMPOUNDS OF FORMULAE I-17, I-18, AND I-27

[0187] Strain CNB476 was grown in a 500-ml flask containing 100 ml of the first vegetative medium consisting of the following per liter of deionized water: glucose, 4 g; Bacto tryptone, 3 g; Bacto casitone, 5 g; and synthetic sea salt (Instant Ocean, Aquarium Systems), 30 g. The first seed culture was incubated at 28 degree C for 3 days on a rotary shaker operating at 250 rpm. Five ml of the first seed culture was inoculated into a 500-ml flask containing 100 ml of the second vegetative medium consisting of the following per liter of deionized water: starch, 10 g; yeast extract, 4 g; peptone, 2 g; ferric sulfate, 40 mg; potassium bromide, 100 mg; calcium carbonate, 1 g; and sodium bromide, 30 g. The second seed cultures were incubated at 28°C for 7 days on a rotary shaker operating at 250 rpm. Approximately 2 to 3 gram of sterile Amberlite XAD-7 resin were added to the second seed culture. The second seed culture was further incubated at 28°C for 2 days on a rotary shaker operating at 250 rpm. Five ml of the second seed culture was inoculated into a 500-ml flask containing 100 ml of the second vegetative medium. The third seed culture was incubated at 28°C for 1 day on a rotary shaker operating at 250 rpm. Approximately 2 to 3 gram of sterile Amberlite XAD-7 resin were added to the third seed culture. The third seed culture was further incubated at 28°C for 2 days on a rotary shaker operating at 250 rpm. Five ml of the third culture was inoculated into a 500-ml flask containing 100 ml of the second vegetative medium. The fourth seed culture was incubated at 28°C for 1 day on a rotary shaker operating at 250 rpm. Approximately 2 to 3 gram of sterile Amberlite XAD-7 resin were added to the fourth seed culture. The fourth seed culture was further

incubated at 28°C for 1 day on a rotary shaker operating at 250 rpm. Five ml each of the fourth seed culture was inoculated into ten 500-ml flasks containing 100 ml of the second vegetative medium. The fifth seed cultures were incubated at 28°C for 1 day on a rotary shaker operating at 250 rpm. Approximately 2 to 3 grams of sterile Amberlite XAD-7 resin were added to the fifth seed cultures. The fifth seed cultures were further incubated at 28°C for 3 days on a rotary shaker operating at 250 rpm. Four ml each of the fifth seed culture was inoculated into one hundred and fifty 500-ml flasks containing 100 ml of the production medium having the same composition as the second vegetative medium. Approximately 2 to 3 grams of sterile Amberlite XAD-7 resin were also added to the production culture. The production cultures were incubated at 28°C for 6 day on a rotary shaker operating at 250 rpm. The culture broth was filtered through cheese cloth to recover the Amberlite XAD-7 resin. The resin was extracted with 2 times 3 liters ethyl acetate followed by 1 time 1 liter ethyl acetate. The combined extracts were dried in vacuo. The dried extract, containing 0.42 g of the compound Formula I-17 and 0.16 gram the compound of Formula I-18, was then processed for the recovery of the compounds.

EXAMPLE 5

PURIFICATION OF COMPOUNDS OF FORMULA I-17, I-18 AND I-27

[0188] The pure compounds of Formula I-17 and I-18 were obtained by reversed-phase HPLC as described below:

Column	ACE 5 C18-HL
Dimensions	15 cm X 21 mm ID
Flow rate	14.5 ml/min
Detection	214 nm
Solvent	Gradient of 35% Acetonitrile/65% H_2O to 90% Acetonitrile/10% H_2O over 15 min

[0189] Crude extract (100 mg) was dissolved in 15 ml of acetonitrile. Aliquots (900 ul) of this solution were injected onto a reversed-phase HPLC column using the conditions described above. Compounds of Formulae I-17 and I-18 eluted at 7.5 and 9 minutes,

respectively. Fractions containing the pure compounds were first concentrated using nitrogen to remove organic solvent. The remaining solution was then frozen and lyophilized to dryness.

[0190] An alternative purification method for Compound I-17 and I-18 was developed for larger scale purification and involved fractionation of the crude extract on a normal phase VLC column. Under these conditions, sufficient amounts of several minor metabolites were identified, including compound I-27. The crude extract (2.4 g) was dissolved in acetone (10 ml) and this solution adsorbed onto silica gel (10 cc) by drying *in vacuo*. The adsorbed crude extract was loaded on a normal phase silica VLC column (250 cc silica gel, column dimensions 2.5 cm diameter by 15 cm length) and washed with a step gradient of hexane / EtOAc, increasing in the percentage of hexane in steps of 5% (100 ml solvent per step). The majority of compound I-16 eluted in the 60% hexane / 40% EtOAc wash while the majority of compound I-17 eluted in the 50% hexane / 50% ethyl acetate wash. Final separation of the compounds was achieved using C18 HPLC chromatography (ACE 5 μ C18-HL, 150 mm X 21 mm ID) using an isocratic solvent system consisting of 35% ACN / 65% H2O. Under these conditions, compound I-27 eluted at 11 minutes, compound I-17 eluted at 12.00 minutes, traces of compound A eluted at 23.5 minutes, and compound I-18 eluted at 25.5 minutes. The resulting samples were dried *in vacuo* using no heat to remove the aqueous solvent mixture. The spectroscopic data for these samples of compound I-16 and compound I-18 were found to be identical with those of samples prepared from earlier purification methods. The sample of compound I-18 was found to contain 8% of the lactone hydrolysis product and was further purified by washing through a normal phase silica plug (1 cm diameter by 2 cm height) and eluting using a solvent mixture of 20% EtOAc / 80% Hexanes (25 ml). The resulting sample was found to contain pure compound I-18.

[0191] The fractions containing compound I-27 described above were further purified using normal phase semipreparative HPLC (Phenomenex Luna Si 10 μ, 100 Å; 250 x 10 mm id) using a solvent gradient increasing from 100% hexane to 100% EtOAc over 20 minutes with a flowrate of 4 ml/min. Compound I-27 eluted as a pure compound after 11.5 minutes (0.8 mg, 0.03% isolated yield from dried extract weight).

[0192] Compound of Formula I-17: UV (Acetonitrile/ H_2O) λ_{max} 225(sh) nm. High Res. Mass (APCI): m/z 280.156 (M+H), Δ_{calc}=2.2 ppm, $C_{15}H_{22}NO_4$.

[0193] Compound of Formula I-18: UV (Acetonitrile/ H_2O) λ_{max} 225(sh) nm. High Res. Mass (APCI): m/z 358.065 (M+H), Δ_{calc}= -1.9 ppm, $C_{15}H_{21}NO_4Br$.

[0194] Compound I-27: UV (Acetonitrile/H_2O) λ_{max} 225(sh) nm; MS (HR-ESI), *m/z* 280.1556 (M+H) Δ_{calc}= 2.7 ppm ($C_{15}H_{22}NO_4$); ^{1}H NMR (DMSO-d_6).

EXAMPLE 6

PREPARATION OF COMPOUND OF FORMULA I-19 FROM I-16

[0195] A sample of compound of Formula I-16 (250 mg) was added to an acetone solution of sodium iodide (1.5 g in 10 ml) and the resulting mixture stirred for 6 days. The solution was then filtered through a 0.45 micron syringe filter and injected directly on a normal phase silica HPLC column (Phenomenex Luna 10u Silica, 25 cm x 21.2 mm) in 0.95 ml aliquots. The HPLC conditions for the separation of compound formula I-19 from unreacted I-16 employed an isocratic HPLC method consisting of 24% ethyl acetate and 76% hexane, in which the majority of compound I-19 eluted 2.5 minutes before compound I-16. Equivalent fractions from each of 10 injections were pooled to yield 35 mg compound I-19. Compound I-19: UV (Acetonitrile/H_2O) 225 (sh), 255 (sh) nm; ESMS, *m/z* 406.0 (M+H); HRMS (ESI), *m/z* 406.0513 $[M+H]^+$, Δ_{calc}= -0.5 ppm, $C_{15}H_{21}NO_4I$; ^{1}H NMR in DMSO-d_6.

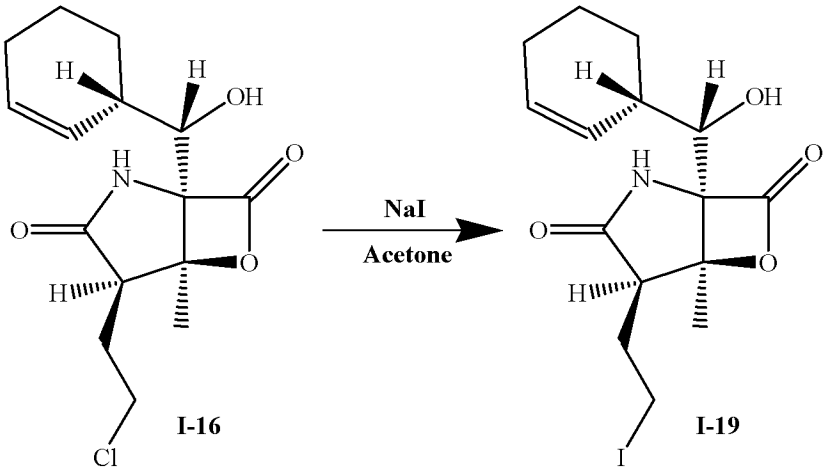

EXAMPLE 7

SYNTHESIS OF THE COMPOUNDS OF FORMULAE I-2, I-3, AND I-4

[0196] Compounds of Formulae I-2, I-3 and I-4 can be synthesized from compounds of Formulae I-16, I-17 and I-18, respectively, by catalytic hydrogenation.

Exemplary Depiction of Synthesis

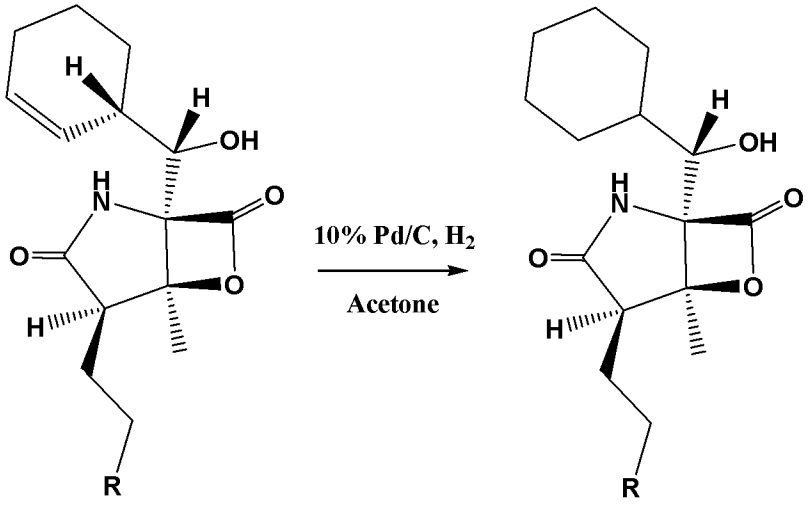

I-16: R=Cl
I-17: R=H
I-18: R=Br

I-2: R=Cl
I-3: R=H
I-4; R=Br

Example 7A: Catalytic Hydrogenation of Compound of Formula I-16

[0197] Compound of Formula I-16 (10 mg) was dissolved in acetone (5 mL) in a scintillation vial (20 mL) to which was added the 10% (w/w) Pd/C (1-2mg) and a magnetic stirrer bar. The reaction mixture was stirred in a hydrogen atmosphere at room temperature for about 15 hours. The reaction mixture was filtered through a 3 cc silica column and washed with acetone. The filtrate was filtered again through 0.2 μm Gelman Acrodisc to remove any traces of catalyst. The solvent was evaporated off from filtrate under reduced pressure to yield the compound of Formula I-2 as a pure white powder: UV (acetonitrile/H_2O): λ_{max} 225 (sh) nm.

Example 7B: Catalytic Hydrogenation of Compound of Formula I-17

[0198] Compound of Formula I-17 (5 mg) was dissolved in acetone (3 mL) in a scintillation vial (20 mL) to which was added the 10% (w/w) Pd/C (about 1mg) and a magnetic stirrer bar. The reaction mixture was stirred in a hydrogen atmosphere at room temperature for about 15 hours. The reaction mixture was filtered through a 0.2 μm Gelman Acrodisc to remove the catalyst. The solvent was evaporated off from filtrate to yield the compound of Formula I-3 as a white powder which was purified by normal phase HPLC using the following conditions:

Column: Phenomenex Luna 10u Silica

Dimensions: 25 cm x 21.2 mm ID

Flow rate: 14.5 ml/min

Detection: ELSD

Solvent: 5% to 60% EtOAc/Hex for 19 min, 60 to 100% EtOAc in 1 min, then 4 min at 100% EtOAc

[0199] Compound of Formula I-3 eluted at 22.5 min as a pure compound: UV (acetonitrile/H_2O): λ_{max} 225 (sh) nm. Formula I-3: m/z 282 (M+H), 304 (M+Na).

Example 7C: Catalytic Hydrogenation of Compound of Formula I-18

[0200] 3.2 mg of compound of Formula I-18 was dissolved in acetone (3 mL) in a scintillation vial (20 mL) to which was added the 10% (w/w) Pd/C (about 1 mg) and a magnetic stirrer bar. The reaction mixture was stirred in hydrogen atmosphere at room temperature for about 15 hours. The reaction mixture was filtered through a 0.2 μm Gelman Acrodisc to remove the catalyst. The solvent was evaporated off from filtrate to yield the compound of Formula I-4 as a white powder which was further purified by normal phase HPLC using the following conditions:

Column: Phenomenex Luna 10u Silica

Dimensions: 25 cm x 21.2 mm ID

Flow rate: 14.5 ml/min

Detection: ELSD

Solvent: 5% to 80% EtOAc/Hex for 19 min, 80 to 100% EtOAc in 1 min, then 4 min at 100% EtOAc

[0201] Compound of Formula I-4 eluted at 16.5 min as a pure compound: UV (acetonitrile/H_2O): λ_{max} 225 (sh) nm. Formula I-4: m/z 360 (M+H), 382 (M+Na).

[0202] In addition, high resolution mass spectrometry data were obtained for compounds I-2, I-3, and I-4. Compound I-2: HRMS (ESI), *m/z* 316.1305 $[M+H]^+$, Δ_{calc}= -3.5 ppm, $C_{15}H_{23}NO_4Cl$. Compound I-3: HRMS (ESI), *m/z* 282.1706 $[M+H]^+$, Δ_{calc}= 0.3 ppm, $C_{15}H_{24}NO_4$. Compound I-4: HRMS (ESI), *m/z* 360.0798 $[M+H]^+$, Δ_{calc}= -3.4 ppm, $C_{15}H_{23}NO_4Br$.

EXAMPLE 8

SYNTHESIS OF THE COMPOUNDS OF FORMULAE I-5A AND I-5B

[0203] Compounds of Formula I-5A and Formula I-5B can be synthesized from compound of Formula I-16 by epoxidation with mCPBA.

[0204] Compound of Formula I-16 (101 mg, 0.32 mmole) was dissolved in methylenechloride (30 mL) in a 100 ml of round bottom flask to which was added 79 mg (0.46 mmole) of meta-chloroperbenzoic acid (mCPBA) and a magnetic stir bar. The reaction mixture was stirred at room temperature for about 18 hours. The reaction mixture was poured onto a 20 cc silica flash column and eluted with 120 ml of CH_2Cl_2, 75 ml of 1:1 ethyl acetate/hexane and finally with 40 ml of 100% ethyl acetate. The 1:1 ethyl acetate/hexane fractions yield a mixture of diastereomers of epoxyderivatives, Formula I-5A and I-5B, which were separated by normal phase HPLC using the following conditions:

Column	Phenomenex Luna 10u Silica
Dimensions	25 cm x 21.2 mm ID
Flow rate	14.5 ml/min
Detection	ELSD
Solvent	25% to 80% EtOAc/Hex over 19 min, 80 to 100% EtOAc in 1 min, then 5 min at 100% EtOAc

[0205] Compound Formula I-5A (major product) and I-5B (minor product) eluted at 21.5 and 19 min, respectively, as pure compounds. Compound I-5B was further chromatographed on a 3cc silica flash column to remove traces of chlorobenzoic acid reagent.

Chemical Structures:

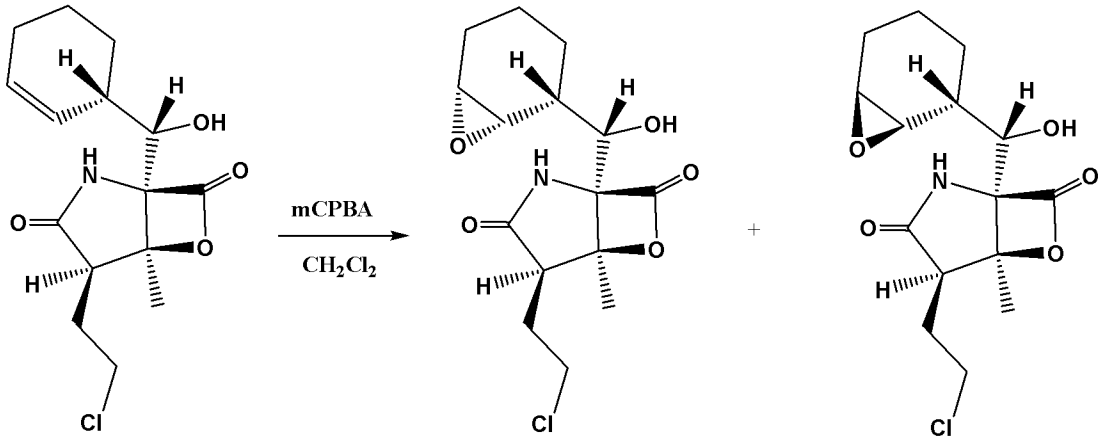

I-16 I-5A (90%) I-5B (10%)

Structural Characterization

[0206] Formula I-5A: UV (Acetonitrile/H_2O) λ_{max} 225 (sh) nm. Low Res. Mass: m/z 330 (M+H), 352 (M+Na); HRMS (ESI), *m/z* 330.1099 $[M+H]^+$, Δ_{calc}= -2.9 ppm, $C_{15}H_{21}NO_5Cl$.

[0207] Formula I-5B: UV (Acetonitrile/H_2O) λ_{max} 225 (sh) nm. Low Res. Mass: m/z 330 (M+H), 352 (M+Na); HRMS (ESI), *m/z* 330.1105 $[M+H]^+$, Δ_{calc}= -0.9 ppm, $C_{15}H_{21}NO_5Cl$.

EXAMPLE 9

SYNTHESIS OF THE COMPOUNDS OF FORMULAE IV-1, IV-2, IV-3 AND IV-4

Synthesis of diol derivatives (Formula IV-2)

[0208] Diols can be synthesized by Sharpless dihydroxylation using AD mix-α and β: AD mix-α is a premix of four reagents, $K_2OsO_2(OH)_4$; K_2CO_3; $K_3Fe(CN)_6$; $(DHQ)_2$-PHAL [1,4-bis(9-O-dihydroquinine)phthalazine] and AD mix-β is a premix of $K_2OsO_2(OH)_4$; K_2CO_3; $K_3Fe(CN)_6$; $(DHQD)_2$-PHAL [1,4-bis(9-O-dihydroquinidine)phthalazine] which are commercially available from Aldrich. Diol can also be synthesized by acid or base hydrolysis of epoxy compounds (Formula I-5A and I-5B) which may be different to that of products obtained in Sharpless dihydroxylation in their stereochemistry at carbons bearing hydroxyl groups

Sharpless Dihydroxylation of Compounds I-16, I-17 and I-18

[0209] Any of the compounds of Formulae I-16, I-17 and I-18 can be used as the starting compound. In the example below, compound of Formula I-16 is used. The starting compound is dissolved in t-butanol/water in a round bottom flask to which is added AD mix-α or

β and a magnetic stir bar. The reaction is monitored by silica TLC as well as mass spectrometer. The pure diols are obtained by usual workup and purification by flash chromatography or HPLC. The structures are confirmed by NMR spectroscopy and mass spectrometry. In this method both hydroxyl groups are on same side.

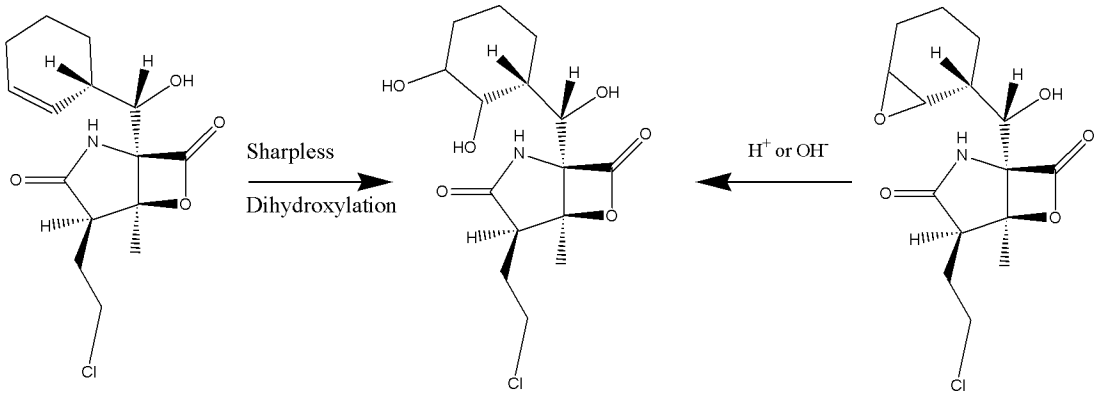

Starting Compound Formula IV-2 Formula I-5

Nucleophilic ring opening of epoxy compounds (I-5):

[0210] The epoxy ring is opened with various nucleophiles like NaCN, NaN_3, NaOAc, HBr, HCl, etc. to creat various substituents on the cyclohexane ring, including a hydroxyl substituent.

Examples:

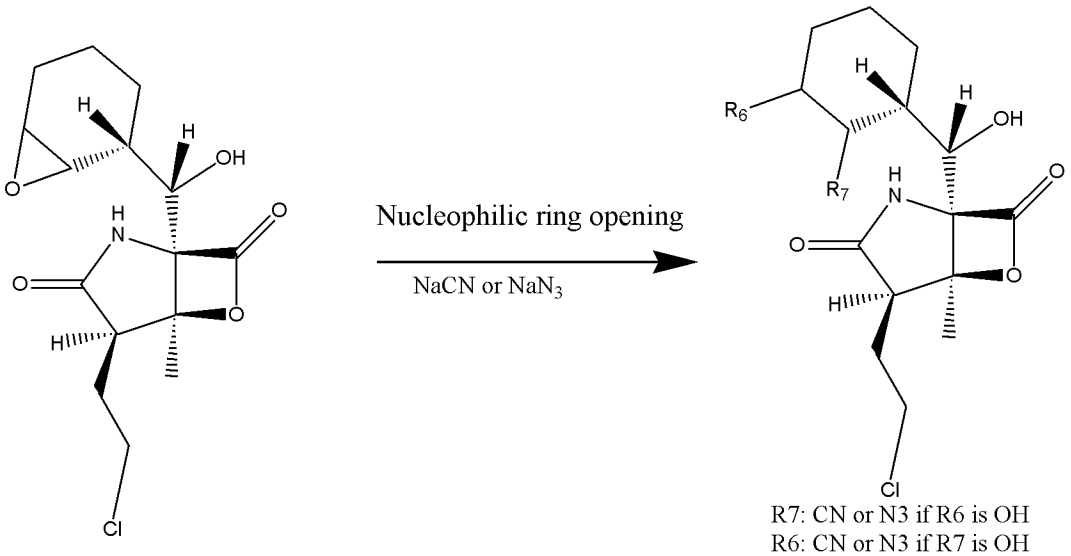

Formula I-5 Formula IV-1

[0211] The epoxy is opened with HCl to make Formula IV-3:

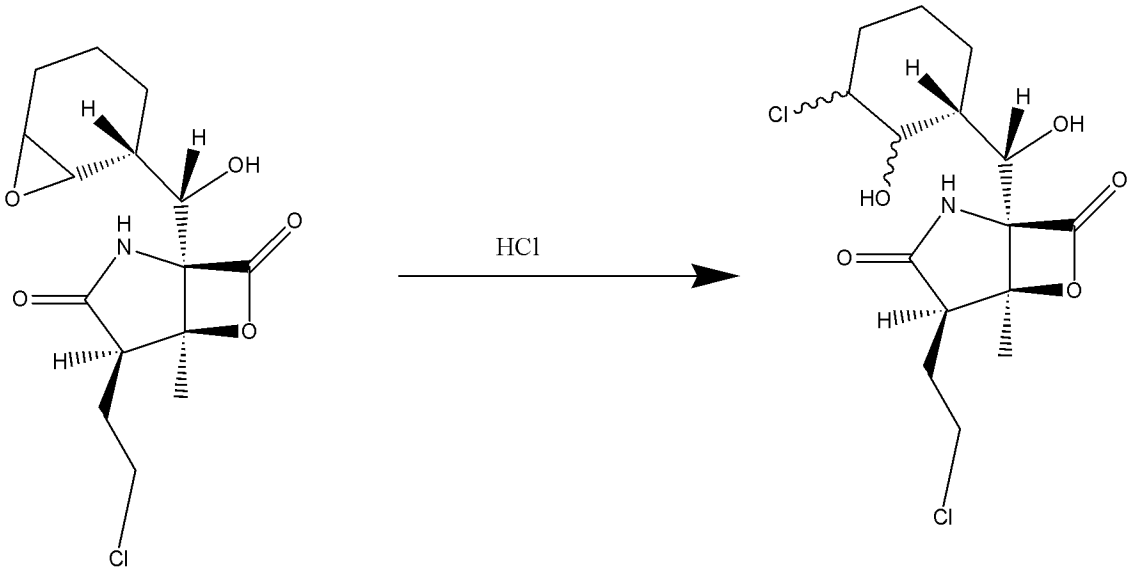

FORMULA I-5 FORMULA IV-3

[0212] Compound of Formula I-5A (3.3 mg) was dissolved in acetonitrile (0.5 ml) in a 1 dram vial to which was added 5% HCl (500 ul) and a magnetic stir bar. The reaction mixture was stirred at room temperature for about an hour. The reaction was monitored by mass spectrometry. The reaction mixture was directly injected on normal phase HPLC to obtain compound of Formula IV-3C as a pure compound without any work up. The HPLC conditions used for the purification were as follows: Phenomenex Luna 10u Silica column (25 cm x 21.2 mm ID) with a solvent gradient of 25% to 80% EtOAc/Hex over 19 min, 80 to 100% EtOAc in 1 min, then 5 min at 100% EtOAc at a flow rate of 14.5 ml/min. An ELSD was used to monitor the purification process. Compound of Formula IV-3C eluted at about 18 min (2.2 mg). Compound of Formula IV-3C: UV (Acetonitrile/H_2O) λ_{max} 225 (sh) nm; ESMS, *m/z* 366 (M+H), 388 (M+Na); HRMS (ESI), *m/z* 366.0875 $[M+H]^+$, Δ_{calc}= 0.0 ppm, $C_{15}H_{22}NO_5Cl_2$; ^1H NMR in DMSO-d_6. The stereochemistry of the compound of Formula IV-3C was determined based on coupling constants observed in the cyclohexane ring in 1:1 C_6D_6/DMSO-d_6.

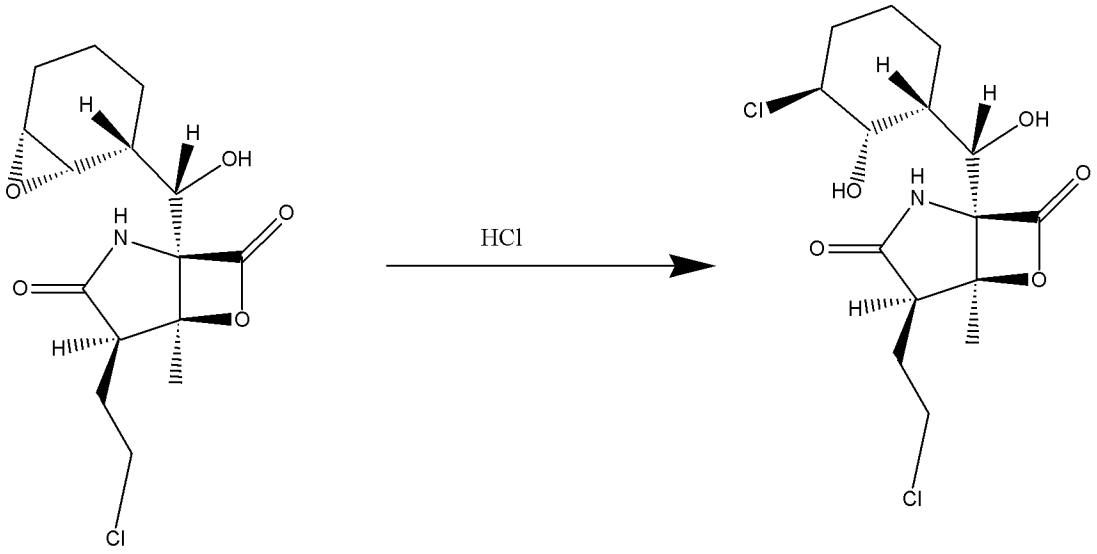

I-5A **IV-3C**

[0213] Reductive ring opening of epoxides (I-5): The compound of Formula is treated with metalhydrides like BH_3-THF complex to make compound of Formula IV-4.

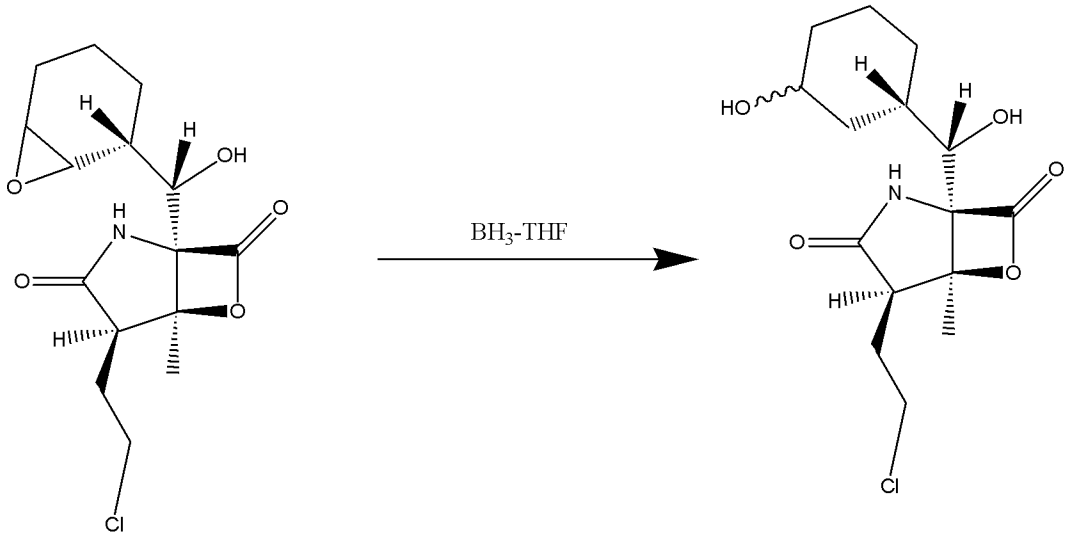

FORMULA I-5 FORMULA IV-4

EXAMPLE 10

SYNTHESIS OF THE COMPOUNDS OF FORMULAE I-13C AND I-8C

[0214] Compound of Formula I-16 (30 mg) was dissolved in CH_2Cl_2 (6 ml) in a scintillation vial (20 ml) to which Dess-Martin Periodinane (122 mg) and a magnetic stir bar

were added. The reaction mixture was stirred at room temperature for about 2 hours. The progress of the reaction was monitored by TLC (Hex:EtOAc, 6:4) and analytical HPLC. From the reaction mixture, the solvent volume was reduced to one third, absorbed on silica gel, poured on top of a 20 cc silica flash column and eluted in 20 ml fractions using a gradient of Hexane/EtOAc from 10 to 100%. The fraction eluted with 30% EtOAc in Hexane contained a mixture of rotamers of Formula I-13C in a ratio of 1.5:8.5. The mixture was further purified by normal phase HPLC using the Phenomenex Luna 10u Silica column (25 cm x 21.2 mm ID) with a solvent gradient of 25% to 80% EtOAc/Hex over 19 min, 80 to 100% EtOAc over 1 min, holding at 100% EtOAc for 5 min, at a flow rate of 14.5 ml/min. An ELSD was used to monitor the purification process. Compound of Formula I-13C eluted at 13.0 and 13.2 mins as a mixture of rotamers with in a ratio of 1.5:8.5 (7 mg). Formula I-13C: UV (Acetonitrile/H_2O) λ_{max} 226 (sh) & 300 (sh) nm; ESMS, *m/z* 312 $(M+H)^+$, 334 $(M+Na)^+$; HRMS (ESI), *m/z* 312.1017 $[M+H]^+$, Δ_{calc}= 4.5 ppm, $C_{15}H_{19}NO_4Cl$; ^1H NMR inDMSO-d_6.

[0215] The rotamer mixture of Formula I-13C (4 mg) was dissolved in acetone (1 ml) in a scintillation vial (20 ml) to which a catalytic amount (0.5 mg) of 10% (w/w) Pd/C and a magnetic stir bar were added. The reaction mixture was stirred in a hydrogen atmosphere at room temperature for about 15 hours. The reaction mixture was filtered through a 0.2 μm Gelman Acrodisc to remove the catalyst. The solvent was evaporated from the filtrate to yield compound of Formula I-8C as a colorless gum which was further purified by normal phase HPLC using a Phenomenex Luna 10u Silica column (25 cm x 21.2 mm ID) with a solvent gradient of 25% to 80% EtOAc/Hex over 19 min, 80 to 100% EtOAc over 1 min, holding at 100% EtOAc for 5 min, at a flow rate of 14.5 ml/min. An ELSD was used to monitor the purification process. Compound of Formula I-8C (1 mg) eluted at 13.5 min as a pure compound. Formula I-8C: UV (Acetonitrile/H_2O) λ_{max} 225 (sh) nm; ESMS, *m/z* 314 $(M+H)^+$, 336 $(M+Na)^+$; HRMS (ESI), *m/z* 314.1149 $[M+H]^+$, Δ_{calc}= 3.3 ppm, $C_{15}H_{21}NO_4Cl$; ^1H NMR inDMSO-d_6.

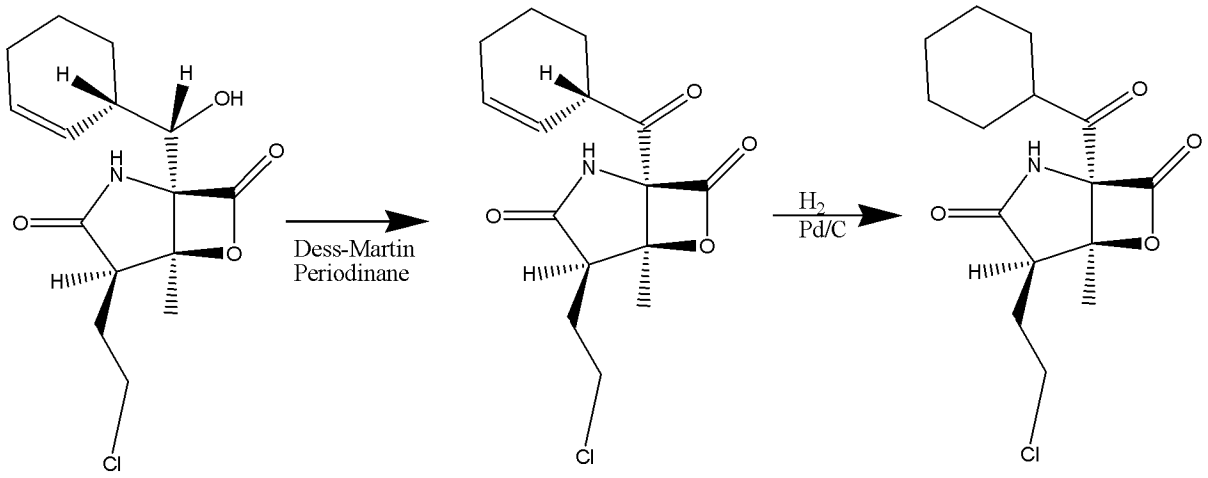

I-16 I-13C I-8C

EXAMPLE 11

SYNTHESIS OF THE COMPOUND OF FORMULA I-25 FROM I-13C

[0216] The rotamer mixture of Formula I-13C (5 mg) was dissolved in dimethoxy ethane (monoglyme; 1.5 ml) in a scintillation vial (20 ml) to which water (15 µl (1% of the final solution concentration)) and a magnetic stir bar were added. The above solution was cooled to -78°C on a dry ice-acetone bath, and a sodium borohydride solution (3.7 mg of $NaBH_4$ in 0.5 ml of monoglyme (created to allow for slow addition)) was added drop-wise. The reaction mixture was stirred at -78°C for about 14 minutes. The reaction mixture was acidified using 2 ml of 4% HCl solution in water and extracted with CH_2Cl_2. The organic layer was evaporated to yield mixture of compound of formulae I-25 and I-16 in a 9.5:0.5 ratio as a white solid, which was further purified by normal phase HPLC using a Phenomenex Luna 10u Silica column (25 cm x 21.2 mm ID). The mobile phase was 24% EtOAc/76% Hexane, which was held isocratic for 19 min, followed by a linear gradient of 24% to 100% EtOAc over 1 min, and held at 100% EtOAc for 3 min; the flow rate was 25 ml/min. An ELSD was used to monitor the purification process. Compound of formula I-25 (1.5 mg) eluted at 11.64 min as a pure compound. Compound of Formula I-25: UV (Acetonitrile/H_2O) λ_{max} 225 (sh) nm; ESMS, *m/z* 314 $(M+H)^+$, 336 $(M+Na)^+$; HRMS (ESI), *m/z* 314.1154 $[M+H]^+$, Δ_{calc}= -0.6 ppm, $C_{15}H_{21}NO_4Cl$; ^1H NMR in DMSO-d_6.

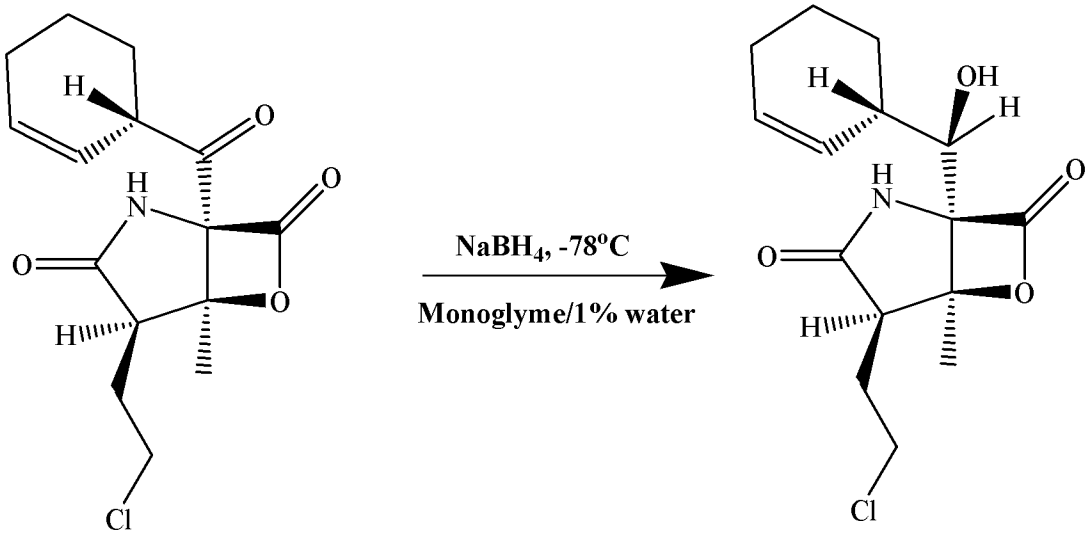

I-13C **I-25 (95%)**

EXAMPLE 12

SYNTHESIS OF THE COMPOUNDS OF FORMULAE I-31, I-32 AND I-49 FROM I-13C; AND COMPOUNDS OF FORMULAE I-33, I-34, I-35 AND I-36 FROM I-31 AND I-32

[0217] A rotamer mixture of the Compound of Formula I-13C (20 mg) was dissolved in acetone (4 ml) in a scintillation vial (20 ml) to which a catalytic amount (3 mg) of 10% (w/w) Pd/C and a magnetic stir bar were added. The reaction mixture was stirred at room temperature for about 15 hours. The reaction mixture was filtered through a 0.2 μm Gelman Acrodisc to remove the catalyst. The solvent was evaporated from the filtrate to yield a mixture of diastereomers of hydroxy derivatives of Formulae I-31 and I-32 (1:1) and a minor compound I-49, which were separated by reversed phase HPLC using Ace 5u C18 column (150 mm x 22 mm ID) with a solvent gradient of 90% to 30% H_2O/Acetonitrile over 15 min, 70 to 100% Acetonitrile over 5 min, holding at 100% Acetonitrile for 4 min, at a flow rate of 14.5 ml/min. A diode array detector was used to monitor the purification process. Compound I-31 (2 mg), I-32 (2 mg) and I-49 (0.2 mg) eluted at 10.6, 10.8 and 11.54 min, respectively, as pure compounds. I-31: UV (Acetonitrile/H_2O) λ_{max} 250 (sh) nm; ESMS *m/z* 328.1 $(M+H)^+$ & 350.0 $(M+Na)^+$. I-32: UV (Acetonitrile/H_2O) λ_{max} 250 (sh) nm; ESMS, *m/z* 328.1 $(M+H)^+$ & 350.0 $(M+Na)^+$. I-49: UV (Acetonitrile/H_2O) λ_{max} 250 (sh) and 320 nm; ESMS, *m/z* 326.0 $(M+H)^+$, 343.1 $(M+H_2O)^+$ & 348.0 $(M+Na)^+$.

[0218] In an alternate method, compounds I-31, I-32 and I-49 were separated by normal phase HPLC using Phenomenex Luna 10u Silica column (25 cm x 21.2 mm ID) with a solvent gradient of 10% to 100% Hexane/EtOAc over 24 min, holding at 100% EtOAc for 3 min, at a flow rate of 14.5 ml/min. ELSD was used to monitor the purification process.

[0219] The ketone of the compounds of formula I-31 and I-32 can be reduced by using sodium borohydride at 0 to -10°C in monoglyme solvent for about 14 minutes. The reaction mixture can be acidified using 4% HCl solution in water and extracted with CH_2Cl_2. The organic layer can be evaporated to yield the mixtures of compounds of formulae I-33, I-34, I-35 and I-36 which can be separated by chromatographic methods.

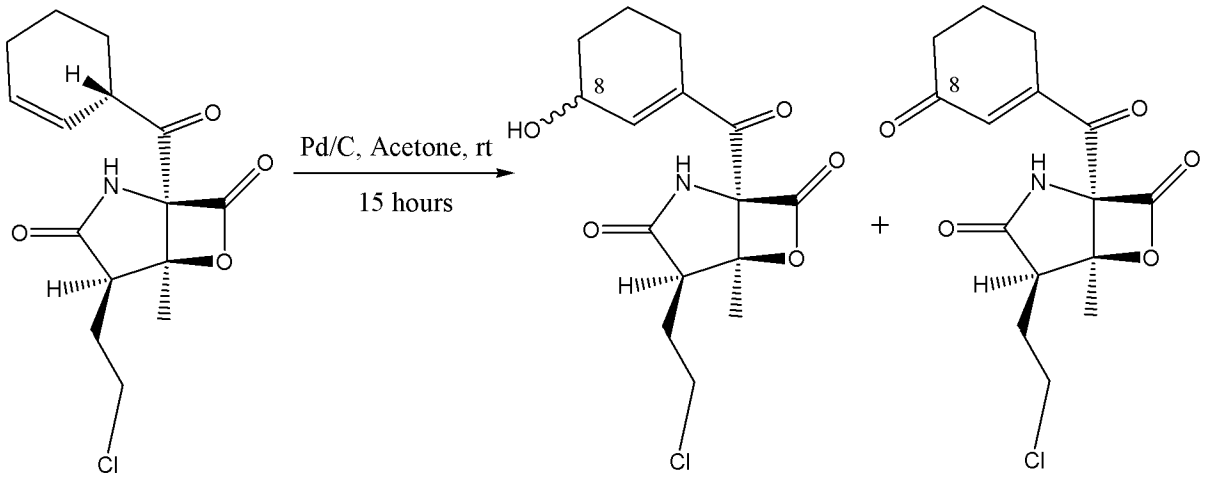

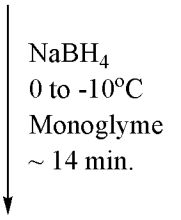

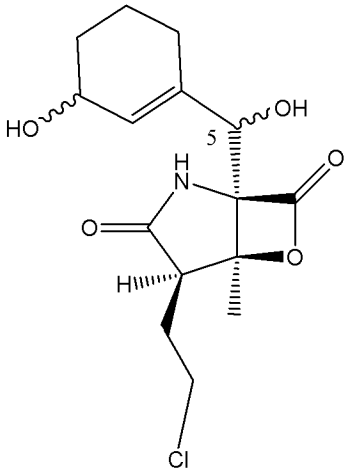

I-33, I-34, I-35 and I-36

EXAMPLE 13

SYNTHESIS OF THE COMPOUND OF FORMULAE I-21 FROM I-19

[0220] Acetone (7.5 ml) was vigorously mixed with 5 N NaOH (3 ml) and the resulting mixture evaporated to a minimum volume *in vacuo*. A sample of 100 µl of this solution was mixed with compound of Formula I-19 (6.2 mg) in acetone (1 ml) and the resulting biphasic mixture vortexed for 2 minutes. The reaction solution was immediately subjected to

preparative C18 HPLC. Conditions for the purification involved a linear gradient if 10% acetonitrile/90% water to 90% acetonitrile/ 10% water over 17 minutes using an Ace 5 μ C18 HPLC column of dimensions 22 mm id by 150 mm length. Compound of Formula I-21 eluted at 9.1 minutes under these conditions to yield 0.55 mg compound. Compound of Formula I-21: UV (Acetonitrile/H_2O) 225 (sh), ESMS, *m/z* 296.1 (M+H); ^{1}H NMR in DMSO-d_6.

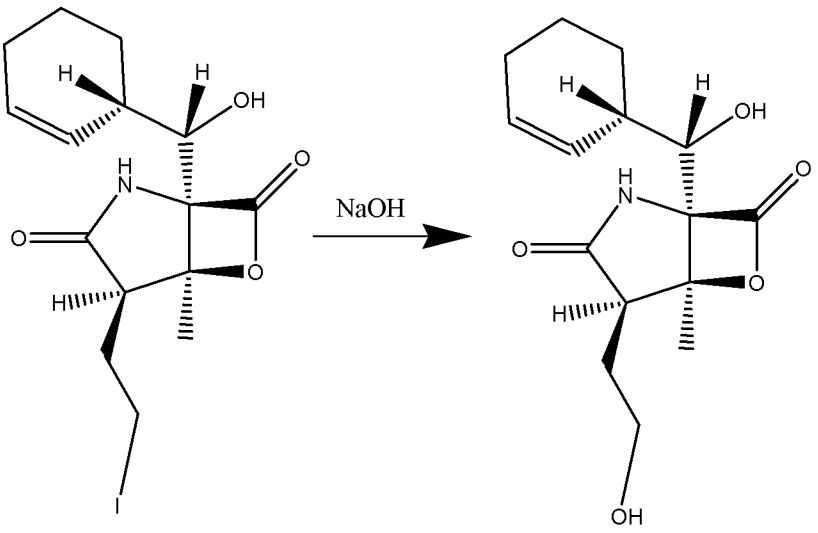

I-19 I-21

EXAMPLE 14

SYNTHESIS OF THE COMPOUND OF FORMULAE I-22 FROM I-19

[0221] A sample of 60 mg sodium propionate was added to a solution of compound of Formula I-19 (5.3 mg) in DMSO (1 ml) and the mixture sonicated for 5 minutes, though the sodium propionate did not completely dissolve. After 45 minutes, the solution was filtered through a 0.45 μ syringe filter and purified directly using HPLC. Conditions for the purification involved a linear gradient if 10% acetonitrile/90% water to 90% acetonitrile/ 10% water over 17 minutes using an Ace 5 μ C18 HPLC column of dimensions 22 mm id by 150 mm length. Under these conditions, compound of Formula I-22 eluted at 12.3 minutes to yield 0.7 mg compound (15% isolated yield). UV (Acetonitrile/H_2O) 225 (sh), ESMS, *m/z* 352.2 (M+H); HRMS (ESI), *m/z* 352.1762 $[M+H]^+$, Δ_{calc}= 0.6 ppm, $C_{18}H_{26}NO_6$; ^{1}H NMR in DMSO-d_6.

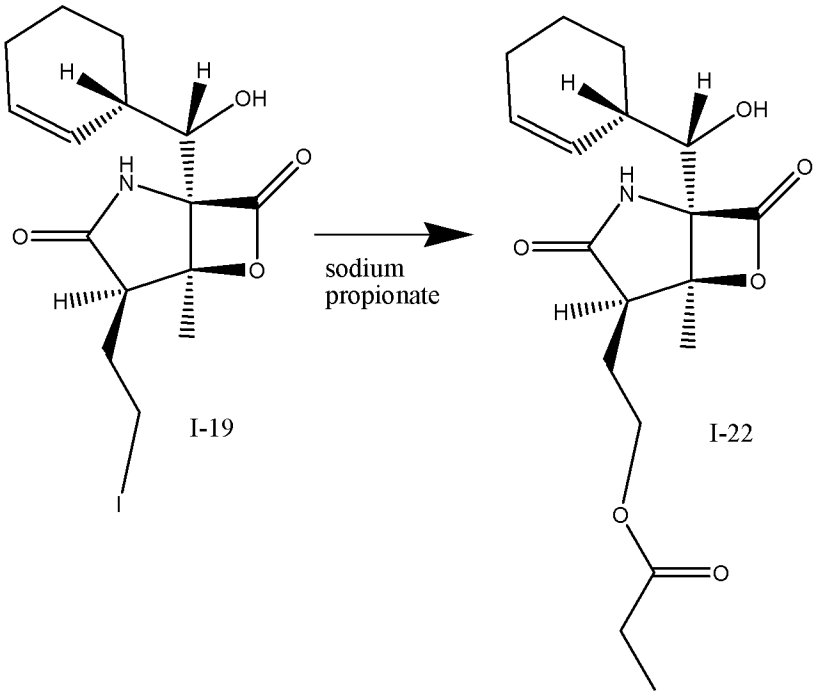

EXAMPLE 15

SYNTHESIS OF THE COMPOUND OF FORMULA I-29 FROM I-19

[0222] A sample of NaN_3 (80 mg) was dissolved in DMSO (1 ml) and transferred to a vial containing Compound I-19 (6.2 mg) which was contaminated with approximately 10% Compound I-16. The solution was incubated at room temperature for 1 hr prior to purification on C18 HPLC (ACE 5µ C18-HL, 150 mm X 21 mm ID) using a solvent gradient of 10% acetonitrile/90% H_2O to 90% acetonitrile/10% H_2O over 17 minutes. Using this method, the desired azido derivative I-29 co-eluted with Compound I-16 contaminant at 12.5 minutes (4.2 mg, 85% yield). A 2.4 mg portion of compound I-29 was further purified using additional C18 HPLC chromatography (ACE 5µ C18-HL, 150 mm X 21 mm ID) using an isocratic solvent gradient consisting of 35% acetonitrile / 65% H_20. Under these conditions compound I-29 eluted after 20 minutes, while Compound I-16 eluted after 21.5 minutes. The resulting sample consisted of 1.1 mg Compound I-29 was used for characterization in biological assays.

[0223] Compound I-29: UV (Acetonitrile/H_2O) 225 (sh), ESMS, *m/z* 321.1 (M+H); ^1H NMR in DMSO-d_6.

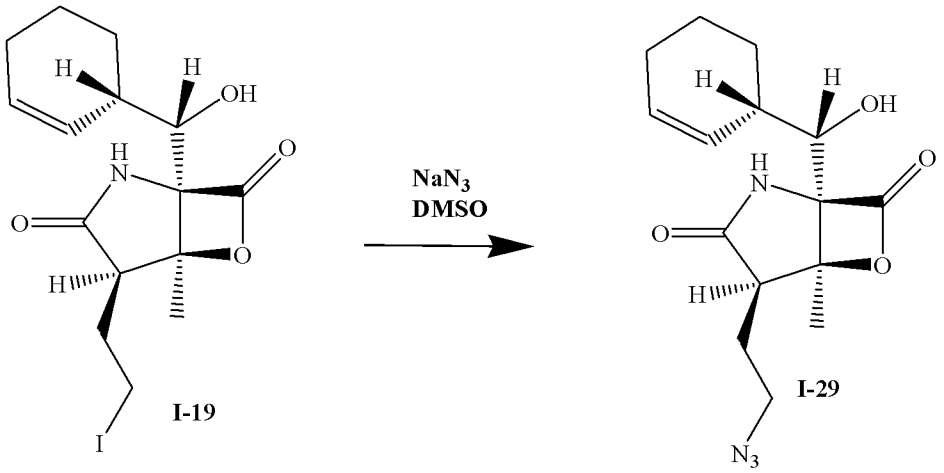

EXAMPLE 16

SYNTHESIS OF THE COMPOUNDS OF FORMULAE I-37 AND I-38 FROM I-19

[0224] The compounds of Formulae I-37 and I-38 can be prepared from the compound of Formula I-19 by cyano-de-halogenation or thiocyanato-de-halogenation, respectively. Compound I-19 can be treated with NaCN or KCN to obtain compound I-37. Alternatively, Compound I-19 can be treated with NaSCN or KSCN to obtain compound I-38.

Synthesis of the compound of Formula I-38 from I-19:

[0225] The compound of formula I-19 (10.6 mg, 0.02616 mmol) was dissolved in 1.5 ml of acetone in a scintillation vial (20 ml) to which sodium thiocyanate (10.0 mg, 0.1234 mmol), triethylamine (5µl, 0.03597 mmol) and a magnetic stir bar were added. The reaction mixture was stirred at room temperature for 72 hours. The reaction mixture was concentrated *in vacuo* to yield the compound I-38. Compound I-38 was purified by normal phase HPLC using a Phenomenex Luna 10µ Silica column (25cm x 21.2 mm ID) with a solvent gradient of 0 to 95% H_2O/Acetonitrile over 21 min, at a flow rate of 14.5 ml/min. Diode array detector was used to monitor the purification process. Compound I-38 (3.0 mg, 34% yield) eluted at 18.0 min as a pure compound. I-38: UV Acetonitrile/H_2O λ_{max} 203 (sh) nm; ESMS *m/z* 337.1 $(M+H)^+$ & 359.1 $(M+Na)^+$.

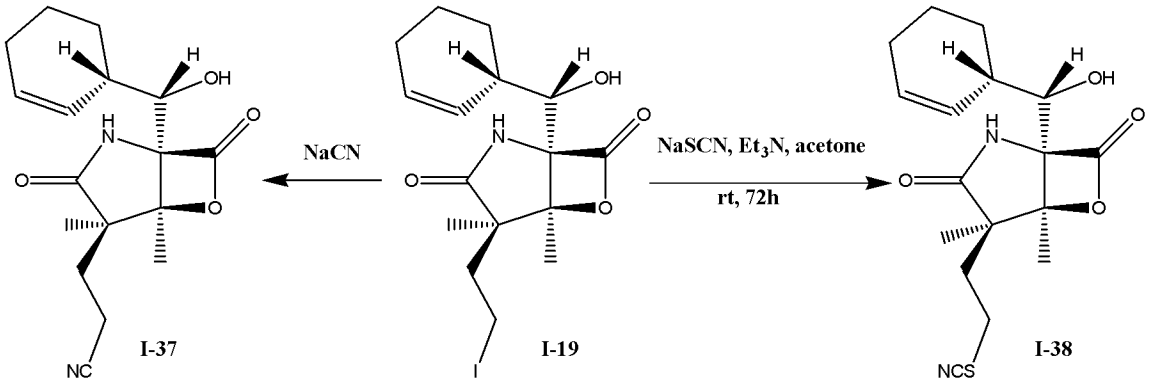

EXAMPLE 17

SYNTHESIS OF THE COMPOUND OF FORMULA I-39 FROM I-19

[0226] Thiols and thioethers of the Formula I-39 can be formed by dehalogenation of the compound of Formula I-19. Thiols (R=H) can be formed by treatment of Compound I-19 with NaSH, for example, while thioethers (R=alkyl) can be formed by treatment of Compound I-19 with salts of thiols, or alternatively, by treatment with thiols themselves by running the reaction in benzene in the presence of DBU.

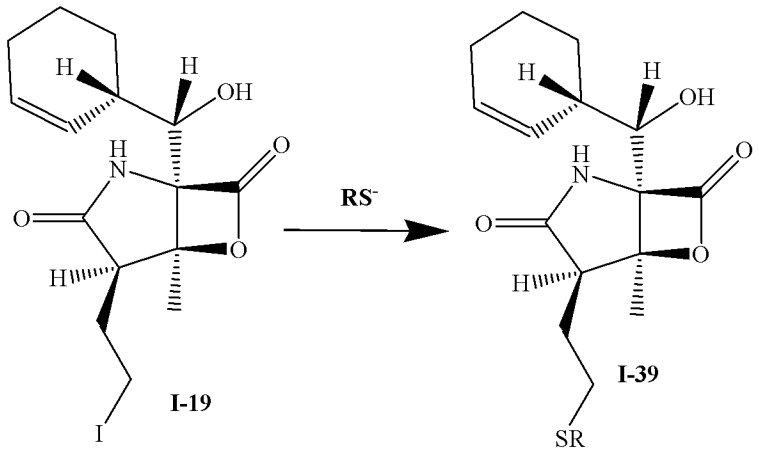

EXAMPLE 18

SYNTHESIS OF THE COMPOUND OF FORMULA I-40 FROM I-39

[0227] Sulfoxides (n=1) and sulfones (n=2) of the Formula I-40 can be formed by oxidation of thioethers of the Formula I-39, for example, with hydrogen peroxide or other oxidizing agents.

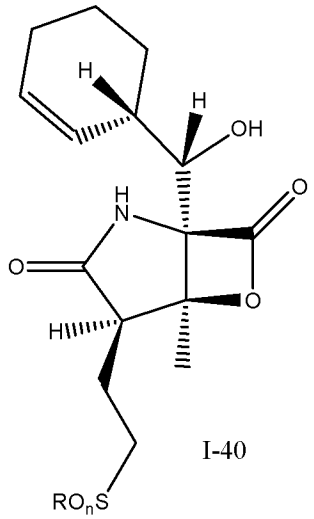

I-40

EXAMPLE 19

SYNTHESIS OF THE COMPOUND OF FORMULA I-41A FROM I-21

[0228] The compound of the Formula I-41A can be prepared by treatment of the compound of Formula I-21 (or a protected derivative of I-21, where the C-5 alcohol or lactam NH are protected, for example) with methyl sulfonyl chloride (mesyl chloride) in pyridine, for example, or by treatment with mesyl chloride in the presence of triethylaminde. Other sulfonate esters can be similarly prepared.

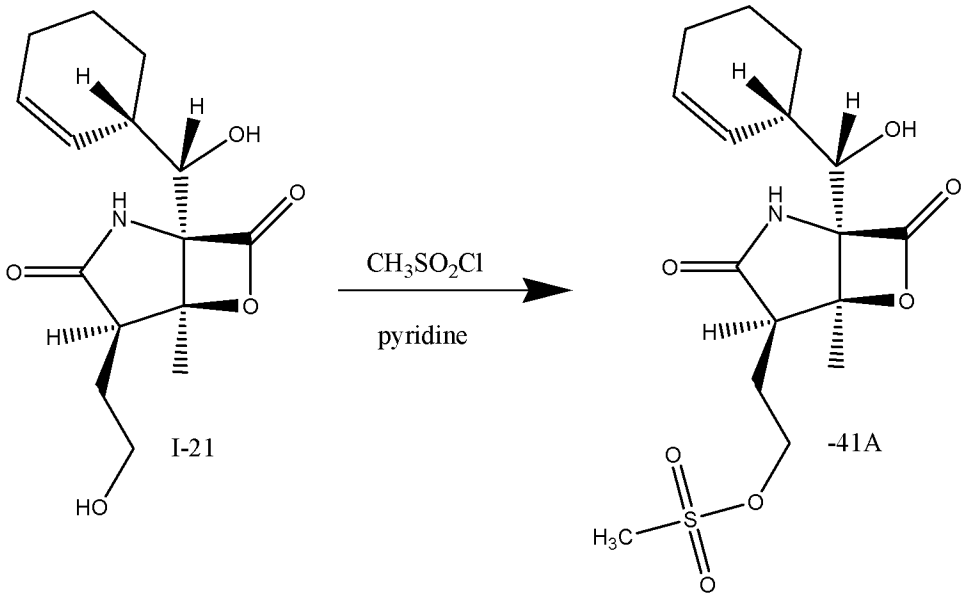

EXAMPLE 20

SYNTHESIS OF THE COMPOUND OF FORMULA I-46 FROM I-19 OR I-41A

[0229] The alkene of the Formula I-46 can be prepared by dehydroiodination of the compound of Formula I-19, or by hydro-mesyloxy elimination of the compound of Formula I-41A, for example, by treatment with base.

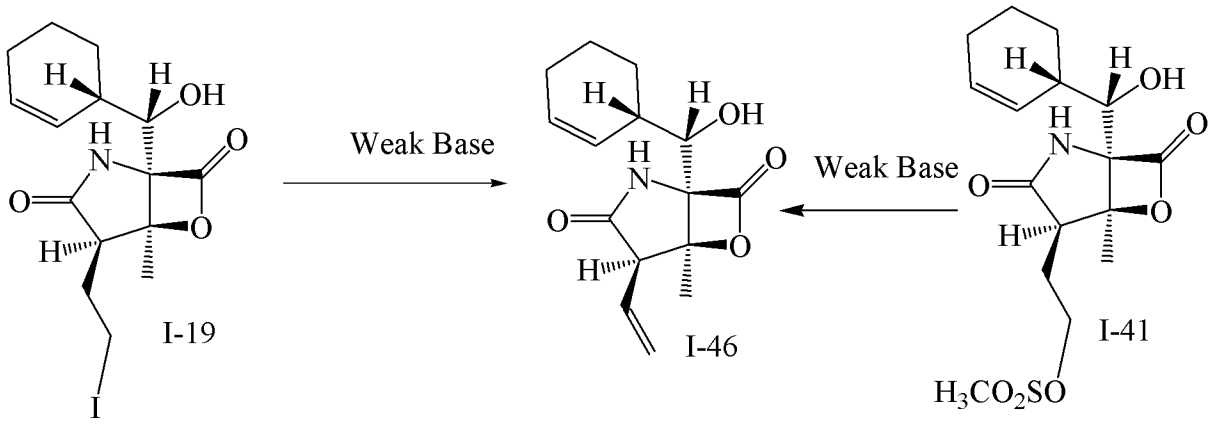

EXAMPLE 21

SYNTHESIS OF THE COMPOUND OF FORMULA I-42A

[0230] Synthesis of boronic acids or esters, for example, the compound of the Formula I-42A, can be achieved as outlined in the retrosynthetic scheme below. Hydroboration of the alkene of Formula I-46 gives the corresponding alkyl borane, which can be converted to the corresponding boronic acid or ester, for example, the compound of the Formula I-42A.

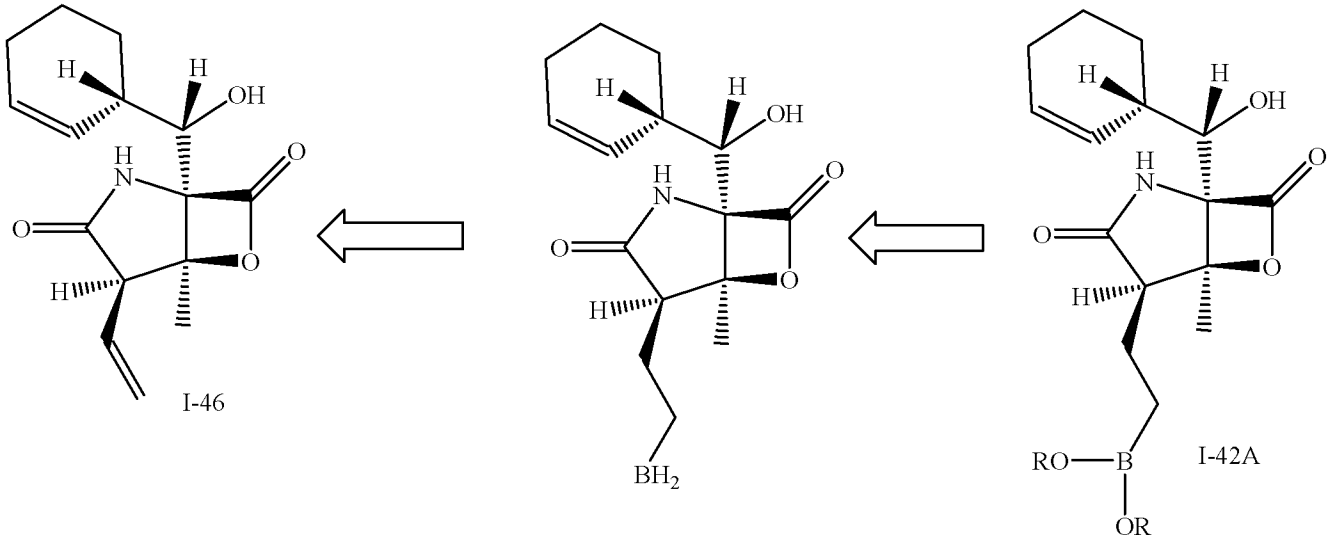

EXAMPLE 22

SYNTHESIS OF THE COMPOUND OF FORMULA I-43A

[0231] The compound of the Formula I-43A can be prepared by treatment of the compound of Formula I-19 with triphenyl phosphine to make a phosphorus ylide, which can be treated with various aldehydes, for example, glyoxylic acid methyl ester, to make Formula I-43A.

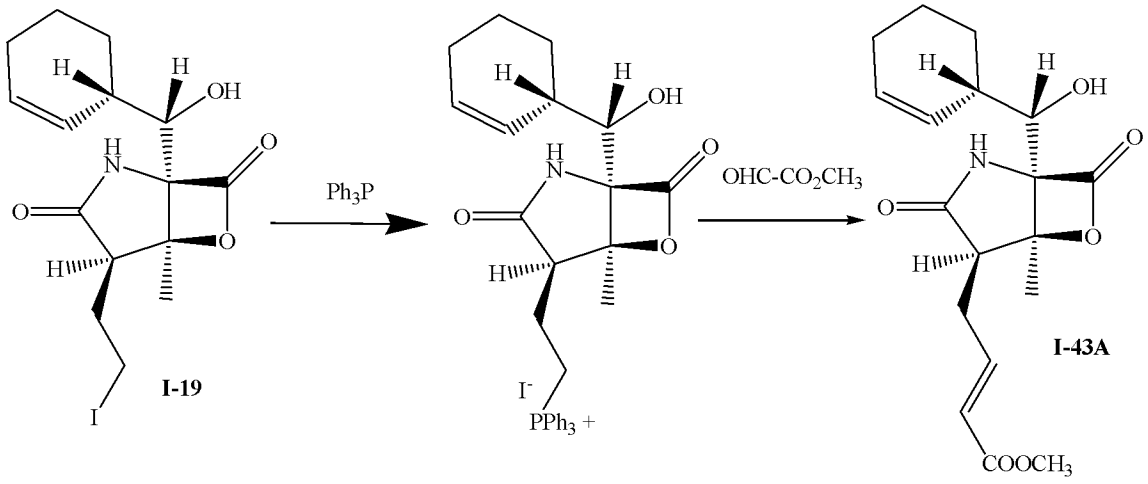

EXAMPLE 23

SYNTHESIS OF THE COMPOUND OF FORMULA I-30 FROM I-19

[0232] A portion of CuI (100 mg) was placed in a 25 ml pear bottom flask and flushed with Ar gas for 30 minutes. Ar gas flow was maintained through the flask throughout the course of the reaction. The vessel was cooled to -78 °C prior to addition of dry THF (5 ml) followed by the immediate dropwise addition of a solution of methyllithium in dry THF (5.0 ml, 1.6 M) with vigorous stirring. A solution of Compound I-19 in dry THF (12 mg Compound I-19, 1 ml THF) was added slowly to the clear dialkylcuprate solution and the resulting mixture stirred at -78 °C for 1 hr. The reaction was quenched by washing the THF solution through a plug of silica gel (1 cm diameter by 2 cm length) along with further washing using a solution of 50% EtOAc / 50% hexanes (50 ml). The combined silica plug washes were dried *in vacuo* and subjected to further C18 HPLC purification in 2 injections (ACE 5μ C18-HL, 150 mm X 21 mm ID) using an isocratic solvent gradient consisting of 35% acetonitrile / 65% H_20. Compound I-30 eluted under these conditions at 23.5 minutes and yielded 2.4 mg material (27% isolated yield) at 90.8% purity as measured by analytical HPLC. An alternative normal phase purification method can be utilized using Phenomenex Luna 10μ Silica column (25cm x 21.2 mm ID) with a solvent gradient consisting of 100% hexanes/ethyl acetate to 0% hexanes over 20 minutes. Compound I-30 eluted under these conditions at 16.5 minutes and yielded 3.0 mg material (41% isolated yield) at 97.1% purity as measured by analytical HPLC.

[0233] Compound I-30: UV (Acetonitrile/H_2O) 225 (sh), ESMS, *m/z* 294.1 (M+H); HRMS (ESI), *m/z* 294.1696 $[M+H]^+$, Δ_{calc}= -3.2 ppm, $C_{16}H_{24}NO_4$; ^1H NMR in DMSO-d_6.

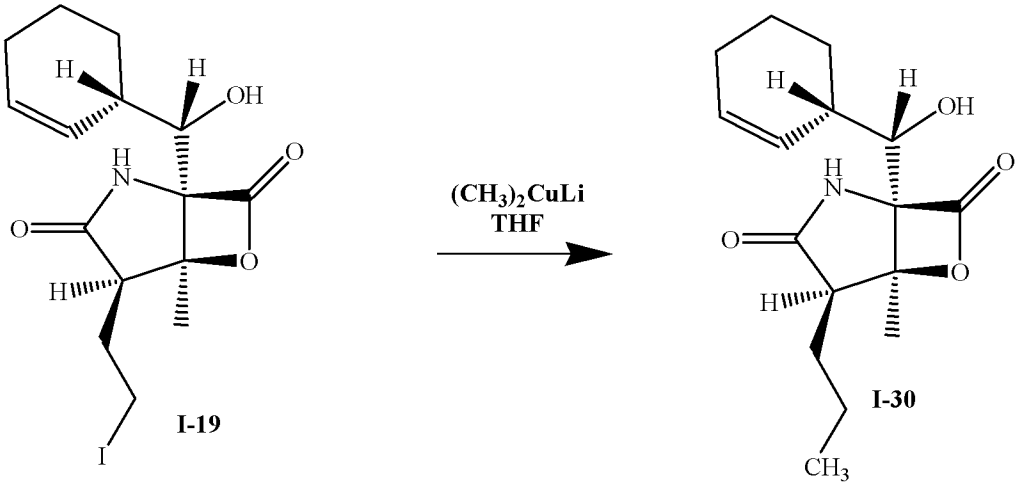

[0234] Compound I-30 can also be obtained by saline fermentation of strain CNB476. In one example, CNB476 was transferred to 500-mL flasks containing 100 mL production medium consisting of the following per liter of deionized water: starch, 10 g; yeast extract, 4 g; Hy-Soy, 4 g; ferric sulfate, 40 mg; potassium bromide, 100mg; calcium carbonate, 1g; and synthetic sea salt, 30g. The production cultures were incubated at 28°C and 250 rpm for 1 day. Approximately 2 g of sterile Amberlite XAD-7 resin was added to the production cultures. The production cultures were further incubated for 5 days. The resin was recovered from the broth and extracted with ethyl acetate. The extract was dried *in vacuo*. The dried extract (8 g) was then processed for the recovery of Compound I-30.

[0235] The crude extract was processed by flash chromatography using a Biotage Flash system. The flash chromatography was developed by the following step gradient: i) Hexanes (1L); I) 10% EtOAc in hexanes (1L); Ii) 20% EtOAc in hexanes, first elution (1L); iv) 20% EtOAc in hexanes, second elution (1L); v) 20% EtOAc in hexanes, third elution (1L); vi) 25% EtOAc in hexanes (1L); vI) 50% EtOAc in hexanes (1L); vIi) EtOAc (1L). Fractions containing Compound I-30 was further purified by normal phase HPLC using an isocratic solvent system of 24% EtOAc/hexanes followed by a 100% EtOAc. Compound I-30 eluted 22 minutes into the isocratic portion of the run.

[0236] Fractions enriched in Compound I-30 were further processed by normal phase HPLC using a 27 minute linear gradient from 15% hexanes/85% EtOAc to 100% EtOAc. Compound I-30 eluted after 15 min.

EXAMPLE 24

SYNTHESIS OF THE COMPOUND OF FORMULAE I-44 AND VI-1A FROM I-16

[0237] The compound of Formula I-16 (30 mg, 0.096 mmol) was dissolved in CH_2Cl_2 (9 ml) in a scintillation vial (20 ml) to which triethylamine (40 µl, 0.29 mmol), methyl-3-mercapto propionate (thiol, 250 µl) and a magnetic stir bar were added. The reaction mixture was stirred at room temperature for about 4 hours. The solvent was evaporated from the reaction mixture to yield a mixture of compounds of Formulae I-44 and VI-1A (19:1), which were separated by reversed phase HPLC using Ace 5u C18 column (150 mm x 22 mm ID) with a solvent gradient of 35% to 90% H_2O/Acetonitrile over 17 min, 90 to 100% Acetonitrile over1 min, holding at 100% Acetonitrile for 1 min, at a flow rate of 14.5 ml/min. Diode array detector was used to monitor the purification process. Compounds I-44 (20 mg) and VI-1A (1 mg) eluted at 11.68 and 10.88 min, respectively, as pure compounds. Compound I-44: UV (Acetonitrile/H_2O) λ_{max} 240 (sh) nm; ESMS *m/z* 434.0 $(M+H)^+$ & 456.0 $(M+Na)^+$. Compound VI-1A: UV (Acetonitrile/H_2O) λ_{max} 220 (sh) nm; ESMS, *m/z* 398.0 $(M+H)^+$ & 420.0 $(M+Na)^+$.

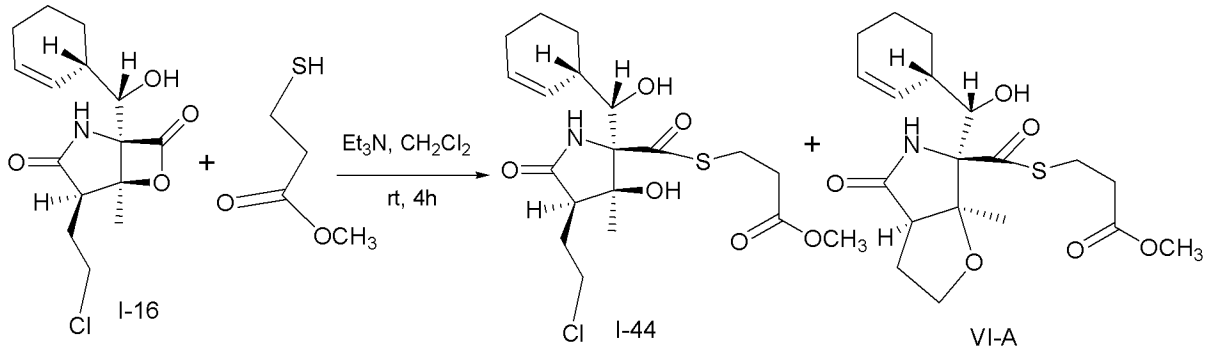

EXAMPLE 25

OXIDATION OF SECONDARY HYDROXYL GROUP IN COMPOUNDS OF FORMULAE I-16, I-17 AND I-18 AND REACTION WITH HYDROXY OR METHOXY AMINES

[0238] Any of the compounds of Formulae I-16, I-17 and I-18 can be used as the starting compound. The secondary hydroxyl group in the starting compound is oxidized using either of the following reagents: pyridinium dichromate (PDC), pyridinium chlorochromate (PCC), Dess-Martin periodinane or oxalyl chloride (Swern oxidation) (Ref: Organic Syntheses, collective volumes I-VII). Preferably, Dess-Martin periodinane can be used as a reagent for this

reaction. (Ref: Fenteany G. *et al.* Science, **1995**, *268*, 726-73). The resulting keto compound is treated with hydroxylamine or methoxy amine to generate oximes.

Examples:

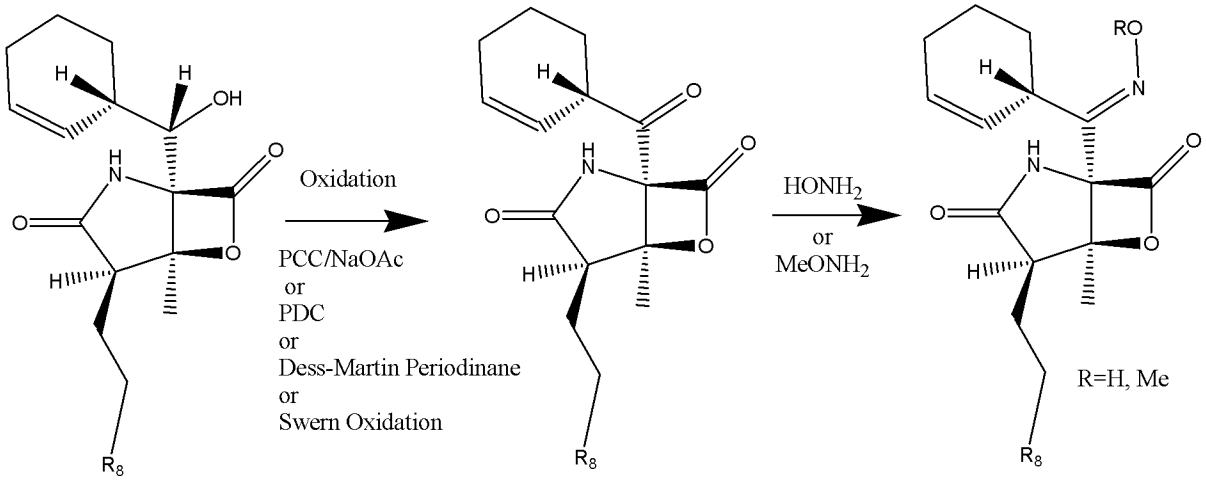

Starting Compound I-13 I-9

EXAMPLE 26

REDUCTIVE AMINATION OF KETO-DERIVATIVE

[0239] The keto derivatives, for example Formula I-8 and I-13, are treated with sodium cyanoborohydride ($NaBH_3CN$) in the presence of various bases to yield amine derivatives of the starting compounds which are subsequently hydrogenated with 10%Pd/C, H_2 to reduce the double bond in the cyclohexene ring.

Example:

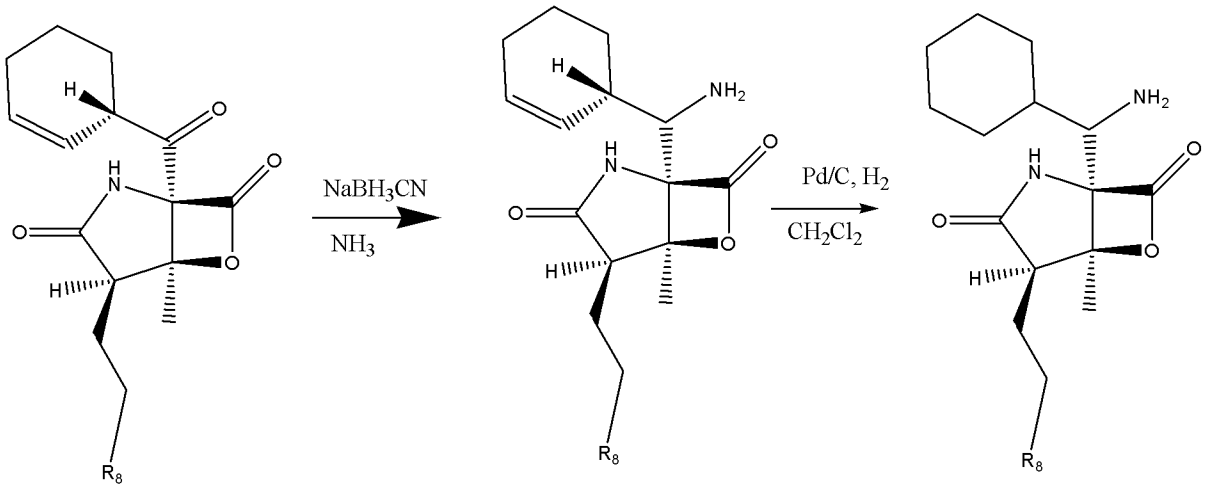

I-13 I-11 I-12

EXAMPLE 27

CYCLOHEXENE RING OPENING

[0240] Any compound of Formulae I-16, I-17 and I-18 can be used as a starting compound. The Starting Compounds can be protected, for example, at the alcohol and/or at the lactam nitrogen positions, and treated with OsO_4 and $NaIO_4$ in THF-H_2O solution to yield dial derivatives which are reduced to the alcohol with $NaBH_4$. The protecting groups can be removed at the appropriate stage of the reaction sequence to produce I-7 or I-6.

Example:

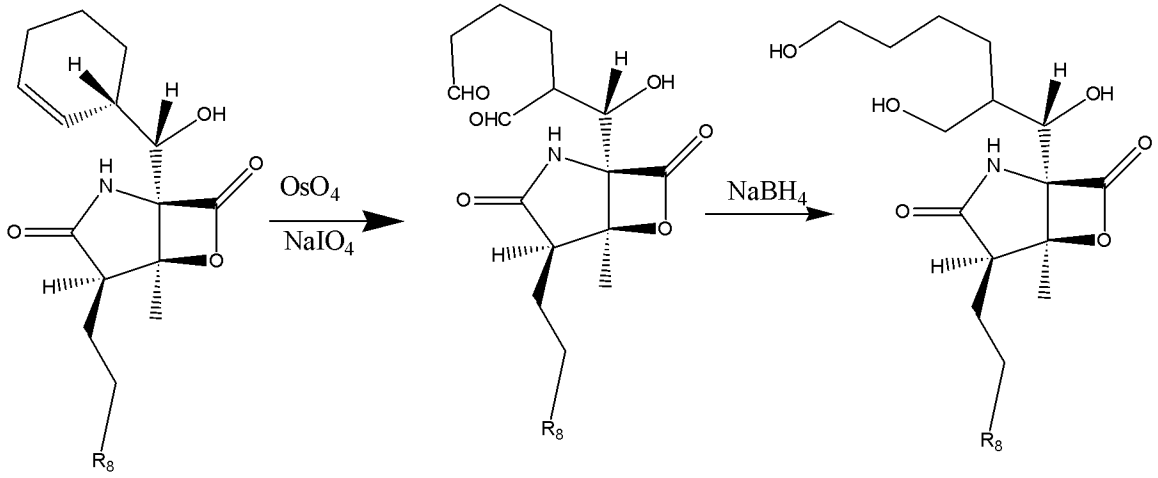

Starting Compound I-7 I-6

EXAMPLE 28

DEHYDRATION OF ALCOHOL FOLLOWED BY ALDEHYDE FORMATION AT LACTONE-LACTAM RING JUNCTION

[0241] A starting compound of any of Formulae I-16, I-17 or I-18 is dehydrated, for example, by treatment with mesylchloride in the presence of base, or, for example, by treatment with Burgess reagent or other dehydrating agents. The resulting dehydrated compound is treated with OsO_4, followed by $NaIO_4$, or alternatively by ozonolysis, to yield an aldehyde group at the lactone-lactam ring junction.

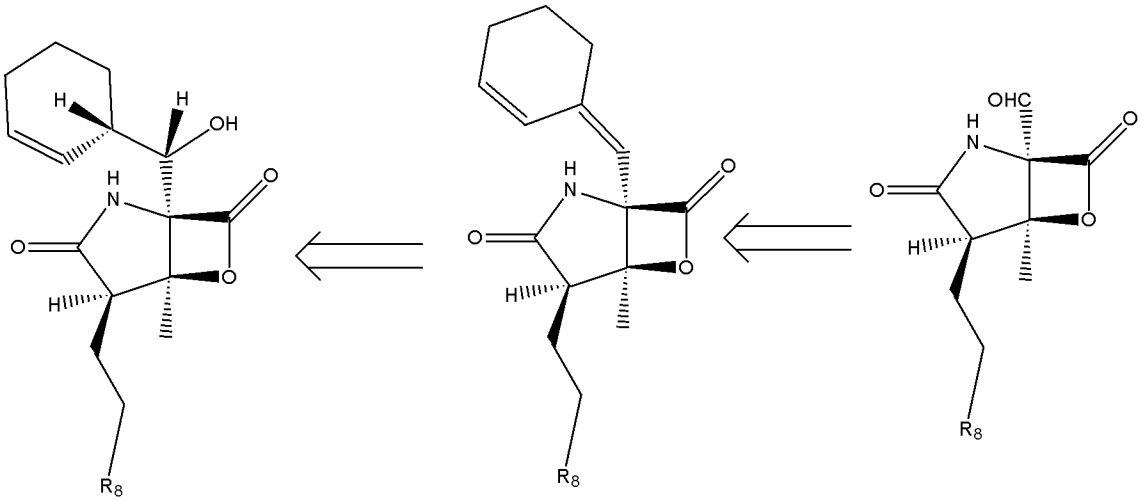

Starting Compound I-6 I-1

EXAMPLE 29

OXIDATION OF THE CYCLOHEXENE RING TO PRODUCE CYCLOHEXADIENES OR A PHENYL RING

[0242] A Starting Compound, such as the ketone of Formula I-13C, is treated with Pd/C to produce a cyclohexadiene derivative. The new double bond can be at any position of the cyclohexene ring. The ketone can be reduced, for example, with sodium borohydride, to obtain the corresponding secondary alcohol(s). Alternatively, the cyclohexadiene derivative can be further treated, for example with DDQ, to aromatize the ring to a phenyl group. Similarly, the ketone can be reduced, for example, with sodium borohydride, to obtain the corresponding secondary alcohol(s).

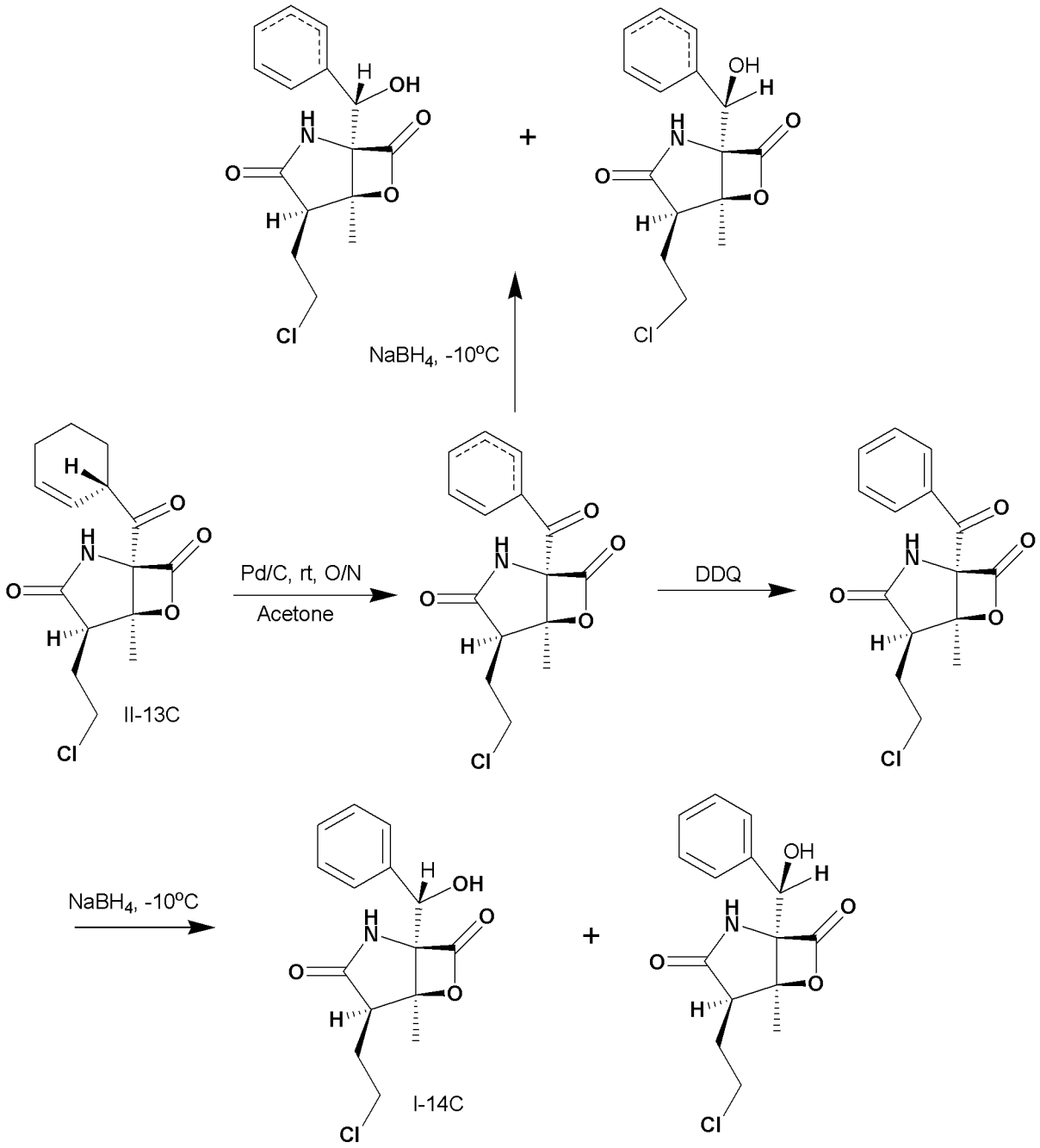

[0243] As an alternate method, the starting compound, such as the compound of Formula I-49, can be treated, for example with TMSCl to produce cyclohexadiene derivative. The cyclohexadiene derivative can be further treated, for example with DDQ, to aromatize the ring to a phenyl group. The OTMS on the phenyl group can be removed, for example, with acid or base. Similarly, the ketone can be reduced, for example, with sodium borohydride, to obtain the corresponding secondary alcohol(s).

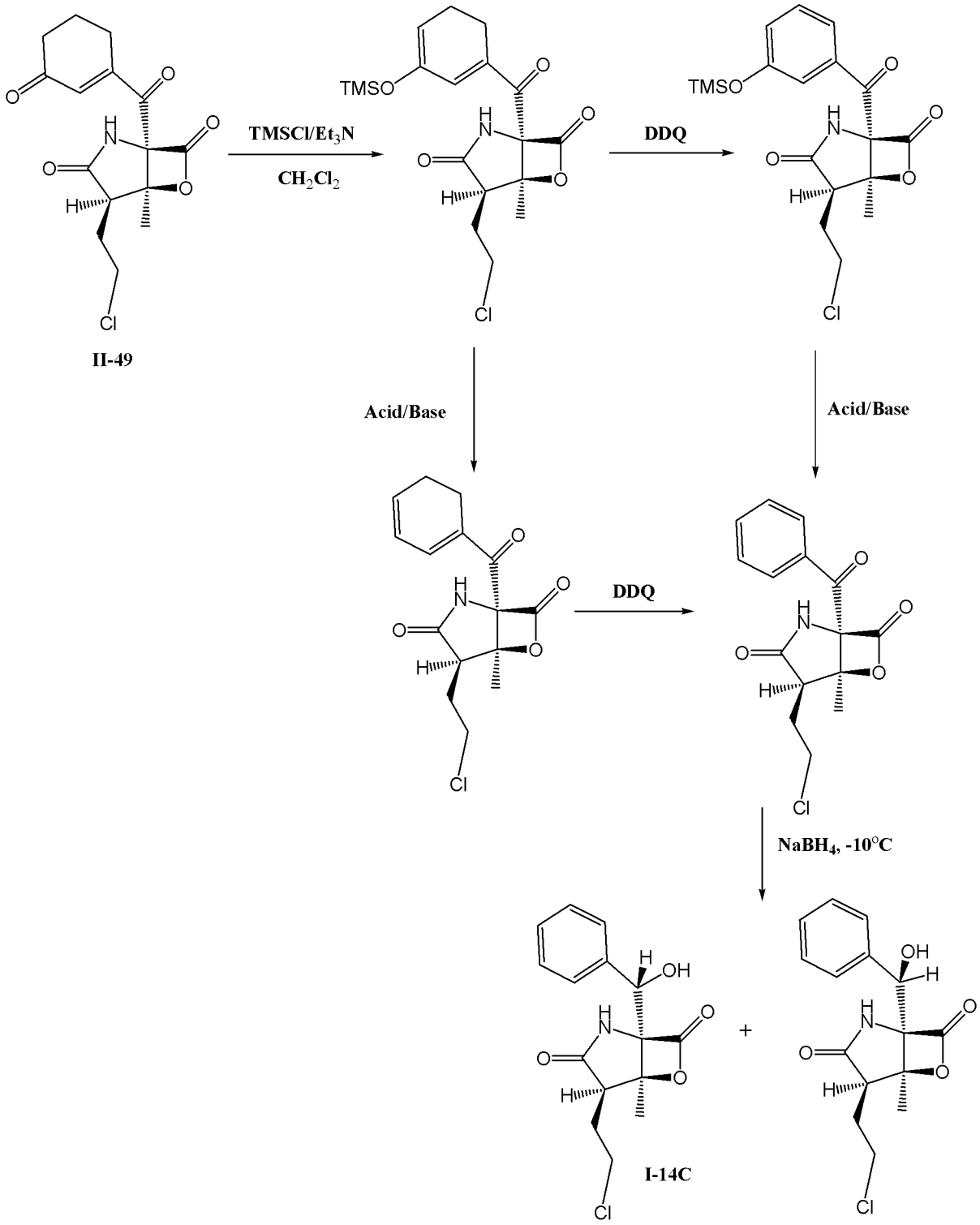
TMSCl/Et3N
CH2Cl2
DDQ
Acid/Base
Acid/Base
DDQ
NaBH4, -10°C
II-49
I-14C
TMSO
TMSO
OH
H
Cl
N
O

EXAMPLE 30

SYNTHESIS OF THE COMPOUND OF FORMULA I-47 FROM I-17

[0244] The compound of Formula I-17 (25 mg, 0.0896 mmol) was dissolved in CH_2Cl_2 (9 ml) in a scintillation vial (20 ml) to which triethylamine (38 µl, 0.27 mmol), methyl-3-mercapto propionate (thiol, 250 µl) and a magnetic stir bar were added. The reaction mixture was stirred at room temperature for about 4 hours. The solvent was evaporated from the reaction mixture to yield the compound of Formulae I-47, which was further purified by normal phase HPLC using Phenomenex Luna 10u Silica column (25 cm x 21.2 mm ID) with a solvent gradient of 10% to 100% Hexane/EtOAc over 24 min, holding at 100% EtOAc for 3 min, at a flow rate of 14.5 ml/min. ELSD was used to monitor the purification process. Compound I-47 (15 mg) eluted at 10.98 min as pure compound. Compound I-47: UV (Acetonitrile/H_2O) λ_{max} 240 (sh) nm; ESMS *m/z* 400.1 $(M+H)^+$ & 422.1 $(M+Na)^+$.

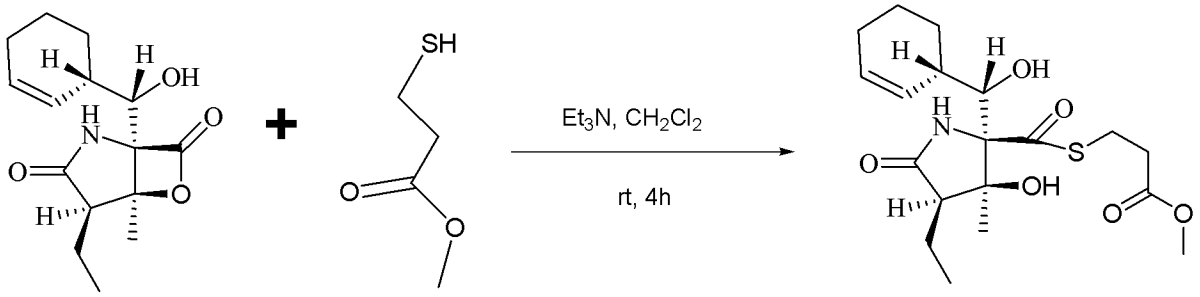

I-17 I-47

EXAMPLE 31

SYNTHESIS OF THE COMPOUND OF FORMULAE I-48 AND VI-1B FROM I-16

[0245] The compound of Formula I-16 (15 mg, 0.048 mmol) was dissolved in 1:1 ratio of ACN/DMSO (8 ml) in a scintillation vial (20 ml) to which triethylamine (40 µl, 0.29 mmol), Glutathione (44.2 mg, 0.144 mmol) and a magnetic stir bar were added. The reaction mixture was stirred at room temperature for about 3 hours. The solvent was evaporated from the reaction mixture to yield the compound of Formula I-48, which was purified by reversed phase HPLC using Ace 5u C18 column (150 mm x 22 mm ID) with a solvent gradient of 10% to 70% H_2O/Acetonitrile over 15 min, 70 to 100% Acetonitrile over 5 min, holding at 100% Acetonitrile for 4 min, at a flow rate of 14.5 ml/min. Diode array detector was used to monitor the

purification process. Compound I-48 (10 mg) eluted as a pure compound at 8.255 min. Compound I-48: UV (Acetonitrile/H_2O) λ_{max} 235 (sh) nm; ESMS *m/z* 621.0 $(M+H)^+$. Compound I-48 was unstable in solution and converted to compound VI-1B which appeared as a mixture of I-48 and VI-1B in the ratio of 7:3. Compound VI-1B: UV (Acetonitrile/H_2O) λ_{max} 235 (sh) nm; ESMS, *m/z* 585.2 $(M+H)^+$.

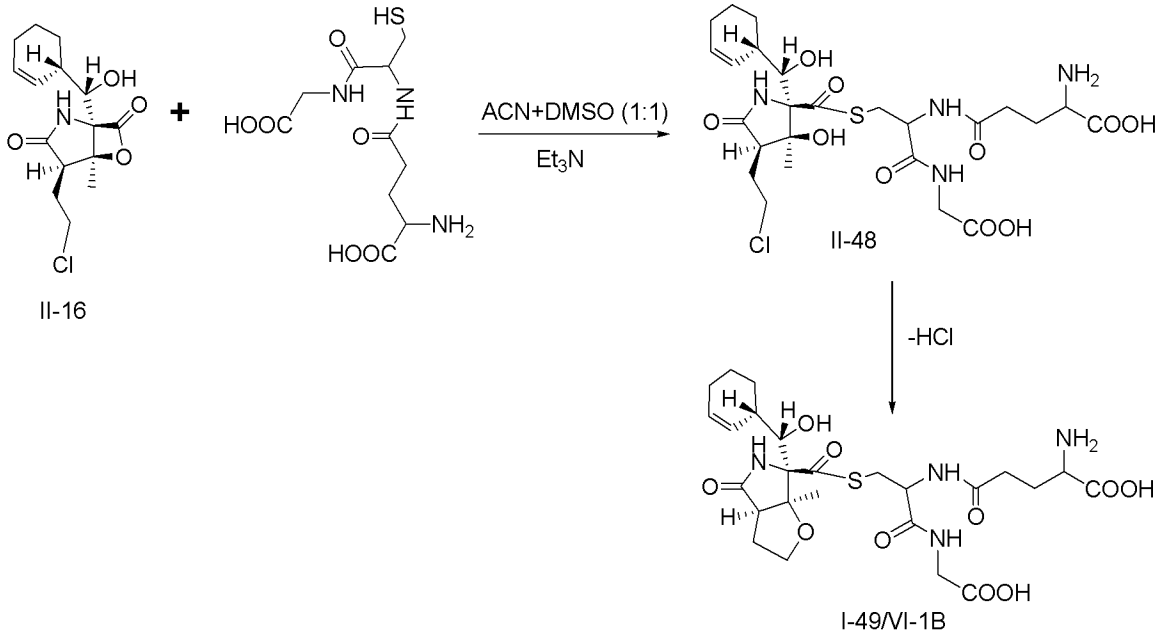

EXAMPLE 32

SYNTHESIS OF THE COMPOUND OF FORMULA I-50 AND VI-1C FROM I-16

[0246] The compound of Formula I-16 (10 mg, 0.032 mmol) was dissolved in CH_2Cl_2 (9 ml) in scintillation vial (20 ml) to which triethylamine (26.5 µl, 0.192 mmol), N-Acetyl-L-Cysteine methyl ester (17mg, 0.096 mmol) and a magnetic stir bar were added. The reaction mixture was stirred at room temperature for about 4 hours. The solvent was evaporated from the reaction mixture to yield the mixture of compounds of Formulae I-50 and VI-1C, which were further purified by normal phase HPLC using Phenomenex Luna 10u Silica column (25 cm x 21.2 mm ID) with a solvent gradient of 10% to 100% Hexane/EtOAc over 24 min, holding at 100% EtOAc for 3 min, at a flow rate of 14.5 ml/min. ELSD was used to monitor the purification process. Compounds I-50 (2 mg) and VI-1C (0.2 mg) were eluted at 10.39 and 10.57 min, respectively as pure compounds. Compound I-50: UV (Acetonitrile/H_2O) λ_{max} 230

(sh) nm; ESMS *m/z* 491.1 $(M+H)^+$ & 513.0 $(M+Na)^+$. Compound VI-1C: UV (Acetonitrile/H_2O) λ_{max} 215 (sh) nm; ESMS *m/z* 455.1 $(M+H)^+$ & 577.0 $(M+Na)^+$

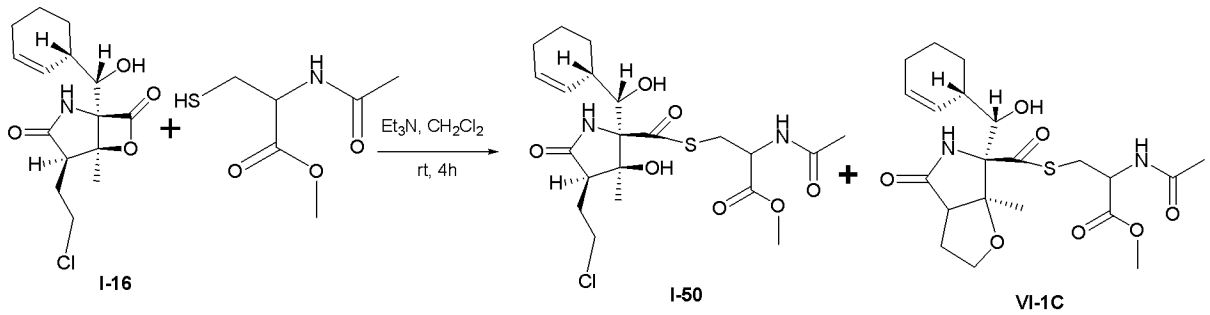

I-16 I-50 VI-1C

EXAMPLE 33

FORMULATION TO BE ADMINISTERED ORALLY OR THE LIKE

[0247] A mixture obtained by thoroughly blending 1 g of a compound obtained and purified by the method of the embodiment, 98 g of lactose and 1 g of hydroxypropyl cellulose is formed into granules by any conventional method. The granules are thoroughly dried and sifted to obtain a granule preparation suitable for packaging in bottles or by heat sealing. The resultant granule preparations are orally administered at between approximately 100 ml/day to approximately 1000 ml/day, depending on the symptoms, as deemed appropriate by those of ordinary skill in the art of treating cancerous tumors in humans.

EXAMPLE 34

PROLONGED G1 ARREST PRIMES MYELOMA CELLS TO KILLING BY CHEMOTHERAPY

[0248] MM1.S cells were cultured in the presence and absence of 0.25 uM of PD 0332991 (PD) for 24 hr before treatment with 4nm Salinosporamide A (NPI) for 24 hr. The percentage of viable cells was determined by adding BrdU followed by FACS analysis. Total viable cells were determined by trypan blue exclusion and presented as a percentage of the number of cells at the start. The loss of mitochondria depolarization was assayed using the JC-1 dye. The results are depicted in Figures 1A-1C. The results indicate synergistic killing of cycling cells with preferential killing in the S phase, given the concomitant loss of S phase cells and gain of dead cells as well as the proportion, but not the absolute number, of G2/M cells.

Inhibition of Cdk4/6 by PD 0332991 prolonged G1 arrest but did not induce apoptosis, because the cessation of BrdU uptake was coincidental with a striking increase in the proportion of cells in G1 but not dead cells. Prolonging G1 arrest induced by PD 0332991, therefore, primes myeloma cells to killing by Salinosporamide A and overcomes chemoresistance through synergistic induction of mitochondrial depolarization.

EXAMPLE 35

PRIMING PRIMARY MYELOMA CELLS TO OVERCOME CHEMORESISTANCE BY SUSTAINED G1 ARREST

[0249] In some bortezomib-refractory cases, primary myeloma cells (MM 10) were susceptible to salinosporamide A, but were rendered sensitive to bortezomib by PD 0332991 pretreatment, by 4 hours and increased with time due to caspase activation as indicated by the cleavage of poly (AOP-ribose) polymerase-1 (PARP) (Fig. 2A).

[0250] In still other bortezomib-refractory cases, BM myeloma cells (MM11) remained resistance to bortezomib (6 nM) ex vivo for 3 days even in the presence PD 0332991. However, replacing salinosporamide A for bortezomib led to a drastic loss of viability, to near eradication by day 7 in the presence of PD 0332991 (Fig. 2B). While it remains possible that similar level of killing might be achieved by prolonging bortezomib treatment further, these results demonstrate that bortezomib resistance can be overcome by salinosporamide A, in particular in combination with sustained G1 arrest induced by PD 0332991. Consistent with this possibility, PD 0332991 pretreatment for 24 hours rendered BM myeloma cells (MM 12) that were extremely resistant to both bortezomib and salinosporamide A moderately sensitive to salinosporamide A (Fig. 2C).

[0251] Thus, combining sustained G1-arrest induced by PD 0332991 with a selective proteasome inhibitor induces synergistic killing of primary BM myeloma cells and overcomes chemoresistance despite protection by BM stromal cells.

Supplementary Table 1.- Clinical Information of Myeloma Cases in This Study

Figure	MM#	Age	Dx	Stage	Ig Isotype	Prior Tx
2A	10	55	MM	III	Gκ	Y
2B	11	84	MM	II	‘κ	Y*

2C	12	57	MM	II	‘λ	Y

Dx, Diagnosis; MM, multiple myeloma; Stage, Durie-Salmon staging; Ig, Immunoglobuling (‘denotes absence of immunoglobulin heavy chains); Prior Tx: Y – Treated, N – Treatment Naïve, Y* - Resistant to bortezomib, Y** - Responding to bortezomib.

[0252] The examples described above are set forth solely to assist in the understanding of the embodiments. Thus, those skilled in the art will appreciate that the methods may provide derivatives of compounds.

[0253] One skilled in the art would readily appreciate that the present invention is well adapted to carry out the objects and obtain the ends and advantages mentioned, as well as those inherent therein. The methods and procedures described herein are presently representative of preferred embodiments and are exemplary and are not intended as limitations on the scope of the invention. Changes therein and other uses will occur to those skilled in the art which are encompassed within the spirit of the invention.

[0254] It will be readily apparent to one skilled in the art that varying substitutions and modifications can be made to the embodiments disclosed herein without departing from the scope and spirit of the invention.

[0255] All patents and publications mentioned in the specification are indicative of the levels of those skilled in the art to which the invention pertains. All patents and publications are herein incorporated by reference to the same extent as if each individual publication was specifically and individually indicated to be incorporated by reference.

[0296] The invention illustratively described herein suitably can be practiced in the absence of any element or elements, limitation or limitations which is not specifically disclosed herein. The terms and expressions which have been employed are used as terms of description and not of limitation, and there is no intention that in the use of such terms and expressions indicates the exclusion of equivalents of the features shown and described or portions thereof. It is recognized that various modifications are possible within the scope of the invention. Thus, it should be understood that although the present invention has been specifically disclosed by preferred embodiments and optional features, modification and variation of the concepts herein disclosed can

be resorted to by those skilled in the art, and that such modifications and variations are considered to be falling within the scope of the embodiments of the invention.

WHAT IS CLAIMED IS:

1. A method of treating cancer comprising administering to an animal PD 0332991 in combination with a compound having the structure of Formula I, or a pharmaceutically acceptable salt or pro-drug ester thereof, wherein PD 0332991 and the compound of Formula I have the structures:

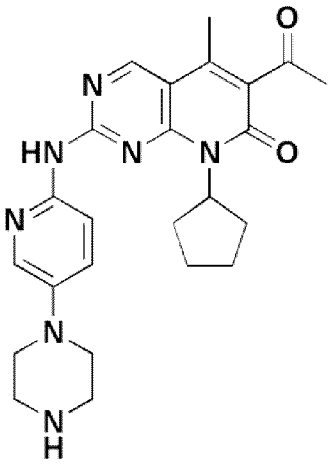

PD 0332991

and

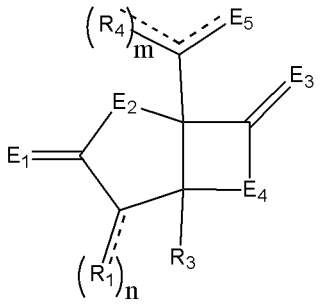

Formula I

wherein R_1, R_3, and R_4 are separately selected from the group consisting of a hydrogen, a halogen, a mono-substituted, a poly-substituted or an unsubstituted variant of the following residues: saturated C_1-C_{24} alkyl, unsaturated C_2-C_{24} alkenyl or C_2-C_{24} alkynyl, acyl, acyloxy, alkyloxycarbonyloxy, aryloxycarbonyloxy, cycloalkyl, cycloalkenyl, alkoxy, cycloalkoxy, aryl, heteroaryl, arylalkoxy carbonyl, alkoxy carbonylacyl, amino, aminocarbonyl, aminocarboyloxy, nitro, azido, phenyl, cycloalkylacyl, hydroxy, alkylthio, arylthio, oxysulfonyl, carboxy, cyano, thio, sulfoxide, sulfone, sulfonate esters, thiocyano, boronic acids and esters, and halogenated alkyl including polyhalogenated alkyl;

wherein m is equal to 1 or 2;

wherein n is equal to 1 or 2;

wherein each of E_1, E_2, E_3 and E_4 is a substituted or unsubstituted heteroatom; and

wherein E_5 is selected from the group consisting of OH, O, OR_{10}, S, SR_{11}, SO_2R_{11}, NH, NH_2, NOH, NHOH, NR_{12}, and $NHOR_{13}$.

2. The method of Claim 1, wherein R_{10-13} are selected from the group consisting of hydrogen and a substituted or unsubstituted variant of any of the following: C_{1-24} alkyl, aryl, and heteroaryl.

3. The method of Claim 1, wherein the cancer is a hematological malignancy.

4. The method of Claim 3, wherein the hematological malignancy is multiple myeloma.

5. The method of Claim 1, wherein the animal is a mammal.

6. The method of Claim 1, wherein the animal is a human.

7. The method of Claim 1, wherein the animal is a rodent.

8. The method of Claim 1, further comprising co-administering another chemotherapeutic agent.

9. The method of Claim 8, wherein the additional chemotherapeutic agent is selected from the group consisting of Adriamycin, Doxorubicin, 5-Fluorouracil, Cytosine arabinoside ("Ara-C"), Cyclophosphamide, Thiotepa, Busulfan, Cytoxin, Taxol, Toxotere, Methotrexate, Cisplatin, Melphalan, Vinblastine, Bleomycin, Etoposide, Ifosfamide, Mitomycin C, Mitoxantrone, Vincreistine, Vinorelbine, Carboplatin, Teniposide, Daunomycin, Carminomycin, Aminopterin, Dactinomycin, Mitomycins, Esperamicins, Melphalan, tamoxifen and onapristone.

10. The method of Claim 8, wherein the additional chemotherapeutic agent is a proteasome inhibitor.

11. The method of Claim 9, wherein the proteasome inhibitor is bortezomib.

12. The method of Claim 8, wherein the additional chemotherapeutic agent is a histone deacetylase inhibitor.

13. The method of Claim 12, wherein the histone deacetylase inhibitor is selected from the group consisting of MS-275, APHA compound 8, Apicidin, (−)-Depudecin, sodium butyrate, Scriptaid, Sirtinol, Trichostatin A, Valproic acid (VPA) and Vorinostat (suberoylanilide hydroxamic acid (SAHA)).

14. The method of Claim 8 wherein the additional chemotherapeutic agent is a vascular disrupting agent.

15. The method of Claim 14, wherein the vascular disrupting agent is NPI-2358.

16. The method of Claim 14, wherein the vascular disrupting agent is combratostatin CA4P.

17. A method of treating cancer comprising administering to an animal PD 0332991 in combination with a compound having the structure of Formula I-15, or a pharmaceutically acceptable salt or pro-drug ester thereof:

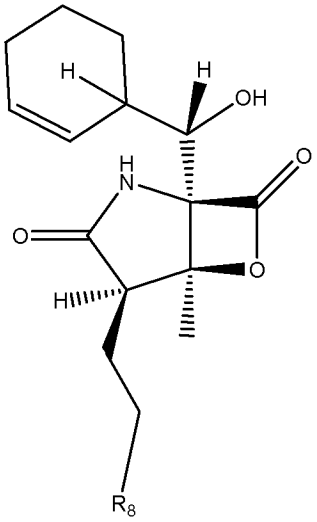

I-15

wherein R_8 is hydrogen, fluorine, chlorine, bromine or iodine.

18. The method of Claim 17, wherein the compound is:

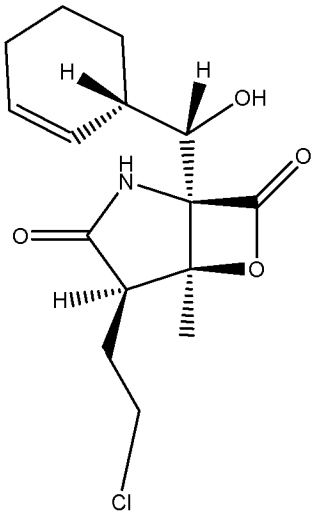

I-16

19. The method of Claim 17, wherein the cancer is multiple myeloma.

20. The method of Claim 17, wherein the animal is a mammal.

21. The method of Claim 17, wherein the animal is a human.

22. The method of Claim 17, wherein the animal is a rodent.

23. The method of Claim 17, further comprising co-administering another chemotherapeutic agent.

24. The method of Claim 23, wherein the additional chemotherapeutic agent is selected from the group consisting of Adriamycin, Doxorubicin, 5-Fluorouracil, Cytosine arabinoside ("Ara-C"), Cyclophosphamide, Thiotepa, Busulfan, Cytoxin, Taxol, Toxotere, Methotrexate, Cisplatin, Melphalan, Vinblastine, Bleomycin, Etoposide, Ifosfamide, Mitomycin C, Mitoxantrone, Vincreistine, Vinorelbine, Carboplatin, Teniposide, Daunomycin, Carminomycin, Aminopterin, Dactinomycin, Mitomycins, Esperamicins, Melphalan, tamoxifen and onapristone.

25. The method of Claim 23, wherein the additional chemotherapeutic agent is a proteasome inhibitor.

26. The method of Claim 25, wherein the proteasome inhibitor is bortezomib.

27. The method of Claim 25, wherein the proteasome inhibitor is carfilzomib.

28. The method of Claim 23, wherein the additional chemotherapeutic agent is a histone deacetylase inhibitor.

29. The method of Claim 28, wherein the histone deacetylase inhibitor is selected from the group consisting of MS-275, APHA compound 8, Apicidin, (−)-Depudecin, sodium butyrate, Scriptaid, Sirtinol, Trichostatin A, Valproic acid (VPA) and Vorinostat (suberoylanilide hydroxamic acid (SAHA)).

30. The method of Claim 23, wherein the additional chemotherapeutic agent is a vascular disrupting agent.

31. The method of Claim 30, wherein the vascular disrupting agent is NPI-2358.

32. The method of Claim 30, wherein the vascular disrupting agent is combratostatin CA4P.

33. A method of inhibiting the growth of a cancer cell comprising contacting the cell with a combination of PD 0332991 and a compound having the structure of Formula I, or a pharmaceutically acceptable salt or pro-drug ester thereof:

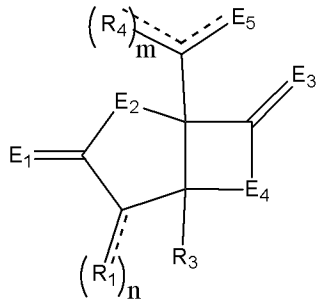

Formula I

wherein R_1, R_3, and R_4 are separately selected from the group consisting of a hydrogen, a halogen, a mono-substituted, a poly-substituted or an unsubstituted variant of the following residues: saturated C_1-C_{24} alkyl, unsaturated C_2-C_{24} alkenyl or C_2-C_{24} alkynyl, acyl, acyloxy, alkyloxycarbonyloxy, aryloxycarbonyloxy, cycloalkyl, cycloalkenyl, alkoxy, cycloalkoxy, aryl, heteroaryl, arylalkoxy carbonyl, alkoxy carbonylacyl, amino, aminocarbonyl, aminocarboyloxy, nitro, azido, phenyl, cycloalkylacyl, hydroxy, alkylthio, arylthio, oxysulfonyl, carboxy, cyano, thio, sulfoxide, sulfone, sulfonate esters, thiocyano, boronic acids and esters, and halogenated alkyl including polyhalogenated alkyl;

wherein m is equal to 1 or 2;

wherein n is equal to 1 or 2;

wherein each of E_1, E_2, E_3 and E_4 is a substituted or unsubstituted heteroatom; and

wherein E_5 is selected from the group consisting of OH, O, OR_{10}, S, SR_{11}, SO_2R_{11}, NH, NH_2, NOH, NHOH, NR_{12}, and $NHOR_{13}$.

34. A method of inhibiting the growth of a cancer cell comprising contacting the cell with a combination of PD 0332991 and a compound having the structure of Formula I-15, or a pharmaceutically acceptable salt or pro-drug ester thereof:

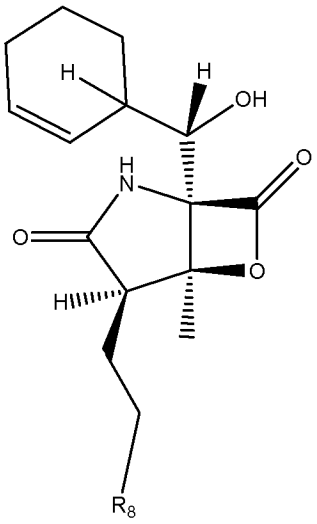

wherein R_8 is hydrogen, fluorine, chlorine, bromine or iodine.

35. The method of Claim 34, wherein the compound is:

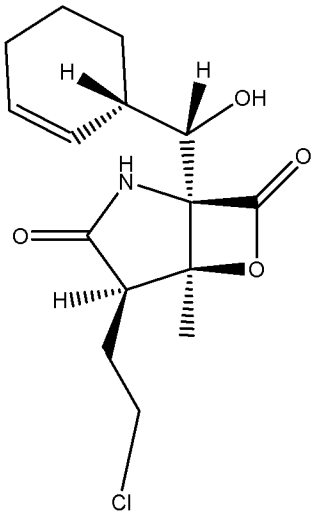

I-16

36. A method of inducing apoptosis of a cancer cell comprising contacting the cell with a combination of PD 0332991 and a compound having the structure of Formula I, and a pharmaceutically acceptable salt or pro-drug ester thereof:

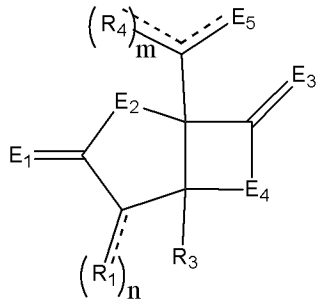

Formula I

wherein R_1, R_3, and R_4 are separately selected from the group consisting of a hydrogen, a halogen, a mono-substituted, a poly-substituted or an unsubstituted variant of the following residues: saturated C_1-C_{24} alkyl, unsaturated C_2-C_{24} alkenyl or C_2-C_{24} alkynyl, acyl, acyloxy, alkyloxycarbonyloxy, aryloxycarbonyloxy, cycloalkyl, cycloalkenyl, alkoxy, cycloalkoxy, aryl, heteroaryl, arylalkoxy carbonyl, alkoxy carbonylacyl, amino, aminocarbonyl, aminocarboyloxy, nitro, azido, phenyl, cycloalkylacyl, hydroxy, alkylthio, arylthio, oxysulfonyl, carboxy, cyano, thio, sulfoxide, sulfone, sulfonate esters, thiocyano, boronic acids and esters, and halogenated alkyl including polyhalogenated alkyl;

wherein m is equal to 1 or 2;

wherein n is equal to 1 or 2;

wherein each of E_1, E_2, E_3 and E_4 is a substituted or unsubstituted heteroatom; and

wherein E_5 is selected from the group consisting of OH, O, OR_{10}, S, SR_{11}, SO_2R_{11}, NH, NH_2, NOH, NHOH, NR_{12}, and $NHOR_{13}$;

37. A method of inducing apoptosis of a cancer cell comprising contacting the cell with a combination of PD 0332991 and a compound having the structure of Formula I-15 and a pharmaceutically acceptable salt or pro-drug ester thereof:

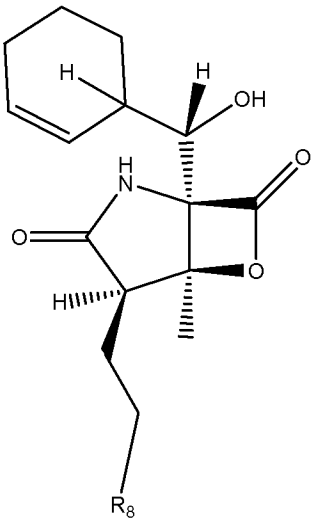

wherein R_8 is hydrogen, fluorine, chlorine, bromine or iodine.

38. The method of Claim 37, wherein the compound is:

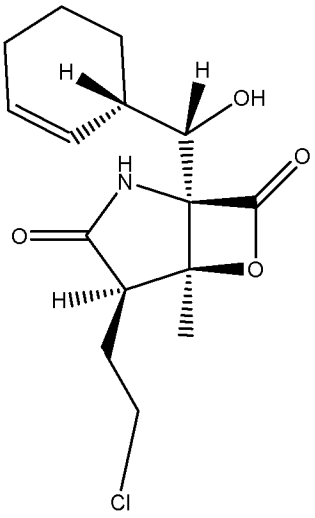

I-16

TARGETING CDK4 and CDK6 IN COMBINATION CANCER THERAPY

Abstract of the Disclosure

Disclosed are methods of treating cancer comprising administering to the animal, combination of PD 0332991 and a therapeutically effective amount of a heterocyclic compound of Formula I. The animal is a mammal, preferably a human or a rodent.

6295869
112608

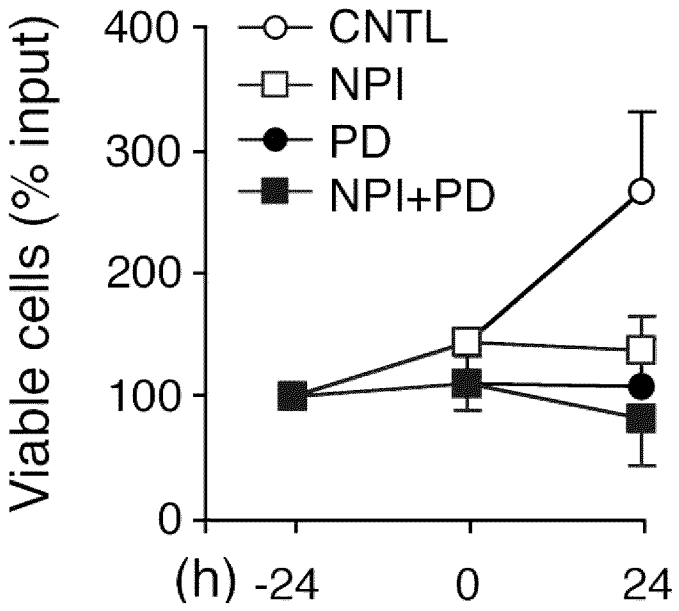
Viable cells (% input)
400
300
200
100
0
CNTL
NPI
PD
NPI+PD
(h) -24
0
24

FIG. 1A

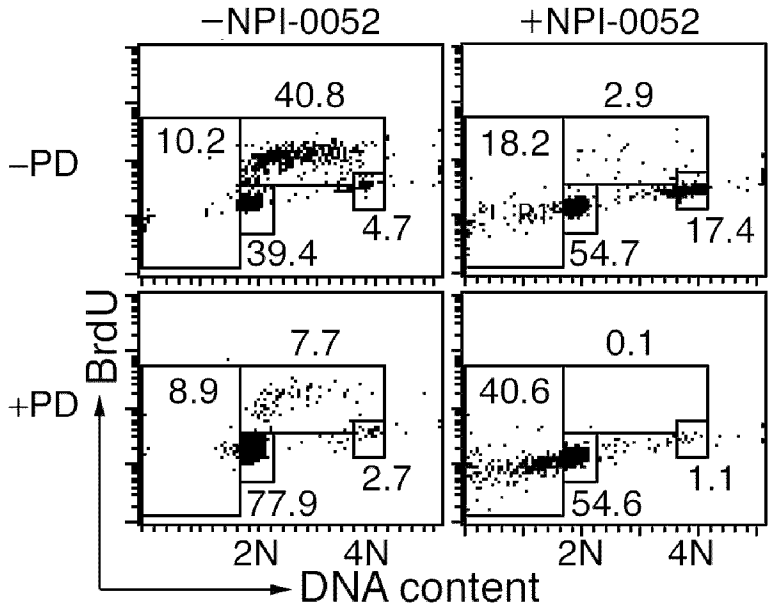
−NPI-0052
+NPI-0052
−PD
+PD
BrdU
40.8
10.2
39.4
4.7
2.9
18.2
54.7
17.4
7.7
8.9
77.9
2.7
0.1
40.6
54.6
1.1
2N
4N
2N
4N
DNA content

FIG. 1B

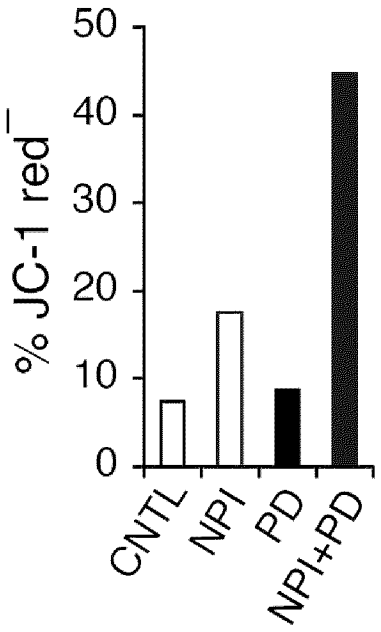
50
40
30
20
10
0
% JC-1 red⁻
CNTL
NPI
PD
NPI+PD

FIG. 1C

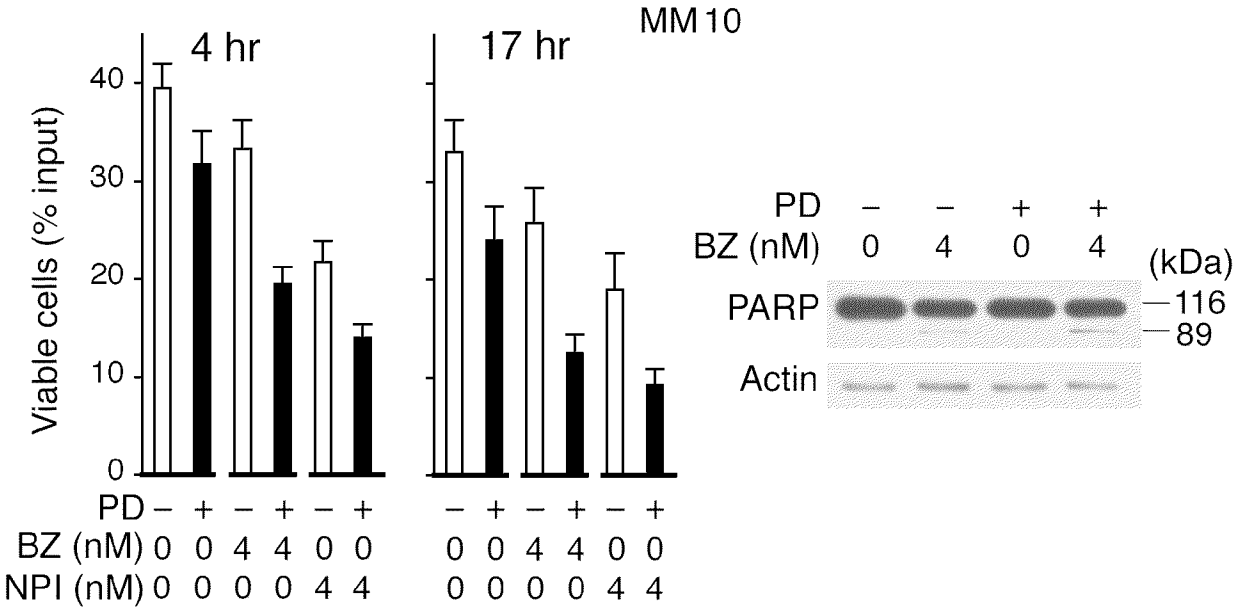
MM 10
4 hr
17 hr
Viable cells (% input)
40
30
20
10
0
PD – + – + – + – + – + – +
BZ (nM) 0 0 4 4 0 0 0 0 4 4 0 0
NPI (nM) 0 0 0 0 4 4 0 0 0 0 4 4
PD – – + +
BZ (nM) 0 4 0 4
(kDa)
PARP
116
89
Actin

FIG. 2A

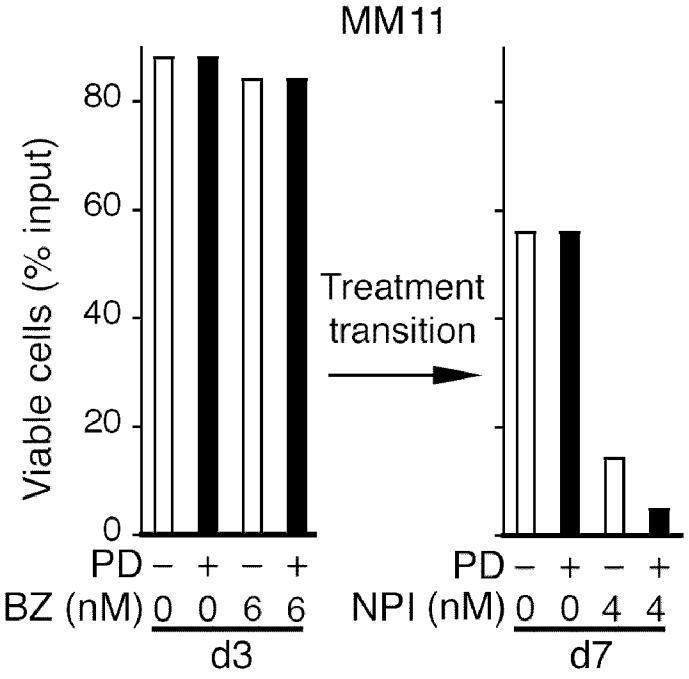
MM11
Viable cells (% input)
80
60
40
20
0
Treatment
transition
PD – + – +
BZ (nM) 0 0 6 6
d3
PD – + – +
NPI (nM) 0 0 4 4
d7

FIG. 2B

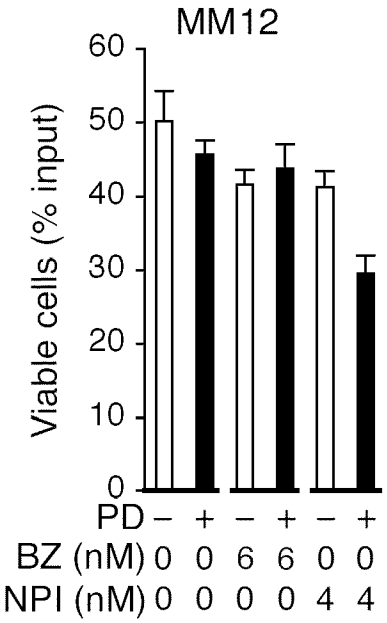
MM12
Viable cells (% input)
60
50
40
30
20
10
0
PD – + – + – +
BZ (nM) 0 0 6 6 0 0
NPI (nM) 0 0 0 0 4 4

FIG. 2C

[Proc Amer Assoc Cancer Res, Volume 46, 2005]

Cellular and Molecular Biology 21: Apoptosis 2: Chemotherapeutic Agents I
Abstract #1721

The proteasome inhibitor NPI-0052 sensitizes pancreatic cancer cells to TRAIL *in vitro* and *in vivo*

Robert H. I. Andtbacka, Sanaz Khanbolooki, Maria S. Pino, Keyi Zhu and David J. McConkey

UT M. D. Anderson Cancer Ctr., Houston, TX

Introduction: The tumor necrosis factor-related apoptosis-inducing ligand (TRAIL) is a potent inducer of apoptosis in pancreatic cancer. However, many pancreatic cancer cell lines are resistant to TRAIL. We have previously shown that proteasome inhibitors alone and in combination with other cytotoxic agents can induce apoptosis in resistant pancreatic cancer cell lines. Whether proteasome inhibitors can sensitize pancreatic cancer cell lines to TRAIL is not established. Hypothesis: We hypothesized that NPI-0052 (NPI - Nereus Pharmaceuticals), a new proteasome inhibitor, would sensitize TRAIL resistant pancreatic cancer cell lines to TRAIL. Methods: We studied the effects of NPI as a single agent and in combination with recombinant human TRAIL (rhTRAIL - R&D Systems) on a panel of 7 pancreatic cancer cell lines in vitro. Propidium-Iodide with FACS analysis and caspase-3 activity were used for in vitro evaluation of apoptosis. An orthotopic L3.6pl pancreatic cancer Nude mouse model was used for the in vivo study. The mice were treated with NPI at 0.075 mg/kg or rhTRAIL at 8.3 mg/kg as single agents or in combination. Results: The dose response to NPI was heterogeneous among the pancreatic cancer cell lines studied. L3.6pl, CFPAC1, HPAF2 and BXPC3 were highly sensitive to NPI with IC_{50} of 50nM. In L3.6pl apoptosis was observed after 8 hours and peaked at 24 hours, reaching a maximum apoptosis rate of 60% at 10μM NPI. 10 ng/ml rhTRAIL in L3.6pl induced apoptosis rates of 25%. Combination treatment with 50nM NPI and low dose rhTRAIL resulted in an increase in apoptosis from 50% to over 75%, indicating an additive effect of rhTRAIL. PANC1, MiaPaCa2 and Hs766T were highly resistant to NPI with apoptosis rates of less than 35%. PANC1 and MiaPaCa2 were also highly resistant to rhTRAIL with apoptosis rates of less than 25%. When NPI and low dose rhTRAIL were used in combination in these cells, apoptosis rates increased dramatically to over 90% after 8 hours of exposure, indicating a synergistic effect of NPI and rhTRAIL. In vivo, mice treated with NPI alone exhibited a minimal reduction in tumor load and mice treated with rhTRAIL alone had a 65% mean reduction in tumor load ($p<0.02$). The combination of NPI and rhTRAIL resulted in a 92% mean

reduction in tumor load (p=0.003), suggesting a synergistic effect of NPI and rhTRAIL in vivo. Conclusion: The NPI-0052 proteasome inhibitor induces apoptosis in pancreatic cancer cell lines. NPI also sensitizes TRAIL resistant pancreatic cancer cells to TRAIL and significantly reduces the tumor load in vivo. Combination therapy with NPI-0052 and TRAIL may provide a new therapeutic regimen in human pancreatic cancer.

A novel orally active proteasome inhibitor induces apoptosis in multiple myeloma cells with mechanisms distinct from Bortezomib

Dharminder Chauhan,[1,4] Laurence Catley,[1,4] Guilan Li,[1] Klaus Podar,[1] Teru Hideshima,[1] Mugdha Velankar,[1] Constantine Mitsiades,[1] Nicolas Mitsiades,[1] Hiroshi Yasui,[1] Anthony Letai,[1] Huib Ovaa,[3] Celia Berkers,[3] Benjamin Nicholson,[2] Ta-Hsiang Chao,[2] Saskia T.C. Neuteboom,[2] Paul Richardson,[1] Michael A. Palladino,[2] and Kenneth C. Anderson[1,*]

[1]The Jerome Lipper Multiple Myeloma Center, Department of Medical Oncology, Dana-Farber Cancer Institute, Harvard Medical School, Boston, Massachusetts 02115
[2]Nereus Pharmaceuticals, San Diego, California 92121
[3]Harvard Medical School, Boston, Massachusetts 02115
[4]These authors contributed equally to this work.
*Correspondence: kenneth_anderson@dfci.harvard.edu

Summary

Bortezomib therapy has proven successful for the treatment of relapsed and/or refractory multiple myeloma (MM); however, prolonged treatment is associated with toxicity and development of drug resistance. Here, we show that the novel proteasome inhibitor NPI-0052 induces apoptosis in MM cells resistant to conventional and Bortezomib therapies. NPI-0052 is distinct from Bortezomib in its chemical structure, effects on proteasome activities, mechanisms of action, and toxicity profile against normal cells. Moreover, NPI-0052 is orally bioactive. In animal tumor model studies, NPI-0052 is well tolerated and prolongs survival, with significantly reduced tumor recurrence. Combining NPI-0052 and Bortezomib induces synergistic anti-MM activity. Our study therefore provides the rationale for clinical protocols evaluating NPI-0052, alone and together with Bortezomib, to improve patient outcome in MM.

Introduction

The successful development of Bortezomib/PS-341 Velcade therapy for treatment of relapsed/refractory multiple myeloma (MM) has established proteasome inhibition as an effective therapeutic strategy. The dipeptide boronic acid analog Bortezomib is a potent, highly selective, and reversible proteasome inhibitor that targets the 26S proteasome complex and inhibits its function (Adams et al., 1999). Besides inhibiting NF-κB, Bortezomib has pleiotropic effects on MM biology by targeting (1) cell cycle regulatory proteins; (2) the unfolded protein response (UPR) pathway; (3) p53-mediated apoptosis; and (4) DNA repair mechanisms; as well as (5) classical stress response pathways via both intrinsic (caspase-9-mediated) and extrinsic (caspase-8-mediated) cell death cascades. Specifically, Bortezomib activates c-Jun amino-terminal kinase (JNK) (Chauhan et al., 2003), which triggers mitochondrial apoptotic signaling: release of cytochrome-c (cyto-c) and second mitochondrial activator of caspases (Smac) from mitochondria to cytosol, followed by activation of caspase-9 and caspase-3 (Chauhan and Anderson, 2003). Despite the potent anti-MM activity of Bortezomib, both intrinsic and acquired resistance has already been observed in MM patients (Anderson, 2004). The mechanisms conferring Bortezomib resistance are now being defined (Chauhan et al., 2005). Nonetheless, the combination of Bortezomib with other novel and conventional agents can overcome Bortezomib resistance (Chauhan et al., 2005).

Recent studies have focused on developing other proteasome inhibitors as therapeutics in cancer. NPI-0052 is one such molecule derived from fermentation of Salinospora, a new marine gram-positive actinomycete (Macherla et al., 2005). In the present study, we show that both NPI-0052 and Bortezomib can be distinguished by chemical structure, their effects on proteasomal activities, and differential toxicity profiles

SIGNIFICANCE

The ubiquitin-proteasome pathway modulates intracellular protein degradation. The multienzyme protease 26S proteasome degrades misfolded proteins; conversely, blockade of the proteasomal degradation pathways results in accumulation of unwanted proteins and cell death. Because cancer cells proliferate to a greater extent than normal cells, the rate of protein translation and degradation is also higher. This notion led to the development of proteasome inhibitors as cancer therapeutics. Recently, the FDA approved the first proteasome inhibitor, Bortezomib (Velcade), for treatment of relapsed/refractory multiple myeloma (MM). This study shows that the orally bioavailable novel proteasome inhibitor NPI-0052 is cytotoxic to MM cells, with reduced toxicity against normal cells compared to Bortezomib, providing the framework for clinical trials of NPI-0052 in MM.

against normal cells. NPI-0052 induces apoptosis in MM cell lines and patient cells. Both biochemical and genetic studies show that NPI-0052-induced cell death, in contrast to that triggered by Bortezomib, relies primarily on caspase-8-mediated signaling pathways. In vivo studies show that NPI-0052 significantly inhibits tumor growth in mice, is well tolerated, and prolongs survival. Based on their structural and mechanistic differences, NPI-0052 and Bortezomib show synergistic anti-MM activity. Finally, current Bortezomib therapy requires intravenous (i.v.) administration, whereas NPI-0052 is orally bioactive. Overall, our study provides the rationale for clinical protocols evaluating NPI-0052 to inhibit tumor cell growth, overcome conventional and Bortezomib resistance, limit toxicity profiles, and improve patient outcome in MM.

Results and discussion

NPI-0052 is structurally distinct from Bortezomib and inhibits all three protease activities within the proteasome both in vitro and in vivo

The naturally occurring and synthetic inhibitors of the ubiquitin-proteasome pathway include peptide aldehydes, peptide boronates, nonpeptide inhibitors, peptide vinyl sulfones, and peptide epoxyketones (Adams, 2004; Adams et al., 1999; Chauhan et al., 2005). Bortezomib/PS-341/Velcade is a boronic acid dipeptide derivative and inhibits proteasome function via interaction of boronic acid at the C terminus of Bortezomib with an active threonine site in the proteasome (Adams et al., 1999) (Figure 1A). NPI-0052 is a nonpeptide proteasome inhibitor and shares structural features with another proteasome inhibitor, Omuralide (Figure 1A), which inhibits proteasome activity by covalently modifying the active site threonine residues of the proteasome (Corey and Li, 1999). Omuralide is clasto-lactacystin β-lactone, the active form of the well-known proteasome inhibitor lactacystin (Corey and Li, 1999). Despite the structural similarity with Omuralide, NPI-0052 can be distinguished by the presence of a uniquely methylated C3 ring juncture, chlorinated alkyl group at C2, and cyclohexene ring at C5 (Figure 1A). Evaluation of the effects of NPI-0052, Omuralide, and Bortezomib on cathepsin A activity show that Omuralide is a more specific inhibitor of cathepsin A (IC_{50} = 65 ± 6 nM). Both NPI-0052 and Bortezomib also inhibited cathepsin A with different IC_{50} (NPI-0052, 1.4 ± 0.1 μM; Bortezomib, 14 ± 5 μM).

Omuralide is known to inhibit all three protease activities in the proteasome: the chymotrypsin-like (CT-L), trypsin-like (T-L), and caspase-like (C-L) activities (Corey and Li, 1999); however, the effect of NPI-0052 on these proteasome activities is undefined. We therefore examined whether NPI-0052 affects these proteasome activities using human erythrocyte 20S proteasomes and fluorogenic peptide substrates. We also simultaneously compared the effect of Bortezomib on proteasome activities. Both NPI-0052 and Bortezomib inhibit all three proteasome activities, albeit at different concentrations (Figures 1B–1D). Results show that (1) NPI-0052 inhibits CT-L and T-L activities at lower concentrations than Bortezomib, and (2) higher concentrations of NPI-0052 than Bortezomib are required to inhibit C-L activity. Our in vitro data suggest that NPI-0052, like Bortezomib, targets proteasomes.

We next compared the effects of NPI-0052 and Bortezomib on all three proteasome activities in vivo in mice. For these studies we selected the MTD dose for each agent. Based on our previous study (LeBlanc et al., 2002), the MTD of Bortezomib is 1.0 mg/kg (i.v.) given twice weekly. Additional experimentation in beige-nude-xid (BNX) mice established the MTD of NPI-0052 at 0.15 mg/kg (i.v.) twice weekly (data not shown). Mice were treated with a single dose of NPI-0052 (0.15 mg/kg i.v.) or Bortezomib (1 mg/kg i.v.); blood samples were collected at 90 min, 24 hr, 48 hr, 72 hr, or 168 hr; and whole blood cells were then analyzed for proteasome activity (Figure 2). NPI-0052 completely inhibited CT-L activity by 90 min, which was recoverable by 168 hr (Figure 2A), whereas Bortezomib-inhibited CT-L activity was markedly restored at 24 hr (Figure 2B). T-L activity is significantly inhibited (50% inhibition) by NPI-0052 at 90 min, 24 hr, 48 hr, and 72 hr and is restored by 168 hr (Figure 2C); in contrast, Bortezomib enhances T-L activity, which remains elevated even at 168 hr (Figure 2D). Finally, NPI-0052 inhibits C-L activity at 90 min, 24 hr, 48 hr, and 72 hr, and this activity recovered at 168 hr (Figure 2E), whereas Bortezomib significantly inhibits C-L activity at 90 min, 24 hr, 48 hr, and 72 hr and is similarly recoverable at 168 hr (Figure 2F). Therefore, after NPI-0052 treatment, all three proteasome activities remain inhibited at 72 hr and were restored to significant levels by 168 hr. These data suggest that NPI-0052 and Bortezomib differentially affect all three proteasome activities.

NPI-0052 is orally bioactive

Previous studies showed that Bortezomib is orally active (Palombella et al., 1998; Teicher et al., 1999); however, the current Bortezomib therapy in MM is administered i.v. The rationale for using the i.v. route instead of oral administration may include bioavailability, rapid distribution (Adams et al., 1999), solubility, and reversibility/half-life issues. We therefore next examined whether NPI-0052 is also orally bioactive. Mice were treated with various oral and i.v. concentrations of NPI-0052; at 90 min whole-blood lysates (WBL) were analyzed for proteasome activity. Oral administration of NPI-0052 significantly inhibits CT-L activity of 20S proteasomes in a dose-dependent manner between 0.025 mg/kg and 0.50 mg/kg (Figure 3A). Both T-L and C-L activities were also inhibited, albeit to lesser extent (data not shown). These findings show that NPI-0052 given orally inhibits proteasome activity in vivo.

NPI-0052 targets nuclear factor-κB

A major rationale for using Bortezomib therapeutically is its ability to inhibit nuclear factor-κB (NF-κB) activation (Adams, 2002; Hideshima et al., 2002; Russo et al., 2001). We therefore next asked whether NPI-0052 similarly affects NF-κB activation. To address this issue, a stable HEK-293 clone was generated carrying a luciferase reporter gene under the regulation of 5× NF-κB binding sites. Stimulation of these cells with human TNF-α leads to increased luciferase activity due to NF-κB activation. Pretreatment of NF-κB/luc HEK-293 cells with NPI-0052 results in a significant ($p < 0.001$) dose-dependent decrease of luciferase activity after TNF-α stimulation (Figure 3B), indicating inhibition of NF-κB. Bortezomib also downregulates NF-κB activity, but at higher concentrations than NPI-0052 (Figure 3B). These findings indicate that NPI-0052 is a more potent inhibitor of NF-κB than Bortezomib.

Activation of NF-κB triggers transcription and secretion of various proinflammatory cytokines, such as TNF-α, interleukin-1-β (IL-1-β), and interleukin-6 (IL-6), which mediate the growth and survival of tumor cells (Adams, 2002; Hideshima et al.,

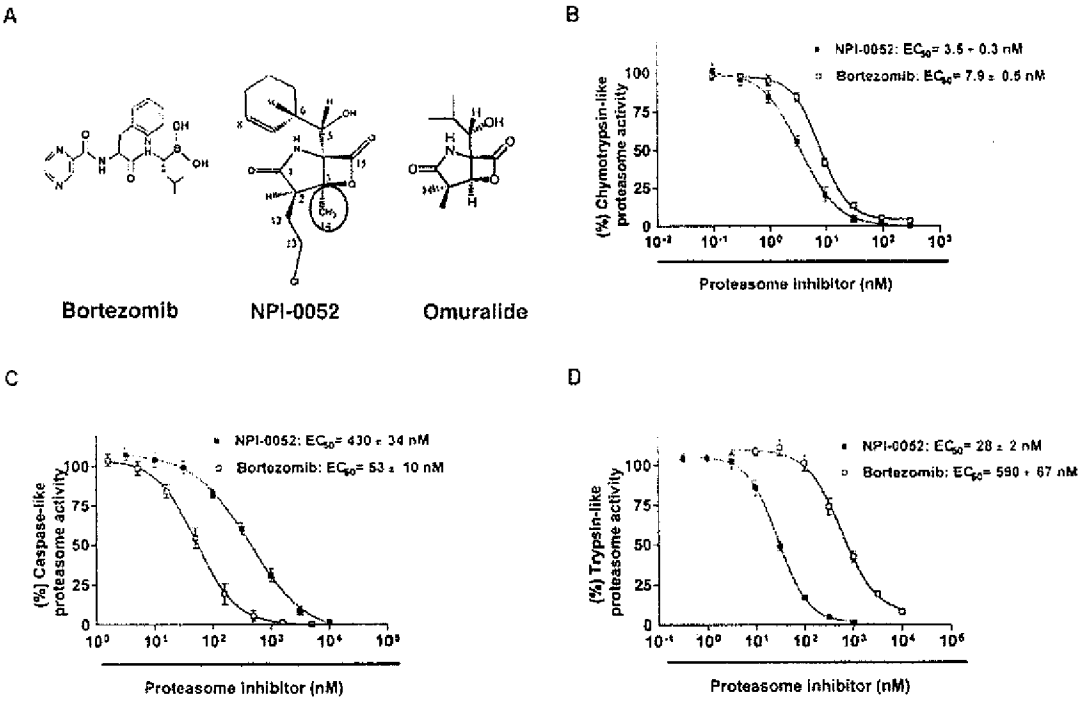

Figure 1. The proteasome inhibitor NPI-0052 is structurally distinct from Bortezomib/PS-341 and attenuates proteasome activity in vitro

A: Chemical structures of the proteasome inhibitors Bortezomib, NPI-0052, and Omuralide.

B–D: NPI-0052 and Bortezomib inhibit CT-L, C-L, and T-L proteasome activities in human erythrocyte derived 20S proteasomes. The EC_{50} values are the drug concentration at which 50% maximal relative fluorescence is inhibited.

2002; Russo et al., 2001). Inhibition of cytokine synthesis and function by means of proteasome inhibition thereby has clinical benefit. Since both NPI-0052 and Bortezomib inhibit NF-κB, we examined the effect of these agents on LPS-induced cytokine production in human peripheral blood mononuclear cells (PBMNCs). NPI-0052 inhibited LPS-triggered secretion of all three cytokines at lower concentrations than Bortezomib (Figure 3C). These findings show that NPI-0052, like Bortezomib, targets NF-κB and related cytokine secretion.

NPI-0052 blocks proteasome activity in MM cells

Our preclinical and clinical studies have already shown Bortezomib to be an effective therapy in MM (Hideshima and Anderson, 2002; Richardson et al., 2005). Our recent study showed the composition of active proteasome in MM.1S cell line and the proteasome targets of Bortezomib in these cells (Berkers et al., 2005). In that study, we utilized a novel methodology to measure proteasome activity by immunoblotting using DansylAhx$_3$L$_3$VS as a probe (Berkers et al., 2005). The results from this method correlated with those obtained using fluorogenic substrates and, in addition, allow for determining subunit specificity of a given proteasome inhibitor (details provided in the Experimental Procedures). In the present study, we examined the effects of NPI-0052 and Bortezomib on the catalytic activities of proteasome subunits. Cells were cultured in the presence or absence of various concentrations of either NPI-0052 (2 nM, low toxic dose; 7 nM, IC_{50}; and 20 nM, highly toxic to MM.1S cells), and compared these effects with those triggered by Bortezomib (2 nM, low toxic dose; 5 nM, IC_{50}; and 20 nM, highly toxic to MM.1S cells). Competition experiments between either NPI-0052 or Bortezomib and DansylAhx$_3$L$_3$VS revealed that NPI-0052 (7 nM) markedly inhibits the CT-L activity as represented by β-5 (β-5) subunit of the proteasome (Figure 3D). Furthermore, NPI-0052 also decreased the DansylAhx$_3$L$_3$VS labeling of the β-1 (C-L activity) and β-2 (T-L activity) in a dose-dependent manner. Slightly higher concentrations of Bortezomib are necessary to markedly inhibit β-5 and β-1 subunits, whereas β-2 subunits are not inhibited. Together, these findings demonstrate the ability of NPI-0052 to inhibit all three proteasome activities in MM cells and are consistent with in vitro results using fluorogenic substrates shown in Figures 1 and 2.

NPI-0052 inhibits growth and triggers apoptosis in MM cells

We next asked whether NPI-0052-induced proteasome inhibition correlates with cytotoxicity in MM cells. Treatment for 24 hr of MM cell lines (MM.1S, RPMI-8226, OPM2, U266), including those that are resistant to the conventional anti-MM agents Dexamethasone (Dex) (MM.1R) and Doxorubicin (Dox-40), with

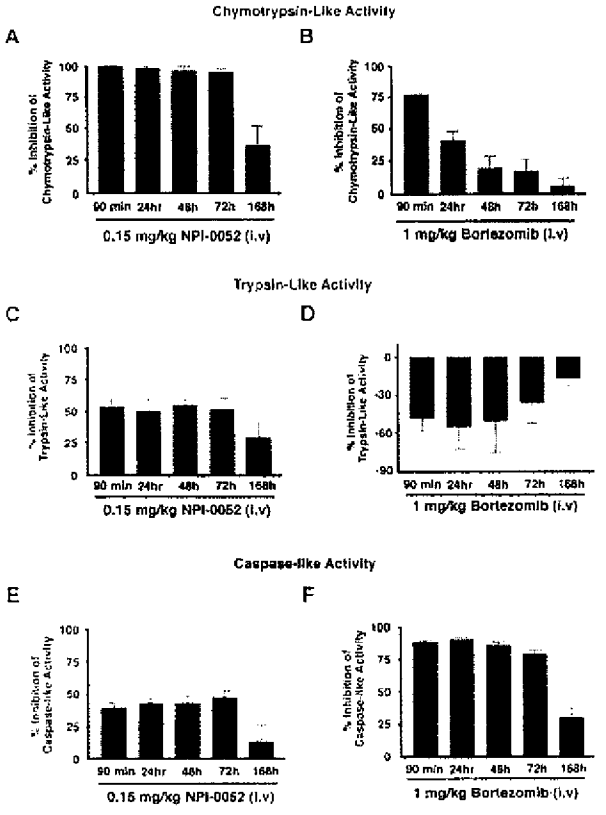

Figure 2. NPI-0052 and Bortezomib differentially affect proteasome activities in vivo

Mice (n = 5) were treated with either NPI-0052 (**A**, **C**, and **E**) or Bortezomib (**B**, **D**, and **F**) at their respective MTD (1 mg/kg for Bortezomib and 0.15 mg/kg for NPI-0052) for the indicated times, and blood samples were analyzed for CT-L, C-L, and T-L proteasome activities. The data represent percent inhibition compared to vehicle control-treated animals from two independent experiments with similar results.

NPI-0052 induces a dose-dependent significant ($p < 0.005$) decrease in viability of all cell lines (IC_{50} range 7–24 nM) (Figure 4A). To determine whether NPI-0052 similarly affects purified patient cells, tumor cells from nine MM patients relapsing after multiple prior therapies including Dex, melphalan, Bortezomib, and Thalidomide were treated for 24 hr with NPI-0052 (10 nM) and then analyzed for apoptosis. NPI-0052 induced significant apoptosis in these cells, as measured by DNA fragmentation assays ($p < 0.005$) (Figure 4B). Importantly, of nine patients examined four were refractory to Bortezomib therapy, and five were resistant to Thalidomide and Dex therapies. Patients were deemed to be refractory to Bortezomib when they had progressive disease while on Bortezomib therapy. In addition, data from the phase II clinical studies in MM show that only 35% of patients with relapsed/refractory MM respond to the treatment with Bortezomib; and in this context, the 65% of patients who were nonresponders were considered to be a Bortezomib-resistant patient population. We next examined whether cells from such patient populations are affected by Bortezomib treatment in vitro and whether NPI-0052 exerts a cytotoxic effect in these cells. CD138-positive cells from seven MM patients were treated with Bortezomib (10 nM) and NPI-0052 (10 nM) in vitro and then analyzed for viability (Figure 4C). Results demonstrate a varying sensitivity to Bortezomib in vitro, with a 15%–50% decrease in viability; however, all patient cells were significantly more sensitive to NPI-0052 ($IC_{50} \leq 10$ nM in 6 of 7 patients) (Figure 4C).

The finding that cells from Bortezomib-refractory patients are sensitive to the treatment with Bortezomib in vitro suggests that extracellular factors, such as the BM microenvironment, play a role in conferring drug resistance in vivo. Absence of the BM milieu under the ex vivo culture conditions may restore sensitivity of MM cells to Bortezomib; however, the activation of intrinsic cellular drug mechanisms cannot be excluded. Additionally, as noted above, NPI-0052 and Bortezomib differentially affect proteasome activities, which may explain their variable in vitro cytotoxicity. Furthermore, it is unclear at present whether alteration in any proteasome subunit confers Bortezomib resistance versus sensitivity. Our data obtained from viability studies suggest that NPI-0052 is a more potent inducer of MM cell apoptosis than Bortezomib in tumor cells obtained from Bortezomib-refractory MM patients.

NPI-0052 does not affect viability of patient MM-derived bone marrow stromal cells

Interaction of MM cells with bone marrow stromal cells (BMSCs) induces cytokine secretion, which mediates paracrine growth of MM cells, as well as protects against drug-induced apoptosis (Hideshima and Anderson, 2002). We examined whether NPI-0052 affects viability of BMSCs. Treatment of BMSCs (patients 1–5) for 24 hr with NPI-0052 (20 nM) does not induce apoptosis in these cells, whereas NPI-0052 triggered a significant (10- to 12-fold) increase in apoptosis of purified patient MM cells (Figure 4D). Importantly, NPI-0052 significantly decreased the secretion of IL-6 triggered by adhesion of MM cells to BMSCs (IC_{50}, 80–100 nM; $p < 0.05$), as is observed using Bortezomib (Anderson, 2004). Together, these results suggest that NPI-0052 does not directly affect BMSC viability, but blocks the secretion of BMSC-derived MM cell growth factor IL-6 within the BM milieu.

NPI-0052 overcomes recombinant human interleukin-6- and recombinant human insulin-like growth factor-I-mediated antiapoptotic effects

Both IL-6 and IGF-I trigger growth and protect against chemotherapy-induced apoptosis in MM cells (Chauhan and Anderson, 2003; Xu et al., 1997). We therefore next examined whether NPI-0052 overcomes this protective effect of IL-6 or IGF-I. Neither recombinant human interleukin-6 (rhIL-6) nor recombinant human insulin-like growth factor-I (rhIGF-I) blocks NPI-0052-triggered cytotoxicity in MM.1S cells (Figure 4E). As in our prior studies (Chauhan and Anderson, 2003; Mitsiades et al., 2002a), both rhIL-6 and rhIGF-I block Dex-induced decreases in MM.1S cell viability. High serum levels of IL-6 or IGF-I contribute to clinical chemoresistance and treatment failure (Hideshima and Anderson, 2002), and our data therefore suggest a remarkable ability of NPI-0052 to induce MM cell apoptosis even in the presence of IL-6 or IGF-I.

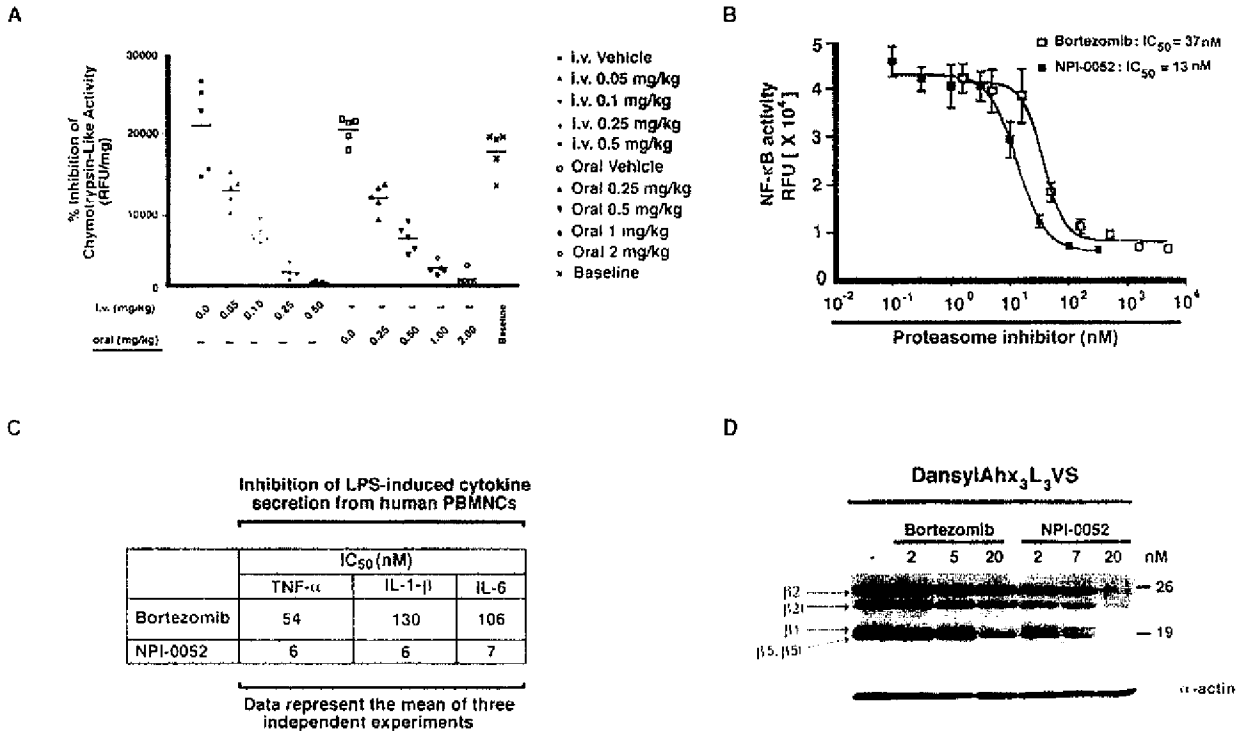

Figure 3. Orally bioactive NPI-0052 Inhibits cytokine secretion, NF-κB, and proteasome activities

A: NPI-0052 is orally bioactive. Mice (n = 5) were administered NPI-0052 i.v. or orally, and CT-L activity of the 20S proteasome in WBC lysates was determined. Relative fluorescence units (RFU) were normalized for protein concentrations of the cell lysates. The 20S proteasome activity of the individual mice is shown, with the horizontal bar representing the average activity. Baseline represents 20S proteasome activity observed in WBC lysates prepared from untreated mice.

B and C: NPI-0052 inhibits NF-κB and the cytokine secretion. Effect of NPI-0052 and Bortezomib on NF-κB activity in NF-κB/Luc HEK-293 cells and LPS-triggered cytokine secretion in PBMNCs.

D: Competition experiment between NPI-0052 or Bortezomib and DansylAhx$_3$L$_3$VS (upper panel). The three distinct catalytic activities of proteasome are represented by β-1 for caspase-like, β-2 for trypsin-like, and activity β-5 for chymotrypsin-like activities. The β-2i and β-5i are the interferon-inducible subunits to form immunoproteasomes with altered catalytic specificity that help production of antigenic peptides. Fillers were reprobed with anti-α-actin Ab to show equal protein loading. Blots shown are representative of two independent experiments.

NPI-0052 blocks vascular endothelial growth factor-induced migration of MM cells

Vascular endothelial growth factor (VEGF) is elevated in the MM BM microenvironment, and our studies showed that VEGF triggers growth, migration, and angiogenesis in MM (Podar et al., 2002). We therefore asked whether NPI-0052 affects VEGF-triggered MM cell migration. VEGF alone markedly increases MM.1S cell migration; conversely, NPI-0052 significantly ($p < 0.05$) inhibits VEGF-dependent MM cell migration (Figure 4F). The short exposure time of MM.1S cells to NPI-0052 did not affect survival of MM cells (viability > 95%). These findings indicate that NPI-0052 may negatively regulate homing of MM cells to the BM, as well as their egress into the peripheral blood.

NPI-0052 inhibits human MM cell growth in vivo and prolongs survival in a murine model

Having shown that NPI-0052 induces apoptosis in MM cells in vitro, we next examined the in vivo efficacy of NPI-0052 using our human plasmacytoma xenograft mouse model (LeBlanc et al., 2002). As noted above, NPI-0052 has achieved therapeutically effective levels of proteasome inhibition after oral administration in mice, and we therefore administered NPI-0052 orally. Treatment of tumor-bearing mice with NPI-0052, but not vehicle alone, significantly ($p < 0.001$) inhibits MM tumor growth and prolongs survival ($p < 0.001$) of these mice (Figures 5A–5C). The concentrations of NPI-0052 administered were well tolerated by mice, without significant weight loss (see Figure S1 in the Supplemental Data available with this article online). Moreover, no neurological behavioral changes were observed even after 12 weeks of NPI-0052 treatment. Analysis at day 300 showed no recurrence of tumor in 57% of the NPI-0052-treated mice (Figure 5C). In addition, histologic analysis performed on the inoculation sites confirmed the disappearance of plasma cells in the NPI-0052- versus vehicle-treated mice (Figure 5D, left and right panels, respectively). These data demonstrate the potent antitumor activity of NPI-0052 in vivo. Importantly, these findings also show that NPI-0052 is orally

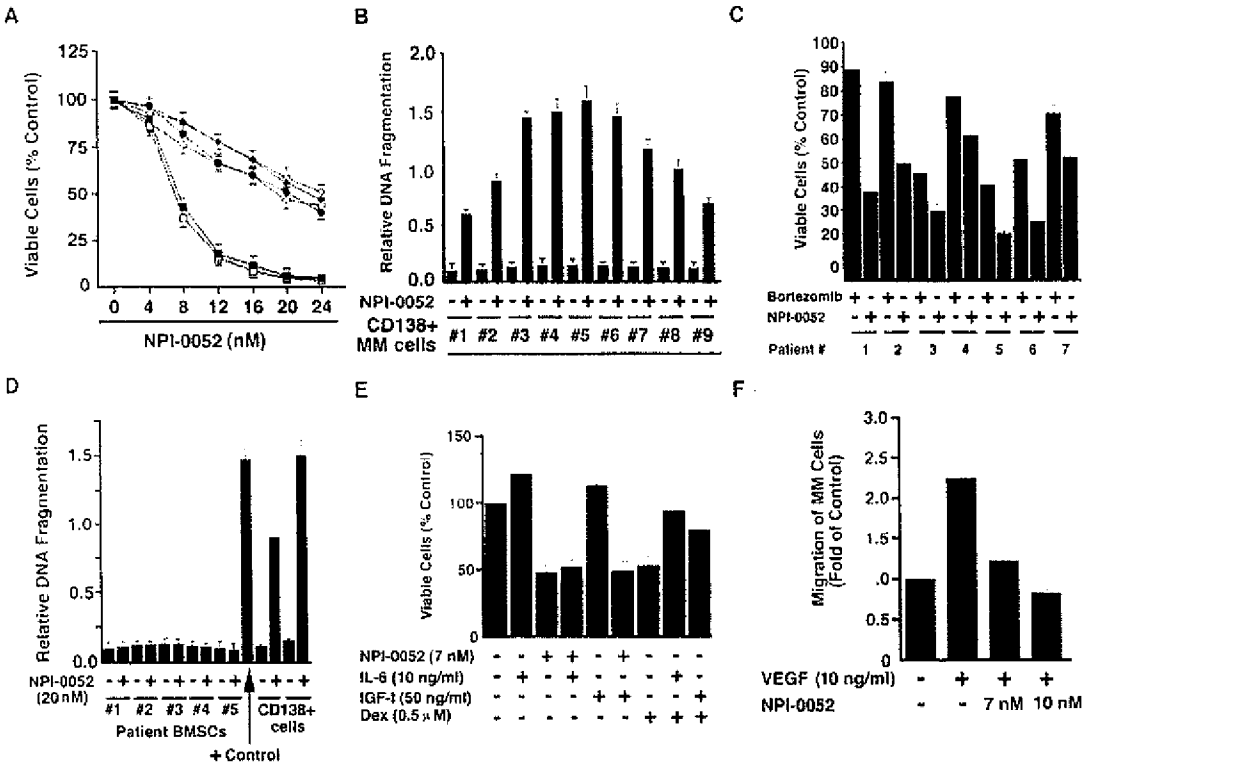

Figure 4. NPI-0052 Induces Apoptosis in Human MM Cells

A: MTT assays were performed after incubation of MM.1S (black squares), MM.1R (white boxes), RPMI-8226 (black circles), Dox-40 (black squares), OPM2 (white circles), and U266 (white diamonds) human MM cells with indicated concentrations of NPI-0052 for 24 hr. Data represent mean ± SD (error bars) from three independent experiments ($p < 0.005$ for all cell lines).

B: Purified MM cells from patients were treated for 24 hr with NPI-0052 (10 nM) and then analyzed for apoptosis. Data represent mean ± SD (error bars) of triplicate samples ($p < 0.005$ for all patient MM cells).

C: Tumor cells from MM patients refractory (patients 1, 2, 4, and 7) or sensitive (patients 3, 5, and 6) to Bortezomib therapy were treated with either NPI-0052 (10 nM) or Bortezomib (10 nM) for 24 hr and then analyzed for viability. Shown is mean ± SD (error bars) of duplicate samples ($p < 0.004$ for all samples).

D: Effect of NPI-0052 on bone marrow (BM) microenvironment. Patient MM-derived BM stromal cells (BMSCs) were treated for 24 hr with NPI-0052 (20 nM) and then analyzed for apoptosis. Purified MM cells from two of these five MM patients were similarly examined. Data represent mean ± SD (error bars) from triplicate samples ($p < 0.005$).

E: MM.1S cells were treated for 24 hr with the indicated concentrations of NPI-0052 or Dex, in the presence or absence of rhIL-6 or rhIGF-1, and then analyzed for viability. Shown is mean ± SD (error bars) of three independent experiments ($p < 0.04$ for all samples).

F: MM.1S MM cells were treated with indicated concentrations of NPI-0052 for 4 hr (viability > 95%), washed, and then treated for 24 hr with rhVEGF (10 ng/ml), followed by analysis in a transwell migration assay. Data represent mean ± SD (error bars) of two independent experiments ($p < 0.005$ for all samples).

bioactive, which together with the in vivo proteasome inhibition studies (Figures 2 and 3A), provides the preclinical framework for its evaluation as an oral agent in phase I trials in MM.

Comparative analysis of in vivo antitumor activity of NPI-0052 and Bortezomib

Our prior study using the human plasmacytoma xenograft mouse model established the MTD of Bortezomib at 1 mg/kg (i.v.) (LeBlanc et al., 2002). Using the same animal model, we obtained the MTD of NPI-0052 at 0.15 mg/kg (i.v.) (data not shown). For the comparative study, we therefore selected the MTD of each agent. Mice were treated with NPI-0052 (0.15 mg/kg i.v.) or Bortezomib (1.0 mg/kg i.v.) twice weekly, the optimal dose and schedule reported for Bortezomib (LeBlanc et al., 2002). Both agents significantly reduced the tumor progression ($p < 0.01$) and prolonged survival ($p = 0.0137$) (Figures 5E and 5F).

Mechanisms mediating anti-MM activity of NPI-0052

We first studied mitochondria, given their critical role in apoptosis (Bossy-Wetzel and Green, 1999). NPI-0052 decreases $\Delta\Psi m$, evidenced by an increased number of CMXRos-negative cells ($p < 0.005$) (Figure 6A), and also triggers O_2^- production in MM.1S cells (Figure 6B). Moreover, NPI-0052 decreases mitochondrial cyto-c and Smac (Figure 6C, upper and middle left panels), coupled with a concurrent accumulation of these proteins in the cytosol (Figure 6C, upper and middle right panels). As in previous studies (Chauhan et al., 2001; Chauhan et

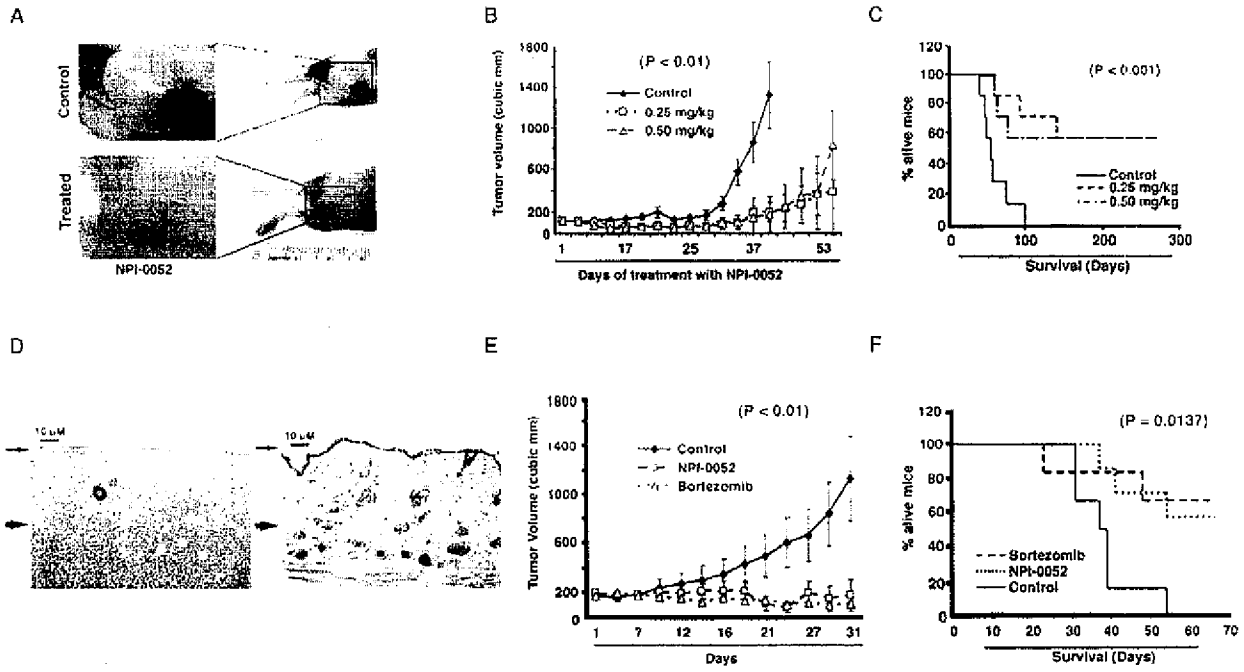

Figure 5. NPI-0052 inhibits human plasmacytoma growth and increases survival in immune-deficient BNX mice

A: Photographs. The mouse on the upper panel received oral doses of vehicle alone, whereas the mouse in the lower panel received oral NPI-0052 (0.25 mg/kg twice weekly). Left panels are enlargements of subcutaneous plasmacytomas growing on the flanks of the mice.

B: Kinetics of myeloma xenograft growth. Mice (n = 7) received NPI-0052 orally at the indicated doses twice weekly. A significant delay in tumor growth in NPI-0052-treated mice was noted compared to vehicle-treated control mice, as early as day 15 ($p < 0.001$). No significant differences between the NPI-0052 treatment groups were observed.

C: Kaplan-Meier plots showing survival for mice treated with NPI-0052 at the indicated concentrations. NPI-0052-treated mice show significantly increased survival ($p < 0.001$) compared to the untreated group. The mean overall survival (OS) was 58 days (95% confidence interval [CI]: 44–73 days) in the control cohort versus 196 days (95% CI: 130–262 days) and 182 days (95% CI: 107–258 days) in groups treated with 0.25 and 0.5 mg/kg NPI-0052, respectively. A statistically significant prolongation in mean OS compared with control mice was observed in animals treated with 0.25 mg/k ($p = 0.0019$) and 0.5 mg/kg ($p = 0.0074$).

D: Histology. Tissue sections of inoculation sites from a treated and a control mouse were examined under an Olympus BX60 inverted microscope (Olympus, Lake Success, NY) equipped with Hoffman objective lenses (×10/×20/×40; Diagnostic Instruments, Sterling Heights, MI) connected to a SPOT One Digital Camera (Diagnostic Instruments). Images were then processed using Adobe Photoshop software (Adobe, San Jose, CA). Left panel shows extensive subcutaneous infiltration with plasma cells replacing the subcutaneous connective tissue and fat. Right panel shows disappearance of the subcutaneous tumor in a mouse treated with NPI-0052. The thin arrow indicates the cutaneous layer, and the thick arrow shows subcutaneous tissue. Scale bar, 10 μM (micrometers).

E: Comparative analysis of NPI-0052- and Bortezomib-triggered effects on myeloma xenograft growth. Treatment with either 0.15 mg/kg NPI-0052 or 1.0 mg/kg Bortezomib (n = 7 per group) significantly delayed tumor growth versus control group ($p < 0.01$).

F: Treatment with either 0.15 mg/kg NPI-0052 or 1.0 mg/kg Bortezomib significantly increases survival ($p < 0.0137$) compared to treatment with either vehicle alone. A statistically significant prolongation in mean OS compared with control mice was observed in animals treated with Bortezomib ($p = 0.003$) and NPI-0052 ($p = 0.01$).

al., 1997), the release of cyto-c and Smac from mitochondria to cytosol correlates with caspase-9 activation (Figure 6D). Besides caspase-9, NPI-0052 also activates caspase-8 (Figure 6E), followed by activation of downstream effector caspase-3 (Miller, 1999), and proteolytic cleavage of PARP (Figure 6F, lower and upper panels). Together, these findings show that NPI-0052, like Bortezomib, triggers both mitochondria-dependent and -independent signaling pathways.

Differential requirement of caspases and mitochondrial signaling during NPI-0052- and Bortezomib-induced MM cell apoptosis

We next defined the requirement for caspase-8 versus caspase-9 during NPI-0052- and Bortezomib-induced apoptosis. Incubation of MM.1S cells with pan-caspase inhibitor (Z-VAD-FMK) markedly abrogates both NPI-0052- and Bortezomib-induced apoptosis (Figure 7A). Inhibition of caspase-8 (IETD-FMK) led to a significant decrease in NPI-0052-triggered cell death, and inhibition of caspase-9 (LEHD-FMK) only moderately blocked NPI-0052-triggered decreased viability in MM.1S cells ($p < 0.005$; $n = 4$), whereas Bortezomib-induced decreases in viability are equally blocked by either caspase-8 or caspase-9 inhibitor ($p < 0.005$; $n = 4$) (Figure 7A). These biochemical data were confirmed by genetic studies using dominant-negative (DN) strategies. Treatment of DN-caspase-8-transfected MM cells with NPI-0052 (IC_{50}, 7 nM) markedly increases survival of these cells, compared to the cells transfected with DN-caspase-9 (Figure 7B). In contrast, treatment of either DN-caspase-8 or DN-caspase-9-

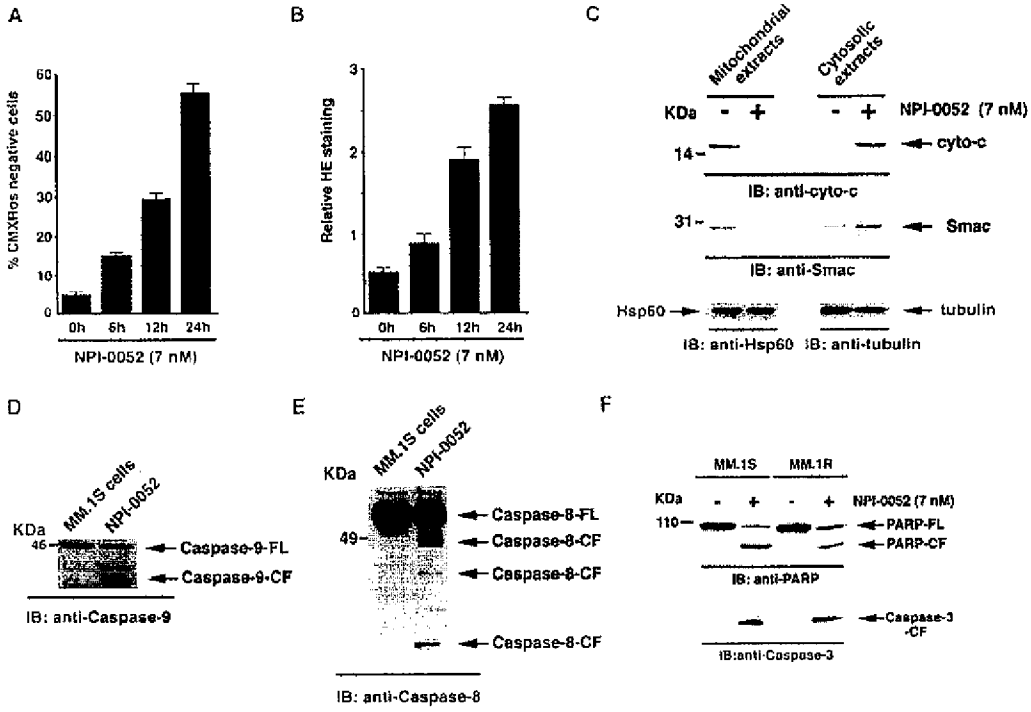

Figure 6. NPI-0052-induced apoptotic signal transduction

A: MM.1S cells were treated with NPI-0052 (7 nM) for the indicated times and then analyzed by flow cytometry for alterations in mitochondrial membrane potential ($\Delta\Psi m$). Data are mean ± SD (error bars) of two independent experiments ($p < 0.005$).

B: MM.1S cells were treated with NPI-0052 for the indicated times, stained with dihydroethidium, and analyzed by flow cytometry. Shown is mean ± SD (error bars) of two independent experiments ($p < 0.005$).

C: Immunoblot analysis of NPI-0052-treated MM.1S cells showing alterations of cyto-c and Smac levels (upper and middle panels). Blots were reprobed with anti-Hsp60 and anti-tubulin Abs (lower left and lower right panels).

D–F: MM.1S cells were treated for 24 hr with NPI-0052 (7 nM) and harvested; cytosolic proteins were subjected to immunoblot analysis using anti-caspase-9, -caspase-8, and -caspase-3 and PARP Abs. "FL" indicates full length; "CF" denotes cleaved fragment. Blots shown are representative of three independent experiments.

tranfected MM.1S cells with Bortezomib (IC_{50}, 5 nM) increased the survival to a similar extent. The functional specificity of DN-caspase-8 and DN-caspase-9 was confirmed by treatment of MM.1S cells with known inducers of caspase-9 (Dex) and caspase-8 in these cells (anti-Fas MoAb) (Chauhan et al., 1997) (Figure 7C). These data suggest that (1) NPI-0052-induced MM cell apoptosis is predominantly mediated by caspase-8; and (2) Bortezomib-induced apoptosis requires both caspase-8 and caspase-9 activation.

We next determined whether inhibition of an upstream signaling pathway that leads to caspase-8 activation affects the response to NPI-0052 or Bortezomib. The Fas-associated death domain (FADD) protein is an essential part of the death-inducing signaling complexes (DISCs) that assemble upon engagement of TNF receptor family members, such as Fas (Strasser et al., 2000), resulting in proteolytic processing and autoactivation of pro-caspase-8 (Strasser et al., 2000). Since both NPI-0052 and Bortezomib trigger caspase-8 activation, we examined the role of FADD during this event in MM cells using DN-FADD. Blockade of FADD with DN-FADD significantly attenuated NPI-0052-induced cytotoxicity compared to the empty vector-transfected MM.1S cells (42% ± 2.0% viable cells in vector-transfected cells versus 76% ± 5.1% viable cells in DN-FADD-transfected cells; $p < 0.05$) (Figure 7D). DN-FADD decreases NPI-0052-induced caspase-8 activation; however, minimal caspase-8 activation is still noted (data not shown), which may be due to upstream activators of caspase-8 other than FADD. Importantly, treatment of DN-FADD-transfected MM.1S cells with Bortezomib results in only a 16% increase in survival compared to vector-transfected cells (39% ± 2.4% viable cells in vector-transfected cells versus 55% ± 4.1% viable cells in DN-FADD-transfected cells; $p < 0.05$) (Figure 7D). These data, coupled with caspase-8 or caspase-9 inhibition studies, suggest that NPI-0052 relies more on FADD-caspase-8 signaling axis than does Bortezomib, further confirming differential mechanism of action of NPI-0052 versus Bortezomib in MM cells.

To further address this issue, we examined the alterations in Bax, a proapoptotic protein that translocates from cytosol to mitochondria during apoptosis, inhibits Bcl-2, and facilitates

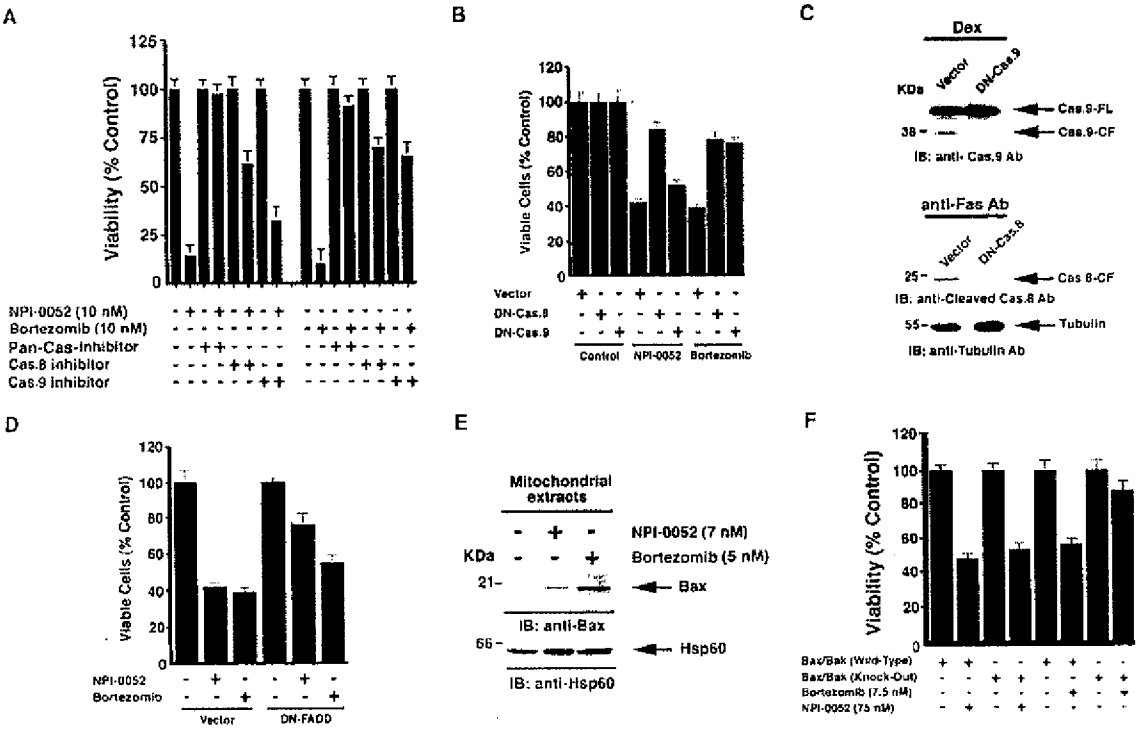

Figure 7. Role of caspase-8 versus caspase-9 during NPI-0052- and Bortezomib-induced apoptosis

A: MM.1S cells were treated for 24 hr with NPI-0052 (10 nM) or Bortezomib (10 nM) in the presence or absence of pan-caspase, caspase-8, or caspase-9 inhibitors and then assessed for viability. Shown is mean ± SD (error bars) of four independent experiments ($p < 0.004$).

B: MM.1S cells transfected with vector alone, DN-caspase-8 (Cas.8), or DN-Cas.9 were treated for 48 hr with NPI-0052 (7 nM) or Bortezomib (5 nM) and then analyzed for cell viability.

C: Control for functional specificity of DN-Cas.9 and DN-Cas.8. MM.1S cells were transiently transfected with vector alone, DN-Cas.9, or DN-Cas.8 and treated for 24 hr with either Dexamethasone (Dex; 5 μM) (upper panel) or anti-Fas MoAb (lower panels). Cytosolic extracts were analyzed by immunoblotting with anti-Cas.9, anti-Cleaved Cas.8, or anti-tubulin Abs. Blots shown are representative of two independent experiments.

D: Vector- or DN FADD-transfected MM.1S cells were treated for 48 hr with NPI-0052 (7 nM) or Bortezomib (5 nM) and then analyzed for cell viability.

E: Mitochondrial protein extracts from NPI-0052- or Bortezomib-treated MM.1S cells were subjected to immunoblot analysis with anti-Bax (upper panel) or anti-Hsp60 (lower panel) Abs.

F: The MEFs Bax and Bak (wild-type or double knockout) were treated with NPI-0052 or Bortezomib and analyzed for viability. Data represent mean + SD (error bars) of three independent experiments ($p < 0.05$).

release of cyto-c and activation of caspase-9 (Guo et al., 2003; Wei et al., 2001). NPI-0052 induces little, if any, increase in Bax levels in mitochondria, whereas Bortezomib triggers a significant accumulation of Bax in mitochondria (Figure 7E, upper panel). Previous studies showed that oligomerization of Bax with another proapoptotic Bcl-2 family member, Bak, facilitates release of cyto-c from mitochondria to the cytosol, resulting in caspase-9 activation and cell death (Wei et al., 2001). Reports in Bax/Bak knockout mice showed that these proteins are required for mitochondria-mediated cell death (Wei et al., 2001). We therefore examined the effects of Bortezomib and NPI-0052 on DKO mouse embryonic fibroblasts lacking both Bax and Bak. Deletion of Bax and Bak markedly inhibits Bortezomib- but not NPI-0052-mediated cytotoxicity (Figure 7F). These findings indicate that, in contrast to NPI-0052-, Bortezomib-mediated cell death requires mitochondrial apoptotic signaling via Bax and Bak.

A recent study showed that Bax and Bak can also localize in the endoplasmic reticulum (ER) and that ER stress can trigger caspase-12 activation (Zong et al., 2003). Bortezomib induces ER stress (Mitsiades et al., 2002b) and activates ER-resident caspase-12 in MM cells (Landowski et al., 2005). Another study showed that caspase-12 and caspase-4 are not required for caspase-dependent ER stress-induced apoptosis (Obeng and Boise, 2005). Whether caspase-12 or caspase-4 has an obligate role during NPI-0052-triggered cell death remains to be examined.

Differential effects of NPI-0052 and Bortezomib on Bcl-2-overexpressing MM cells

As noted above, during apoptosis Bax neutralizes the anti-apoptotic function of Bcl-2, thereby facilitating the cyto-c release and caspase-9 activation (Rathmell and Thompson, 2002; Willis et al., 2003). Bcl-2 also confers drug resistance in

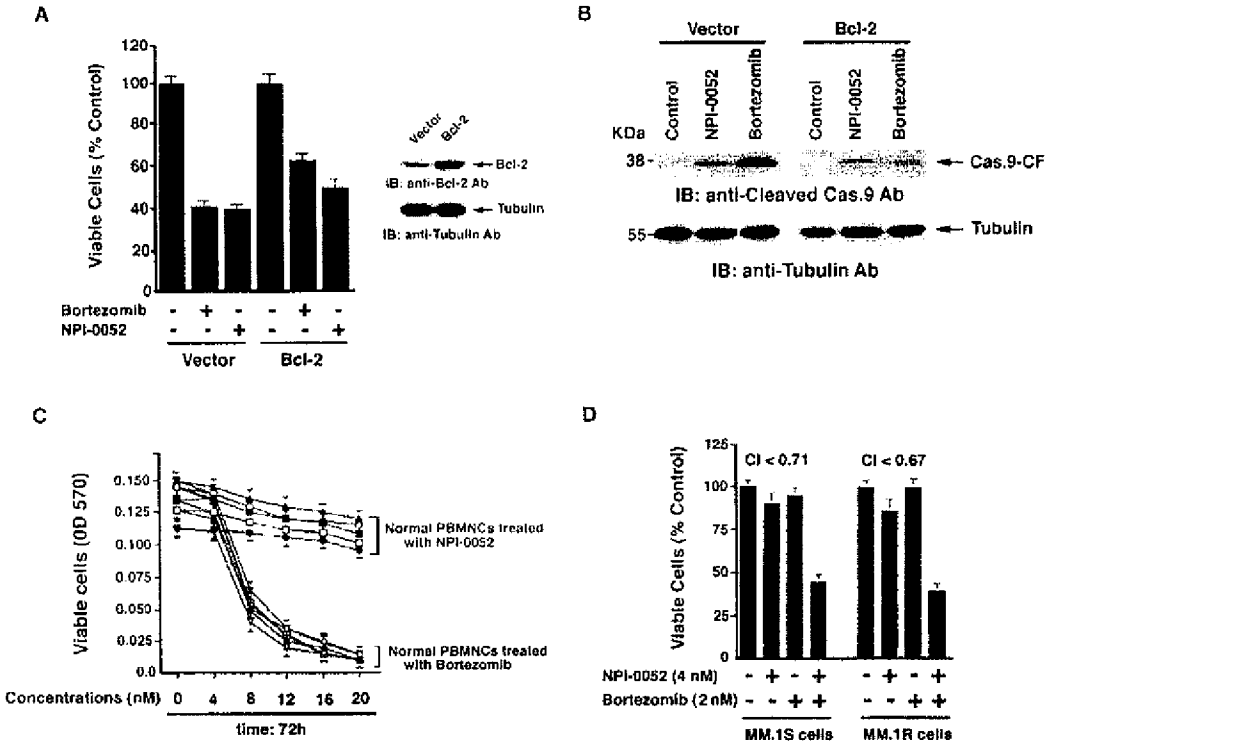

Figure 8. NPI-0052 decreases survival in Bcl-2-overexpressing MM.1S cells

A: Left panel: empty vector- or Bcl-2-transfected MM.1S cells were treated for 48 hr with NPI-0052 (10 nM) or Bortezomib (10 nM) and then analyzed for viability. Results are mean ± SD (error bars) of three independent experiments. Right panel: Bcl-2 protein levels in MM.1S cells transfected with Bcl-2 or empty (neo) vector.

B: Vector- or Bcl-2 transfected MM.1S cells were treated for 48 hr with NPI-0052 (7 nM) or Bortezomib (5 nM), and cytosolic extracts were analyzed by immunoblotting with anti Cleaved Cas.9 or anti-tubulin Abs. Blots shown are representative of two independent experiments.

C: Differential cytotoxicity of NPI-0052 and Bortezomib against lymphocytes from healthy donors. Normal lymphocytes from five healthy donors were treated with indicated concentrations of NPI-0052 or Bortezomib and then analyzed for viability. Data are mean ± SD (error bar) of three independent experiments ($p = 0.27$ from Jonckheere-Terpstra test for trend).

D: NPI-0052 and Bortezomib trigger synergistic anti-MM activity. Low doses of NPI-0052 and Bortezomib trigger synergistic anti-MM activity in MM cells. MM.1S and MM.1R cells were treated for 24 hr with indicated concentrations of NPI-0052, Bortezomib, or NPI-0052 + Bortezomib and then assessed for viability. Shown is mean ± SD (error bars) of three independent experiments ($p < 0.005$). Combination index (CI) of <1 indicates synergy.

cancer cells, including MM (Hideshima and Anderson, 2002), and provides partial protection against Bortezomib-induced killing (Mitsiades et al., 2002b). We therefore next asked whether ectopic expression of Bcl-2 in MM.1S cells affects the ability of NPI-0052 or Bortezomib to trigger cytotoxicity and postmitochondrial apoptotic signaling in MM cells. Overexpression of Bcl-2 promotes a modest increase in viability of cells treated with both agents: for NPI-0052, 50% ± 2.6% viability in Bcl-2-transfected cells versus 39% ± 1.5% viability in vector-transfected cells ($p < 0.05$); and for Bortezomib, 61% ± 2.9% viability in Bcl-2-transfected cells versus 40% ± 2.1% viability in vector-transfected cells ($p < 0.05$) (Figure 8A). Importantly, the increased survival of Bcl-2 transfectants in response to Bortezomib was greater (21%) than that in response to NPI-0052 (11%) ($p < 0.04$; $n = 3$) (Figure 8A). Moreover, Bortezomib triggers significant caspase-9 cleavage in control vector-transfected cells, which is markedly attenuated (3-fold decrease by densitometry) in Bcl-2-transfected cells; in contrast, NPI-0052-induced caspase-9 cleavage is minimally affected by Bcl-2 overexpression (Figure 8B). These findings, together with the viability results, suggest that Bcl-2 provides more protection against Bortezomib than NPI-0052.

NPI-0052 and Bortezomib have differential effects on normal lymphocytes

Our data demonstrate that NPI-0052 and Bortezomib proteasome inhibitors have differential mechanisms of action. It is also possible, due to differences in their chemical structure, specificity, or signaling mechanisms, that these agents may have different cytotoxic activities against normal cells. To address this issue, we compared the effects of NPI-0052 and Bortezomib on normal lymphocytes. NPI-0052 does not significantly decrease viability of normal lymphocytes ($p = 0.27$ from Jonckheere-Terpstra [J-T] trend test) even at the increased

doses (20 nM) (Figure 8C). Higher concentrations of NPI-0052 at 50 and 100 nM decrease the viability of lymphocytes by 25% and 50%, respectively. These data suggest that normal cells are not completely refractory to NPI-0052. In contrast, Bortezomib significantly decreases the survival of lymphocytes even at the low concentrations of 6–10 nM (Figure 8C), as is observed in clinical studies (Adams, 2002; Richardson, 2004). Importantly, the IC_{50} for patient MM cells of NPI-0052 or Bortezomib is at concentrations that do not affect viability of normal lymphocytes; however, dose escalation of each agent suggests a larger therapeutic index for NPI-0052 than for Bortezomib. Moreover, a 50% decrease in viability of normal CCD-27sk fibroblasts is observed at 317 ± 17 nM NPI-0052 versus 15 ± 3 nM Bortezomib ($p < 0.05$), suggesting that NPI-0052 has significantly reduced cytotoxicity against normal cells than Bortezomib.

We further examined whether NPI-0052 or Bortezomib alters proteasome activity in normal lymphocytes and skin fibroblasts. Both NPI-0052 and Bortezomib significantly inhibit proteasome activity in these cells: 20 nM NPI-0052 or Bortezomib triggers 99% or 59 ± 11% inhibition of CT-L proteasome activity, respectively (data not shown). Thus, although 20 nM NPI-0052 does not trigger significant cytotoxicity in normal lymphocytes, it reduces CT-L proteasome activity in these cells. Similarly, treatment of normal CCD-27sk fibroblasts at the IC_{50} for NPI-0052 (317 nM) or Bortezomib (15 nM) also inhibits proteasome activity (data not shown). Bortezomib inhibits 20S proteasome activity in murine WBCs at 1 hr post-i.v. injections (Adams et al., 1999). Furthermore, these data are consistent with the clinical observation showing a similar degree of proteasome inhibition in blood from responders versus nonresponders to Bortezomib therapy (Adams, 2002; Richardson, 2004). Nonetheless, these findings demonstrate a selective anti-MM activity of NPI-0052.

Combined Bortezomib and NPI-0052 treatment triggers synergistic apoptosis in MM cells

The proteasome inhibitors Bortezomib and NPI-0052 are distinct, providing the rationale for combining these agents to enhance anti-MM activity. MM.1S or MM.1R MM cells were treated with both NPI-0052 and Bortezomib simultaneously across a range of concentrations and analyzed for viability. Results demonstrate that NPI-0052 and Bortezomib induce synergistic cytotoxicity (Figure 8D; shown are the representative results from minimally toxic and maximally synergistic concentrations of each agent). Isobologram analysis confirmed synergistic anti-MM activity of Bortezomib with NPI-0052 (combination index < 1.0). Importantly, combining low doses of these two agents does not significantly affect the viability of normal lymphocytes (Figure S2). While the definitive demonstration of decreased toxicity of combination therapy awaits results of careful clinical trials, the synergy observed in vitro may allow for use of lower doses and decreased toxicity.

The mechanisms mediating the enhanced cytotoxicity of the combination may simply reflect higher levels of proteasome inhibition with the two-drug regimen, and our ongoing studies are examining this issue in MM animal models using various parameters to determine the proteasome activity profiles of combination therapy, such as drug route, dose, and sequence of administration. Nonetheless, our present study shows that these two agents trigger differential apoptotic signaling pathways, which may account for the enhanced cytotoxicity upon combined treatment. Activation of different apoptotic signaling cascades provides the basis for combining two drugs to enhance cell death (Chauhan and Anderson, 2003). Another recent study also showed that Bortezomib sensitizes to TRAIL-induced apoptosis in genitourinary cancer cells via p21 accumulation and enhanced caspase-8 activation (Lashinger et al., 2005). Combination therapy with Bortezomib and NPI-0052 therefore may (1) allow use of subtoxic concentrations of each agent and (2) permit escalating synergistic doses of these agents to increase the apoptotic threshold, thereby enhancing anti-MM activity.

Collectively, our study shows the following: (1) a novel proteasome inhibitor, NPI-0052, inhibits proteasome activity both in vitro and in vivo at pharmacologically achievable concentrations and exhibits a different proteasome inhibition profile than Bortezomib; (2) NPI-0052 is a more potent inhibitor of NF-κB and related cytokine secretion than Bortezomib; (3) NPI-0052 induces apoptosis in MM cells resistant to conventional and Bortezomib therapies, without affecting normal lymphocyte viability; (4) NPI-0052 does not affect viability of BMSCs; (5) NPI-0052 induces MM cell apoptosis even in the presence of MM growth factors, such as IL-6 or IGF-1; (6) NPI-0052 blocks VEGF-induced migration of MM cells, confirming its antiangiogenic activity; (7) NPI-0052 overcomes drug resistance conferred by the antiapoptotic protein Bcl-2; (8) NPI-0052-induced apoptosis in MM cells is associated with loss of $\Delta\Psi m$, increase in O_2^- production, release of cyto-c/Smac, and activation of caspase-8, caspase-9, and caspase-3; (9) both biochemical and genetic evidence indicate that NPI-0052, in contrast to Bortezomib, relies more on the FADD-caspase-8-mediated cell death signaling pathway; (10) combinations of low doses of NPI-0052 and Bortezomib trigger synergistic anti-MM activity; (11) NPI-0052 inhibits MM tumor growth in vivo, as well as prolongs, survival without reoccurrence of tumor in 57% mice; and finally, (12) NPI-0052 is orally bioactive. Together, these findings provide the framework for clinical trials of NPI-0052, either alone or in combination with Bortezomib, to enhance clinical efficacy, reduce toxicity, and overcome drug resistance in patients with relapsed/refractory MM.

Experimental procedures

In vitro and in vivo proteasome activity assays

Proteasome activity assays were performed using purified human erythrocyte-derived 20S proteasomes, as previously described (Lightcap et al., 2000). In vivo comparative analysis of proteasome activities were performed as follows. Single i.v. administration of NPI-0052: NPI-0052 was dissolved in 100% DMSO and serially diluted with 5% Solutol (Solutol HS 15, polyethylene glycol 660 12-hydroxystearate; BASF, Shreveport, LA), yielding a final concentration of 2% DMSO. The vehicle control consisted of 2% DMSO and 98% (5% Solutol). Male Swiss-Webster mice (n = 5) were treated with a single dose of NPI-0052 (0.15 mg/kg) or Bortezomib (1 mg/kg); blood samples were collected at 90 min, 24 hr, 48 hr, 72 hr, or 168 hr; and whole blood cells were then analyzed for proteasome activity. Further details are found in the Supplemental Data.

Assaying proteasome activity by immunoblotting

The method has been described previously (Berkers et al., 2005). Briefly, the principle is as follows: DansylAhx$_3$L$_3$VS is a proteasome inhibitor that covalently modifies all active proteasome subunits with comparable affinity (Bogyo et al., 1998; Kessler et al., 2001). This proteasome probe is equipped with a dansyl-sulfonamidohexanoyl hapten and can be visualized by immunoblotting using polyclonal antibodies against the dansyl moiety.

in the assay, sites that are not targeted by NPI-0052 or Bortezomib are labeled by DansylAhx$_3$L$_3$VS and visualized on Western blot, while sites that are targeted by NPI-0052 or Bortezomib cannot be seen. Equal amounts of protein (60 μg) from Bortezomib- or NPI-0052-treated MM.1S cells were incubated with 0.6 μM DansylAhx$_3$L$_3$VS at 37°C and subjected to immunoblotting using an anti-dansyl-sulfonamidohexanoyl polyclonal Ab (1:500, rabbit; Molecular Probes, Carslbad, CA).

Human plasmacytoma xenograft models

All experiments involving animals were approved by an institutional Animal Care and Use Committee. The xenograft tumor formation was performed as previously described (LeBlanc et al., 2002). Briefly, mice (n = 7/group) were inoculated subcutaneously in the flank with 3×10^7 MM.1S MM cells in 100 μl of RPMI-1640 media. NPI-0052 treatment was started after the development of measurable tumor (120–180 mm^3 size). NPI-0052 (0.25 mg/kg or 0.5 mg/kg) was given orally twice a week. For comparative studies, mice were treated by the i.v. route with NPI-0052 (0.15 mg/kg) or Bortezomib (1 mg/kg) twice a week. Tumor measurements were taken on alternate days with a caliper, and tumor volume was calculated according to the equation 1/2 (length [mm] × width [mm]]^2. Animals were sacrificed if the tumor was ≥2 cm or exhibited visible signs of necrosis.

Expression vectors and transfections

MM.1S cells were transiently transfected using Cell line Nucleofecto kit V, according to the manufacturer's instructions (Amaxa Biosystems, Germany), with vector alone, DN-caspase-8, DN-caspase-9, or DN-FADD and cotransfected with vector containing green fluorescence protein (GFP) alone. Following transfections, GFP-positive cells were selected by flow cytometry, treated with NPI-0052 or Bortezomib, and analyzed for viability.

Statistical analysis

Nonparametric tests and mixed models were used to analyze the data. This includes the Wilcoxon signed rank test to compare proliferation in untreated and treated patient cells and the J-T trend test for measuring the viability of lymphocytes and cell lines resistant to conventional therapy. Wilcoxon rank-sum test was used for measuring change in the tumor volume, the Kaplan-Meier method was used for survival analysis, and log-rank analysis was used for statistical significance.

Isobologram analysis

Isobologram analysis was performed using the CalcuSyn software program (Biosoft, Ferguson, MO and Cambridge, UK), and a combination index (CI) of <1.0 indicates synergism (Chou and Talalay, 1984).

Supplemental data

Information on MM cell lines and culture medium, reagents, purification of CD138-positive MM patient BM samples, PBMNC preparation from normal healthy donors, cytotoxicity and apoptosis assays, transwell migration assays, protein extraction, mitochondrial assays, immunoblotting, and antibodies can be found in the Supplemental Data. The Supplemental Data include two supplemental figures as well as the Supplemental Experimental Procedures and can be found with this article online at http://www.cancercell.org/cgi/content/full/8/5/407/DC1/.

Acknowledgments

We thank Dr. Stanley Korsmeyer (Dana-Farber Cancer Institute, Boston, MA) for providing MEF cell lines and for critical discussion. We are thankful to Drs. Kapil Bhalla (H. Lee Moffitt Cancer Center and Research Institute, Tampa, FL) and Yuri Lazebnik (The Cold Spring Harbor Laboratory, NY) for providing dominant-negative caspase-8, caspase-9, and FADD constructs. We thank Gordafaried Deyanat-Yazdi for technical assistance with proteasome assays, Paula Neri and Melissa Rooney for help in animal studies, and Deli He for competition assays. This work was supported by NIH grants RO 1 CA50947, PO-1 CA 78373, and SPORE P50 CA100707; a Doris Duke Distinguished Clinical Research Scientist Award (K.C.A.); a Multiple Myeloma Research Foundation (MMRF) Senior Research Award (D.C.); The Myeloma Research Fund; The Cure Myeloma Fund; and The National Foundation of Cancer Research.

Received: January 12, 2005
Revised: July 2, 2005
Accepted: October 22, 2005
Published: November 14, 2005

References

Adams, J. (2002). Preclinical and clinical evaluation of proteasome inhibitor PS-341 for the treatment of cancer. Curr. Opin. Chem. Biol. *6*, 493–500.

Adams, J. (2004). The proteasome: a suitable antineoplastic target. Nat. Rev. Cancer *4*, 349–360.

Adams, J., Palombella, V.J., Sausville, E.A., Johnson, J., Destree, A., Lazarus, D.D., Maas, J., Pien, C.S., Prakash, S., and Elliott, P.J. (1999). Proteasome inhibitors: a novel class of potent and effective antitumor agents. Cancer Res. *59*, 2615–2622.

Anderson, K.C. (2004). Bortezomib therapy for myeloma. Curr. Hematol. Rep. *3*, 65.

Berkers, C.R., Verdoes, M., Lichtman, E., Fiebiger, E., Kessler, B.M., Anderson, K.C., Ploegh, H.L., Ovaa, H., and Galardy, P.J. (2005). Activity probe for in vivo profiling of the specificity of proteasome inhibitor bortezomib. Nat. Methods *2*, 357–362.

Bogyo, M., Shin, S., McMaster, J.S., and Ploegh, H.L. (1998). Substrate binding and sequence preference of the proteasome revealed by active-site-directed affinity probes. Chem. Biol. *5*, 307–320.

Bossy-Wetzel, E., and Green, D.R. (1999). Apoptosis: checkpoint at the mitochondrial frontier. Mutat. Res. *434*, 243–251.

Chauhan, D., and Anderson, K.C. (2003). Mechanisms of cell death and survival in multiple myeloma (MM): Therapeutic implications. Apoptosis *8*, 337–343.

Chauhan, D., Pandey, P., Ogata, A., Teoh, G., Krett, N., Halgren, R., Rosen, S., Kufe, D., Kharbanda, S., and Anderson, K.C. (1997). Cytochrome-c dependent and independent induction of apoptosis in multiple myeloma cells. J. Biol. Chem. *272*, 29995–29997.

Chauhan, D., Hideshima, T., Rosen, S., Reed, J.C., Kharbanda, S., and Anderson, K.C. (2001). Apaf-1/cytochrome c-independent and Smac-dependent induction of apoptosis in multiple myeloma (MM) cells. J. Biol. Chem. *276*, 24453–24456.

Chauhan, D., Li, G., Hideshima, T., Podar, K., Mitsiades, C., Mitsiades, N., Munshi, N., Kharbanda, S., and Anderson, K.C. (2003). JNK-dependent release of mitochondrial protein, Smac, during apoptosis in multiple myeloma (MM) cells. J. Biol. Chem. *278*, 17593–17596.

Chauhan, D., Hideshima, T., and Anderson, K.C. (2005). Proteasome inhibition in multiple myeloma: therapeutic implication. Annu. Rev. Pharmacol. Toxicol. *45*, 465–476.

Chou, T.C., and Talalay, P. (1984). Quantitative analysis of dose-effect relationships: the combined effects of multiple drugs or enzyme inhibitors. Adv. Enzyme Regul. *22*, 27–55.

Corey, E.J., and Li, W.D. (1999). Total synthesis and biological activity of lactacystin, omuralide and analogs. Chem. Pharm. Bull. (Tokyo) *47*, 1–10.

Guo, B., Zhai, D., Cabezas, E., Welsh, K., Nouraini, S., Satterthwait, A.C., and Reed, J.C. (2003). Humanin peptide suppresses apoptosis by interfering with Bax activation. Nature *423*, 456–461.

Hideshima, T., and Anderson, K.C. (2002). Molecular mechanisms of novel therapeutic approaches for multiple myeloma. Nat. Rev. Cancer *2*, 927–937.

Hideshima, T., Chauhan, D., Richardson, P., Mitsiades, C., Mitsiades, N., Hayashi, T., Munshi, N., Dong, L., Castro, A., Palombella, V., et al. (2002). NF-κB as a therapeutic target in multiple myeloma. J. Biol. Chem. *277*, 16639–16647.

Kessler, B.M., Tortorella, D., Altun, M., Kisselev, A.F., Fiebiger, E., Hekking,

B.G., Ploegh, H.L., and Overkleeft, H.S. (2001). Extended peptide-based inhibitors efficiently target the proteasome and reveal overlapping specificities of the catalytic β-subunits. Chem. Biol. *8*, 913–929.

Landowski, T.H., Megli, C.J., Nullmeyer, K.D., Lynch, R.M., and Dorr, R.T. (2005). Mitochondrial-mediated disregulation of Ca2+ is a critical determinant of Velcade (PS-341/bortezomib) cytotoxicity in myeloma cell lines. Cancer Res. *65*, 3828–3836.

Lashinger, L.M., Zhu, K., Williams, S.A., Shrader, M., Dinney, C.P., and McConkey, D.J. (2005). Bortezomib abolishes tumor necrosis factor-related apoptosis-inducing ligand resistance via a p21-dependent mechanism in human bladder and prostate cancer cells. Cancer Res. *65*, 4902–4908.

LeBlanc, R., Catley, L.P., Hideshima, T., Lentzsch, S., Mitsiades, C.S., Mitsiades, N., Neuberg, D., Goloubeva, O., Pien, C.S., Adams, J., et al. (2002). Proteasome inhibitor PS-341 inhibits human myeloma cell growth in vivo and prolongs survival in a murine model. Cancer Res. *62*, 4996–5000.

Lightcap, E.S., McCormack, T.A., Pien, C.S., Chau, V., Adams, J., and Elliott, P.J. (2000). Proteasome inhibition measurements: clinical application. Clin. Chem. *46*, 673–683.

Macherla, V.R., Mitchell, S.S., Manam, R.R., Reed, K.A., Chao, T.H., Nicholson, B., Deyanat-Yazdi, G., Mai, B., Jensen, P.R., Fenical, W.F., et al. (2005). Structure-activity relationship studies of salinosporamide A (NPI-0052), a novel marine derived proteasome inhibitor. J. Med. Chem. *48*, 3684–3687.

Miller, L.K. (1999). An exegesis of IAPs: salvation and surprises from BIR motifs. Trends Cell Biol. *9*, 323–328.

Mitsiades, C.S., Mitsiades, N., Poulaki, V., Schlossman, R., Akiyama, M., Chauhan, D., Hideshima, T., Treon, S.P., Munshi, N.C., Richardson, P.G., and Anderson, K.C. (2002a). Activation of NF-κB and upregulation of intracellular anti-apoptotic proteins via the IGF-1/Akt signaling in human multiple myeloma cells: therapeutic implications. Oncogene *21*, 5673–5683.

Mitsiades, N., Mitsiades, C.S., Poulaki, V., Chauhan, D., Fanourakis, G., Gu, X., Bailey, C., Joseph, M., Libermann, T.A., Treon, S.P., et al. (2002b). Molecular sequelae of proteasome inhibition in human multiple myeloma cells. Proc. Natl. Acad. Sci. USA *99*, 14374–14379.

Obeng, E.A., and Boise, L.H. (2005). Caspase-12 and caspase-4 are not required for caspase-dependent endoplasmic reticulum stress-induced apoptosis. J. Biol. Chem. *280*, 29578–29587.

Palombella, V.J., Conner, E.M., Fuseler, J.W., Destree, A., Davis, J.M., Laroux, F.S., Wolf, R.E., Huang, J., Brand, S., Elliott, P.J., et al. (1998). Role of the proteasome and NF-κB in streptococcal cell wall-induced polyarthritis. Proc. Natl. Acad. Sci. USA *95*, 15671–15676.

Podar, K., Tai, Y.T., Lin, B.K., Narsimhan, R.P., Sattler, M., Kijima, T., Salgia, R., Gupta, D., Chauhan, D., and Anderson, K.C. (2002). Vascular endothelial growth factor-induced migration of multiple myeloma cells is associated with β1 integrin- and phosphatidylinositol 3-kinase-dependent PKCα activation. J. Biol. Chem. *277*, 7875–7881.

Rathmell, J.C., and Thompson, C.B. (2002). Pathways of apoptosis in lymphocyte development, homeostasis, and disease. Cell Suppl. *109*, S97–S107.

Richardson, P.G. (2004). A review of the proteasome inhibitor bortezomib in multiple myeloma. Expert Opin. Pharmacother. *5*, 1321–1331.

Richardson, P.G., Sonneveld, P., Schuster, M.W., Irwin, D., Stadtmauer, E.A., Facon, T., Harousseau, J.L., Ben-Yehuda, D., Lonial, S., Goldschmidt, H., et al. (2005). Bortezomib or high-dose dexamethasone for relapsed multiple myeloma. N. Engl. J. Med. *352*, 2487–2498.

Russo, S.M., Tepper, J.E., Baldwin, A.S., Jr., Liu, R., Adams, J., Elliott, P., and Cusack, J.C., Jr. (2001). Enhancement of radiosensitivity by proteasome inhibition: implications for a role of NF-κB. Int. J. Radiat. Oncol. Biol. Phys. *50*, 183–193.

Strasser, A., O'Connor, L., and Dixit, V.M. (2000). Apoptosis signaling. Annu. Rev. Biochem. *69*, 217–245.

Teicher, B.A., Ara, G., Herbst, R., Palombella, V.J., and Adams, J. (1999). The proteasome inhibitor PS-341 in cancer therapy. Clin. Cancer Res. *5*, 2638–2645.

Wei, M.C., Zong, W.X., Cheng, E.H., Lindsten, T., Panoutsakopoulou, V., Ross, A.J., Roth, K.A., MacGregor, G.R., Thompson, C.B., and Korsmeyer, S.J. (2001). Proapoptotic BAX and BAK: a requisite gateway to mitochondrial dysfunction and death. Science *292*, 727–730.

Willis, S., Day, C.L., Hinds, M.G., and Huang, D.C. (2003). The Bcl-2-regulated apoptotic pathway. J. Cell Sci. *116*, 4053–4056.

Xu, F., Gardner, A., Tu, Y., Michl, P., Prager, D., and Lichtenstein, A. (1997). Multiple myeloma cells are protected against dexamethasone-induced apoptosis by insulin-like growth factors. Br. J. Haematol. *97*, 429–440.

Zong, W.X., Li, C., Hatzivassiliou, G., Lindsten, T., Yu, Q.C., Yuan, J., and Thompson, C.B. (2003). Bax and Bak can localize to the endoplasmic reticulum to initiate apoptosis. J. Cell Biol. *162*, 59–69.

Dual targeting of the proteasome regulates survival and homing in Waldenstrom Macroglobulinemia

Aldo M. Roccaro,[1,2] Xiaoying Jia,[1] Antonio Sacco,[1] Molly Melhem,[1] Anne-Sophie Moreau,[1] Xavier Leleu,[1] Hai T. Ngo,[1] Judith Runnels,[1] Abdelkareem Azab,[1] Feda Azab,[1] Nicholas Burwick,[1] Mena Farag, [1] Steven P. Treon,[1] Michael A. Palladino,[4] Teru Hideshima,[1] Dharminder Chauhan,[1] Kenneth C. Anderson,[1] Irene M. Ghobrial[1]

[1] Medical Oncology, Dana-Farber Cancer Institute, and Harvard Medical School, Boston, MA, USA
[2] Dept. Blood Disease, Brescia, Italy.
[3] Dept. of Internal Medicine and Clinical Oncology, University of Bari Medical School, Bari, Italy
[4]Nereus Pharmaceuticals, San Diego, CA

Corresponding author.

Irene M. Ghobrial, MD
Medical Oncology, Dana-Farber Cancer Institute,
44 Binney Street, Mayer 548A, Boston, MA, 02115.
Phone: (617)-632-4198 ; Fax: (617)-632-4862
Email: irene_ghobrial@dfci.harvard.edu

Supported in part by R21 1R21CA126119-01A1, International Waldenstrom Macroglobulinemia Foundation (IWMF), the Leukemia and Lymphoma Research Foundation, and the Lymphoma Research Foundation.

Running Title: Combination of NPI-0052 and bortezomib in Waldenstrom Macroglobulinemia
Scientific subheading: Neoplasia
Keywords: Waldenstrom Macroglobulinemia, Bortezomib, NPI-0052, NF-κB, Akt

Abstract count:

Word count:

The authors (IMG, KCA) declare Grant support by Millennium Inc.

Abstract

Walderstrom's Macroglobulinemia (WM) is a biologically unique low grade B-cell lymphoma characterized by high protein turnover. In this study, we dissect the biological role of the proteasome in WM using two proteasome inhibitors, bortezomib and NPI-0052, that have non-overlapping activities. We first demonstrated that the novel proteasome inhibitor NPI-0052 leads to inhibition of proliferation and induction of apoptosis in WM cells. We then demonstrated that the combination of NPI-0052 and bortezomib leads to synergistic cytotoxicity on WM cells leading to inhibition of nuclear translocation of p65 NF-κB, and synergistic induction of caspases-3, -8, -9 and PARP cleavage. These two agents led to inhibition of the canonical and non-canonical NF-κB pathways. We further dissected the mechanism of synergy of these two agents and demonstrated that they act synergistically through their differential activity on Akt activity and on chymotripsin-like (CT-L), caspase-like (CL) and trypsin-like (T-L) activities of the proteasome. We demonstrated that NPI-0052-induced cytotoxicity was completely abrogated in an Akt knockdown cell line, indicating that its major activity is mediated through the Akt pathway, while bortezomib modestly activated Akt. NPI-0052 and bortezomib inhibited migration and adhesion *in vitro* and homing of WM cells *in vivo*. Since IL-6 and NF-κB induction by adhesion are two major pathways regulated by the proteasome, we demonstrated that NPI-0052 and bortezomib overcome resistance induced by mesenchymal cells and by the addition of IL-6 in a co-culture *in vitro* system. Finally, we demonstrated that the combination of NPI-0052 and bortezomib did not induce cytotoxicity on stem cells using colony-formation assays. Theses studies provide a stronger understanding of the biological role of the proteasome and signaling pathways regulated by this pathway in WM, and provide the preclinical basis for studying the activity of combinations of proteasome inhibitors in WM and other low-grade lymphomas.

Introduction

Although considered a rare disease, Waldenström's Macroglobulinemia (WM) is becoming a model low-grade lymphoma to test and validate therapeutic compounds that are specifically active in this biologically unique malignancy. WM is characterized by the presence of lymphoplasmacytic cells in the bone marrow and the secretion of IgM monoclonal protein in the serum, indicating that WM cells present a high protein turnover.[1-3] Protein metabolism is a tightly regulated process, and inhibition of its turnover may lead to apoptosis in malignant cells, such as with proteasome inhibitors.[4,5] The major activity of proteasome inhibitors is through targeting the IL-6 and NF-κB signaling pathways. Both these pathways are critical regulators of survival and proliferation in B-cell malignancies including WM.[6-8] Previous studies have demonstrated that adhesion of multiple myeloma cells to stromal cells induces NF-κB activation, which in turn regulates IL-6 excretion by stromal cells. [9,10]

The multicatalytic ubiquitin-proteasome pathway is responsible for the degradation of eukaryotic cellular proteins. This pathway also controls the activation of NF-κB by regulating degradation of IκBα. NF-κB plays a critical role in regulating many cellular responses including immunity, inflammation, proliferation, survival, and angiogenesis.[11] Inactive NF-κB complexes with its inhibitor, IκBα, and remains sequestered in the cytosol. A variety of stimuli trigger the phosphorylation of IκB by IκB kinase (IKK).[12] Phosphorylated IκB is then a target for ubiquination and proteasome mediated degradation, which in turn releases NF-κB to translocate from the cytosol to the nucleus. Once in the nucleus, NF-κB stimulates transcription of numerous cytokines, chemokines, and cell adhesion molecules. NF-κB is constitutively activated in numerous hematologic malignancies, including plasma cell dyscrasias like multiple myeloma.[10] This pathway also interacts with the PI3K/Akt pathway, a critical regulator of survival in WM cells based on our previous studies.[13] Akt indirectly activates NF-κB through direct phosphorylation and activation of IκB kinase alpha (IKKα), thereby inducing degradation of NF-κB inhibitor alpha (IκBα) by the ubiquitin-proteasome pathway.[10]

One of the most extensively studied proteasome inhibitors is bortezomib (Millennium Inc, Cambridge, MA). Bortezomib inhibits the ubiquitin-26S proteasome pathway, which regulates the turnover of a vast number of intracellular proteins, has become an exciting target in a variety of malignancies, most notably multiple myeloma.[14] The proper functioning of this system is crucial for cell cycle regulation, gene transcription, and signal transduction. Inhibition of the proteasome effectively increases the presence of IκBα and prevents NF-κB release to the nucleus. Based on its activity in multiple myeloma, single agent bortezomib was tested in WM in phase II trials and achieved 40-80% responses.[15]

These striking clinical responses indicate that proteasome activity is critical for the survival of WM cells. Similarly, other proteasome inhibitors have been recently developed including NPI-0052 (Salinosporamide A, Nereus Inc, San Diego, CA). NPI-0052 has a different chemical structure, toxicity profile, and mechanism of action than bortezomib. It regulates all three activities of the proteasome, and apoptosis mediated by this agent appears to be predominately through the caspase-8 cell death cascade.[16]

In this study, we sought to determine the activity of the new proteasome inhibitor NPI-0052 in WM on the canonical and non-canonical NF-κB pathways in WM, and to determine its cytotoxic activity in combination with bortezomib. In addition, we investigated mechanisms of synergistic activity of these two agents on WM cells and in the presence of the bone marrow milieu, including their activity on the different catalytic activities of the proteasome, on the PI3K/Akt pathway and on caspases cleavage. Finally, we determined the effect of these two agents alone and in combination on homing and adhesion of WM cells *in vitro* and *in vivo* to the bone marrow. These studies provide a stronger understanding of the biological role of the proteasome and signaling pathways regulated by this pathway in WM, and provide the preclinical basis for studying the activity of combinations of proteasome inhibitors in WM and other low-grade lymphomas.

Material and methods

Cells

The WM cell lines (BCWM.1; WM-WSU) and IgM secreting low grade lymphoma cell lines (MEC-1; Namalwa) were used in this study. The BCWM.1 is a recently described WM cell line that has been developed from a patient with untreated WM.[17] The cells express the typical lymphoplasmacytic phenotype. Kariotypic and multiplex fluorescent in situ hybridization (M-FISH) studies did not demonstrate cytogenetic abnormalities in this cell line (Santos). WSU-WM was kindly provided by Dr. Al Katib (Wayne State University, Detroit, MI). MEC-1 was a gift from Dr. Kay (Mayo Clinic, Rochester, MN). RL was purchased from the American Tissue Culture Collection (Manassas, VA). All cell lines were cultured at 37°C in RPMI-1640 containing 10% fetal bovine serum (FBS; Sigma Chemical, St Louis, MO), 2 mM L-glutamine, 100 U/mL penicillin, and 100 μg/mL streptomycin (GIBCO, Grand Island, NY).

Primary WM cells were obtained from bone marrow (BM) samples from previously treated WM patients using $CD19^+$ microbead selection (Miltenyi Biotec, Auburn, CA) with over 90% purity as confirmed by flow cytometric analysis with monoclonal antibody reactive to human CD20-PE (BD-Bioscience, San Jose, CA). Peripheral blood mononuclear cells (PBMCs) were obtained from healthy subjects by Ficoll-Hipaque density sedimentation. Cells were cultured at 37°C in RPMI-1640 containing 10% fetal bovine serum (FBS; Sigma Chemical, St Louis, MO), 2 mM L-glutamine, 100 U/mL penicillin, and 100 μg/mL streptomycin (GIBCO, Grand Island, NY). Approval for these studies was obtained from the Dana-Farber Cancer Institute Institutional Review Board. Informed consent was obtained from all patients and healthy volunteers in accordance with the Declaration of Helsinki protocol.

Reagents

NPI-0052 was provided by Nereus Pharmaceuticals (San Diego, CA). Bortezomib was obtained from Millennium Pharmaceuticals Inc. (Cambridge, MA). Fluorogenic substres, suc-LLVY-amc and z-LLE-amc, were from Calbiochem (San Diego, CA).

Growth inhibition assay

The inhibitory effect of NPI-0052, alone or in combination with Bortezomib, on WM cell growth was assessed by measuring 3-(4,5-dimethylthiazol-2-yl)-2,5-diphenyltetrazolium bromide (MTT; Chemicon International, Temecula, CA) dye absorbance as previously described.[18] Briefly, cells were seeded at a density of 4×10^4 cells per well in a 96-well plate and treated with NPI-0052, bortezomib, or the combination. MTT (10 μL) was added to each well for the last 4 hours of 24-hour and/or 48-hour cultures. Absorbance was measured at 570/630 nm using a spectrophotometer (Molecular Devices, Sunnyvale, CA). All experiments were performed in triplicate.

DNA synthesis

WM cell lines and $CD19^+$ primary WM cells were incubated in the presence of RPMI (10% FBS) with NPI-0052 (2.5-40 nM), for 48 hours at 37°C. DNA synthesis was measured by [^{3}H]-thymidine ([^{3}H]-TdR; Perkin Elmer, Boston, MA) uptake, as previously described.[18] Cells were pulsed with ([^{3}H]-TdR (0.0185 MBq/well [0.5 μCi/well0 during the last 8 hours (cell lines) or 24 h ($CD19^+$ primary WM cells) of 48 hours cultures. All experiments were performed in triplicate.

Detection of apoptosis

Annexin V-FITC and PI staining were used to detect and quantify apoptosis by flow cytometry. BCWM.1 cells (1×10^6 cells/well) were cultured in 24-well plates (Costar, Cambridge, MA) for 24 hours with NPI-0052 (2.5-30nM) or control media. Cells were then harvested in cold PBS and pelleted by centrifugation for 5 minutes at 1500 rpm. They were subsequently resuspended at 1×10^6 cells/mL in binding buffer (Hepes buffer, 10 mM, pH 7.4, 150 mM NaCl, 5 mM KCl, 1 mM $MgCl_2$, 1.8 mM $CaCl_2$), stained with annexin V-FITC and PI, and incubated in the dark for 15 minutes. Cells were processed with a Epics Altra flow cytometer (Coulter Immunology, Hialeha, FL), as previously described.[13]

Immunoblotting

BCWM.1 cells were harvested and lysed using lysis buffer (Cell Signaling technology, Beverly, MA) reconstituted with 5 mM NaF, 2 mM Na_3VO_4, 1 mM PMSF (polymethilsulfonyl fluoride), 5 μg/mL leupeptine, and 5 μg/mL aprotinin. Whole-cell lysates (50 μg/lane) were subjected to sodium dodecyl sulfate-polyacrylamide gel eletrophoresis (SDS-PAGE) and transferred to polyvinyldene fluoride (PVDF) membrane (Bio-Rad Laboratories, Hercules, CA). The antibodies used for immunoblotting included: anti-phospho (p)-Akt (Ser473), -Akt, -p-GSK3α-β (Ser21/9), -p-ERK1/2 (Thr202/Tyr204), -caspase-3, -caspase-8, -caspase-9, -PARP, -mcl1, -survivin, and -p-S6 ribosomal (Cell Signaling Technology, Beverly, MA); -α-tubulin antibodies (Santa Cruz Biotechnology, Santa Cruz, CA). Nuclear extracts of the cells were prepared using the Nuclear extraction kit (Panomics Inc., Redwood City, CA, USA) and subjected to immunoblotting with anti-p-p65, p50/p105 and -nucleolin antibodies (Santa Cruz Biotechnology).

***In vitro* Akt kinase assay**

In vitro Akt kinase assay (Cell Signaling Technology, Beverly, MA) was performed as previously described.[18] Briefly, BCWM.1 cells were cultured in the presence or absence of NPI-0052 (10nM), alone or in combination with Bortezomib (10nM), for 4 hours, and subsequently lysed in 1X lysis buffer. Lysates were then immunoprecipitated with immobilized Akt primary antibody and incubated with gentle rocking overnight at 4°C. Cell lysate/immobilized antibody were microcentrifuged and pellets were washed twice with 1X cell lysis buffer, and twice with 1X kinase buffer. Pellets were resuspended in 1X kinase buffer supplemented with ATP and GSK-3 fusion protein, and then incubated for 30 minutes at 30°C. Samples were run on SDS-PAGE and transferred to PVDF membrane. Kinase activity was detected by immunoblotting with p-GSK-3α/β (Ser21/9) antibody (Cell Signaling, Beverly, MA).

Lentivirus shRNA vector construction and Akt gene transduction.

To further determine the role of NPI-0052 in the regulation of the Akt pathway, we established an Akt knockout BCWM.1 cell line using a lentivirus transfection system,

as previously described.[19-21] The sense and antisense oligonucleotide sequence for construction of Akt shRNA were as follows: Clone #10162: target sequence GGACAAGGACGGGCACATTAA; #10163: target sequence CGAGTTTGAGTACCTGAAGCT.

NF-κB activity

NF-κB activity was investigated using the Active Motif TransAM kits, a DNA-binding ELISA-based assay (Active Motif North America, Carlsbad, CA). Briefly, BCWM.1 cells were treated with NPI-0052 (10nM), bortezomib (10nM), alone or in combination for 4 hours and stimulated with TNF-α (10ng/mL) during the last 20 minutes of culture. NFκBp65 transcription factor-binding to its consensus sequence on the plate-bound oligonucleotide was studied from nuclear extracts, following manufacturer procedure.

20S proteasome activity

The chymotrypsin-like, trypsin-like, and caspase-like activity of the 20S proteasome of leukemia cells was determined by measurement of fluorescence generated from the cleavage of the fluorogenic substrates suc-LLVY-amc, boc-LRR-amc, and z-LLE-amc, respectively.[22] Cells were incubated for 4 hours in the presence of diluent or NPI-0052 10nM, bortezomib 10nM, or bortezomib + NPI-0052, washed with phosphate buffered saline (PBS) and resuspended in 300 μL of a solution containing 20 mM Tris (tris(hydroxymethyl)aminomethane), pH 7.5, 0.1 mM EDTA (ethylenediaminetetraacetic acid), pH 8.0, 20% glycerol, 0.05% Nonidet-P40, 1 mM 2-ß mercaptoethanol, 1 mM adenosine triphosphate (ATP) and lysed by freezing and thawing 3 times on dry ice. After centrifugation, supernatants were combined with substrate buffer (50 mM HEPES [N-2-hydroxyethylpiperazine-N'-2-ethanesulfonic acid], pH 7.5, 5 mM EGTA (ethylene glycol tetraacetic) acid pH 7) and the specific fluorogenic substrate in a 96-well plate and analyzed on a spectrofluorometer Mithras LB940 (Berthold Technologies, Oak Ridge, TN), using an excitation of 380 nm and an emission of 460 nm.

Effect of NPI-0052 and bortezomib on paracrine WM cell growth in the BM

To evaluate growth stimulation and signaling in WM cells adherent to bone marrow stromal cells (BMSCs), 3 x 10^4 BCWM.1 cells were cultured in BMSC-coated 96-well plates for 48 hours in the presence or absence of NPI-0052 alone or combined with Bortezomib. DNA synthesis was measured as described.[18]

Transwell migration assay

We performed transwell migration assay (Costar; Corning, Acton, MA) using BCWM.1 cells in the presence or absence of 30 nM SDF-1.[13] In brief, cells were suspended in 1% FCS media and were placed (2 x 10^5 cells) in the upper chambers of the transwell plates with serial concentrations of SDF-1 in the lower chambers in 1 mL of 1% FCS media. After 4 hours at 37°C, cells that migrated to the lower chambers were counted. Triplicates of each concentration were performed, and the means and standard deviations were calculated.

Adhesion assay

BCWM.1 cells were pre-treated with NPI-0052 (10nM) either alone or in combination with bortezomib (10nM) for 4 hours, then we used an *in vitro* adhesion assay coated with fibronectin, a ligand of VLA-4, following the manufacturer recommendations (EMD Biosciences, San Diego, CA). Calcein AM was used to measure adherent cells and the degree of fluorescence was measured using a spectrophotometer (485-520). BSA-coated well served as negative control.

Immunofluorescence

The effect of NPI-0052 in combination with bortezomib on the TNF-α-induced nuclear translocation of p65 was examined by an immunocytochemical method using an epifluorescence microscope [redacted] and a Photometrics Coolsnap CF color camera (Nikon, Lewisville, TX) as previously described.[23]

***In vivo* flow cytometry**

The effects of NPI-0052 either alone or in combination with bortezomib on homing *in vivo* were tested using Balb/c mice with *in vivo* flow cytometry as previously

described.[24,25] Briefly, BCWM.1 cells were treated with each agent either alone or in combination, or control PBS, for 4 hours, and then injected to the mice. Treated cells and untreated cells were fluorescently labelled by incubation with carbocyanine membrane dye, "DiI" (1,1'-dioctadecyl-3,3,3',3'-tetramethylindocarbocyanine perchlorate) and "DiR" (1,1'-dioctadecyl-3,3,3',3'-tetramethyl indotricarbocyanine Iodide) 5μM for 30 minutes, respectively (Molecular Probes, Carlsbad, Ca). Each mouse received both DiI-labeled and DiR-labeled cells. Fluorescence signal was detected on an appropriate artery in the ear and digitized for analysis with Matlab software developed in house, as described.[24,25]

Statistical analysis

Statistical significance of differences in drug-treated *versus* control cultures was determined using Student's *t*-test. The minimal level of significance was $p<0.05$. The interaction between NPI-0052 and Bortezomib was analyzed by isobologram analysis using the CalcuSyn software program (Biosoft, Ferguson, MO) to determine if the combinations were additive or synergistic. This program is based on the Chou-Talalay method, which calculates a combination index (CI) to indicate additive or synergistic effects. When CI=1, effects are additive; when CI<1.0, effects are synergistic. Results from viability assay (MTT) were expressed as fraction of cells killed by the single drug or the combination in drug-treated versus untreated cells.[18]

Results

NPI-0052 inhibits DNA synthesis and induces cytotoxicity of WM cells

WM and IgM-secreting cell lines next were cultured for 48 hours in the presence of NPI-0052 (2.5-40nM). As shown in Figure 1A, NPI-0052 inhibited BCWM.1 proliferation, as measured by [^{3}H]-thymidine uptake assay, with an IC_{50} of 15nM. NPI-0052 demonstrated similar activity on all cell lines tested, with IC_{50} between 20 and 30nM at 48 hours (Figure 1B). We next studied the cytotoxic effect of NPI-0052 (2.5-40nM) on cell lines and WM patient cells by MTT assay. NPI-0052 decreased survival of BCWM.1 cells (IC_{50}, 18nM; Figure 1A) and other IgM-secreting cell lines (IC_{50} 30-40nM; Figure 1C). Similarly, NPI-0052 induced cytotoxicity in primary $CD19^+$ cells isolated from three patients with WM (IC_{50} 20-30nM; Figure 1D). In contrast, NPI-0052 had no cytotoxic effect on PBMCs from 3 healthy volunteers (data not shown). These results demonstrate that NPI-0052 triggers significant cytotoxicity in tumor cell lines and patient WM cells, without toxicity in normal PBMCs.

NPI-0052 induces apoptosis in WM cells.

We examined the molecular mechanisms whereby NPI-0052 induces cytotoxicity in WM cells. We demonstrated that NPI-0052 induced dose-dependent apoptosis, as evidenced by Apo2.7 staining in flow cytometry analysis. The percentage of apoptotic BCWM.1 cells increased from 5% (untreated) to 21.2% and 40% after 48 hours of treatment with NPI-0052 5nM and 20nM respectively (Fig. 1E). Similar data were obtained on other IgM secreting cell lines (data not shown).

We next determined mechanisms whereby NPI-0052 induces apoptosis in WM, and demonstrated that NPI-0052 induced caspase-8 and PARP cleavage in a dose-dependent manner (Fig. 1F), without affecting caspase-3 and -9 (data not shown). Moreover NPI-0052 induced down-modulation of the anti-apoptotic protein Mcl-1, with an increased release of the second mitochondria-derived activator of caspases (Smac/DIABLO) from the mitochondria to the cytosol (Fig. 1F). It has been reported that Smac/DIABLO can abrogate the protective effects of inhibitors of apoptosis proteins (IAPs), such as X-linked inhibitor of apoptosis (XIAP).[26] We therefore, treated BCWM.1

cells with NPI-0052 (2.5-20nM) for 12 hours and demonstrated that NPI-0052 down-regulated the expression of XIAP in a dose-dependent manner, accompanied by an inhibition of other IAPs members, such as c-IAP and survivin (Fig. 1F).

NPI-0052 and bortezomib synergistically induce cytotoxicity of WM cells

Previous studies have shown that the novel proteasome inhibitor NPI-0052 induces apoptosis in MM cells with mechanism distinct from bortezomib.[16] We therefore, investigated whether the combination of two proteasome inhibitors, NPI-0052 and bortezomib, could be synergistic in inducing cytotoxicity in WM cells. BCWM.1 cells were cultured with NPI-0052 (2.5, 5 and10nM) for 48 hours, in the presence or absence of bortezomib (5-10nM). NPI-0052 showed a significant cytotoxic effects when combined with bortezomib in BCWM.1 cells, as demonstrated using MTT assays at 48 hours (Fig. 2A). NPI-0052 (5nM) induced cytotoxicity in 12.4% of BCWM.1 cells, which was increased to 39.8% and 69.4% in the presence of bortezomib at 5nM (Combination Index, CI: 0.72) and10nM (CI: 0.6), respectively, indicating synergism. Isobologram analysis, fractions affected and the combination indexes for each of these combinations are summarized in Fig. 2B-C. Similar data were observed on IgM secreting cell lines and primary $CD19^+$ cells (data not shown).

To better define the mechanisms of NPI-0052/bortezomib-induced cytotoxicity, we investigated the effect of NPI-0052 (10nM), either alone or in combination with bortezomib 10nM, on BCWM.1 cells using immunoblotting after 12 hours treatment. Interestingly, we demonstrated that PARP cleavage was significantly higher using the combination compared to the effect of each agent alone. To further dissect whether apoptosis is mediated through the intrinsic or extrinsic pathways, we investigate the effect of NPI-0052, bortezomib and the combination on caspases-3, 8 and 9. As shown in Figure 2D, we demonstrated that single agent NPI-0052 induced mild capsase-8 cleavage without affecting caspase-3 and 9 cleavage, while bortezomib induced -9 and -3 cleavage, while the combination of NPI-0052 and bortezomib induced significant caspase-3, -8 and -9 cleavage. In addition, previous studies have shown that the release of Smac/DIABLO from the mitochondria to the cytoplasm results in activation of caspase-9-induced apoptotic cascade, and similarly, XIAP, the most effective IAPs member, inhibits

apoptosis through binding to caspase-3 and -9.[26] We therefore investigated the effect of bortezomib and NPI-0052 on Smac/DIABLO and XIAP and as shown in Figure 2D, demonstrated that the combination of the two proteasome inhibitors induced higher release of Smac/DIABLO and a significant decrease of XIAP, more than the effect of each agent alone. Similarly, we demonstrated that the IAP member, c-IAP was strongly downregulated by the combination versus single agent treatment (Fig. 2D). In addition, recent studies have shown that HSP-27 functions as an inhibitor of caspase activation and also inhibits the mitochondrial release of Smac/DIABLO.[27] We showed that NPI-0052 downregulates HSP-27 phosphorylation which in turn leads to increase in the release of SmacDIABLO from the mitochondria and the induction of caspase-9 cleavage. In parallel we showed an upregulation of HSP70, while HSP-90 expression was not modulated (Fig. 2D).

NPI-0052 and bortezomib synergistically inhibit NF-κB activation in WM cells

NF-κB pathway plays a pivotal role in regulating growth and survival of plasma cell malignancies.[10] We therefore sought to investigate whether the combination of the two proteasome inhibitors would lead to a synergistic modulation of this pathway. We first investigated the effect of NPI-0052 either alone or in combination with bortezomib on the NF-κBp65 DNA binding activity, studying nuclear extracts from treated cells using the Active Motif assay. We showed that TNF-α treatment induced NF-κB recruitment to the nucleus in BCWM.1 cells, which was inhibited by NPI-0052 more than bortezomib, and more significantly by the combination of the two proteasome inhibitors (Fig. 3A). In addition, immunoblotting from nuclear extracts demonstrated that p65 phosphorylation and p50NF-κB expression were inhibited by NPI-0052, either alone or in combination with bortezomib, more than bortezomib used as single agent (Fig. 3B). We further confirmed that phospho-p65 translocation from the cytoplasmic compartment to the nucleus was inhibited by the combination of bortezomib and NPI-0052, resulting in a significant increase in p-p65 expression in the cytoplasmic compartment as shown by immunofluorescence (Fig 3D). We next examined whether the combination of NPI-0052 and bortezomib altered the non-canonical NF-κB pathway. Immunoblotting from nuclear extracts showed that two proteasome inhibitors used in combination inhibited the

expression of p52 and RelB, which are mostly activated through the non-canonical pathway (Fig. 3B).[28] Moreover, each agent alone, and more significantly their combination up-regulated the phosphorylation of the inhibitor protein IκB, as shown in Fig. 3C. Taken together, these data demonstrate that the combination of the two proteasome inhibitors regulate both canonical and non-canonical pathways of NF-κB in WM.

NPI-0052 and bortezomib synergistically inhibit PI3K/Akt pathway in WM cells

To further investigate other mechanisms of synergy between NPI-0052 and bortezomib, we sought to determine the effect of these agents on the PI3K/Akt pathway. Previous studies in MM have demonstrated that bortezomib upregulates Akt which may be a potential mechanism of resistance to this agent. We therefore, sought to determine the effect of NPI-0052 and the combination of Akt activation. The PI3K/Akt pathway is implicated in promoting growth and survival of tumor B cells.[29] We first investigated whether NPI-0052 could affect PI3K/Akt signaling pathway in WM cells. BCWM.1 were treated with increasing doses of NPI-0052 (2.5-20nM) for 6 hours. As shown in Figure 4A, NPI-0052 inhibited phosphorylation of Akt (ser473), and downstream GSK3$_{\alpha/\beta}$ and ribosomal protein S6 in a dose dependent manner, with no activity on the phosphorylation of the MAP kinase ERK1/2 (thr202/tyr204). We next investigated the effect of NPI-0052 (10nM), alone or combined with bortezomib (10nM), on Akt kinase activity, using an *in vitro* Akt kinase assay. We showed that NPI-0052 decreased phosphorylation of GSK3α/β fusion protein, while bortezomib did not modulate Akt phosphorylation. The combination of NPI-0052 and bortezomib showed significant inhibition of Akt activity, indicating a possible mechanism of synergy where NPI-0052 overcomes Akt-dependent bortezomib resistance (Fig. 4B). To further validate the role of the Akt pathway in NPI-0052-dependent cytotoxicity, we used an Akt knockdown BCWM.1 cell line established using lentivirus infection[19-21] and demonstrated that in the absence of Akt, the cytotoxic effect of NPI-0052 was abrogated (Fig. 4C), indicating that Akt plays an essential role in the cytotoxic activity of NPI-0052 and that this could be an important differential effect between the two proteasome inhibitors and a mechanism of synergy between them in WM.

NPI-0052 inhibits the three 20S proteolytic activities within the proteasome

We further examined the effect of NPI-0052, Bortezomib, as single agents or in combination, on proteasome activities in BCWM.1 and CD19+ WM cells. Cells were treated with NPI-0052 (10nM) either alone or in combination with bortezomib (10nM), for 4 hours, and the chymotripsin-like (CT-L), caspase-like (CL) and trypsin-like (T-L) activities were measured using distinct fluorogenic peptides specific for each enzymatic activity.[22] As shown in Figure 4D, bortezomib induced 29%, 5% and 69% reduction of the C-L, T-L and CT-L activities, respectively; compared to NPI-0052 which induced 34.3%, 38.7% and 81% reduction of the C-L, T-L and CT-L activities, respectively. Interestingly, the inhibition of the C-L activity significantly increased to 60% when NPI-0052 and bortezomib were used in combination (Fig. 4D). Similar data were obtained on $CD19^+$ primary cells (Fig. 4E*i-iii*).

The combination of NPI-0052 and bortezomib overcomes resistance induced by the bone marrow microenvironment and IL-6

Since the BM microenvironment confers growth and induces drug resistance in malignant cells,[30] we next investigated whether NPI-0052, alone or in combination with bortezomib, inhibits WM cells growth in the context of the BM milieu. BCWM.1 cells were cultured with NPI-0052 (2.5-20nM) and/or bortezomib (10nM) in the presence or absence of BMSCs, for 48 hours. The viability of BMSCs, assessed by MTT was not affected by NPI-0052 treatment (data not shown). Using [^{3}H]-TdR uptake assay, adherence of BCWM.1 cells to BMSCs triggered an increase of 55% in proliferation, which was inhibited by NPI-0052 in a dose-dependent manner. This effect was significantly enhanced by the combination with bortezomib (Fig. 5A), confirming that the combination of the two proteasome inhibitors enhanced the antitumor activity of each drug used as a single agent, even in presence of BMSCs.

Since IL-6 and NF-kB induction by adhesion are two major pathways regulated by the proteasome, we further investigated the effect of the two proteasome inhibitors on cytotoxicity of WM cells in the presence of IL-6. Previous studies using gene expression analysis in WM have demonstrated an upregulation in IL-6 signaling.[31] IL-6 also

promotes plasmacytoid lymphocyte growth in WM, and serum IL-6 levels reflect tumor burden and disease severity.[32]. We therefore tested whether the addition of recombinant human IL-6 (25 ng/mL) can overcome the cytotoxic effect of NPI-0052 and bortezomib on WM cells. As shown in Figure 5B, IL-6 induced proliferation of BCWM.1 cell, and the addition of NPI-0052 (2.5-20nM), bortezomib (10nM), or the combination inhibited IL-6-induced proliferation of BCWM.1 cells, indicating that NPI-0052, alone or more significantly in combination with bortezomib, overcomes resistance induced by IL-6. In addition, IL-6 induced phosphorylation of Akt and STAT-3.[18,33] NPI-0052 and bortezomib inhibited IL-6-triggered Akt and STAT-3 phosphorylation, which were more significantly down-regulated with the combination of NPI-0052 and bortezomib (Fig. 5C). We next investigated whether the two proteasome inhibitors, used as single agent or in combination, could also target non-malignant hematoopoietic cells. We found that NPI-0052 (10nM, 20nM), bortezomib (10nM) and the combination did not affect the growth of BM hematopoietic progenitor cells as shown using colony-formation assay (Fig.5D).

NPI-0052 and bortezomib inhibit migration and adhesion of WM cells *in vitro* and homing *in vivo*.

Previous studies have demonstrated that the PI3K/Akt pathway regulates migration and adhesion in B cells[13], and that adhesion induces activation of the NF-κB pathway. We therefore, sought to investigate the effect of NPI-0052 and bortezomib on the migration and adhesion of WM cells. We first demonstrated that stromal derived factor-1 (SDF-1), one of the important regulators of migration in B-cells,[24] induced migration in BCWM.1 cells at 30nM SDF-1. To study the effect of NPI-0052 on the migration of WM cells, BCWM.1 cells were incubated with NPI-0052 (10nM), either alone or in combination with bortezomib (10nM), for 4 hours (these doses and duration of incubation did not induce apoptosis in WM cells as confirmed by trypan blue and Apo2.7 staining by flow cytometry, data not shown). Cells were then subjected to migration as previously described.[24] NPI-0052 slightly inhibited WM cells migration towards SDF-1, which was significantly inhibited when NPI-0052 was used in combination with bortezomib. in

combination with bortezomib induced significant inhibition of BCWM.1 cells migration (Fig. 6A).

We also tested the effect of NPI-0052 and bortezomib on adhesion *in vitro* in WM. We found that NPI-0052 induced significant inhibition of adhesion to fibronectin when used in combination with bortezomib (Fig. 6B). Previous studies have shown that FN induces members of NF-κB family transcription factors.[34] We therefore, examined the effect of NPI-0052 and bortezomib on NF-kB activity in the presence or absence of fibronectin. As shown in Fig. 6C, FN induced a significant increase in p65 phosphorylation and p50NF-κB expression, which were inhibited by NPI-0052, bortezomib, and more significantly by the two drugs in combination.

We have previously shown that adhesion of neoplastic cells to BM microenvironment confers resistance to apoptosis.[35] Therefore, we sought to investigate the effect of NPI-0052 either alone or in combination with bortezomib, on homing in WM *in vivo*. DiI-labeled BCWM.1 cells treated with NPI-0052 (10nM, 4 hours), alone or in combination with bortezomib (5nM), or DiR-labeled untreated BCWM.1 cells used as control were injected in the tail vein of BALB/c mice, followed by *in vivo* flow cytometry every 5 minutes for 45 minutes after injection. Neither NPI-0052 nor bortezomib used as single agents significantly inhibited homing of WM cells to the bone marrow, as demonstrated by a rapid decrease of circulating BCWM.1 cells which was observed in the untreated cells as well as on cells treated with NPI-0052 or bortezomib (data not shown). Interestingly, we demonstrated that pretreatment of BCWM.1 with NPI-0052 in combination with bortezomib resulted in a significant inhibition of homing with a decrease of 45% of cells in the circulation at 45 minutes compared to a decreased of 77% obtained in the untreated cells, suggesting that when the two proteasome inhibitors were used together there is an inhibition in the homing of WM cells to the bone marrow (Fig. 5D).

Discussion

WM is a biologically unique low grade B –cell lymphoma characterized by high protein turnover. Little is known about the signaling pathways regulating survival and proliferation in this disease. Clinical studies have demonstrated that bortezomib induces

significant cytotoxicity in WM cells,[15] indicating an important role of the proteasome in WM. In this study, we dissect the biological role of the proteasome in WM using two proteasome inhibitors that have non-overlapping activities.[16] We first demonstrated that the novel proteasome inhibitor NPI-0052 leads to inhibition of proliferation and induction of apoptosis in WM cell lines and CD19+ primary WM cells at doses consistent with previous studies and achievable *in vivo*.[23,36] We then demonstrated that the combination of NPI-0052 and bortezomib leads to synergistic cytotoxicity on WM cell lines, IgM secreting cell lines and patient cells. These two agents lead to inhibition of nuclear translocation of p65 NF-κB, with activity on the canonical and non-canonical NF-κB pathway, and synergistic induction of caspases 3, 8 and 9 cleavage as well as PARP cleavage and induction of Smac/DIABLO. This study begins to delineate the role of the canonical and non-canonical NF-κB pathways in WM.

We further dissected the mechanism of synergy of these two agents and demonstrated that they act synergistically through: the differential activity on Akt pathway; and the differential activity on chymotrypsin-like, caspase-like and trypsin-like activities of the 20S proteasome. We demonstrated that NPI-0052 induced cytotoxicity was completely abrogated in an Akt knockdown cell line, indicating that its major activity is mediated through the Akt pathway, while bortezomib modestly activated Akt activity. Previous studies have demonstrated that activation of the Akt survival pathway may be one of the mechanisms of resistance of malignant B cells to bortezomib. In this study, we demonstrate that the major activity of NPI-0052 is mediated through inhibition and not activation of Akt and therefore, its combination with bortezomib may overcome resistance to bortezomib *in vivo*.

We then showed that NPI-0052 and bortezomib inhibit migration and adhesion of WM cells to cytokines or fibronectin present in the BM microenvironment. Adhesion of WM cells to fibronectin led to NF-κB stimulation, which was abrogated by NPI-0052 and bortezomib. In addition, the combination of NPI-0052 and bortezomib led to inhibition of homing of WM cells *in vivo* in our homing model. Since IL-6 and NF-κB induction by adhesion are two major pathways regulated by the proteasome, we demonstrated that NPI-0052 and bortezomib overcome resistance induced by mesenchymal cells and the addition of IL-6 in a co-culture *in vitro* system. Finally, we demonstrated that the

combination of these two agents does not induce cytotoxicity on hematopoietic stem cells using colony-formation assays. These studies demonstrate that the combination of NPI-0052 and bortezomib is active even in the presence of the bone marrow microenvironment. Little is known about the role of the bone marrow microenvironment in WM. Here, we demonstrate that adhesion of WM cells to the bone marrow milieu induces NF-κB activation and IL-6 induces Akt activation, which were both down-regulated in presence of NPI-0052 either alone, and more significantly in combination with bortezomib. The combination of the two agents overcomes the protective effect of the bone marrow niches, without affecting the growth and differentiation of normal hematopoetic components. In addition, homing is a complex process that is regulated by migration and adhesion of malignant cells to their specific bone marrow niches. In this study, we demonstrate that NPI-0052 and bortezomib inhibit migration and adhesion of WM cells as well as their homing *in vivo*. Together, theses studies provide a stronger understanding of the biological role of the proteasome pathway in WM, and provide the preclinical framework for studying in clinical trials the combination of NPI-0052 and bortezomib in WM and other low-grade lymphomas.

TEXT LEGEND

Figure 1. NPI-0052 induces decrease in DNA synthesis, triggers cytotoxicity and induces apoptosis in WM cells.

(A) Thymidine uptake assay and cytotoxicity assessed by MTT. BCWM.1 cells were cultured with NPI-0052 (2.5-40 nM) for 48 hours. (B) Thymidine uptake assay. Several IgM-secreting cell lines, WM-WSU (♦), MEC-1 (■), Namalwa were cultured with NPI-0052 (2.5-40 nM) for 48 hours. (C) Several IgM secreting cell lines, WM-WSU, MEC-1, Namalwa were cultured with NPI-0052 for 48 hours. Cytotoxicity was assessed by MTT assay. (D) Freshly isolated bone marrow $CD19^+$ tumor cells from 3 patients with WM were cultured with NPI-0052 (2.5-40 nM [E]; 2.5-80 nM [F]). Cytotoxicity was assessed by MTT assay. (E) BCWM.1 were cultured with NPI-0052 for 48 hours at doses that range from 2 to 30 nM and the percentage of cells undergoing apoptosis was studied by Apo2.7 staining. (F) BCWM.1 cells were cultured with NPI-0052 (2.5-20 nM) for 12 hours. Whole cell lysates were subjected to Western blotting using anti-caspase 8, -PARP, -Mcl1, -Smac/DIABLO, -cIAP, -XIAP, -survivin, and -α-tubulin antibodies.

Figure 2. NPI-0052-induced cytotoxicity is enhanced in combination with bortezomib.

(A) BCWM.1 cells were cultured with NPI-0052 (2.5, 5 and 10 nM) for 48 hours, in the presence or absence of bortezomib (5 and 10 nM). Cytotoxicity was assessed by MTT assay. (B) Representative isobologram of NPI-0052 associated to bortezomib with the CalcuSyn software demonstrating synergy for the combination. (C) Combination indexes (C.I.) and fractions affected (FA) of the combinations of NPI-0052 and bortezomib. All experiments were repeated in triplicate. (D) BCWM.1 were cultured with NPI-0052 (10 nM) in presence or absence of bortezomib (10 nM) for 12 hours. Whole cell lysate were subjected to Western blotting using anti-caspase-8, -9, -3, -PARP, -Smac/DIABLO, -cIAP, -XIAP, -survivin, -p-HSP27, -HSP27, -HSP70, -HSP90 and α-tubulin antibodies.

Figure 3. NPI-0052 and bortezomib inhibit NF-κB function in WM cells.

(A) BCWM.1 cells were cultured with either NPI-0052 (10 nM), bortezomib (10 nM), or the combination for 4 hours, then TNF-α (10 ng/mL) was added for the last 20 minutes. NF-κBp65 transcription factor-binding to its consensus sequence on the plate-bound oligonucleotide was studied from nuclear extract. Wild type and mutant are wild type and mutated consensus competitor oligonucleotides, respectively. All results represent means (±sd) of triplicate experiments. (B;C) BCWM.1 cells were cultured with either NPI-0052 (10nM), bortezomib (10nM), or the combination for 4 hours, and TNF-α (10 ng/mL) was added for the last 20 minutes. Cytoplasmic and nuclear extracts were subjected to western blotting using anti-p-NF-κBp65, - NF-κBp50, -NF-κBp52 IkBα, -RelB, -p-IκB, -IκB, -nucleolin and -α-tubulin antibodies. (D) BCWM.1 cells were cultured with NPI-0052 (10nM) and bortezomib (10nM) for 4 hours, or control medium, and TNF-α (10 ng/mL) was added for the last 20 minutes. Immunocytochemical analysis was assessed as described in Materials and Methods.

Figure 4. NPI-0052 inhibits Akt pathway and synergizes with bortezomib in inhibiting Akt and 20S proteasome activities.

(A) BCWM.1 were cultured with NPI-0052 (2.5-20nM) for 6 hours. Whole cell lysate were subjected to Western blotting using anti -p-Akt, -Akt, -p-GSK3α/β, -p-S6R, -p-ERK, and -α-tubulin antibodies. (B) *In vitro* Akt kinase assay. BCWM.1 cells were cultured with control media or NPI-0052 (2.5-20nM) for 6 hours. Whole cell lysates were immunoprecipitated with anti-Akt antibody. Then the immunoprecipitated was washed and subjected to *in vitro* kinase assay according to manufacturer's protocol. Western blotting used anti-p-GSK3α/β and anti-Akt antibodies. (C) BCWM.1 cells were transduced with Akt shRNA for 48 hours. Mock: control plasmid. BCWM.1 transfected cells or BCWM.1 control cells were treated with NPI-0052 (2.5-20nM) for 48 hours. Cytotoxicity was assessed by MTT assay. Whole cell lysates were subjected to western blotting using anti-p-Akt, -Akt, and α-tubulin antibodies (insert panel C). (D) BCWM.1 cells or primary $CD19^+$ tumor cells from 2 patients with WM (E *i, ii, iii*) were incubated for 4 hours in the presence of diluent or 10 nM NPI-0052, Bortezomib 10 nM, or

Bortezomib + NPI-0052. The chymotrypsin-like (CT-L), trypsin-like (T-L), and caspase-like (C-L) activity of the 20S proteasome of BCWM.1 was determined by measurement of fluorescence generated from the cleavage of the fluorogenic substrates suc-LLVY-amc, boc-LRR-amc, and z-LLE-amc, respectively.

Figure 5. Neither growth factors nor adherence to BMSCs protect against NPI-0052-induced cytotoxicity.

(A) BCWM.1 cells were cultured with control media, and with NPI-0052 (2.5-20 nM), with and without bortezomib (10 nM) for 48 hours, in the presence or absence of BMSCs. Cell proliferation was assessed using [^{3}H]-thymidine uptake assay. All data represent mean (±sd) of triplicate experiment. (B) BCWM.1 were cultured with control media or NPI-0052 (2.5-20 nM), with and without bortezomib (10 nM) for 48 hours, in presence or absence of IL-6 (25 ng/mL) (10 μM). Proliferation was assessed by thymidine uptake assay. (C) BCWM.1 cells were cultured with control media or NPI-0052 (10 nM) with and without bortezomib (10 nM) for 8 hours. Cells were then stimulated with IL-6 (25 ng/mL) for 10 minutes. Whole cell lysates were subjected to western blotting using anti-p-AKT, anti-AKT, anti-p-STAT3 and anti–α-tubulin. (D) Colony-forming cell assay. Negative fraction after CD19$^+$ selection of bone marrow mononuclear cells was cultured using methylcellulose semisolid technique in absence or presence of NPI-0052 (10nM, 20nM) either alone or in combination with borteomib 10nM, and BFU-E, CFU-GM, CFU-M and CFU-GEMM were counted at day 14th. All experiments have been done in triplicate.

Figure 6. NPI-0052 inhibited migration and adhesion of BCWM.1 cells *in vitro* and homing *in vivo.*

(A) Transwell migration assay showing inhibition of migration of BCWM.1 in the presence of NPI-0052 (2.5-20 nM), bortezomib (10 nM), or NPI-0052 (10 nM) in combination with bortezomib (10 nM). SDF-1 30nM was placed in the lower chambers and induced migration as compared to control with no SDF-1 (Ctrl, control). SDF-1 was placed in the lower chambers of the NPI-0052/bortezomib-treated wells. (B) Adhesion assay with BCWM.1 cells in the presence or absence of NPI-0052 (10nM), either alone

or in combination with bortezomib (10 nM). BCWM.1 cells demonstrated increased adhesion in fibronectin-coated wells (control) as compared to BSA-coated wells (BSA, bovine serum albumin). All data represent mean (±sd) of triplicate experiments. (C) BCWM.1 cells were cultured with control media or NPI-0052 (10 nM) with and without bortezomib (10 nM) for 4 hours, in presence or absence of fibronectin (FN). Nuclear extracts were subjected to western blotting using anti-p-p65, -p50, and –nucleolin antibodies. (D) *In vivo* flow cytometry. DiI-labeled treated cells and DiR- labeled untreated cells were injected in the tail vein of 2 BALB/c mice. Cells were counted every 5 min for 45 minutes as described in Material and Methods.

1. Treon SP, Gertz MA, Dimopoulos M, et al. Update on treatment recommendations from the Third International Workshop on Waldenström's macroglobulinemia. Blood 2006;107:3442-6.
2. Ghobrial IM, Gertz MA, Fonseca R. Waldenstrom macroglobulinaemia. Lancet Oncol 2003;4:679-85.
3. Owen RG, Treon SP, Al-Katib A, et al. Clinicopathological definition of Waldenström's macroglobulinemia: consensus panel recommendations from the Second International Workshop on Waldenström's Macroglobulinemia. Semin Oncol 2003;30:110-5.
4. Adams J. The proteasome: structure, function, and role in the cell. Cancer Treat Rev. 2003;29;3-9.
5. Adams J. The development of proteasome inhibitors as anticancer drugs. Cancer Cell. 2004;5:417-21.
6. Panwalkar A, Verstovsek S, Giles F. Nuclear factor-kappaB modulation as a therapeutic approach in hematologic malignancies. Cancer. 2004;100:1578-89
7. Karin M. Nuclear factor-kappaB in cancer development and progression. Nature. 2006;441:431-6.
8. Hatzimichael EC, Christou L, Bai M, Kolios G, Kefala L, Bourantas KL. Serum levels of IL-6 and its soluble receptor (sIL-6R) in Waldenstrom's macroglobulinemia. Eur J Haematol 2001;66(1):1-6.
9. Chauhan D, Uchiyama H, Akbarali Y, Urashima M, Yamamoto K, Libermann TA and Anderson KC. 1996; 87:1104-1112
10. Hideshima T, Chauhan D, Richardson P, Mitsiades C, Mitsiades N, Hayashi T, Munshi N, Dang L, Castro A, Palombella V, Adams J and Anderson KC. NF-kB as a therapeutic target in multiple myeloma. 2002. J. Biol. Chem., 277:16639-16647
11. Heilbig G, Christopherson KW, Bhat-Nakshatri P, et al. NF-kB promotes breast cancer cell migration and metastasis by inducing the expression of the chemokine receptor CXCR4. The Journal of Biological Chemistry. 2003;278:21631-21638
12. O'Dea EL, Barken D, Peralta RQ, Tran KT, Werner SL, Kearns JD, Levchenko A, Hoffmann A. A homeostatic model of IkappaB metabolism to control constitutive NF-kappaB activity. Mol Syst Biol. 2007;3:111. Epub 2007 May 8.
13. Leleu X, Jia X, Runnels J, Ngo HT, Moreau AS, Farag M, Spencer JA, Pitsillides CM, Hatjiharissi E, Roccaro A, O'sullivan G, McMillin DW, Moreno D, Kiziltepe T, Carrasco R, Treon SP, Hideshima T, Anderson KC, Lin CP, Ghobrial IM. The Akt pathway regulates survival and homing in Waldenstrom Macroglobulinemia. Blood. 2007 Aug 30; [Epub ahead of print]
14. Hideshima T, Mitsiades C, Akiyama M, et al. Molecular mechanisms mediating antimyeloma activity of proteasome inhibitor PS-341. Blood 2003;101:1530-4.
15. Treon SP, Hunter ZR, Matous J, et al. Multicenter Clinical Trial of Bortezomib in Relapsed/Refractory Waldenstrom's Macroglobulinemia: Results of WMCTG Trial 03-248. Clin Cancer Res 2007;13:3320-5
16. Chauhan D, Catley L, Li G, Podar K, Hideshima T, Velankar M, Mitsiades C, Mitsiades N, Yasui H, Letai A, Ovaa H, Berkers C, Nicholson B, Chao TH,

Neuteboom ST, Richardson P, Palladino MA, Anderson KC. A novel orally active proteasome inhibitor induces apoptosis in multiple myeloma cells with mechanisms distinct from Bortezomib. Cancer Cell. 2005;8:407-19.
17. Santos D HA, Tournilhac O, Leleu X, et al. Establishment of a Waldenstrom's Macroglobulinemia Cell Line (BCWM.1) with Productive In Vivo Engraftment in SCID-hu Mice. Clin Exp Hematol. 2007 In press.
18. Hideshima T, Catley L, Yasui H, et al. Perifosine, an oral bioactive novel alkylphospholipid, inhibits Akt and induces in vitro and in vivo cytotoxicity in human multiple myeloma cells. Blood 2006;107: 4053-62.
19. Dillon CP, Sandy P, Nencioni A, Kissler S, Rubinson DA, Van Parijs L. Rnai as an experimental and therapeutic tool to study and regulate physiological and disease processes. Annu Rev Physiol. 2005;67:147-173
20. Rubinson DA, Dillon CP, Kwiatkowski AV, Sievers C, Yang L, Kopinja J, Rooney DL, Ihrig MM, McManus MT, Gertler FB, Scott ML, Van Parijs L. A lentivirus-based system to functionally silence genes in primary mammalian cells, stem cells and transgenic mice by RNA interference. Nat Genet. 2003;33:401-406
21. Moreau AS, Jia X, Ngo HT, Leleu X, O'Sullivan G, Alsayed Y, Leontovich A, Podar K, Kutok J, Daley J, Lazo-Kallanian S, Hatjiharisi E, Raab MS, Xu L, Treon SP, Hideshima T, Anderson KC, Ghobrial IM. Protein kinase C inhibitor enzastaurin induces in vitro and in vivo antitumor activity in Waldenstrom's Macroglobulinemia. Blood. 2007
22. Lightcap ES, McCormack TA, Pien CS, Chau V, Adams J, Elliott PJ. Proteasome inhibition measurements: clinical application. Clin Chem 2000; 46:673–683.
23. Ahn KS, Sethi G, Aggarwal BB. Embelin, an inhibitor of X chromosome-linked inhibitor-of-apoptosis protein, blocks nuclear factor-kappaB (NF-kappaB) signaling pathway leading to suppression of NF-kappaB-regulated antiapoptotic and metastatic gene products. Mol Pharmacol. 2007;71:209-19.
24. Alsayed Y, Ngo H, Runnels J., et al. Mechanisms of regulation of CXCR4/SDF-1 (CXCL12)-dependent migration and homing in multiple myeloma. Blood. 2007;109:2708-2717.
25. Sipkins DA, Wei X, Wu JW, Runnels JM, Cote D, Means TK, Luster AD, Scadden DT, Lin CP. In vivo imaging of specialized bone marrow endothelial microdomains for tumour engraftment. Nature. 2005;435:969-73.
26. Chauhan D., Li G., Shringarpure R., et al. Blockade of Hsp27 overcomes bortezomib/proteasome inhibitor PS-341 resistance in lymphoma cells. Cancer Res 2003;63:6174-6177.
27. Chauhan D., Li G., Shringarpure R., et al. Blockade of Hsp27 overcomes bortezomib/proteasome inhibitor PS-341 resistance in lymphoma cells. Cancer Res 2003;63:6174-6177.
28. Monaco C, Evangelos A, Serafim K, et al. Canonical pathway of nuclear factor κB activation selectively regulates proinflammatory and prothrombotic responses in human atherosclerosis. PNAS2004;101:5634-5639.
29. Uddin S, Hussain AR, Siraj AK, et al. Role of phosphatidylinositol 3'-kinase/AKT pathway in diffuse large B-cell lymphoma survival. Blood 2006;108:4178-86.
30. Mitsiades CS, Mitsiades NS, Munshi NC, Richardson PG, Anderson KC. The role of the bone microenvironment in the pathophysiology and therapeutic

management of multiple myeloma: interplay of growth factors, their receptors and stromal interactions. Eur J Cancer. 2006;42:1564-73.
31. Gutierrez N.C., Ocio E.M., de Las Rivas J., et al. Gene expression profiling of B lymphocytes and plasma cells from Waldenstrom's macroglobulinemia: comparison with expression patterns of the same cell counterparts from chronic lymphocytic leukemia, multiple myeloma and normal individuals. Leukemia. 2007;21:541-549.
32. Hatzimichael EC, Christou L, Bai M, Kolios G, Kefala L, Bourantas KL. Serum levels of IL-6 and its soluble receptor (sIL-6R) in Waldenstrom's macroglobulinemia. Eur J Haematol 2001;66(1):1-6.
33. Chatterjee M. Combined disruption of both the MEK/ERK and the IL-6R/STAT3 pathways is required to induce apoptosis of multiple myeloma cells in the presence of bone marrow stromal cells. Blood 2004;104:3712-21.
34. Landowski TH, Olashaw NE, Agrawal D, Dalton W. Cell adhesion-mediated drug resistance (CAM-DR) is associated with activation of NF-kB (RelB/p50) in myeloma cells. Oncogene 2003;22:2417-2421.
35. Moreau AS, Jia X, Ngo H., et al. Protein kinase C inhibitor enzastaurin induces in vitro and in vivo antitumor activity in Waldenstrom macroglobulinemia. Blood. 2007 Jun 1;109(11):4964-72. Epub 2007 Feb 6.
36. Miller C, Ban K, Dujka ME, et al. NPI-0052, a novel proteasome inhibitor, induces caspase-8 and ROS-dependent apoptosis alone and in combination with HDAC inhibitors in leukemia cells. Blood, 2007;110:267-277.

Fig.1

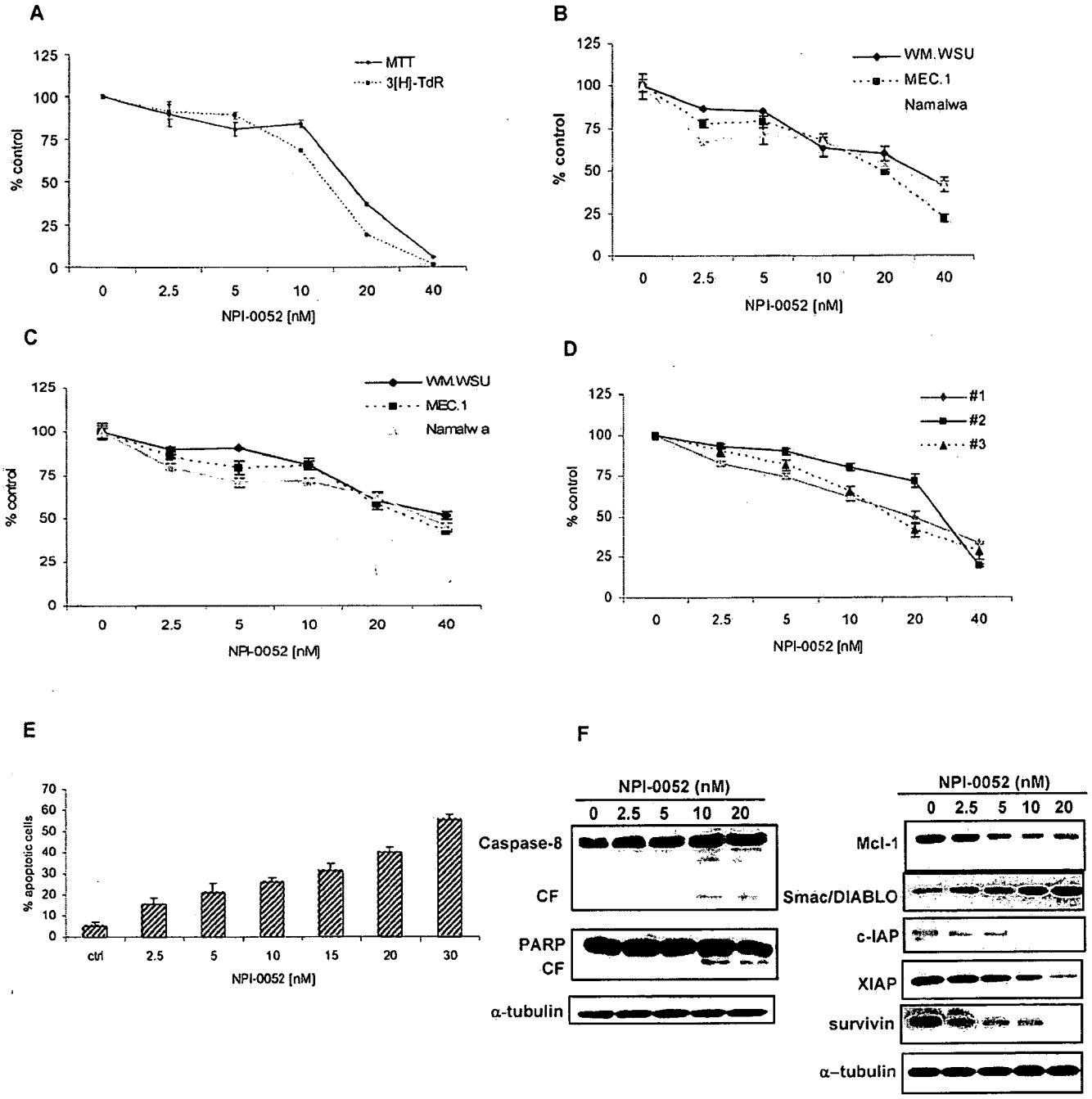
A
MTT
3[H]-TdR
% control
NPI-0052 [nM]
B
WM.WSU
MEC.1
Namalwa
% control
NPI-0052 [nM]
C
WM.WSU
MEC.1
Namalwa
% control
NPI-0052 [nM]
D
#1
#2
#3
% control
NPI-0052 [nM]
E
% apoptotic cells
ctrl
NPI-0052 [nM]
F
NPI-0052 (nM)
0 2.5 5 10 20
Caspase-8
CF
PARP
CF
α-tubulin
NPI-0052 (nM)
0 2.5 5 10 20
Mcl-1
Smac/DIABLO
c-IAP
XIAP
survivin
α-tubulin

Fig. 2

A

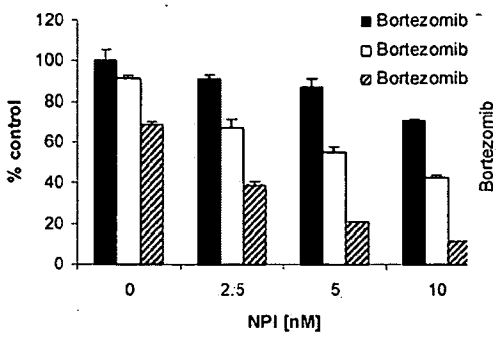

B

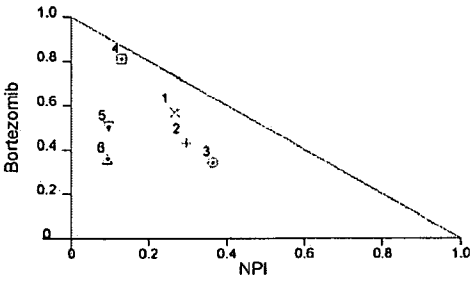

C

B (nM)	N (nM)	F.A.	C.I.
5	2.5	0.25	0.835
5	5	0.39	0.727
5	10	0.53	0.709
10	2.5	0.43	0.941
10	5	0.69	0.601
10	10	0.83	0.454

D

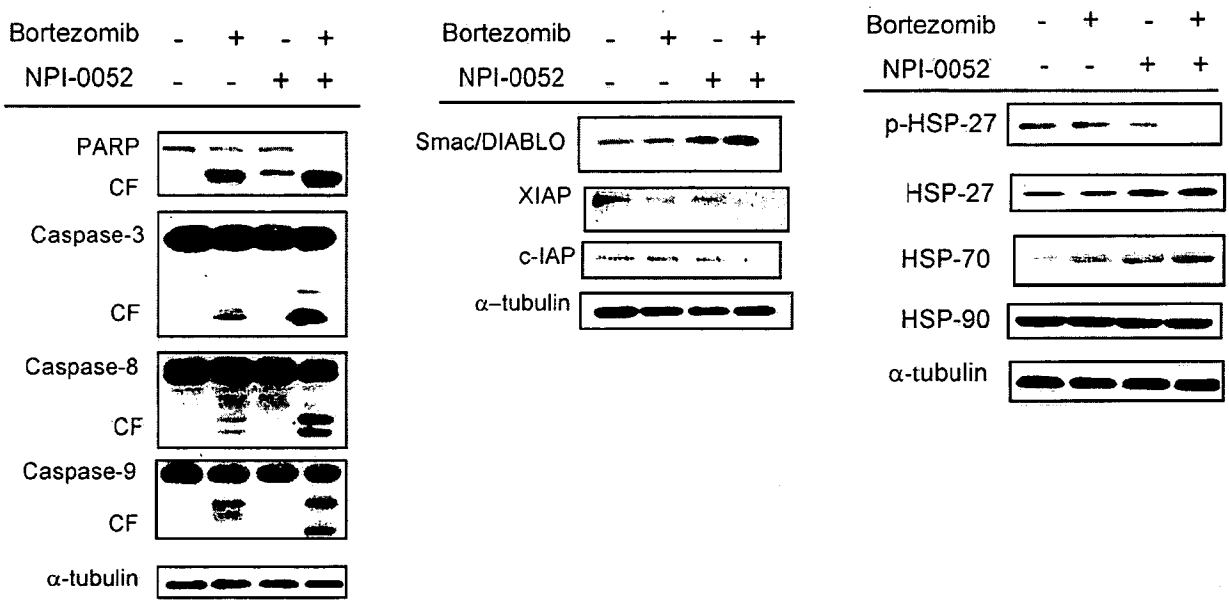

Fig. 3

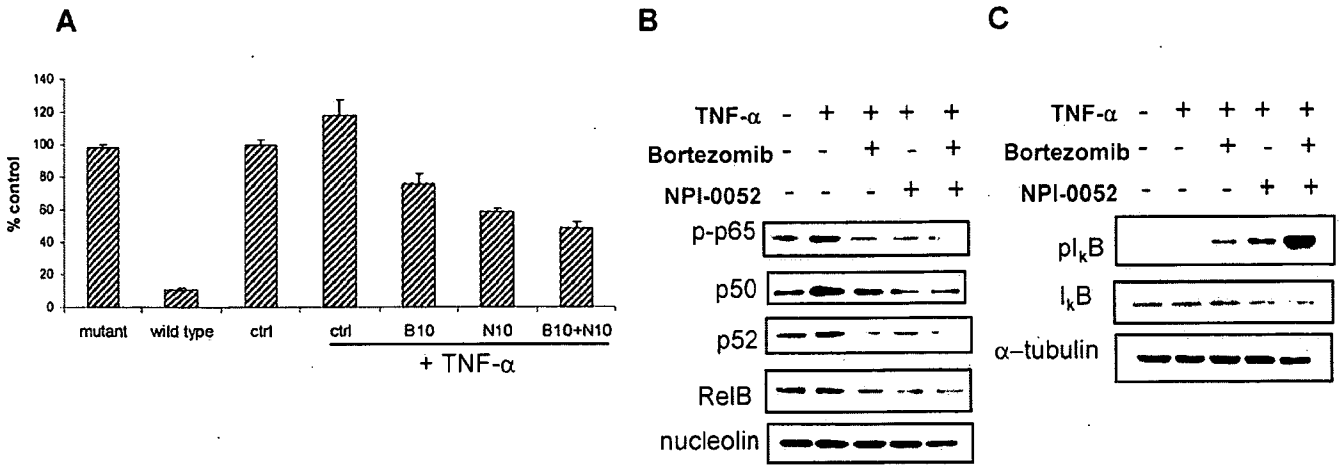
A
% control
140
120
100
80
60
40
20
0
mutant
wild type
ctrl
ctrl
B10
N10
B10+N10
+ TNF-α
B
TNF-α - + + + +
Bortezomib - - + - +
NPI-0052 - - - + +
p-p65
p50
p52
RelB
nucleolin
C
TNF-α - + + + +
Bortezomib - - + - +
NPI-0052 - - - + +
plkB
lkB
α–tubulin

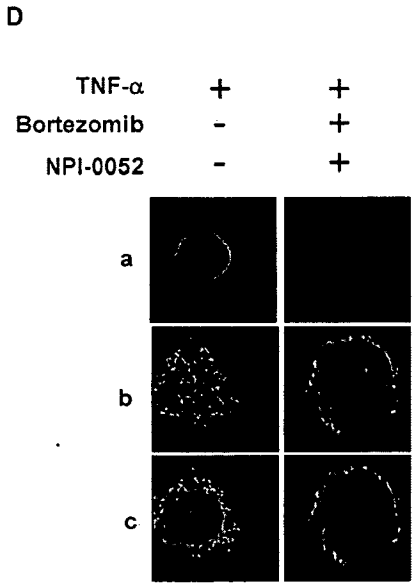
D
TNF-α + +
Bortezomib - +
NPI-0052 - +
a
b
c

Fig. 4

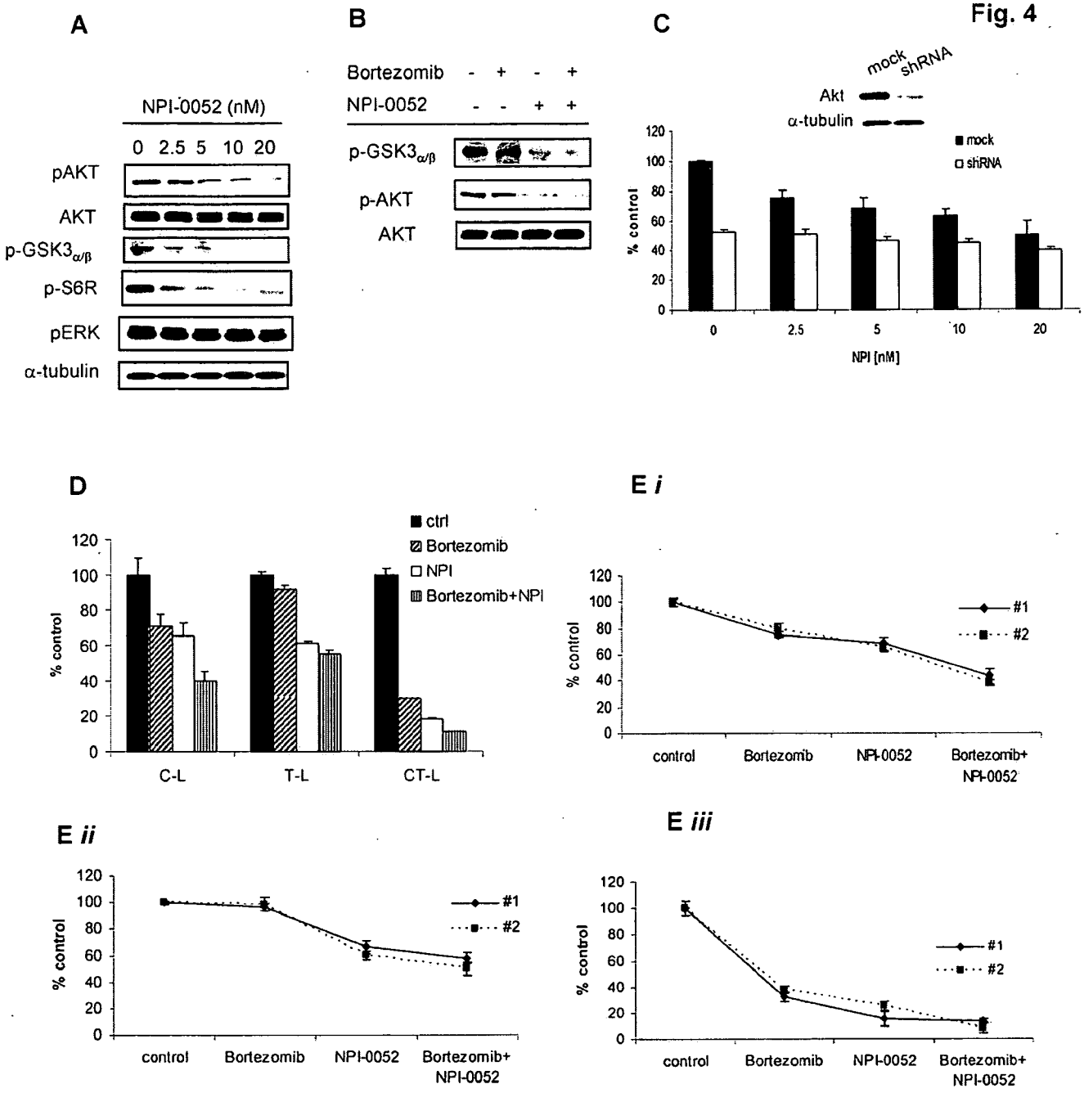
A
NPI-0052 (nM)
0 2.5 5 10 20
pAKT
AKT
p-GSK3α/β
p-S6R
pERK
α-tubulin
B
Bortezomib - + - +
NPI-0052 - - + +
p-GSK3α/β
p-AKT
AKT
C
mock shRNA
Akt
α-tubulin
mock
shRNA
% control
NPI [nM]
D
ctrl
Bortezomib
NPI
Bortezomib+NPI
% control
C-L
T-L
CT-L
E i
#1
#2
% control
control
Bortezomib
NPI-0052
Bortezomib+ NPI-0052
E ii
#1
#2
% control
control
Bortezomib
NPI-0052
Bortezomib+ NPI-0052
E iii
#1
#2
% control
control
Bortezomib
NPI-0052
Bortezomib+ NPI-0052

Fig. 5

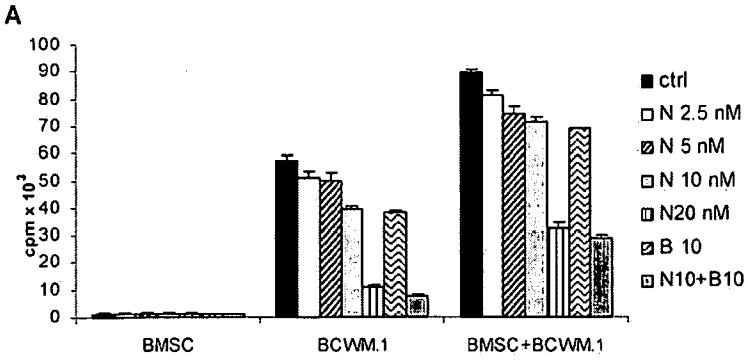
A
100
90
80
70
60
50
40
30
20
10
0
cpm x 10^3
BMSC
BCWM.1
BMSC+BCWM.1
ctrl
N 2.5 nM
N 5 nM
N 10 nM
N20 nM
B 10
N10+B10

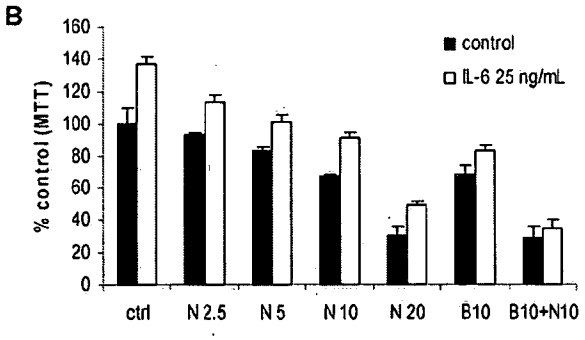
B
160
140
120
100
80
60
40
20
0
% control (MTT)
control
IL-6 25 ng/mL
ctrl
N 2.5
N 5
N 10
N 20
B10
B10+N10

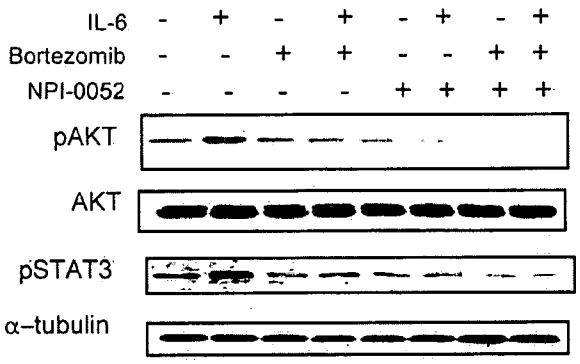
C
IL-6 - + - + - + - +
Bortezomib - - + + - - + +
NPI-0052 - - - - + + + +
pAKT
AKT
pSTAT3
α–tubulin

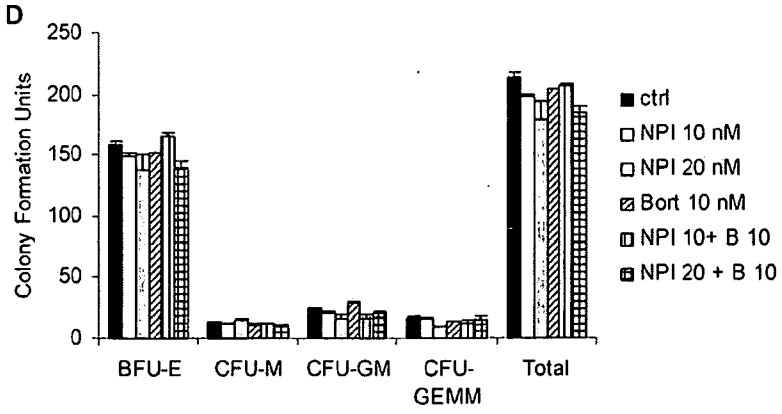
D
250
200
150
100
50
0
Colony Formation Units
BFU-E
CFU-M
CFU-GM
CFU-GEMM
Total
ctrl
NPI 10 nM
NPI 20 nM
Bort 10 nM
NPI 10+ B 10
NPI 20 + B 10

Fig. 6

A

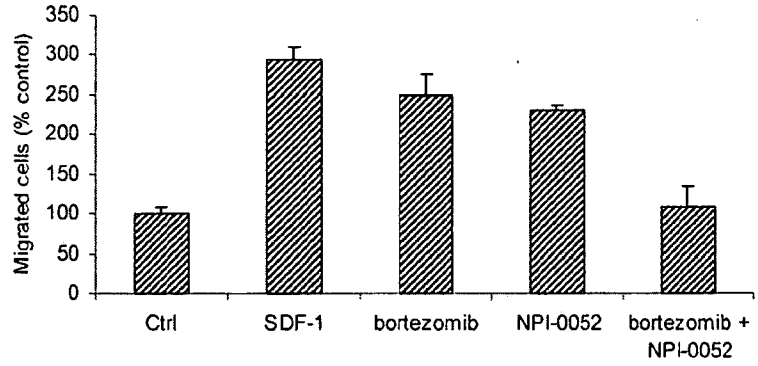
Migrated cells (% control)
350
300
250
200
150
100
50
0
Ctrl
SDF-1
bortezomib
NPI-0052
bortezomib + NPI-0052

B

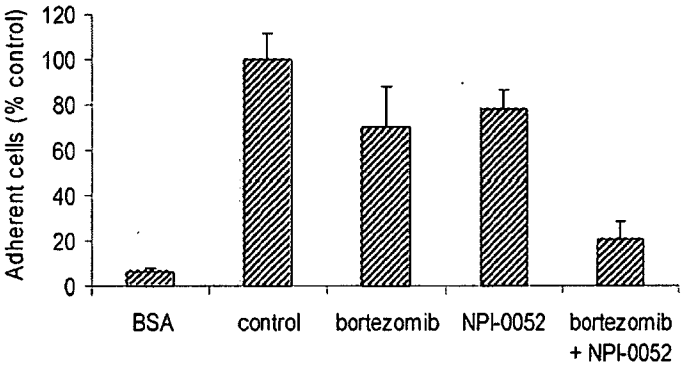
Adherent cells (% control)
120
100
80
60
40
20
0
BSA
control
bortezomib
NPI-0052
bortezomib + NPI-0052

C

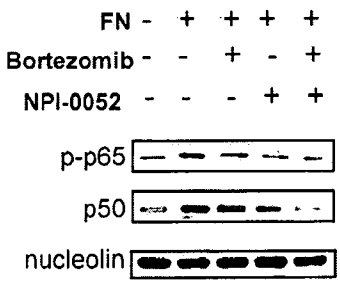
FN - + + + +
Bortezomib - - + - +
NPI-0052 - - - + +
p-p65
p50
nucleolin

D

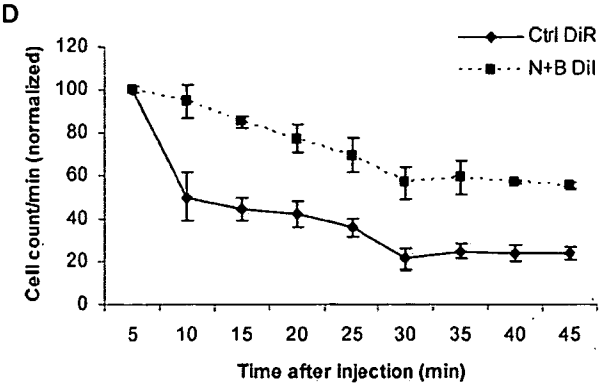
Ctrl DiR
N+B DiI
Cell count/min (normalized)
120
100
80
60
40
20
0
5
10
15
20
25
30
35
40
45
Time after injection (min)

96th Annual Meeting
April 16-20, 2005
Anaheim/Orange County, CA

Print this Page for Your Records Close Window

Abstract Number: 4943

Presentation Title: Oral proteasome inhibitor (NPI-0052) enhances sensitivity to combination Gemcitabine and Erbitux in a pancreatic cancer xenograft model.

Presentation Start/End Time: Tuesday, Apr 19, 2005, 1:00 PM - 5:00 PM

Board Number: Board #15

Author Block: *James C. Cusack Jr.*, *Rong Liu*, *Lijun Xia*, *David Ljungman*, *Rena Bahjat*, *Michael A. Palladino Jr.*. Massachusetts General Hospital, Harvard Medical School, Boston, MA, Nereus Pharmaceuticals, Inc., San Diego, CA

Pancreatic cancer is one of the most resistant cancers to chemotherapy and irradiation. A variety of resistance mechanisms have been demonstrated in pancreatic cancer including the activation of nuclear transcription factor kappa B (NF-κB) and the dysregulation of the epidermal growth factor receptor (EGFR). We have previously demonstrated *in vitro* that the proteasome inhibitor NPI-0052 suppresses both constitutive and chemotherapy-induced NF-κB activation, but does not stabilize p53 expression, suggesting that treatment induced responses are mediated through p53-independent pathways. The current study was performed to determine if oral administration of a potent proteasome inhibitor NPI-0052 (Nereus Pharmaceuticals, San Diego) could alter the sensitivity to the combination treatment of gemcitabine (Gemzar, Eli Lily, Indianapolis, IN) and the antibody to EGFR (Erbitux, Imclone, Princeton, NJ) in a pancreatic cancer xenograft model. To determine the effect of proteasome inhibition on treatment response, panc-1 tumors were established by injecting 5 x 10^6 cells in the flank of female nude mice (nu/nu, 4-5 wks, 18-20g). Treatments were initiated once the tumors reached a mean diameter of 10 mm. Treatment groups (7 mice/group) received twice-weekly combination treatment with Erbitux 33mg/kg i.p., Gemzar 80mg/kg, and/or NPI-0052 0.25mg/kg. We found that the addition of NPI-0052 to the different treatment regimens resulted in an enhanced tumor growth response, including a 2-fold greater response to gemcitabine alone ($p<0.001$,T test), a 1.8-fold greater response to treatment with gemcitabine/Erbitux ($p<0.01$), and a 1.3-fold enhanced response to treatment with NPI-0052 alone compared to gemcitabine alone ($p<0.05$). These results demonstrate that the addition of NPI-0052 significantly enhanced tumor growth response to all treatments studied. Additional studies are underway to evaluate the potential of using orally administered NPI-0052 as an adjunct to combination chemo-and molecular therapy in pancreatic cancer.

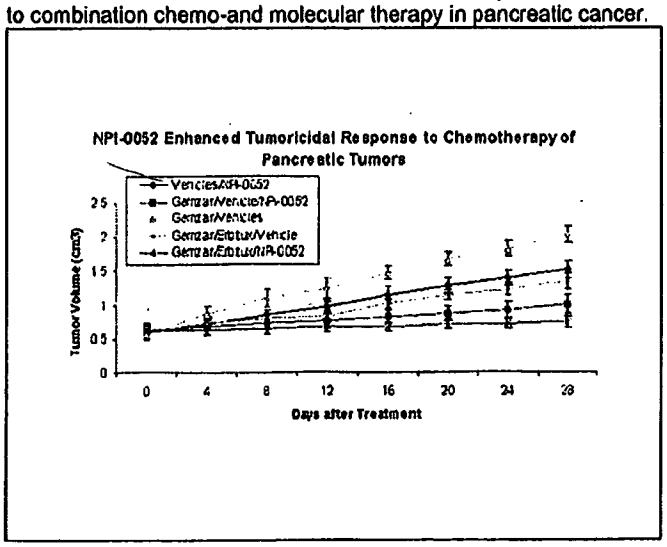

96th Annual Meeting
April 16-20, 2005
Anaheim/Orange County, CA

Selected Abstracts

Returned: 1 citations and abstracts. **Click on down arrow or scroll to see abstracts.**

Eriko Suzuki, Ali Jazirehi, Michael Palladino, and Benjamin Bonavida
Chemosensitization of Drug and Rituximab-Resistant Daudi B-NHL Clones to Drug-Induced Apoptosis by the Proteasome Inhibitor NPI-0052.
ASH Annual Meeting Abstracts 106: 1521.

Abstract 1 of 1 Poster Sessions

Chemosensitization of Drug and Rituximab-Resistant Daudi B-NHL Clones to Drug-Induced Apoptosis by the Proteasome Inhibitor NPI-0052.

Eriko Suzuki[1,*], Ali Jazirehi, PhD[1,*], Michael Palladino, PhD[2] and Benjamin Bonavida, PhD[1]

[1] Department of Microbiology, Immunology, and Molecular Genetics, David Geffen School of Medicine, Jonnson Comprehensive Cancer Center, University of California, Los Angeles, Los Angeles, CA, USA and [2] Nereus Pharmaceuticals, San Diego, CA, USA.

Abstract

Rituximab (chimeric anti-CD20) has been used clinically, alone or in combination with chemotherapy, in the treatment of B-NHL with a good response rate. However, some patients initially do not respond to such treatment and others develop resistance to further treatments. The mechanisms governing unresponsiveness are not known. We have proposed that responsiveness to rituximab treatment may be influenced by the response of the tumor cells to rituximab-mediated cell signaling. In addition, we have reported that rituximab sensitizes B-NHL cell lines to chemotherapy-induced drug apoptosis (see review Jazirehi and Bonavida, 2005, Oncogene 24:2121–2843[Medline]). In an effort to investigate the resistance of NHL response to rituximab treatment, we have generated rituximab resistant clones from the B-NHL cell line Daudi. For these studies, one such clone was examined, Daudi RR1. We have recently reported that rituximab signals the wild type (wt) Daudi and inhibits the constitutively activated NF-KB signaling pathway; this resulted in the selective downregulation of the anti-apoptotic Bcl-xl gene expression and sensitization of the tumor cells to various chemotherapeutically drug-induced apoptosis (Jazirehi, et al., 2005, Cancer Research 65: 264–76). In contrast to wt Daudi, treatment of Daudi RR1 with rituximab failed to modify the NF-KB signaling pathway. Further, examination of Daudi RR1 revealed that the cells exhibited hyperactivation of the NF-KB signaling pathway and overexpression of Bcl-xl and also exhibited higher degree of drug resistance as compared to wt Daudi. We investigated whether inhibition of NF-KB activity by a novel marine-derived orally active proteasome inhibitor, NPI-0052 (Nereus Pharmaceuticals), can sensitize both wt Daudi and Daudi RR1 cells to drug-induced apoptosis. NPI-0052 inhibits all three major proteolytic functions of the proteasome with a significantly different profile compared to Velcade and is active on Velcade resistant multiple myeloma cells (Chauhan, D., et al., Proc Amer Cancer Assoc, 2005, 46: [Abstract#: 6153]). In addition, NPI-0052 inhibits NF-KB activity, cytokine synthesis and exhibit cytostatic and cytotoxic activity in a variety of tumor cell

lines. Both Daudi and Daudi RR1 cells were treated with various concentrations of NPI-0052 (1–30 nM for 1 h) and then treated with CDDP (10–30 ug/ml for 20 h). Cell viability was determined microscopically and apoptosis was determined by PI staining for DNA hypoploidy. The findings reveal that treatment of Daudi and Daudi RR1 with single agent was not cytotoxic; however, combination treatment resulted in significant potentiation of cytotoxicity and synergy was achieved. Current studies are comparing the findings obtained with NPI-0052 with other NF-KB inhibitors for optimal sensitization and synergy with various chemotherapeutic drugs. The present findings demonstrate that NPI-0052 is a potent sensitizing agent that can reverse both rituximab and drug resistance of B-NHL cell lines when used in combination with conventional chemotherapeutic drugs.

97th AACR Annual Meeting
April 1-5, 2006
Washington, DC

Print this Page for Your Records Close Window

Abstract Number:	780
Presentation Title:	**Novel NFκB Inhibitors NPI-1342 / NPI-1387 and proteasome inhibitor NPI-0052 overcome resistance of pancreatic carcinoma to rhTRAIL**
Presentation Start/End Time:	Sunday, Apr 02, 2006, 1:00 PM - 5:00 PM
Location:	Exhibit Hall, Washington Convention Center
Poster Section:	3
Poster Board Number:	15
Author Block:	*Sanaz Khanbolooki, Simona Pino, Robert Andtbacka, Ta-Hsiang Chao, Saskia Neuteboom, Michael A. Palladino, David J. McConkey.* UT M.D. Anderson Cancer Ctr., Houston, TX, Division of Medical Oncology "A" Regina Elena Cancer Institute, Rome, Italy, Nereus Pharamceuticals, San Diego, CA

Pancreatic adenocarcinoma is the fifth leading cause of cancer deaths in the United States, with a 5 year survival rate of less than five percent. Nuclear Factor kappa B (NFκB) is a dimeric transcription factor implicated in suppression of apoptosis, angiogenesis, and metastasis. We investigated the effects of a small molecule inhibitor of the proteasome, NPI-0052, and two novel pimarane diterpene-derived inhibitors of NFκB (NPI-1342 and NPI-1387, Nereus Pharmaceuticals) in human pancreatic cancer cell lines. NPI-0052 is able to inhibit the 3 predominant catalytic active sites associated with proteasome function. It displays high potency and specific activity against the human 20S proteasome, is a potent inhibitor of chemotherapy-induced NFκB activation *in vitro* and promotes chemosensitivity both *in vitro* and *in vivo*. NPI-1342 and 1387 were originally identified in a cell-based screening program for their ability to inhibit LPS-induced TNF-α secretion. Exposure to the agents alone resulted in very little apoptosis, less than 10%. Seven of the 9 cell lines were moderately sensitive to apoptosis induced by Tumor Necrosis Factor related apoptosis-inducing ligand (TRAIL). NPI-0052, 1342, and 1387 reversed TRAIL resistance in the cell lines Panc1 and HS766T. Specific silencing of NFκB/p65 expression mimicked these effects. Combination treatment of NPI-0052 and NPI-1342 or 1387 led to induction of apoptosis as measured by PI FACS analysis. Specifically, levels of DNA fragmentation increased from 4% to 50% in HS766T cells and from 4% to 62% in Panc1 cells. The inhibitory effects of NPI-0052, 1342, 1387 on NFκB were evaluated by EMSA and confirmed by confocal microscopy. Bcl-XL and XIAP expression were downregulated by the inhibitors alone and in combination with TRAIL. Specific silencing of both anti-apoptotic proteins significantly enhanced the cytotoxic effects of TRAIL, 2% to 73%. *In vivo* results from an orthotopic pancreatic xenograft model conclude that mice treated with very low doses of NPI-0052 exhibited a minimal reduction in tumor load and mice treated with rhTRAIL had a 65% mean reduction in tumor load ($p<0.02$). The combination regimen of NPI-0052 and rhTRAIL resulted in a 92% mean reduction in tumor load ($p=0.003$) suggesting a synergistic effect of NPI-0052 and rhTRAIL *in vivo*. Treatment of mice with NPI-1342 alone resulted in a 51% mean reduction in tumor load ($p=0.0067$) demonstrating its efficacy as single agent therapy.
Together, our results strongly suggest that NFκB controls inhibition of apoptosis in human pancreatic cancer cells. We report here for the first time that inhibition of the proteasome as well as effective inhibition of NFκB results in decreased expression of Bcl-XL and XIAP significantly enhancing tumor cell apoptosis. Combined therapy with NFκB inhibitors and/or TRAIL may be a novel therapeutic strategy in this otherwise drug-resistant disease.

97th AACR Annual Meeting
April 1-5, 2006
Washington, DC

Click here to download CME disclosure information

Citation format: Proc Amer Assoc Cancer Res 2006;47:[Abstract #].

The proteasome inhibitor NPI-0052 overcomes TRAIL resistance in human pancreatic cancer cells in vitro and in vivo[1].

Robert Andtbacka[2,3*], Sanaz Khanbolooki[2*], Laura Lashinger[2], Steffan Nawrocki[2], Maria S. Pino[2,4], , Meiling Lu[6], Toni Kwan[6], Vincent Cryns[6], Thiruvengadam Arumugam[2], Craig D. Logsdon[2], Michael Palladino[5], and David J. McConkey[2]

Departments of Cancer Biology[2], Surgical Oncology[3], and Medical Oncology[4], U.T. M.D. Anderson Cancer Center, Houston, Texas 77030

Nereus Pharmaceuticals[5], Inc., San Diego, CA

Center for Endocrinology[6], Feinberg School of Medicine, Northwestern University, Chicago, IL 60611

*Co-first authors.

Running title: NPI-0052 plus TRAIL in pancreatic cancer.

Key words: L3.6pl, Panc-1, salinosporamide A, bortezomib, Velcade, caspase, TUNEL

Address correspondence to:
David McConkey
Department of Cancer Biology – 173
U.T. M.D. Anderson Cancer Center
1515 Holcombe Boulevard
Houston, Texas 77030
Tel. (713) 792-8591
FAX (713) 792-8747
Email: dmcconke@mdanderson.org

Footnotes

[1]Supported by a fellowship from the American Legion Auxiliary (to SK) and the MD Anderson SPORE in Pancreatic Cancer (P20 CA101936). The authors also wish to thank Angela Papageorgiou and Donna Reynolds for their input in the optimization of immunohistochemistry protocols.

[5]Abbreviations:

BCL-X_L: BCL-2-homologous X protein, long form.
DR4: death receptor 4
DR5: death receptor 5
FLIP: flice-like inhibitory protein
IAP: inhibitor of apoptosis protein
IκBα: Inhibitor of kappa B, alpha isoform
IKK: I Kappa B Kinase
NFκB: Nuclear Factor Kappa B
PI /FACS: propidium iodide staining/fluorescence-activated cell sorting
pIκBα: phosphorylated I kappa B alpha
siRNA: small interfering RNA
TNF-α: Tumor Necrosis Factor - alpha
TRAIL: Tumor necrosis factor-related apoptosis-inducing ligand
XIAP: X-linked inhibitor of apoptosis protein

Abstract

Recent studies have demonstrated that the proteasome inhibitor bortezomib (PS-341, Velcade) synergizes with TRAIL to induce apoptosis in solid tumor cell lines in vitro. Here we characterized the effects of the novel proteasome inhibitor, NPI-0052 (salinosporamide A), on TRAIL-induced apoptosis in human pancreatic cancer cells in vitro and in vivo. NPI-0052 interacted with TRAIL to induce additive increases in apoptosis in cells that were highly sensitive to TRAIL and reversed TRAIL resistance in the others. Single-agent therapy with rhTRAIL alone induced a dose-dependent inhibition of growth in drug-sensitive, orthotopic L3.6pl xenografts, and combination therapy with TRAIL plus NPI-0052 produced significantly greater tumor growth inhibition without significant toxicity. Furthermore, although neither single agent had much effect on the growth of drug-resistant, orthotopic Panc-1 tumors, combination therapy induced overt tumor regressions. Immunohistochemical analyses revealed that combination therapy with rhTRAIL plus bortezomib led to synergistic and rapid activation of caspases 8 and 3 and DNA fragmentation, consistent with the results obtained in vitro. Together, our results demonstrate that combination therapy with NPI-0052 plus TRAIL is well tolerated and induces synergistic induction of apoptosis and tumor regressions in vivo. The data support the design and implementation of clinical trials with proteasome inhibitors plus TRAIL in solid tumor patients.

(204 words)

Introduction

Pancreatic cancer is the fourth leading cause of cancer deaths in both men and women, with an incidence that almost exactly matches mortality (1). Even with the emergence of new combination regimens, little has been done in the last 20 years to improve patient prognosis (2), and only 4% of patients survive 5 years from the time of diagnosis according to the American Cancer Society (2). The nucleoside analog, gemcitabine, is currently considered to be the most active agent, but its effects are mostly palliative, and the majority of patients succumb to their disease within 6 months (3). Ongoing studies are evaluating the therapeutic activity of gemcitabine-based combination therapy, but the preliminary results of these trials do not suggest that a major increase in survival will be obtained (3). Therefore, there is a great need to develop more active therapeutic approaches in this disease, and there is particular interest in exploring potential biological targets that have not been targeted to date.

Tumor necrosis factor apoptosis inducing ligand (TRAIL) is a pro-apoptotic cytokine that plays important roles in inflammation and immunity (4). Preclinical studies demonstrated that it is also a very potent stimulus for apoptosis in human cancer cell lines, and unlike its structural and functional homologues TNF and Fas ligand, systemic exposure to TRAIL does not lead to appreciable toxicity in rodents and primates (5). The mechanisms underlying the TRAIL resistance of normal cells are not clear but may be related to their lower expression levels of functional TRAIL receptors (DR4, DR5) relative to cancer cells (6), to expression of non-functional ("decoy") TRAIL receptors (4, 7-9), or to differences in cell cycle control. A multi-center Phase I clinical trial of Apo-2L/TRAIL was recently completed at our institution and others.

Although there is great enthusiasm for using TRAIL in the therapy of pancreatic cancer and other solid tumors, it is appreciated that it will probably not demonstrate much clinical activity as a single agent, especially in tumors that have been exposed to numerous prior regimens. Indeed, preclinical studies demonstrate that approximately 50% of solid tumor cell lines are TRAIL-refractory at baseline (5, 10), prompting a search for agents that combine well with TRAIL to promote cell death. Several laboratories (including our own) have demonstrated that the proteasome inhibitor bortezomib (PS-341, Velcade) is a potent TRAIL-sensitizing agent, even in cancer cells that are completely TRAIL-refractory at baseline (9, 11-21). Proteasome inhibitors are especially attractive for pancreatic cancer therapy because they inhibit the anti-apoptotic transcription factor, NFκB (22), and previous work has established that NFκB is constitutively active in the majority of pancreatic tumors (23). NPI-0052 is a fully synthetic version of the marine compound salinosporamide A (24) that has been developed for cancer therapy (25-27). It is distinct from bortezomib in terms of its effects on 20S proteasome activity and its proteasome-binding properties (bortezomib is a reversible inhibitor whereas NPI-0052 is an irreversible inhibitor) (25-27). Here we assessed the therapeutic efficacy and toxicity of combination therapy with NPI-0052 plus TRAIL in orthotopic human L3.6pl pancreatic tumor xenografts. The results demonstrate that combination therapy is well tolerated and produces very potent effects on tumor growth inhibition and apoptosis.

Materials and Methods

Cell Culture and Reagents

The human pancreatic cancer cell lines Aspc1, BxPC3, Capan2, CfPac1, HPAF2, HS766T, MiaPaca2, and Panc1 were obtained from the American Type Culture Collection (Manassas, VA). The L3.6pl pancreatic adenocarcinoma cell line was derived from COLO-357 following selection for metastases from the pancreas to the liver in nude mice (28). All of the cell lines, with the exception of BxPC3, were maintained in MEM supplemented with 10% Fetal Bovine Serum, MEM vitamin solution, L-glutamine, non-essential amino acids, sodium pyruvate, and penicillin/streptomycin solutions in a 37° incubator under an atmosphere of 5% CO_2 in the air. BxPC3 was maintained under the same conditions in RPMI medium.

NPI-0052 was obtained from Nereus Pharmaceuticals, Inc (San Diego, CA). The rhTRAIL used in vitro was purchased from R& D Systems, Inc. (Minneapolis, MN). For in vivo studies, recombinant soluble His-tagged TRAIL (amino acids 98-281) was expressed in E. Coli by transforming BL-21 cells with a pET15b plasmid containing a partial TRAIL cDNA (29). Clones were isolated and grown to log phase, followed by addition of 1mM isopropyl 1-thio-β-D-galactopyranoside (IPTG) to induce protein expression, and incubated for 2 hours. The bacteria were lysed and the His-tagged protein was purified under native conditions using the QIAexpress system from Qiagen (Valencia, CA). Bacteria were suspended in lysis buffer (50mM NaH_2PO_4, 300mM NaCl, and 10mM imidazole (pH 8.0)) with 100 μg/ml lysozyme. The lysates were sonicated and centrifuged at 10,000g for 20 minutes at 4°C. Lysates were incubated with nickel-nitriloriacetic (NiNta) agarose mixture (Qiagen) for 90 minutes at 4°C while rotating. The lysate-NiNta mixture was loaded onto a column and washed with lysis buffer, and His-tagged TRAIL was eluted in 250mM imidazole. Post elution, fractions

containing high concentrations of TRAIL were collected and stored in aliquots containing 10% glycerol at 80°C.

Quantification of DNA Fragmentation

DNA fragmentation was measured by propidium iodide staining and FACS analysis as described previously (30, 31). After incubation *in vitro*, cells were harvested by trypsinization, pelleted by centrifugation, and resuspended in PBS containing 50 μg/ml propidium iodide, 0.1% Triton-X 100, and 0.1% sodium citrate. Samples were stored at 4°C and analyzed by flow cytometry (FL3 channel).

^{3}H-thymidine proliferation assay.

Cells were plated in 96-well plates at a density of 1×10^4 cells/well. Cells were exposed 24 h later to various concentrations of gefitinib (0.1 μM to 10 μM) in serum free MEM. After 24 hours the medium was removed and replaced with fresh MEM containing 10% FBS and 10 μCi/ml ^{3}H-thymidine (Amersham Biosciences, Piscataway, NJ). The cells were pulsed with ^{3}H-thymidine for 1 hour, lysed by the addition of 0.1 N KOH, and harvested onto fiberglass filters. The incorporated tritium was quantified in a scintillation counter.

Establishment and therapy of orthotopic L3.6pl xenografts

L3.6pl cells were harvested from culture flasks and transferred to serum-free HBSS. Male nude mice were anesthetized with methoxylurane, a small left abdominal flank incision was made, and tumor cells ($1x10^6$ cells) were injected into the subcapsular

region of the pancreas using a 30-gauge needle and a calibrated push button-controlled dispensing device (Hamilton Syringe Company, Reno, NV). To prevent leakage, a cotton swab was held cautiously for 1 minute over the site of injection. The abdominal wound was closed in one layer with wound clips (Autoclip; Clay Adams, Parsippany, NJ). Tumors were established for 10 days. Animals were then injected i.p. with the indicated doses of NPI-0052, rhTRAIL, or combinations of the two every 4 days for a total of 4 treatments. Mice were sacrificed and primary tumors in the pancreas were excised and weighed. For immunohistochemistry, tumor tissue was formalin-fixed and paraffin-embedded.

Establishment and therapy of orthotopic Panc-1 xenografts

Luciferase-transduced Panc-1 cells were used to generate orthotopic tumors and tumor volumes were imaged during the course of therapy as described previously (32). Briefly, one million ($1x10^6$) Panc1 cells stably transduced with a lentiviral luciferase vector were injected into the pancreas of nude mice (8 mice/group). Tumors were established for 14 days. Mice were treated with vehicle, TRAIL (8 mg/kg, 5 days/week), NPI-0052 (0.15 mg/kg, biweekly), or TRAIL plus NPI-0052 via intraperitoneal injection. Tumor volumes were monitored weekly by bioluminescence imaging using a cryogenically cooled imaging system coupled to a data acquisition computer running LivingImage software (Xenogen Corp., Alameda, CA). Before imaging, animals were anesthetized in an acrylic chamber with 1.5% isofluorane/air mixture and injected intraperitoneally with 40 mg/mL of luciferin potassium salt in PBS at a dose of 150 mg/kg body weight. After 10 minutes of incubation with luciferin, mice were placed in a

right lateral decubitus position and a digital grayscale animal image was acquired followed by acquisition and overlay of a pseudocolor image representing the spatial distribution of detected photons emerging from active luciferase within the animal. Signal intensity was quantified as the sum of all detected photons within the region of interest per second. (The minimum tumor-related signal intensity that can be accurately quantified in this model is approximately 10^4 pixels/second.) Therapy was continued for 3 weeks and animals were sacrificed.

Immunohistochemistry and Immunofluorescence

Paraffin-embedded sections were used for analysis of caspase-3, caspase-8, and PCNA. Approximately 5μm- thick sections of formalin-fixed, paraffin-embedded tissue were deparaffinized in xylene, treated serially with dilutions of alcohol [100%, 95%, and 80% ethanol], and subsequently rehydrated in PBS (pH 7.5). Antigen retrieval for the cleaved caspase-3 and -8 antibodies was performed using Borg Decloaker reagent purchased from Biocare (Walnut Creek, CA), and a pressure cooker. The protocol for detection of PCNA employed citrate/PBS-T antigen retrieval with incubation for five minutes in a microwave set on high power. Endogenous peroxidase activity was blocked by incubating tissue sections in 3% hydrogen peroxide diluted in methanol (CD31) or PBS (all others) for 15 minutes. Tissues were washed in PBS three times for three minutes each followed by incubation with the protein blocking solution for 20 minutes at room temperature. The protein blocking solution contained either 5% normal horse serum and 1% normal goat serum in PBS (pH 7.5) (PCNA and CD31 detection) or fish gelatin (TED Pella, Inc., Redding, CA) (cleaved caspase detection) in PBS (pH 7.5).

Excess protein block was drained and tissues were incubated at 4°C overnight with either of the following: rabbit polyclonal anti-caspase-3 antibody (BioCare, Walnut Creek, CA, 1:50), rabbit polyclonal anti-cleaved caspase-8 antibody (Cell Signaling Technology, Beverly, MA, 1:50), mouse monoclonal anti-PCNA antibody (Dako, Carpenteria, CA, 1:100). The tissues were then washed three times for three minutes each and incubated with the following species-specific secondary antibodies: biotinylated anti-rabbit Ig (Biocare) and streptavidin conjugated to horseradish peroxidase (HRP)(Dako, Carpenteria, CA, 1:300)(caspases 3 and 8) or HRP-conjugated anti-mouse IgG2a (Serotec Inc., Raleigh, NC)(PCNA) for one hour at room temperature. Positive staining was visualized by incubating tissue in 3,3'-diaminobenzidine (Research Genetics, Huntsville, AL) for 10-15 minutes. Following three washes in PBS, nuclei were counterstained with Gill's #3 hematoxylin (Sigma, St. Louis, MO) for 10s. Tissue sections were finally washed with distilled H_20 three times and treated with PBS for 1 minute. Slides were mounted with Universal Mount (Research Genetics, Huntsville, AL) prior to imaging. Negative control samples incubated in secondary antibodies alone exhibited no staining.

Images were captured from tumor areas devoid of necrosis under a light microscope at fields of x100 and absorbance was quantified using the Optimas software program (Bioscan, Edmonds, WA). Three different tumors were analyzed from each group, and a minimum of four images was captured from each tumor to yield an average measurement of staining intensity from 12 independent fields. Results were graphed as percentage of positively stained nuclei/cells versus total number of nuclei/cells quantified using the Optimas software (Bioscan, Edmonds, WA).

Quantification of Apoptosis by fluorescent TUNEL

DNA fragmentation was analyzed in frozen sections by FITC-labeled terminal deoxynucleotidyl transferase-mediated dUTP nick end labeling (TUNEL) (Promega, Madison, WI). Percentages of positive cells were determined using the Optimas software program (Bioscan, Edmonds, WA). Data were acquired from four fields in at least three tumors derived from each treatment group, and results are reported as means ± SEMs. To detect apoptotic endothelial cells, frozen sections were stained as described for detection of CD31 as outlined above using a Texas red-conjugated goat anti-rat secondary antibody (Jackson ImmunoResearch Lab, Inc., West Grove, PA) prior to performing the TUNEL analyses.

Results

Effects of NPI-0052 and TRAIL on apoptosis and proliferation in vitro.

We first characterized the effects of NPI-0052 on DNA fragmentation and proliferation in a panel of 8 human pancreatic cancer cell lines. Consistent with our previous observations with bortezomib (31), the cells displayed marked heterogeneity in terms of their sensitivity to proteasome inhibitor-induced apoptosis, with the Panc-1.1 and Panc-1 cells displaying the lowest levels of DNA fragmentation (Fig. 1A). In fact, cells that were previously found to be bortezomib-resistant (31) were also resistant to NPI-0052, and combination therapy with bortezomib plus NPI-0052 did not reverse drug resistance in these cells (R. Andtbacka, data not shown). Nonetheless, NPI-0052 inhibited DNA synthesis in all of the cell lines, including the ones that were most refractory to apoptosis (Fig. 1B and data not shown). These effects are also similar to the effects of bortezomib, which also blocked cell cycle progression in lines that were resistant to apoptosis (33). Kinetic analyses in the L3.6pl cells exposed to 10 nM NPI-0052 revealed that increased levels of apoptosis were first detectable at 8 h and reached a maximum by 24 h (Fig. 1C). Caspase activation appeared to precede endonuclease activation, in that processing of procaspases 8 and 3 was first detectable at 8 h and maximal by 12 h (Fig. 1D). The kinetics of apoptosis induced by NPI-0052 were also quite similar to those observed in cells exposed to borteozmib (33, 34).

We next exposed the same panel of cell lines to increasing concentrations of recombinant human TRAIL and measured apoptosis-associated DNA fragmentation 24 h later by propidium iodide staining and FACS analysis. Highly variable responses were observed (Fig. 1A), with the majority of cell lines displaying relatively modest increases

in DNA fragmentation at high concentrations of TRAIL (<30%, Fig. 2A). Analysis of DNA synthesis by ^{3}H-thymidine incorporation in two of the more resistant cell lines (Panc-1, Panc-1.1) demonstrated that TRAIL did inhibit cell proliferation (Fig. 2B).

Because our group and others has demonstrated that proteasome inhibitors increase TRAIL sensitivity (16, 19), we exposed L3.6pl or Panc-1 cells to TRAIL plus NPI-0052 for 24 h and measured DNA fragmentation by PI/FACS. In the L3.6pl cells exposure to either TRAIL or NPI-0052 induced significant increases in apoptosis, and exposure to both drugs simultaneously produced additive increases in DNA fragmentation (Fig. 2C). In Panc-1 cells neither NPI-0052 nor TRAIL induced substantial DNA fragmentation (Fig. 2C). Strikingly, however, the combination of TRAIL plus bortezomib stimulated increases in apoptosis Panc-1 cells that were equivalent to those observed in the L3.6pl cells (Fig. 2C).

Effects of single agent NPI-0052 on the growth of orthotopic L3.6pl xenografts. In previous studies we demonstrated that bortezomib inhibits the growth of orthotopic L3.6pl tumors (31, 33, 34). We therefore performed studies with this model to identify a maximum tolerated dose (MTD) for NPI-0052 in tumor-bearing animals. Human L3.6pl pancreatic cancer cells were implanted directly in the pancreas glands of nude mice and allowed to grow unperturbed for 10 days. NPI-0052 was then delivered every 4 days via intraperitoneal injection (total of 4 treatments). We sacrificed some animals after two treatments for biomarker analyses at an intermediate point in therapy ("acute" studies), and we also measured relevant biomarkers at the experimental endpoint. All animals treated with 0.075 or 0.15 mg/kg NPI-0052 survived until the end of the experiment (Fig.

3A) and displayed minimal toxicity (Table I). In contrast, 3/10 mice treated with 0.25 mg/kg NPI-0052 died during the course of therapy, and body weights in the group as a whole decreased by >10% (Fig. 3A, Table I). All three doses of drug significantly inhibited tumor growth (Fig. 3A). These effects were associated with dose-dependent decreases in tumor cell proliferation, measured by PCNA immunohistochemistry (Fig. 3B). However, single-agent therapy induced very modest increases in tumor cell apoptosis as measured by fluorescent TUNEL staining or immunohistochemical detection of activated caspase-8 or -3 after 1 week of therapy (Fig. 4). Higher levels of TUNEL staining were observed in tumors isolated from the animals that survived therapy with 0.25 mg/kg NPI-0052, but this increased DNA fragmentation was not associated with increased caspase-8 or -3 activation (Fig. 4).

Effects of combination therapy with NPI-0052 plus TRAIL in orthotopic L3.6pl tumors. We next assessed the toxicity and therapeutic efficacy of combination therapy with NPI-0052 plus TRAIL in the drug-sensitive L3.6pl tumors. We selected an intermediate dose of NPI-0052 (0.075 mg/kg) and combined it with increasing doses of TRAIL (1, 4, and 8 mg/kg). Single-agent therapy with TRAIL produced a dose-dependent inhibition of tumor growth, reaching over 80% inhibition at the highest dose tested (8 mg/kg)(Fig. 4A, Table 2). Single-agent NPI-0052 also produced significant tumor growth inhibition (25%)(Fig. 5A, Table 2), consistent with the previous studies (Fig. 3A, Table 1). However, combination therapy with 1 or 4 mg/kg TRAIL plus 0.075 mg/kg NPI-0052 significantly inhibited tumor growth as compared to therapy with either single agent (Fig. 5A, Table 2). Combination therapy also appeared to inhibit tumor

growth at the highest dose of TRAIL, although these effects did not reach statistical significance (Fig. 5A, Table 2).

Effects of combination therapy on proliferation and apoptosis. We focused on the combination of 4 mg/kg TRAIL plus 0.075 mg/kg NPI-0052 and measured changes in biomarker levels after two doses of drugs (to measure the "acute" changes) and at the experimental endpoint. Analysis of tumor cell proliferation levels by PCNA staining revealed that NPI-0052 had minimal effect, whereas TRAIL reduced proliferation by 50% (Fig. 5B). Combination therapy with NPI-0052 plus TRAIL produced the strongest inhibition of proliferation at both time points (Fig. 5B).

We also characterized the effects of combination therapy on induction of apoptosis, measured by TUNEL staining or by immunohistochemical detection of caspase-8 and -3 activation. By all three measures single-agent therapy with NPI-0052 produced no detectable acute increases in apoptosis (Fig. 6). Levels of DNA fragmentation did increase in tissues exposed to NPI-0052 at the experimental endpoint, which may have been a consequence of the extensive necrosis observed in these tumors (data not shown). Therapy with rhTRAIL did induce increases in DNA fragmentation, caspase-3 activation, and caspase-8 activation, acutely and at the experimental endpoint (Fig. 6). However, combined therapy with NPI-0052 plus TRAIL produced synergistic, acute increases in apoptosis (Fig. 6). Increased levels of apoptosis were also easily detected at the experimental endpoint, but by this time levels of active caspase-8 and -3 had declined from the values observed earlier in the course of therapy (Fig. 6).

Effects of combination therapy on the growth of refractory orthotopic Panc-1 tumors. Although the results we obtained with the L3.6pl xenografts established that

combination therapy with NPI-0052 plus TRAIL produced the desired effects on tumor growth and apoptosis, we were especially interested in testing whether or not the combination would be effective in a model of drug-refractory disease. To address this question we tested the effects of combination therapy with NPI-0052 (0.15 mg/kg, biweekly) plus TRAIL (8 mg/kg, 5 days/week) in luciferase-transduced orthotopic Panc-1 tumors (32). We dosed animals with NPI-0052 8 h prior to administering NPI-0052 to ensure that proteasome inhibition was maximal when the TRAIL reached the tumor. Consistent with our previous experience (32), single-agent TRAIL had very little effect on Panc-1 tumor growth, and the effects of NPI-0052 were cytostatic at best (Fig. 7). However, combination therapy with TRAIL plus NPI-0052 produced tumor regressions (Fig. 7).

Discussion

Bortezomib's promising single agent activity in multiple myeloma and other malignancies (35-38) has prompted the development of chemically distinct proteasome inhibitors that display differences in their effects on 20S proteasome inhibition and their bioavailability. NPI-0052 (salinosporamide A) is a novel marine-derived proteasome inhibitor that, like bortezomib, has been developed for the treatment of cancer (24, 25). However, NPI-0052 differs from bortezomib in terms of its inhibitory effects on the 3 major enzymatic activities of the 20S proteasome and its irreversibility (25, 27). NPI-0052 also induces apoptosis via mechanism(s) that are distinct from those activated by bortezomib in multiple myeloma cells, and bortezomib-resistant multiple myeloma cells can be sensitive to NPI-0052 (26). In a recent study with cells from patients with chronic

lymphocytic leukemia (CLL) we demonstrated that NPI-0052 inhibits the 20S proteasome more rapidly and in a more sustained fashion than does bortezomib (27), which may be important for maximizing the effects of proteasome inhibition in tumor cells in vivo. NPI-0052 is now being evaluated in a Phase I clinical trial at our institution.

Here we characterized the effects of NPI-0052 on cell proliferation and apoptosis in a panel of 8 human pancreatic cancer cell lines. Overall, our results demonstrate that NPI-0052's effects are very similar to those observed in cells exposed to borteozmib. Specifically, NPI-0052 was a potent inhibitor of DNA synthesis (measured by ^{3}H-thymidine incorporation) in all of the cell lines, whereas its effects on apoptosis were much more variable. NPI-0052 also appeared to exert largely cytostatic effects on established orthotopic L3.6pl or Panc-1 tumors that were associated in the L3.6pl tumors with dose-dependent reductions in proliferation (as measured by PCNA staining) and more modest increases in cell death. Cells that we previously found to be refractory to bortezomib-induced apoptosis (31) were cross-resistant to NPI-0052, and combination therapy with bortezomib plus NPI-0052 did not overcome this resistance (R. Andtbacka, unpublished observations). Our findings therefore differ somewhat from recent results obtained in multiple myeloma (26).

Ongoing preclinical studies and clinical trials are attempting to identify the best means of exploiting the unique biological effects of proteasome inhibition within the context of combination chemotherapy. The original rationale for combining proteasome inhibitors with conventional chemotherapy and other modalities was that the latter often activate the survival-associated transcription factor, NFκB, as a side effect of their

actions (39, 40). NFκB activation appears to limit drug-induced apoptosis by upregulating the expression of crucial downstream targets (XIAP, BCL-X_L) (32, 41), and proteasome inhibitors block NFκB activation by preventing the proteasome-mediated degradation of NFκB's inhibitor, IκBα. Apoptosis induced by death receptor ligands (TNFα, TRAIL) appears to be particularly sensitive to NFκB activation status (42), and recent studies have confirmed that proteasome inhibitors and other NFκB antagonists are potent TRAIL-sensitizing agents in vitro (41, 43-55). We have also confirmed that small molecule NFκB inhibitors (PS-1145, NPI-1342) sensitize orthotopic tumors to TRAIL-induced apoptosis in vivo (32)(S. Khanbolooki, manuscript in preparation).

Here we show for the first time that therapeutic doses of TRAIL can be combined with NPI-0052 to promote tumor growth inhibition without inducing prohibitive toxicity in whole animals. The effects of combination therapy were associated with synergistic induction of apoptosis as measured by proteolytic processing of caspases-8 and -3 and DNA fragmentation, effects that were most obvious in tumors harvested at an early point in the course of therapy. Of critical importance was our observation that combination therapy with NPI-0052 plus TRAIL produced regressions of orthotopic Panc-1 tumors that were resistant to therapy with either agent alone (Fig. 7).

In other recent studies we have characterized the molecular mechanisms involved in proteasome inhibitor-mediated TRAIL sensitization in some detail. Predictably, these mechanisms are complex and involve several different (probably independent) biochemical pathways. We have confirmed that NFκB inhibition plays a major role and have identified BCL-X_L and XIAP as two of NFκB's important targets in TRAIL sensitization (32). In addition, proteasome inhibitors promote the accumulation of the

cyclin-dependent kinase inhibitor, p21, and p21 also contributes to sensitization (19). Finally, proteasome inhibitors induce endoplasmic reticular (ER) stress leading to activation of the ER-resident protease, caspase-4 (34), and active caspase-4 also appears to contribute to the enhancement of TRAIL-induced apoptosis (K. Zhu, unpublished observations). Importantly, we have not yet observed toxicity when we have combined more selective chemical inhibitors of NFκB with TRAIL in animals bearing orthotopic pancreatic tumors, and NFκB inhibitors are capable of restoring TRAIL sensitivity in refractory cells in vitro and in vivo (32)(S. Khanbolooki, manuscript in preparation). Thus, it would seem important to compare the effects of non-selective (proteasome inhibitors) and more selective inhibitors of NFκB in terms of their ability to synergize with TRAIL to induce apoptosis and regress refractory tumors in additional preclinical models before advancing to clinical trials of the combinations in patients.

References

1. Jemal A, Thomas A, Murray T, Thun M. Cancer statistics, 2002. CA Cancer J Clin 2002;52:23-47.
2. Niederhuber JE, Brennan MF, Menck HR. The National Cancer Data Base report on pancreatic cancer. Cancer 1995;76:1671-7.
3. Pino SM, Xiong HQ, McConkey D, Abbruzzese JL. Novel therapies for pancreatic adenocarcinoma. Curr Oncol Rep 2004;6:199-206.
4. Ashkenazi A, Dixit VM. Apoptosis control by death and decoy receptors. Curr Opin Cell Biol 1999;11:255-60.
5. Kelley SK, Ashkenazi A. Targeting death receptors in cancer with Apo2L/TRAIL. Curr Opin Pharmacol 2004;4:333-9.
6. Ozawa F, Friess H, Kleeff J, et al. Effects and expression of TRAIL and its apoptosis-promoting receptors in human pancreatic cancer. Cancer Lett 2001;163:71-81.
7. Ibrahim SM, Ringel J, Schmidt C, et al. Pancreatic adenocarcinoma cell lines show variable susceptibility to TRAIL-mediated cell death. Pancreas 2001;23:72-9.
8. Liao Q, Friess H, Kleeff J, Buchler MW. Differential expression of TRAIL-R3 and TRAIL-R4 in human pancreatic cancer. Anticancer Res 2001;21:3153-9.
9. Bai J, Sui J, Demirjian A, Vollmer CM, Jr., Marasco W, Callery MP. Predominant Bcl-XL knockdown disables antiapoptotic mechanisms: tumor necrosis factor-related apoptosis-inducing ligand-based triple chemotherapy overcomes chemoresistance in pancreatic cancer cells in vitro. Cancer Res 2005;65:2344-52.
10. Wang S, El-Deiry WS. TRAIL and apoptosis induction by TNF-family death receptors. Oncogene 2003;22:8628-33.
11. Sayers TJ, Brooks AD, Koh CY, et al. The proteasome inhibitor PS-341 sensitizes neoplastic cells to TRAIL-mediated apoptosis by reducing levels of c-FLIP. Blood 2003;102:303-10.
12. Johnson TR, Stone K, Nikrad M, et al. The proteasome inhibitor PS-341 overcomes TRAIL resistance in Bax and caspase 9-negative or Bcl-xL overexpressing cells. Oncogene 2003;22:4953-63.
13. An J, Sun YP, Adams J, Fisher M, Belldegrun A, Rettig MB. Drug interactions between the proteasome inhibitor bortezomib and cytotoxic chemotherapy, tumor necrosis factor (TNF) alpha, and TNF-related apoptosis-inducing ligand in prostate cancer. Clin Cancer Res 2003;9:4537-45.
14. An J, Sun Y, Fisher M, Rettig MB. Antitumor effects of bortezomib (PS-341) on primary effusion lymphomas. Leukemia 2004;18:1699-704.
15. Yin D, Zhou H, Kumagai T, et al. Proteasome inhibitor PS-341 causes cell growth arrest and apoptosis in human glioblastoma multiforme (GBM). Oncogene 2005;24:344-54.
16. Papageorgiou A, Lashinger L, Millikan R, et al. Role of tumor necrosis factor-related apoptosis-inducing ligand in interferon-induced apoptosis in human bladder cancer cells. Cancer Res 2004;64:8973-9.
17. Matta H, Chaudhary PM. The Proteasome Inhibitor Bortezomib (PS-341) Inhibits Growth and Induces Apoptosis in Primary Effusion Lymphoma Cells. Cancer Biol Ther 2005;4:77-82.

18. Sayers TJ, Murphy WJ. Combining proteasome inhibition with TNF-related apoptosis-inducing ligand (Apo2L/TRAIL) for cancer therapy. Cancer Immunol Immunother 2005.
19. Lashinger LM, Zhu K, Williams SA, Shrader M, Dinney CP, McConkey DJ. Bortezomib abolishes tumor necrosis factor-related apoptosis-inducing ligand resistance via a p21-dependent mechanism in human bladder and prostate cancer cells. Cancer Res 2005;65:4902-8.
20. Ganten TM, Koschny R, Haas TL, et al. Proteasome inhibition sensitizes hepatocellular carcinoma cells, but not human hepatocytes, to TRAIL. Hepatology 2005;42:588-97.
21. Nencioni A, Wille L, Dal Bello G, et al. Cooperative cytotoxicity of proteasome inhibitors and tumor necrosis factor-related apoptosis-inducing ligand in chemoresistant Bcl-2-overexpressing cells. Clin Cancer Res 2005;11:4259-65.
22. Adams J. The development of proteasome inhibitors as anticancer drugs. Cancer Cell 2004;5:417-21.
23. Wang W, Abbruzzese JL, Evans DB, Larry L, Cleary KR, Chiao PJ. The nuclear factor-kappa B RelA transcription factor is constitutively activated in human pancreatic adenocarcinoma cells. Clin Cancer Res 1999;5:119-27.
24. Groll M, Huber R, Potts BC. Crystal structures of Salinosporamide A (NPI-0052) and B (NPI-0047) in complex with the 20S proteasome reveal important consequences of beta-lactone ring opening and a mechanism for irreversible binding. J Am Chem Soc 2006;128:5136-41.
25. Macherla VR, Mitchell SS, Manam RR, et al. Structure-activity relationship studies of salinosporamide A (NPI-0052), a novel marine derived proteasome inhibitor. J Med Chem 2005;48:3684-7.
26. Chauhan D, Catley L, Li G, et al. A novel orally active proteasome inhibitor induces apoptosis in multiple myeloma cells with mechanisms distinct from Bortezomib. Cancer Cell 2005;8:407-19.
27. Ruiz S, Krupnik Y, Keating M, Chandra J, Palladino M, McConkey D. The proteasome inhibitor NPI-0052 is a more effective inducer of apoptosis than bortezomib in lymphocytes from patients with chronic lymphocytic leukemia. Mol Cancer Ther 2006;5:1836-43.
28. Bruns CJ, Harbison MT, Kuniyasu H, Eue I, Fidler IJ. In vivo selection and characterization of metastatic variants from human pancreatic adenocarcinoma by using orthotopic implantation in nude mice. Neoplasia 1999;1:50-62.
29. Lu M, Kwan T, Yu C, et al. Peroxisome proliferator-activated receptor gamma agonists promote TRAIL-induced apoptosis by reducing survivin levels via cyclin D3 repression and cell cycle arrest. J Biol Chem 2005;280:6742-51.
30. Nicoletti I, Migliorati G, Pagliacci MC, Grignani F, Riccardi C. A rapid and simple method for measuring thymocyte apoptosis by propidium iodide staining and flow cytometry. J Immunol Methods 1991;139:271-9.
31. Nawrocki ST, Bruns CJ, Harbison MT, et al. Effects of the proteasome inhibitor PS-341 on apoptosis and angiogenesis in orthotopic human pancreatic tumor xenografts. Mol Cancer Ther 2002;1:1243-53.

32. Khanbolooki S, Nawrocki ST, Arumugam T, et al. Nuclear factor-kappaB maintains TRAIL resistance in human pancreatic cancer cells. Mol Cancer Ther 2006;5:2251-60.
33. Nawrocki ST, Sweeney-Gotsch B, Takamori R, McConkey DJ. The proteasome inhibitor bortezomib enhances the activity of docetaxel in orthotopic human pancreatic tumor xenografts. Mol Cancer Ther 2004;3:59-70.
34. Nawrocki ST, Carew JS, Pino MS, et al. Bortezomib sensitizes pancreatic cancer cells to endoplasmic reticulum stress-mediated apoptosis. Cancer Res 2005;65:11658-66.
35. Richardson PG, Barlogie B, Berenson J, et al. A phase 2 study of bortezomib in relapsed, refractory myeloma. N Engl J Med 2003;348:2609-17.
36. Aghajanian C, Soignet S, Dizon DS, et al. A phase I trial of the novel proteasome inhibitor PS341 in advanced solid tumor malignancies. Clin Cancer Res 2002;8:2505-11.
37. Papandreou CN, Logothetis CJ. Bortezomib as a potential treatment for prostate cancer. Cancer Res 2004;64:5036-43.
38. Scagliotti G. Proteasome inhibitors in lung cancer. Crit Rev Oncol Hematol 2006.
39. Cusack JC, Jr., Liu R, Houston M, et al. Enhanced chemosensitivity to CPT-11 with proteasome inhibitor PS-341: implications for systemic nuclear factor-kappaB inhibition. Cancer Res 2001;61:3535-40.
40. Russo SM, Tepper JE, Baldwin AS, Jr., et al. Enhancement of radiosensitivity by proteasome inhibition: implications for a role of NF-kappaB. Int J Radiat Oncol Biol Phys 2001;50:183-93.
41. Ravi R, Bedi GC, Engstrom LW, et al. Regulation of death receptor expression and TRAIL/Apo2L-induced apoptosis by NF-kappaB. Nat Cell Biol 2001;3:409-16.
42. Aggarwal BB. Nuclear factor-kappaB: the enemy within. Cancer Cell 2004;6:203-8.
43. Thomas RP, Farrow BJ, Kim S, May MJ, Hellmich MR, Evers BM. Selective targeting of the nuclear factor-kappaB pathway enhances tumor necrosis factor-related apoptosis-inducing ligand-mediated pancreatic cancer cell death. Surgery 2002;132:127-34.
44. Lee KY, Park JS, Jee YK, Rosen GD. Triptolide sensitizes lung cancer cells to TNF-related apoptosis-inducing ligand (TRAIL)-induced apoptosis by inhibition of NF-kappaB activation. Exp Mol Med 2002;34:462-8.
45. Kim YS, Schwabe RF, Qian T, Lemasters JJ, Brenner DA. TRAIL-mediated apoptosis requires NF-kappaB inhibition and the mitochondrial permeability transition in human hepatoma cells. Hepatology 2002;36:1498-508.
46. Deeb D, Jiang H, Gao X, et al. Curcumin sensitizes prostate cancer cells to tumor necrosis factor-related apoptosis-inducing ligand/Apo2L by inhibiting nuclear factor-kappaB through suppression of IkappaBalpha phosphorylation. Mol Cancer Ther 2004;3:803-12.
47. Chawla-Sarkar M, Bauer JA, Lupica JA, et al. Suppression of NF-kappa B survival signaling by nitrosylcobalamin sensitizes neoplasms to the anti-tumor effects of Apo2L/TRAIL. J Biol Chem 2003;278:39461-9.
48. Dalen H, Neuzil J. Alpha-tocopheryl succinate sensitises a T lymphoma cell line to TRAIL-induced apoptosis by suppressing NF-kappaB activation. Br J Cancer 2003;88:153-8.

49. Ghosh SK, Wood C, Boise LH, et al. Potentiation of TRAIL-induced apoptosis in primary effusion lymphoma through azidothymidine-mediated inhibition of NF-kappa B. Blood 2003;101:2321-7.
50. Shigeno M, Nakao K, Ichikawa T, et al. Interferon-alpha sensitizes human hepatoma cells to TRAIL-induced apoptosis through DR5 upregulation and NF-kappa B inactivation. Oncogene 2003;22:1653-62.
51. Ehrhardt H, Fulda S, Schmid I, Hiscott J, Debatin KM, Jeremias I. TRAIL induced survival and proliferation in cancer cells resistant towards TRAIL-induced apoptosis mediated by NF-kappaB. Oncogene 2003;22:3842-52.
52. Deeb D, Xu YX, Jiang H, et al. Curcumin (diferuloyl-methane) enhances tumor necrosis factor-related apoptosis-inducing ligand-induced apoptosis in LNCaP prostate cancer cells. Mol Cancer Ther 2003;2:95-103.
53. Nakshatri H, Rice SE, Bhat-Nakshatri P. Antitumor agent parthenolide reverses resistance of breast cancer cells to tumor necrosis factor-related apoptosis-inducing ligand through sustained activation of c-Jun N-terminal kinase. Oncogene 2004;23:7330-44.
54. Karacay B, Sanlioglu S, Griffith TS, Sandler A, Bonthius DJ. Inhibition of the NF-kappaB pathway enhances TRAIL-mediated apoptosis in neuroblastoma cells. Cancer Gene Ther 2004;11:681-90.
55. Huerta-Yepez S, Vega M, Jazirehi A, et al. Nitric oxide sensitizes prostate carcinoma cell lines to TRAIL-mediated apoptosis via inactivation of NF-kappa B and inhibition of Bcl-xl expression. Oncogene 2004;23:4993-5003.

Figure Legends

Figure 1: Concentration-dependent effects of NPI-0052 on proliferation and apoptosis. A. Effects on DNA fragmentation. Cells were exposed to the indicated concentrations of NPI-0052 for 24 h and DNA fragmentation was quantified by PI/FACs as described in Materials and Methods. Mean ± SEM, n = 3. B. Effects of NPI-0052 on DNA synthesis. Cells were exposed to the indicated concentrations of NPI-0052 for 24 h and ^{3}H-thymidine uptake was quantified as described in Materials and Methods. Mean ± SEM, n = 3. C. Time course of NPI-0052-induced DNA fragmentation. L3.6pl cells were exposed to 10 nM NPI-0052 for the times indicated and DNA fragmentation was measured by PI/FAC S. Mean ± SEM, n = 3. D. Time-dependent effects of NPI-0052 on caspase activation. L3.6pl cells were exposed to 10 nM for the times indicated. Cells were then harvested and lysed, and levels of caspase activation were measured as described in Materials and Methods. Top panel: procaspase-8 processing. Middle panel; procaspase-3 processing. Bottom panel: Time-dependent effects on caspase-3-like (DEVDase) activity. Results of one experiment that were representative of 3 independent replicates.

Figure 2: Effects of rhTRAIL on apoptosis and proliferation in vitro. A. Cells were incubated in the absence or presence of the indicated concentrations of rhTRAIL for 24 h and DNA fragmentation was measured by PI/FACS. Mean ± SEM, n = 3. B. Effects of rhTRAIL on cell proliferation, Cells were incubated with the indicated concentrations of TRAIL for 24 h, and DNA synthesis was measured by ^{3}H-thymidine incorporation. Mean ± SEM, n = 3. C. Effects of NPI-0052 on TRAIL-induced apoptosis in vitro.

L3.6pl (sensitive) or Panc-1 (resistant) were incubated with 1 ng/ml (L3.6p) or 50 ng/ml TRAIL without or with 10 nM NPI-0052 for 24h, and DNA fragmentation was measured by PI/FACS. Mean ± SEM, n = 3.

Figure 3: Effects of NPI-0052 on tumor growth and proliferation. A. Effects on tumor growth. Cells (1×10^6) were implanted into the pancreas glands of nude mice. Ten days later therapy was initiated, consisting of NPI-0052 at doses of 0.25, 0,15, or 0.075, delivered once every 4 days via intraperitoneal injection. Animals were treated 4 times before they were sacrificed and tumors were weighed. Mean ± SEM, n = 10. *p < 0,05. B. Effects of NPI-0052 on proliferation. Animals bearing established orthotopic L3.6pl tumors were treated with two (acute studies) or four (chronic studies) doses of NPI-0052. Animals were sacrificed, tumors harvested, tumor sections were stained with an anti-PCNA antibody, and proliferation was quantified as described in Materials and Methods. Mean ± SEM, n = 5. *p < 0.05 versus controls.

Figure 4: Effects of NPI-0052 on apoptosis in vivo. Animals bearing established orthotopic tumors were treated with two (acute studies) or four (chronic studies) doses of NPI-0052. Animals were sacrificed, tumors were harvested, tumor sections were stained for detection of DNA fragmentation (TUNEL) or active caspases, and levels of apoptosis were quantified as described in Materials and Methods. Mean ± SEM, n = 5. *p < 0.05 versus controls.

Figure 5: Effects of combination therapy with TRAIL plus NPI-0052 on L3.6pl tumor growth and proliferation. A. Effects on tumor growth. Cells (1×10^6) were implanted into the pancreas glands of nude mice. Ten days later therapy was initiated, consisting of 0.075 mg/kg NPI-0052 with or without 1, 4, or 8 mg/kg rhTRAIL, delivered once every 4 days via intraperitoneal injection. Animals were treated 4 times before they were sacrificed and tumors were weighed. Mean ± SEM, n = 10. *$p < 0.05$ versus controls; † $p < 0.05$ versus TRAIL alone. B. Effects of therapy on proliferation. Animals bearing established orthotopic L3.6pl tumors were treated with two (acute studies) or four (chronic studies) doses of NPI-0052 with or without TRAIL. Animals were sacrificed, tumors harvested, tumor sections were stained with an anti-PCNA antibody, and proliferation was quantified as described in Materials and Methods. Mean ± SEM, n = 5. *$p < 0.05$ versus controls.

Figure 6: Effects of combination therapy with TRAIL plus NPI-0052 on apoptosis in vivo. Animals bearing established orthotopic L3.6pl tumors were treated with two (acute studies) or four (chronic studies) doses of NPI-0052 with or without TRAIL. Animals were sacrificed, tumors harvested, tumor sections were stained for detection of DNA fragmentation (TUNEL) or active caspases, and levels of apoptosis were quantified as described in Materials and Methods. Mean ± SEM, n = 5. *$p < 0.05$ versus controls.

Figure 7: Effects of combination therapy with TRAIL plus NPI-0052 on the growth of orthotopic Panc-1 xenografts. Animals bearing established tumors were treated with TRAIL (5 days/week), NPI-0052 (biweekly), or both via intraperitoneal injection, and

tumor volumes were monitored continuously throughout the course of therapy by luciferase imaging. Body weights were also measured weekly as a surrogate for toxicity.

A. Representative images obtained from mice at an intermediate point during therapy.

B. Growth curves. Mean ± SEM, n = 8. C. Body weights. Mean ± SEM, n = 8.

TABLE 1. Effect of NPI-0052 on mouse mortality, body weight, and established orthotopic pancreatic tumors [a]

Concentration of NPI-0052 (mg/kg)	Mortality	Tumor incidence	Mean pre-treatment body weight (g)	Mean post-treatment body weight (g)	Mean change in body weight (g)	Mean tumor weight (g)
Control	0 of 10	10 of 10	30.7 (27.7-34.0)	27.2 (20.1-31.7)	-3.5 (-11.5%)	1.625 (0.768-2.432)
0.075	0 of 10	10 of 10	30.1 (27.0-33.8)	25.1 (19.5-29.9)	-5.0 (-16.7%) [b]	1.143 (0.500-1.709) [c]
0.15	0 of 10	10 of 10	26.7 (20.2-29.8)	23.9 (18.7-27.3)	-2.8 (-10.4%)	1.038 (0.305-1.952) [c]
0.25	3 of 10	10 of 10	28.9 (25.6-30.9)	22.7 (20.7-24.5)	-6.2 (-21.4%) [b]	0.588 (0.382-1.201) [d]

[a] Orthotopic tumor were generated by injecting 1 x 10^6 L3.6pl cells into the body of the pancreas of nude mice. Tumors were established for 10 days before the initiation of therapy with NPI-0052 (intraperitoneal injection every 4 days for a total of 4 treatments). Animals were sacrificed 1 day after the last treatment, and assessed for weight, tumor burden and analysis of biological endpoints. Data ranges given in parentheses. [b] Significantly different from pre-treatment weight ($P<0.01$). [c] Significantly different from control tumors ($P<0.05$). [d] Significantly different from control tumors ($P<0.001$).

TABLE 2. Effect of TRAIL and NPI-0052 on mouse mortality, body weight, and established orthotopic pancreatic tumors [a]

Condition	Mortality	Tumor incidence	Mean pre-treatment body weight (g)	Mean post-treatment body weight (g)	Mean change in body weight (g)	Mean tumor weight (g)
Control	0 of 9	9 of 9	28.8 (26.4-31.0)	25.8 (18.6-32.1)	-3.0 (-10.3%)	1.973 (0.667-3.026)
TRAIL 1 mg/kg	0 of 10	10 of 10	29.7 (27.6-31.5)	28.6 (24.2-30.6)	-1.1 (-3.7%)	1.338 (0.746-2.141) [c]
TRAIL 4 mg/kg	0 of 10	10 of 10	27.4 (24.0-30.8)	25.7 (19.2-29.6)	-1.7 (-5.9%)	1.083 (0.146-3.400) [c]
TRAIL 8 mg/kg	0 of 10	10 of 10	28.2 (24.3-32.0)	28.5 (23.7-32.6)	0.3 (1.0%)	0.375 (0.055-0.888) [d]
NPI-0052	0 of 10	10 of 10	29.2 (26.2-33.8)	24.6 (19.5-31.9)	-4.6 (-15.8%) [b]	1.450 (0.468-2.466) [c]
NPI-0052 + TRAIL 1 mg/kg	1 of 10	10 of 10	28.9 (26.5-31.6)	24.8 (19.6-28.1)	-4.1 (-14.3%) [b]	0.925 (0.640-1.816) [c, e]
NPI-0052 + TRAIL 4 mg/kg	0 of 10	10 of 10	29.7 (26.7-31.8)	25.5 (21.3-28.2)	-4.2 (-14.2%) [b]	0.384 (0.070-1.445) [d, e]
NPI-0052 + TRAIL 8 mg/kg	3 of 10	10 of 10	30.1 (27.8-34.2)	25.6 (21.4-28.9)	-4.5 (-15.1%) [b]	0.252 (0.010-0.413) [d]

[a] Orthotopic tumor were generated by injecting 1 x 10^6 L3.6pl cells into the body of the pancreas of nude mice. Tumors were established for 10 days before the initiation of therapy with TRAIL and/or NPI-0052 (concomitant intraperitoneal injection every 4 days for a total of 4 treatments). NPI-0052 was administered at 0.075 mg/kg. Animals were sacrificed 1 day after the last treatment and assessed for weight, tumor burden and analysis of biological endpoints. Data ranges given in parentheses. [b] Significantly different from pre-treatment weight ($P<0.01$). [c] Significantly different from control tumors ($P<0.05$). [d] Significantly different from control tumors ($P<0.001$). [e] Significantly different from TRAIL single agent treatment ($P<0.05$).

Fig. 1A

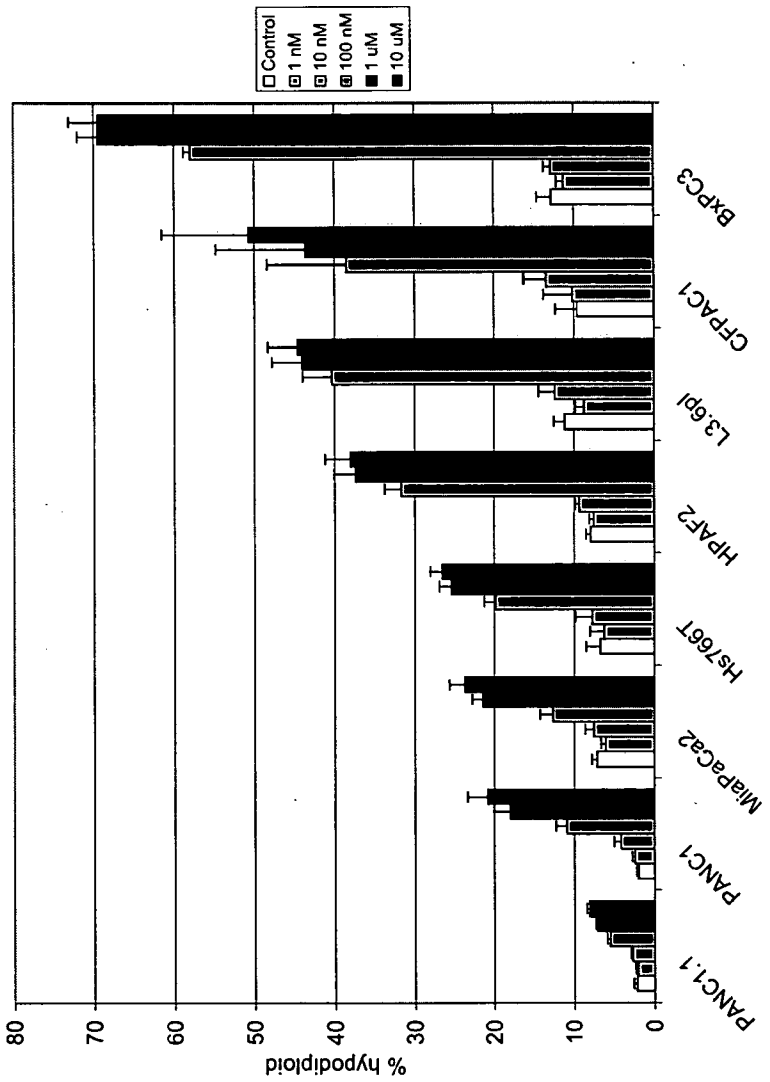
Control
1 nM
10 nM
100 nM
1 uM
10 uM
% hypodiploid
0
10
20
30
40
50
60
70
80
PANC1.1
PANC1
MiaPaCa2
HS766T
HPAF2
L3.6pl
CFPAC1
BxPC3

Fig. 1B

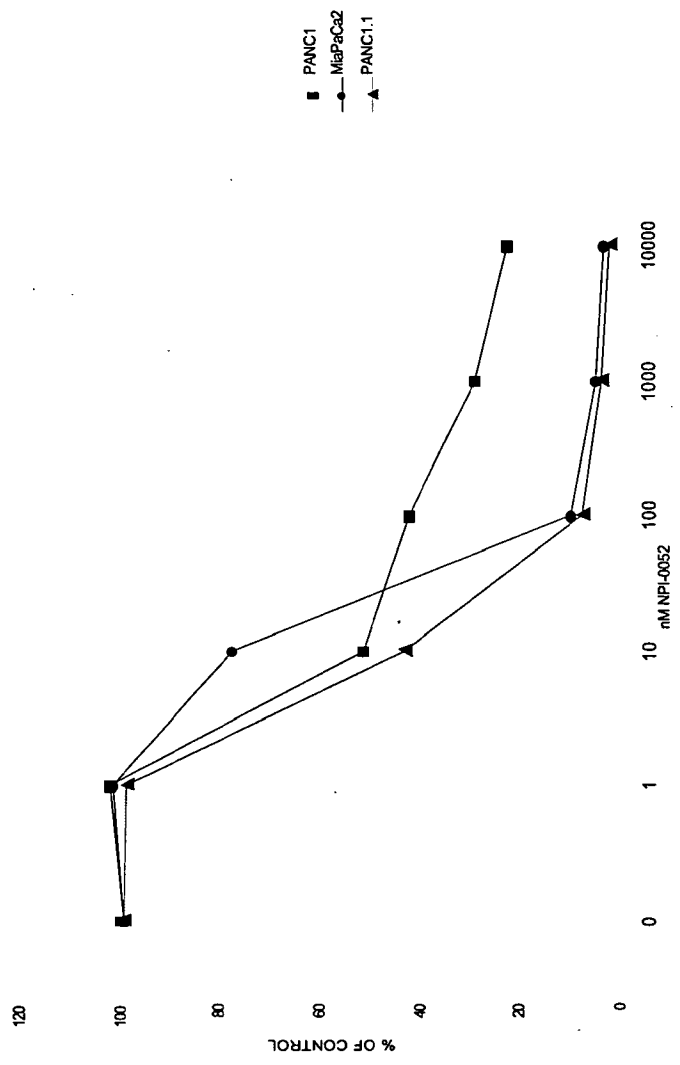
PANC1
MiaPaCa2
PANC1.1
% OF CONTROL
120
100
80
60
40
20
0
0
1
10
100
1000
10000
nM NPI-0052

Fig. 1C

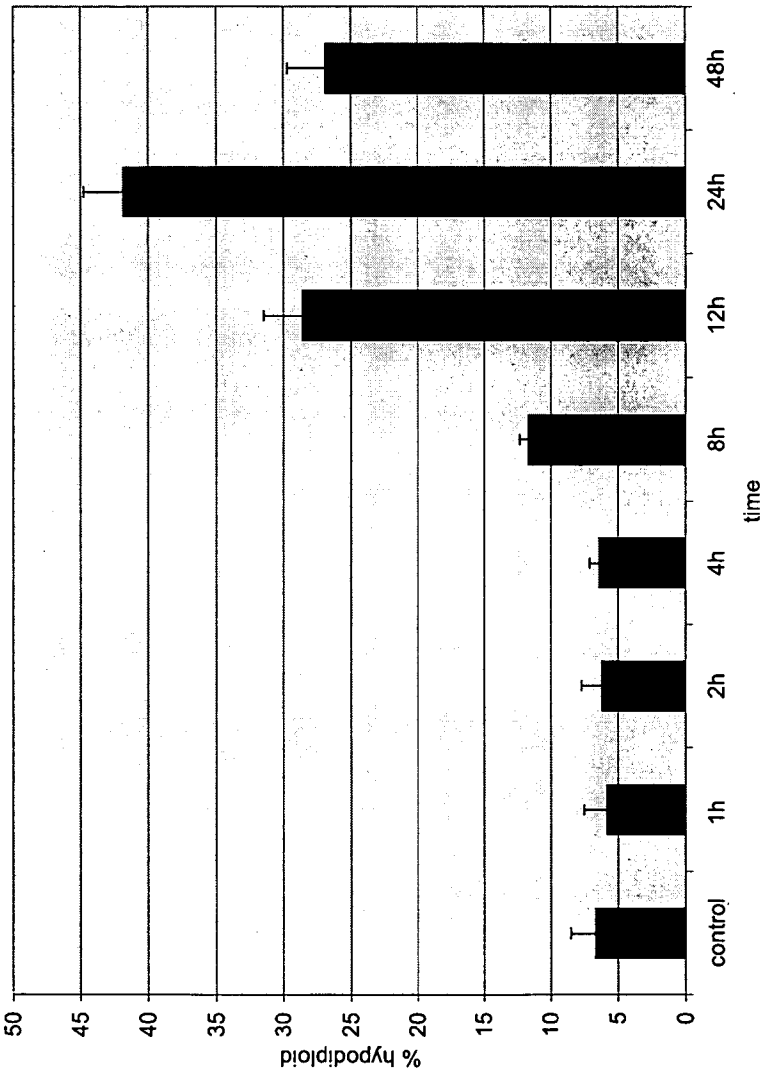
% hypodiploid
0
5
10
15
20
25
30
35
40
45
50
control
1h
2h
4h
8h
12h
24h
48h
time

Fig. 1D

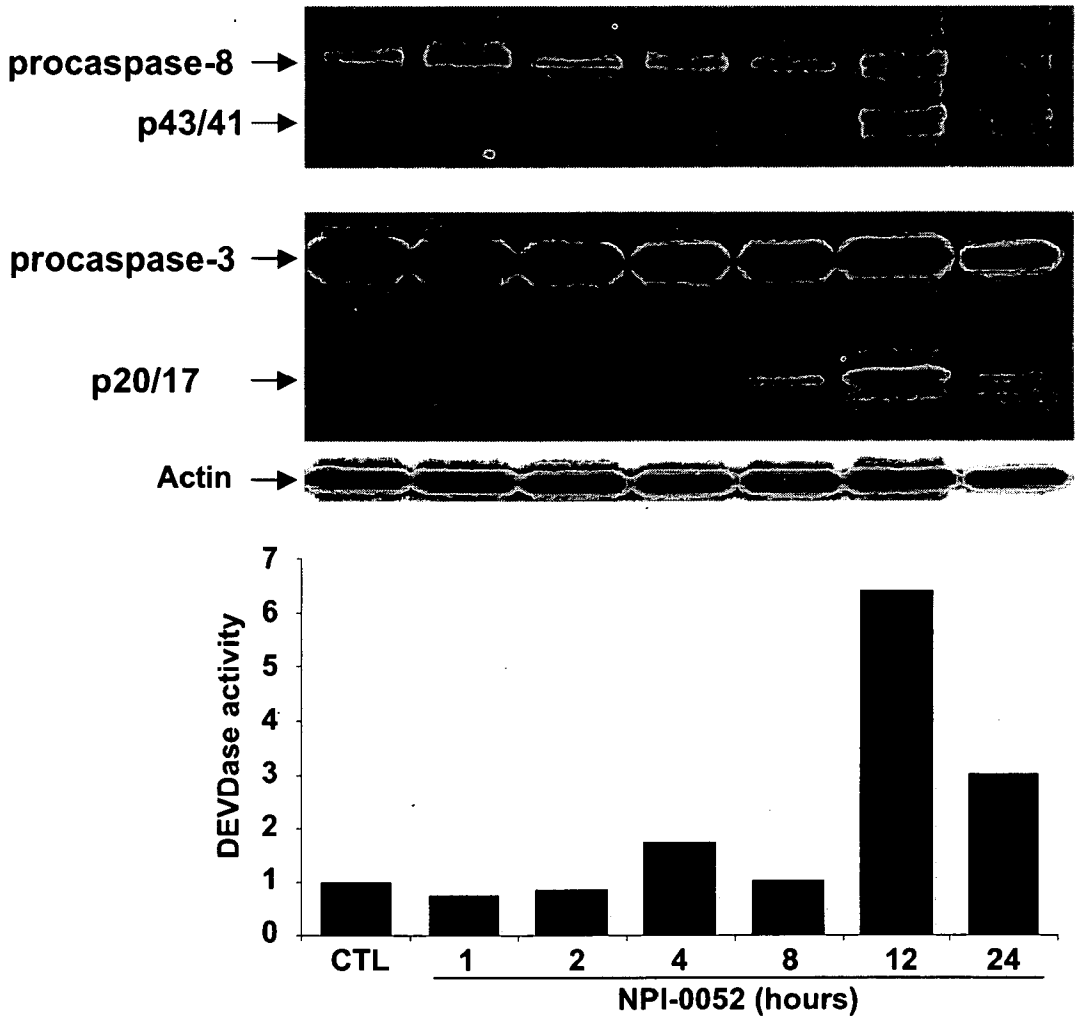
procaspase-8
p43/41
procaspase-3
p20/17
Actin
DEVDase activity
0
1
2
3
4
5
6
7
CTL
1
2
4
8
12
24
NPI-0052 (hours)

Fig. 2A

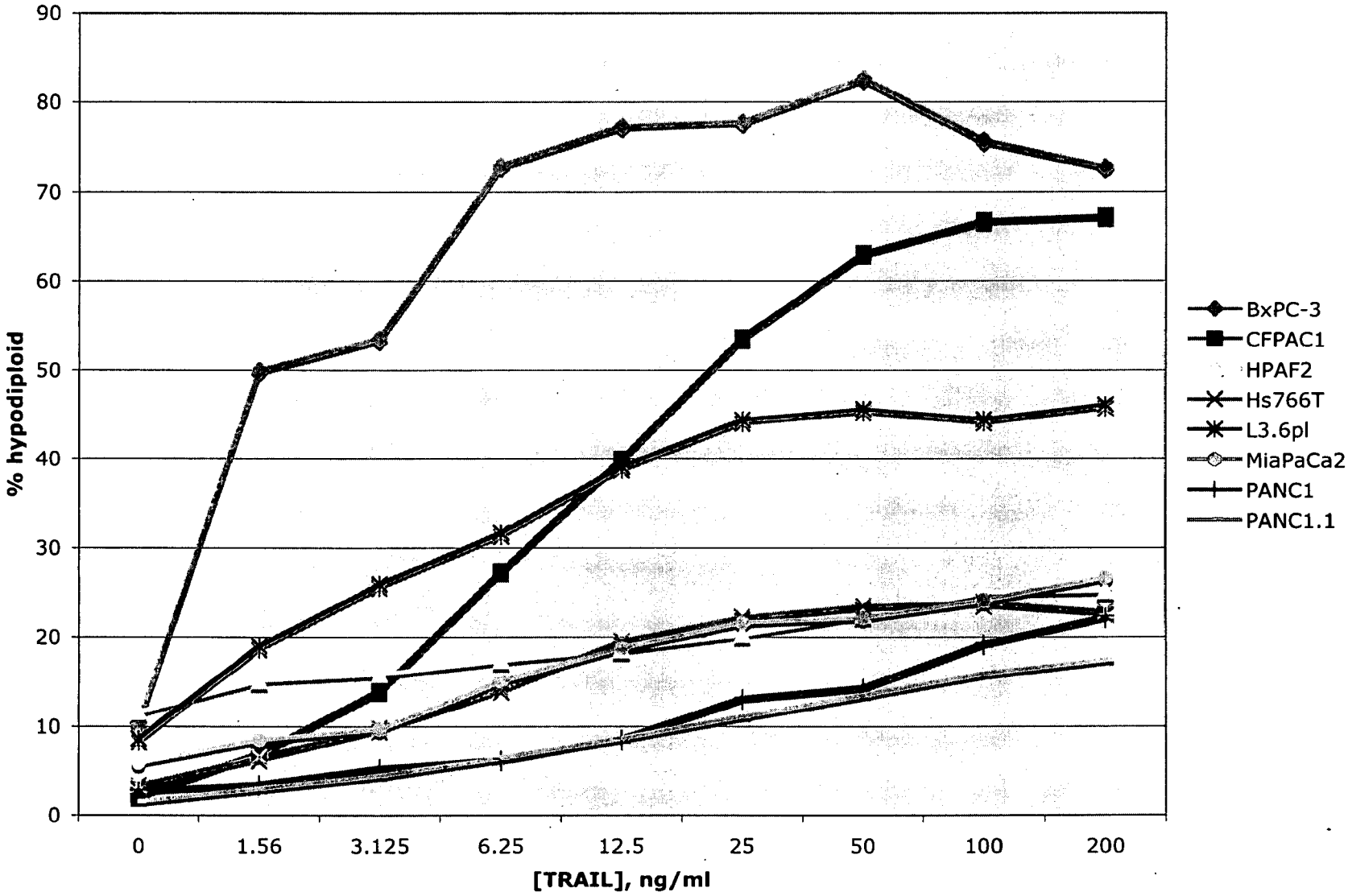
90
80
70
60
50
40
30
20
10
0
% hypodiploid
0
1.56
3.125
6.25
12.5
25
50
100
200
[TRAIL], ng/ml
BxPC-3
CFPAC1
HPAF2
Hs766T
L3.6pl
MiaPaCa2
PANC1
PANC1.1

Fig. 2B

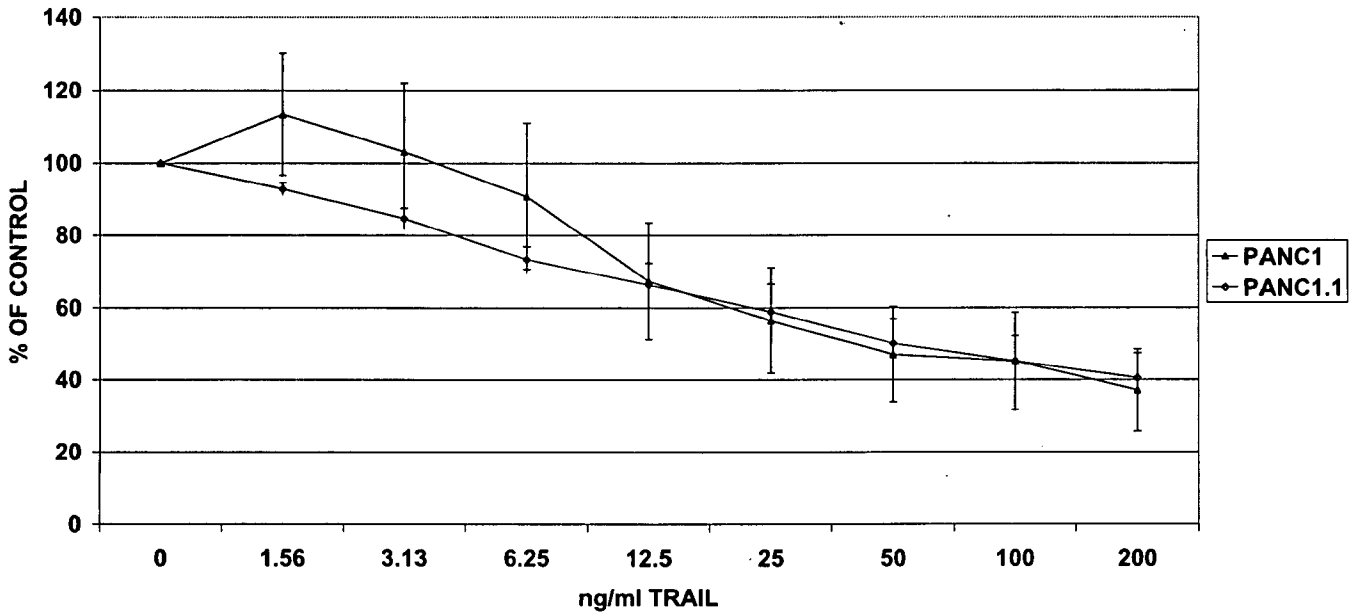
140
120
100
80
60
40
20
0
% OF CONTROL
0
1.56
3.13
6.25
12.5
25
50
100
200
ng/ml TRAIL
PANC1
PANC1.1

Fig. 2C

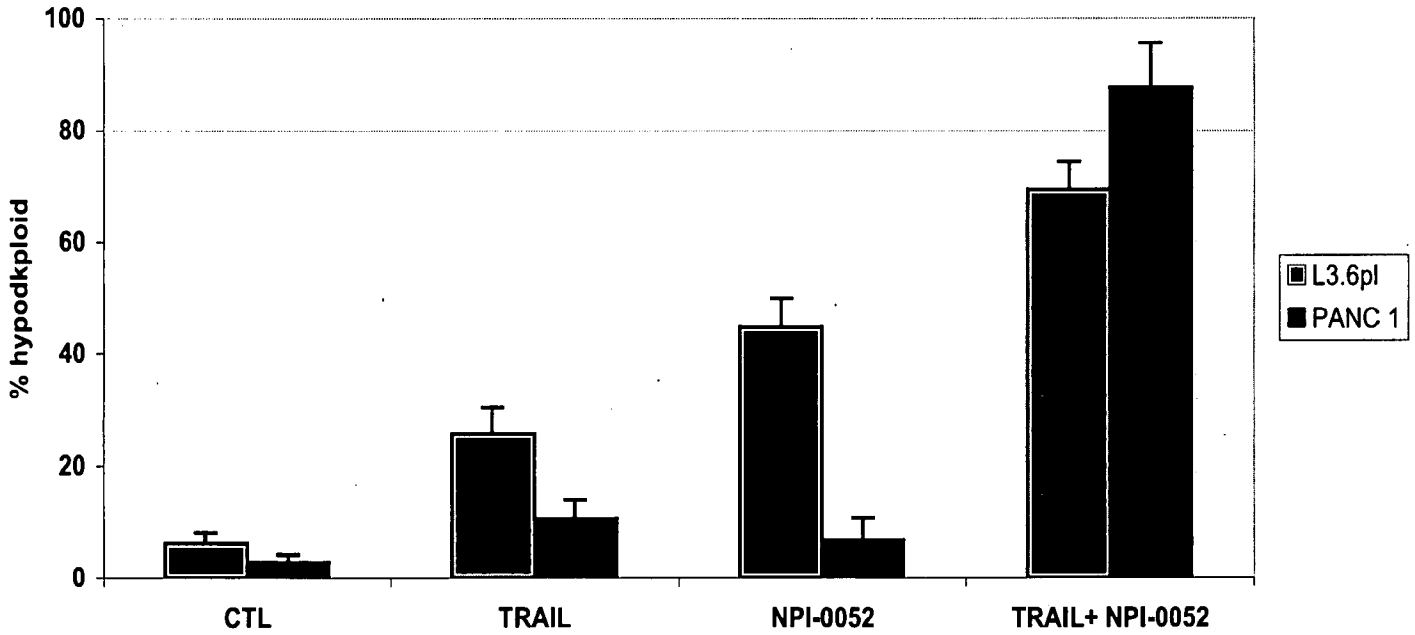
100
80
60
40
20
0
% hypodkploid
CTL
TRAIL
NPI-0052
TRAIL+ NPI-0052
L3.6pl
PANC 1

Fig. 3A

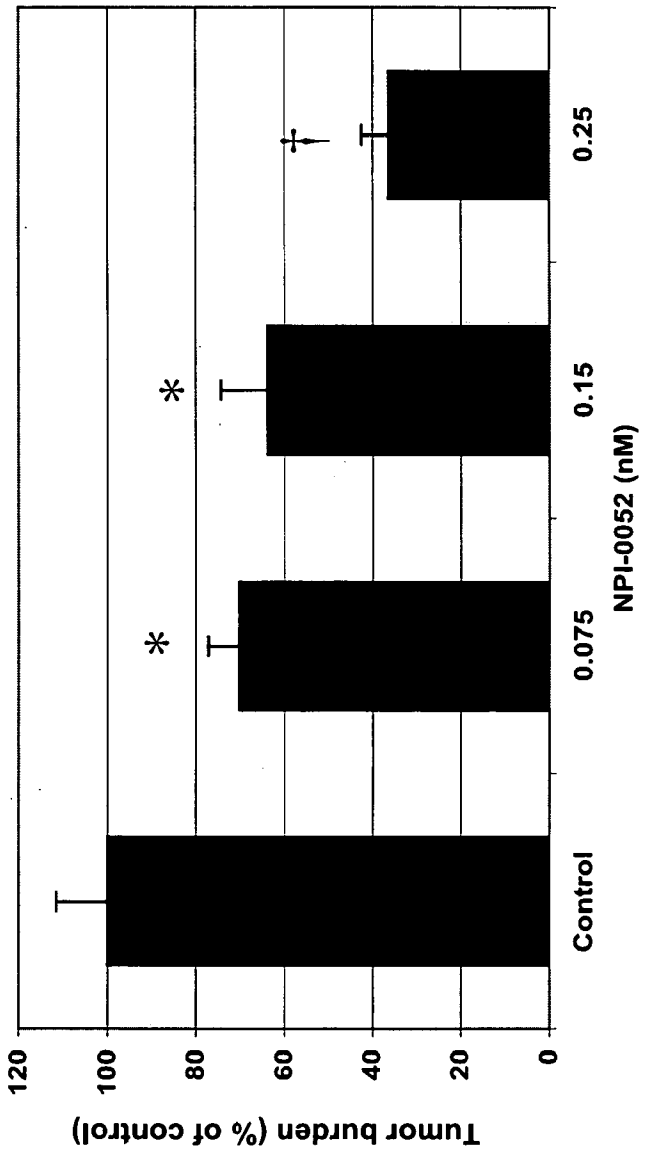
Tumor burden (% of control)
120
100
80
60
40
20
0
Control
0.075
0.15
0.25
NPI-0052 (nM)
*
*
†

Fig. 3B

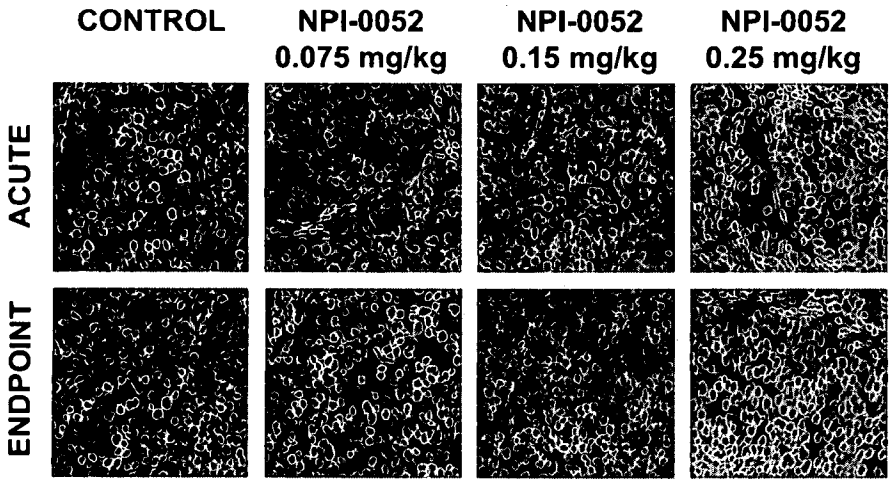
CONTROL
NPI-0052
0.075 mg/kg
NPI-0052
0.15 mg/kg
NPI-0052
0.25 mg/kg
ACUTE
ENDPOINT

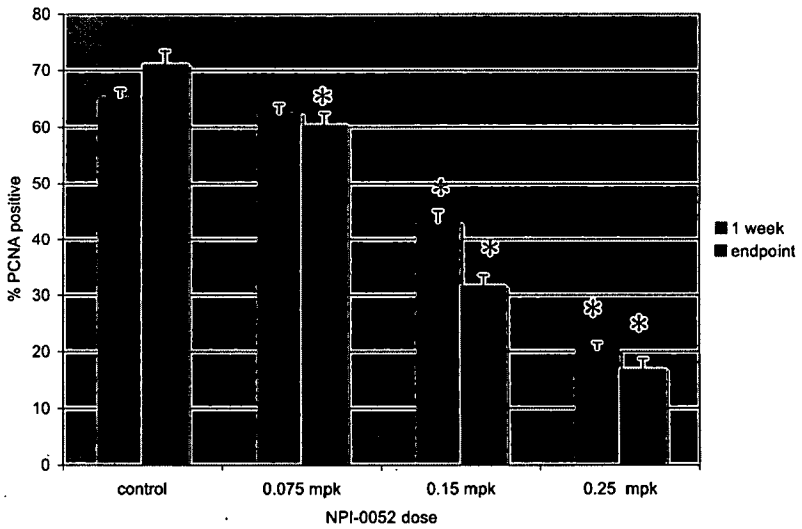
% PCNA positive
80
70
60
50
40
30
20
10
0
control
0.075 mpk
0.15 mpk
0.25 mpk
NPI-0052 dose
1 week
endpoint

Fig. 4

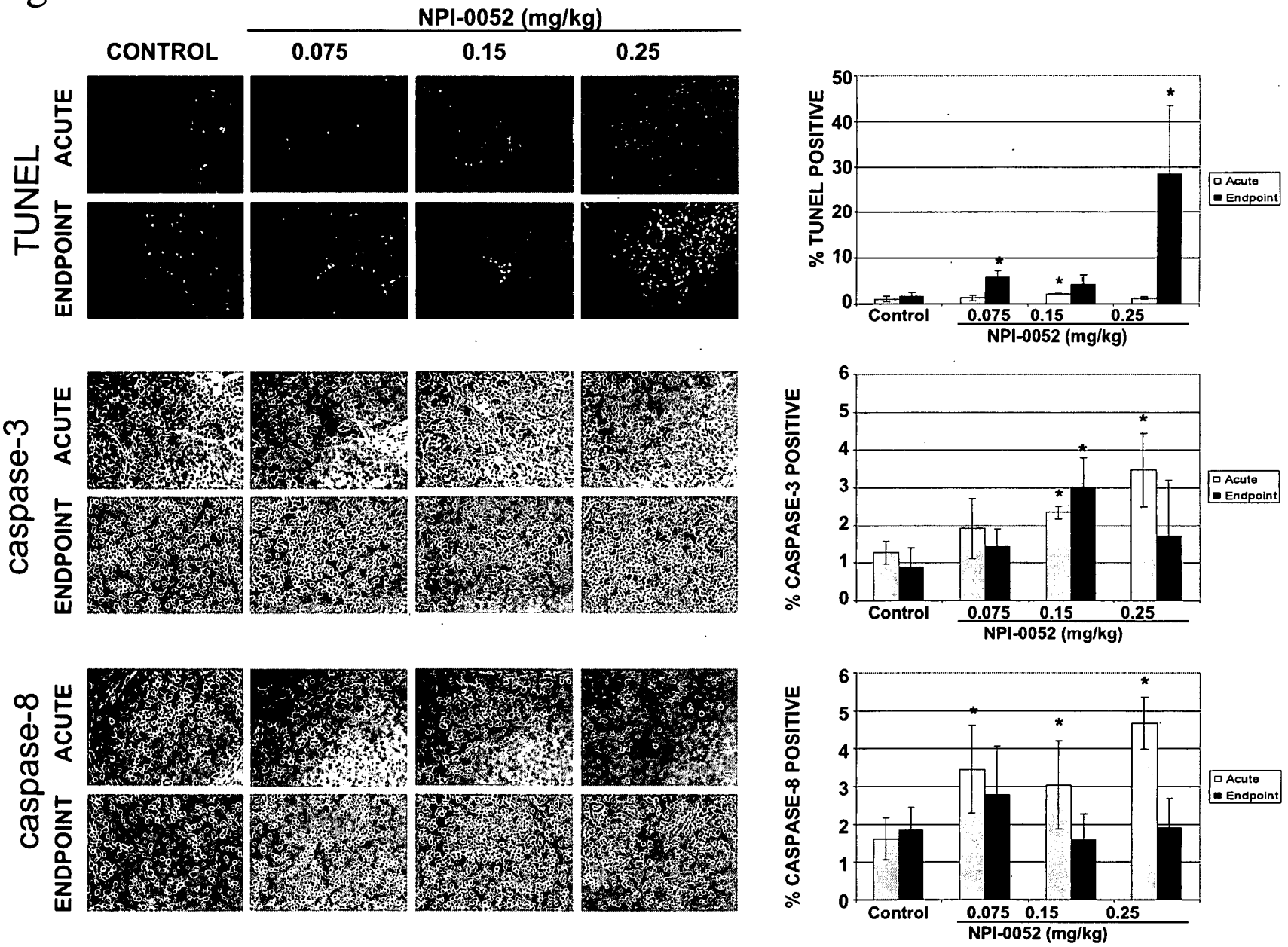
NPI-0052 (mg/kg)
CONTROL
0.075
0.15
0.25
TUNEL
ACUTE
ENDPOINT
caspase-3
ACUTE
ENDPOINT
caspase-8
ACUTE
ENDPOINT
% TUNEL POSITIVE
% CASPASE-3 POSITIVE
% CASPASE-8 POSITIVE
Acute
Endpoint
Control
0.075
0.15
0.25
NPI-0052 (mg/kg)

Fig. 5A

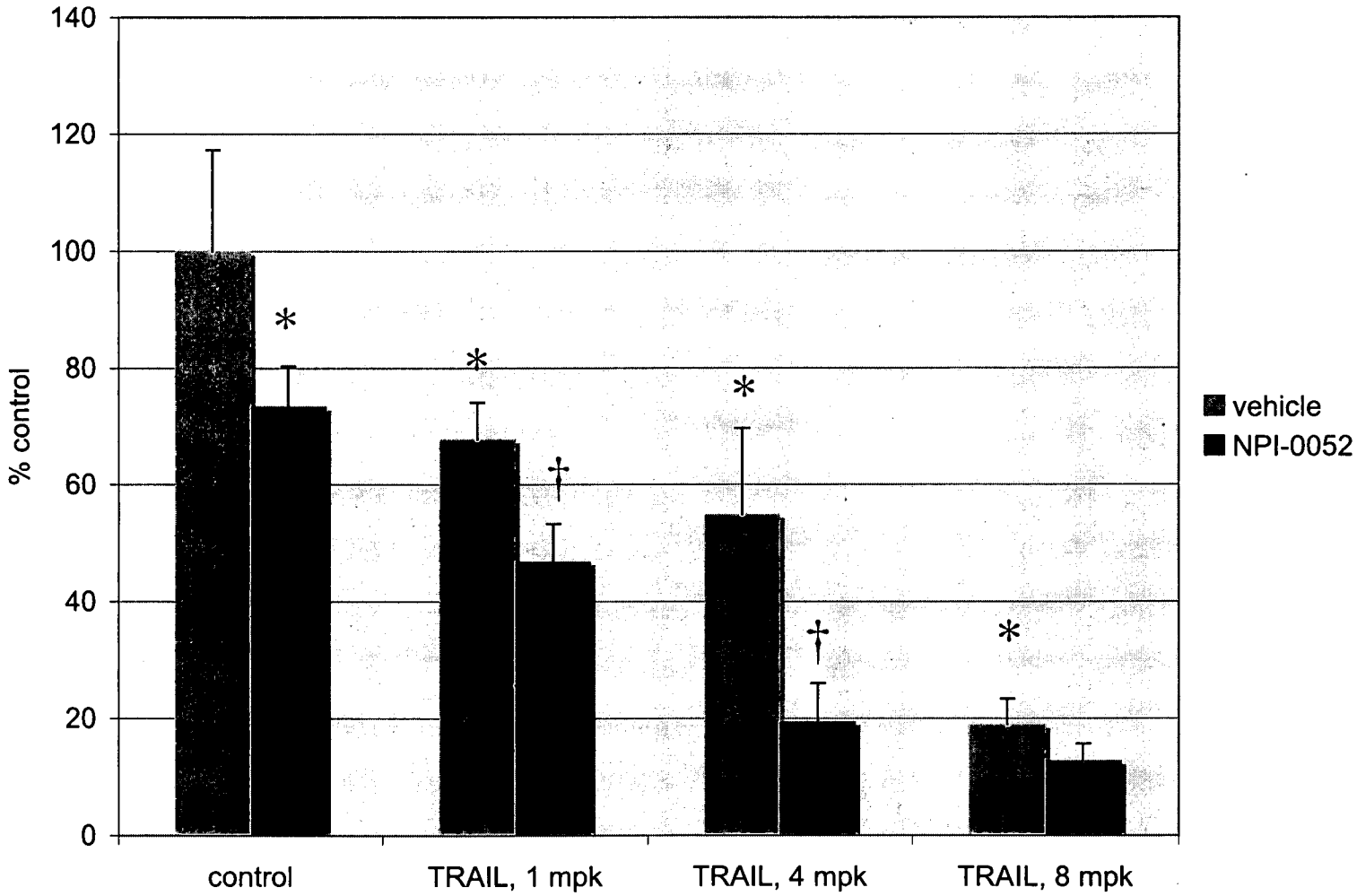
140
120
100
80
60
40
20
0
% control
*
*
*
*
†
†
control
TRAIL, 1 mpk
TRAIL, 4 mpk
TRAIL, 8 mpk
vehicle
NPI-0052

Fig. 5B

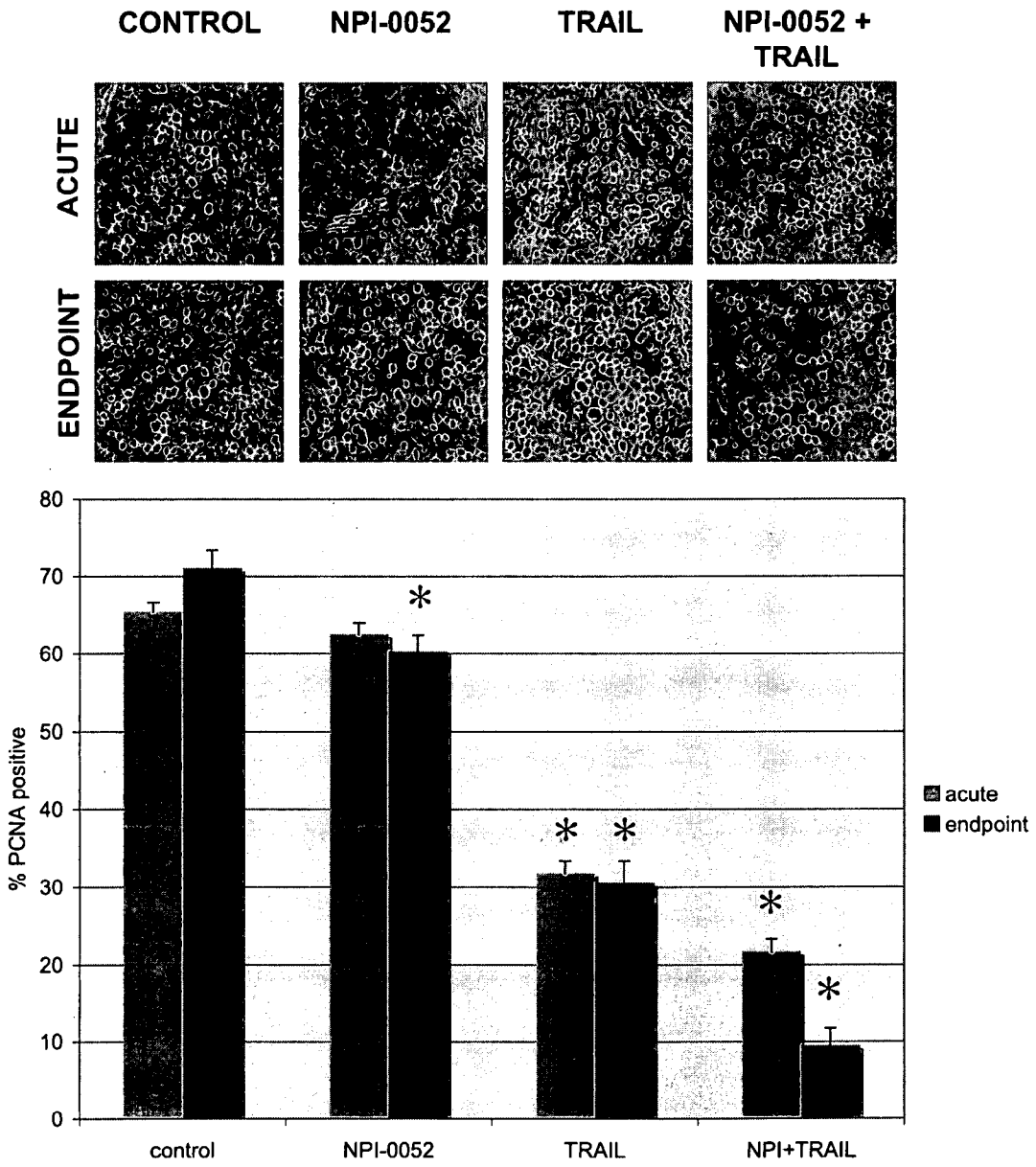
CONTROL
NPI-0052
TRAIL
NPI-0052 + TRAIL
ACUTE
ENDPOINT
% PCNA positive
80
70
60
50
40
30
20
10
0
control
NPI-0052
TRAIL
NPI+TRAIL
acute
endpoint
*

Fig. 6

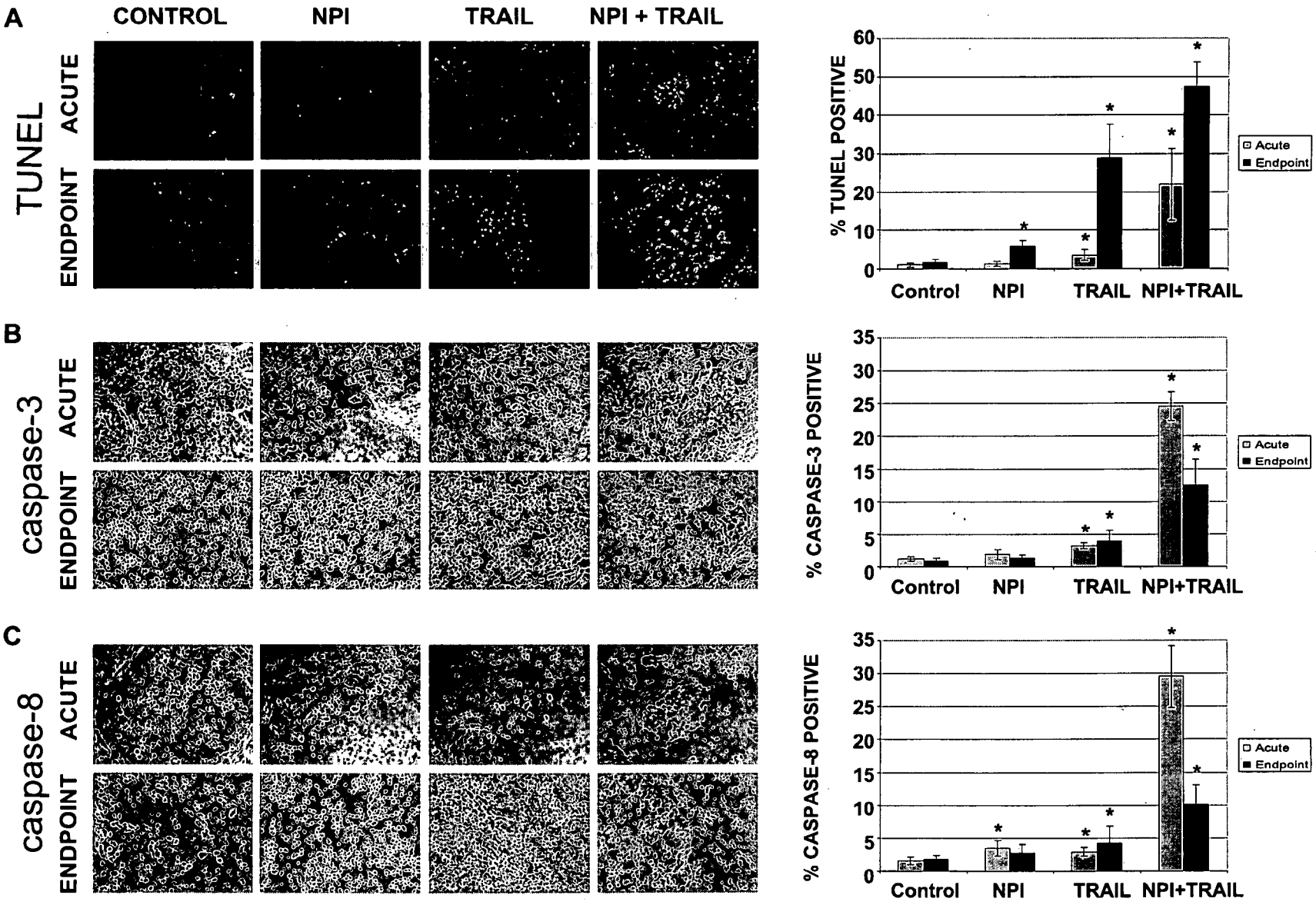
A
CONTROL
NPI
TRAIL
NPI + TRAIL
TUNEL
ACUTE
ENDPOINT
% TUNEL POSITIVE
60
50
40
30
20
10
0
Control
NPI
TRAIL
NPI+TRAIL
Acute
Endpoint
B
caspase-3
ACUTE
ENDPOINT
% CASPASE-3 POSITIVE
35
30
25
20
15
10
5
0
Control
NPI
TRAIL
NPI+TRAIL
Acute
Endpoint
C
caspase-8
ACUTE
ENDPOINT
% CASPASE-8 POSITIVE
35
30
25
20
15
10
5
0
Control
NPI
TRAIL
NPI+TRAIL
Acute
Endpoint

Fig. 7A

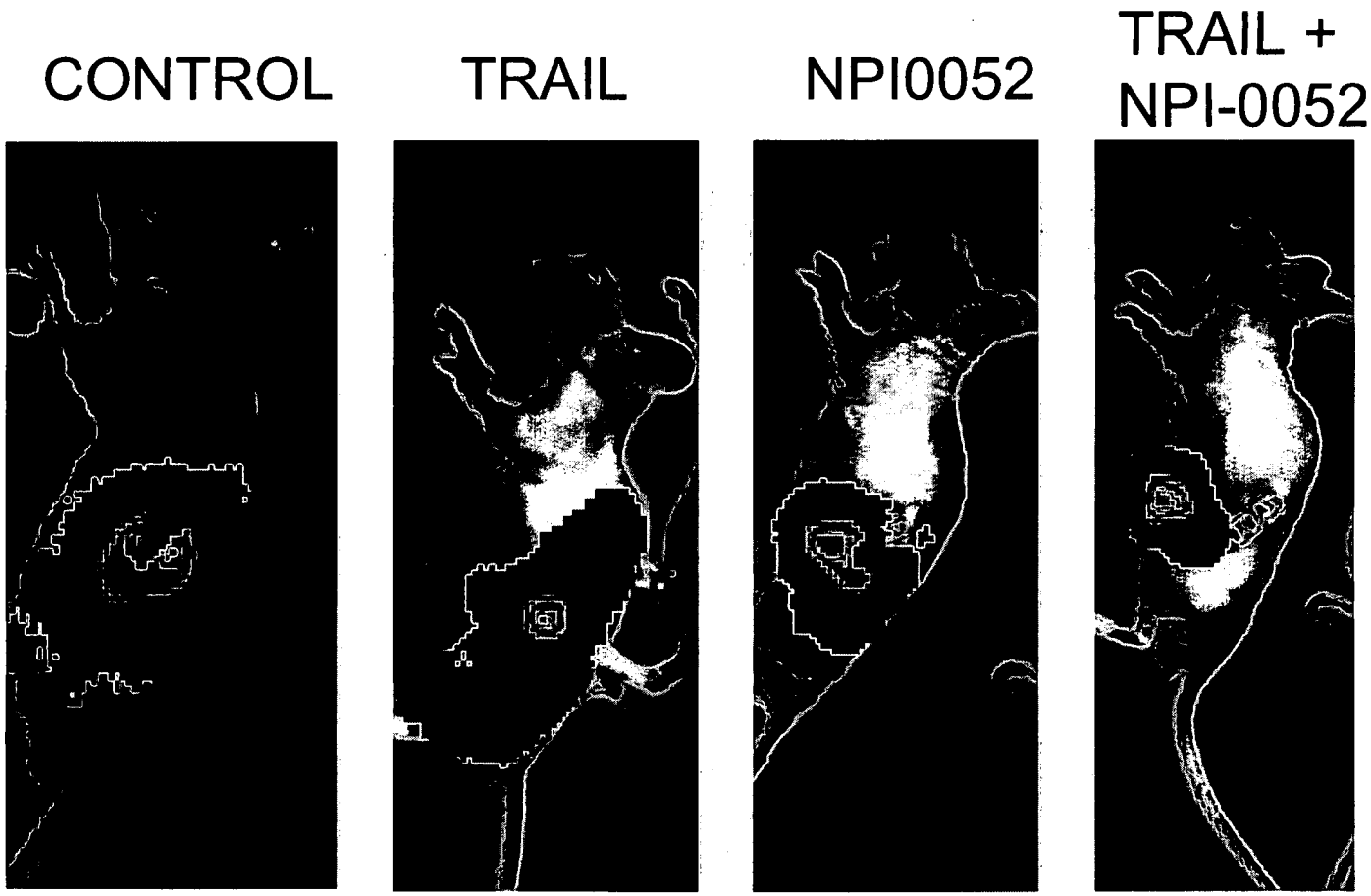

Fig. 7B

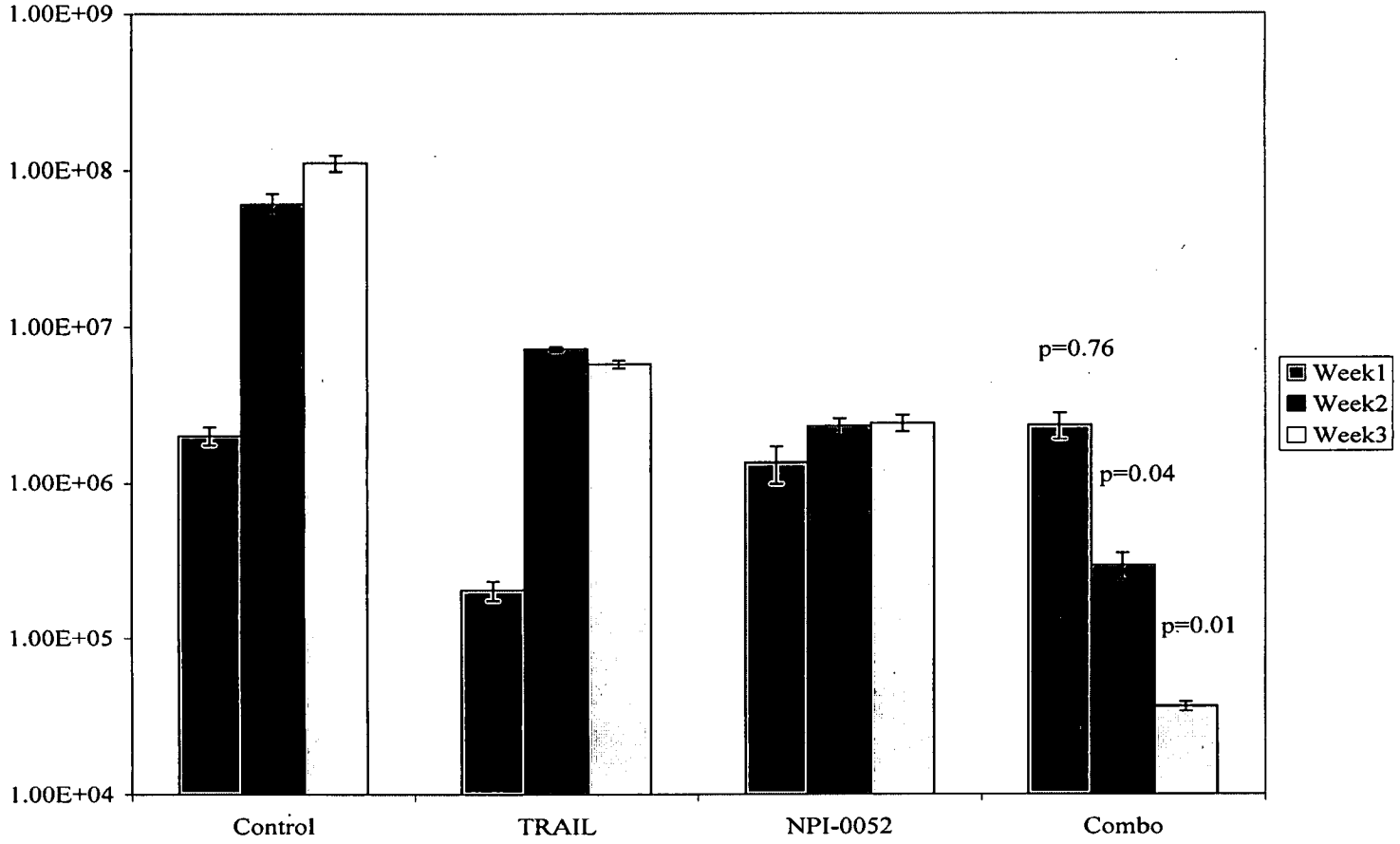
1.00E+09
1.00E+08
1.00E+07
1.00E+06
1.00E+05
1.00E+04
Control
TRAIL
NPI-0052
Combo
p=0.76
p=0.04
p=0.01
Week1
Week2
Week3

Fig. 7C

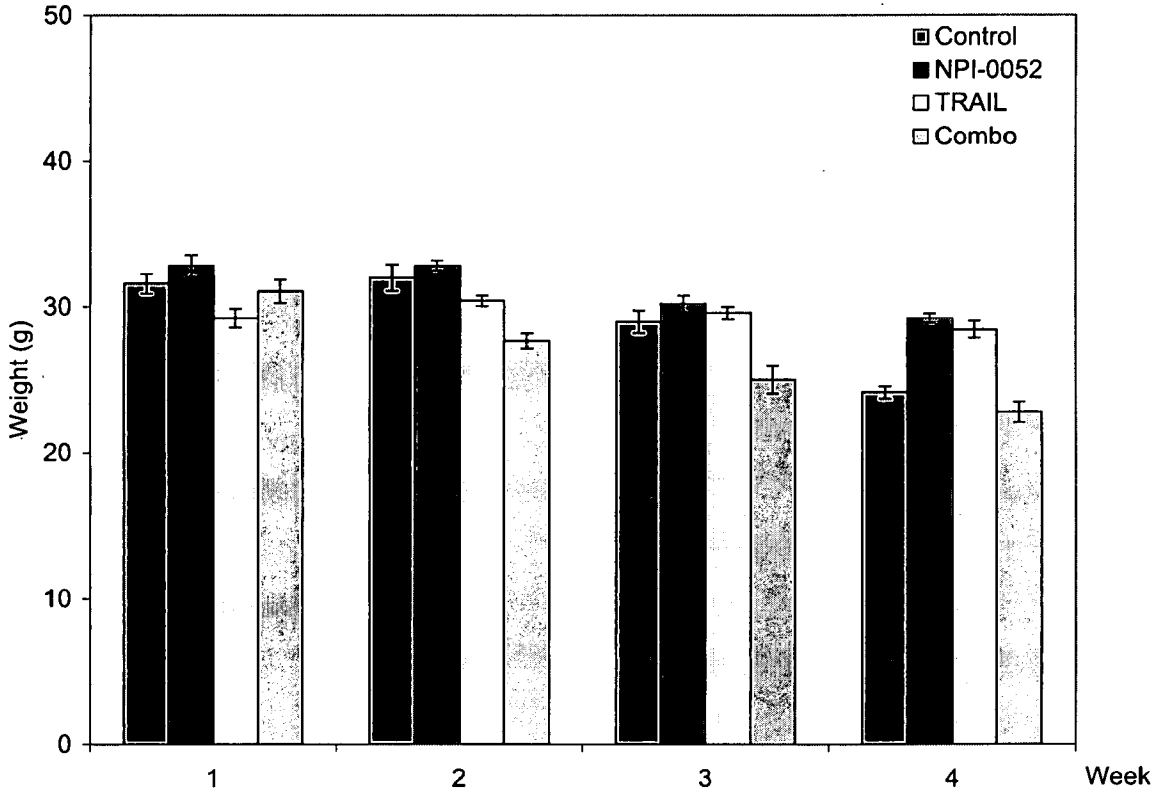
50
40
30
20
10
0
Weight (g)
Control
NPI-0052
TRAIL
Combo
1
2
3
4
Week

The Proteasome Inhibitor NPI-0052 Reduces Tumor Growth and Overcomes Resistance of Prostate Cancer to rhTRAIL via Inhibition of the NF-kB Pathway

Ana Maria Barral[1], Ta-Hsiang Chao[1], Sanaz Kanabolooki[2], Gordafaried Deyanat-Yazdi[1], Benjamin Nicholson[1], David McConkey[2], Michael A. Palladino[1], Saskia T. C. Neuteboom[1]
[1]Nereus Pharmaceuticals Inc., 10480 Wateridge Circle, San Diego, CA 92121, USA
[2]Department of Cancer Biology, The University of Texas M.D. Anderson Cancer Center, Box 173, 1515 Holcombe Boulevard, Houston, TX 77030, USA.

Prostate cancer is characterized by constitutive NF-kappaB (NF-kB) activity, due to increased activity of the IkB kinase complex and an increased turnover of the IkB inhibitory proteins. Furthermore, an inverse correlation between androgen receptor (AR) status and NF-kB activity has been observed in human prostate cancer cell lines. Treatment of hormone-refractory prostate cancer is still a challenge, and agents that inhibit the NF-kB pathway are considered promising therapeutic candidates.

NPI-0052 is a novel proteasome inhibitor that inhibits all three major proteolytic activities of the 20S proteasome both *in vitro* and *in vivo*. As NF-kB is regulated by the activity of the proteasome that degrades the IkB proteins, we explored the effect of NPI-0052 on various prostate cancer cell lines. Our results show that NPI-0052 inhibits the growth of the AR-negative PC-3 cell line with an IC_{50} of 55 nM. Treatment of PC-3 cells with 5 nM NPI-0052 results in 84% inhibition of the 20S proteasome chymotrypsin-like activity, while 5 nM bortezomib inhibits only 32%. Moreover, in clonogenicity assays, a one hour incubation with 50 nM NPI-0052 is sufficient to reduce PC-3 colony formation by more than 80%, in sharp contrast to bortezomib (50 nM, 1h), which only reduces colony formation by 30%.

We demonstrate that the effect of NPI-0052 occurs through blockade of the NF-kB pathway, as shown by accumulation of phosphorylated IkBα, and inhibition of NF-kB nuclear translocation and DNA-binding activity. Cells treated with NPI-0052 arrest in G2/M phase of the cell cycle, and undergo apoptosis as shown by annexin V staining and presence of cleaved PARP in a time- and dose-dependent manner. In addition, it has previously been reported that NPI-0052 exhibits a more rapid cytotoxic effect than bortezomib on lymphocytes from patients with chronic lymphocytic leukemia (Ruiz et al., *Mol Can Ther.* 2006, 5:1836).

Tumor Necrosis Factor Apoptosis Inducing Ligand (TRAIL) is a member of the TNF superfamily, which efficiently induces apoptosis in a variety of human tumor cell lines. However, some tumor cells remain resistant to TRAIL, which in many cases is thought to be mediated by activated NF-kB. Here we show that TRAIL-resistance of LNCaP-Pro5, a human prostate cell line, is reversed by treatment with NPI-0052, an effect mimicked by specific siRNA silencing of NF-kB/p65 expression. Combination treatment of NPI-0052 and TRAIL led to induction of apoptosis as measured by PI/FACS analysis. Specifically, levels of DNA fragmentation increased from 6% to 74% in LNCaP-Pro5 cells and from 5% to 62% in DU145 cells.

In summary, inhibition of the proteasome by NPI-0052 induced apoptosis in prostate cancer cell lines, which was significantly enhanced by combination with TRAIL. Selective blockade of multiple cellular pathways by combined therapy with proteasome inhibitors and/or TRAIL may prove to be a novel strategy for the treatment of hormone-refractory metastatic prostate cancer. NPI-0052 is currently in Phase I clinical trials for treatment of solid tumors/lymphomas and multiple myeloma.